Full Report

IndOOS-2

A roadmap to sustained observations of the Indian Ocean for 2020-2030

Coordinating lead authors

Lisa M. Beal, Jérôme Vialard, Mathew K. Roxy

December 2019

Sponsored by

World Climate Research Programme

United Nations Educational, Scientific and Cultural Organization

Intergovernmental Oceanographic Commission

International Association for the Physical Sciences of the Oceans

Lead Authors: Muthalagu Ravichandran[4,5], Michael J. McPhaden[6], Ming Feng[7], Rick Lumpkin[8], Alakkat S. Unnikrishnan[9], Tong Lee[10,11], Bernadette Sloyan[12,13], Magdalena Andres[14], Aneesh C. Subramanian[15], Lisan Yu[14], Matthieu Lengaigne[2], Toshiaki Shinoda[16],Hariharasubramanian Annamalai[17], Caroline C. Ummenhofer[14], Peter Strutton[18], Yukio Masumoto[19], Tomoki Tozuka[19], Jerry Wiggert[20], Weiqing Han[15], and Raleigh Hood[21].

Lead authors are in chapter order. A complete list of authors is given in Appendix B of the full report.

This report was led by the CLIVAR/IOC-GOOS Indian Ocean Region Panel (IORP) in collaboration with the Sustained Indian Ocean Biogeochemistry and Ecosystem Research programme (SIBER) of IMBeR.

Author Affiliations:

1. Rosenstiel School of Marine and Atmospheric Science, University of Miami, FL, USA
2. LOCEAN-IPSL, Sorbonne Universités (UPMC, Univ. Paris 06)-CNRS-IRD-MNHN, Paris, France
3. Indian Institute of Tropical Meteorology (IITM), India
4. National Centre for Polar and Ocean Research (NCPOR), India
5. Indian National Centre for Ocean Information Services (INCOIS), India
6. NOAA/Pacific Marine Environmental Laboratory (PMEL), Seattle, WA, USA
7. CSIRO Oceans and Atmosphere, Perth, Western Australia, Australia
8. NOAA/Atlantic Oceanographic and Meteorological Laboratory, Miami, FL, USA
9. CSIR-National Institute of Oceanography, Goa, India
10. NASA Jet Propulsion Laboratory (JPL), USA
11. California Institute of Technology, USA
12. CSIRO, Oceans and Atmosphere, Hobart, Australia
13. Centre for Southern Hemisphere Oceans Research, Hobart, Tasmania, Australia
14. Woods Hole Oceanographic Institution (WHOI), Woods Hole, MA, USA
15. University of Colorado, Boulder, USA
16. Texas A&M University-Corpus Christi, USA
17. International Pacific Research Center/Dept. of Oceanography, University of Hawaii, USA
18. Institute for Marine and Antarctic Studies, University of Tasmania, and Australian Research Council Centre of Excellence for Climate Extremes, Australia
19. University of Tokyo, Japan
20. University of Southern Mississippi, USA
21. University of Maryland, Center for Environmental Science, USA

Please use the following citation for the Full Report:

Beal, L. M., Vialard, J., Roxy, M. K. and lead authors 2019: Full Report. IndOOS-2: A roadmap to sustained observations of the Indian Ocean for 2020-2030. CLIVAR-4/2019, GOOS-237, 206 pp. doi: https://doi.org/10.36071/clivar.rp.4.2019

Please use the following citation for the Executive Summary:

Beal, L. M., Vialard, J., Roxy, M. K. and lead authors 2019: Executive Summary. IndOOS-2: A roadmap to sustained observations of the Indian Ocean for 2020-2030. CLIVAR-4/2019, GOOS-237, 8 pp. doi: https://doi.org/10.36071/clivar.rp.4-1.2019

Executive Summary

Lisa M. Beal, Jérôme Vialard, Mathew K. Roxy

Key functions of the Indian Ocean Observing System (IndOOS)

IndOOS is the sustained observing system for the Indian Ocean, a network operated and supported by various national agencies and coordinated internationally under the Global Ocean Observing System (www.goosocean.org) framework by the CLIVAR/IOC-GOOS Indian Ocean Region Panel (see Appendix A for a list of acronyms). The IORP is made up of an international group of scientists and science leaders from countries and institutions within and outside the Indian Ocean region who have a commitment to sustained observations of the Indian Ocean.

About one third of the global population live around the Indian Ocean, many in small islands, developing states and least developed countries that are especially vulnerable to climate impacts. There is growing societal demand for monitoring, understanding, and predicting the state of the Indian Ocean and its climatic influences in a time of accelerating changes and rapid growth in the blue economy. Despite its relatively small size, the Indian Ocean has accounted for 30% of the global oceanic heat content increase over the last two decades, while it is home to 30% of the world's coral reefs and 13% of global wild-catch fisheries. Cyclones, floods, droughts, and heatwaves are becoming more extreme around the Indian Ocean, with anthropogenic climate change increasingly impacting weather patterns and threatening marine and terrestrial resources. Moreover, natural climate phenomena with global impacts, such as the Madden-Julian Oscillation (MJO) and the Indian Ocean Dipole (IOD), originate in the Indian Ocean. The goal of IndOOS is to provide sustained high-quality oceanographic and marine meteorological measurements that can support knowledge-based decision-making and policy development through improved scientific understanding, and ultimately, improved regional weather, ocean, and climate forecasts.

Why IndOOS-2?

The existing IndOOS design was established on the basis of an Implementation Plan drafted by the CLIVAR IORP in 2006. Since then, societal and scientific priorities and measurement technologies have evolved, many practicalities of implementation have been learned, and the pace of climatic and oceanic change has accelerated. The main objective of this document is to review the successes and failures of the IndOOS and to incorporate these practicalities, together with new priorities, into actionable recommendations for future observing system components that will make up IndOOS-2. In essence, the review findings provide a roadmap to address *the clear and urgent need for expansion of a global ocean observing system designed to meet the requirements of a broad suite of users*, as recognized in the GOOS 2030 Strategy.

This review and the resulting roadmap was sponsored by the OOPC, an expert panel of GOOS, as a *system-based evaluation to renovate or fill gaps in the IndOOS and increase its readiness level*. It was conducted and written by a group of sixty international scientists, under the guidance of the IORP in partnership with SIBER and under the scrutiny of an independent review board appointed through various partners of GOOS (see Appendix B for the full list of contributors).

Document overview

A description of the review process that led to IndOOS-2 is given in the Introduction, which also includes background on the societal motivations for observing the Indian Ocean, the broad scientific and operational drivers of the IndOOS, and its observing system components. In the 25 chapters that follow we: (1) Review the current status of the IndOOS, component by component, including past successes and failures (Chapters 1-8); (2) Assess the demands that operational products and forecasts place on the IndOOS (Chapters 9-11); and (3) Articulate the oceanic and climatic phenomena that the observing system must capture (Chapters 12-25). Each chapter identifies a set of essential ocean variables (EOVs) with their required geographical coverage and spatio-temporal resolution as well as a list of Actionable Recommendations for upgrades and enhancements to the observing system that address the most important gaps and needs. Finally, in the Synthesis the major outcomes of these chapters are summarized, the process of consolidating and prioritizing the Actionable Recommendations is described, and the Recommendations are listed in the context of observing system components.

This Executive Summary stands alone and presents a comprehensive summary of the outcomes of the review, providing a roadmap to the proposed evolution of the IndOOS during 2020-2030 in terms of the core findings and a prioritized list of Actionable Recommendations.

Core findings

The first decade or so of IndOOS has provided unprecedented measurements of weather, ocean, and climate phenomena. These observations have, for instance: Supported the study and forecast of tropical cyclones and marine heatwaves (Chapter 12); Improved our understanding of the MJO and MISO (Monsoon Intra-Seasonal Oscillation) and their influence on sub-seasonal variations of the global hydro-climate (Chapters 13-15); Mapped the equatorial and monsoon circulations and captured variability of the Indonesian throughflow (Chapters 14, 17); And elucidated year-to-year climate variations in the tropical Indian Ocean (Indian Ocean Dipole, IOD) and their relationship to tropical Pacific climate variations (El Niño-Southern Oscillation, ENSO) (Chapter 19).

There remain, however, significant limitations and gaps in the existing IndOOS such that, so far, it falls short of meeting many of society's demands for climate forecasting and prediction. These limitations are starkly illustrated by the low prediction skill of sub-seasonal to seasonal forecasts, which lack sufficient information of initial upper-oceanic conditions (Chapter 9), and by large discrepancies in climatologies of heat exchange at the air-sea interface. These discrepancies exceed 30 Wm^{-2} over boundary current and upwelling regions, such as the Agulhas and Somali Current systems and the Java-Sumatra upwelling cells (Chapter 10). IndOOS must also support ocean state estimations that are used to initialize climate predictions and drive biogeochemistry models. Large uncertainties remain in these critical products and, while technical limitations of data assimilation systems are partially to blame, lack of sustained observations, particularly in high flux boundary regions and in the deep ocean, leave these products poorly constrained (Chapter 11).

Several key gaps in the observing system have been identified through the work of this review. The Arabian Sea and western equatorial Indian Ocean have suffered from an extreme lack of observations, largely as a result of piracy and vandalism. Here, the uniquely seasonal Somali Current and western boundary upwelling system are associated with strong oceanic productivity and an expansion of regional sub-surface anoxia (Chapters 18, 20), while semi-annual variability in mixed layer depth and air-sea fluxes influence monsoon variability and predictabil-

ity (Chapters 13, 14). With piracy now dormant, long-planned RAMA sites were finally occupied in the Arabian Sea in June 2018, while a further three remain unoccupied (Chapter 1). **We recommend that IndOOS coverage of the Arabian Sea and western equatorial Indian Ocean, including biogeochemical measurements, be rapidly intensified.**

Better measurements of the mixed layer, the upper oceanic layer that interacts with the atmosphere, and of barrier layers, a salinity-stratified layer below the mixed layer, are needed to improve sub-seasonal to seasonal forecasting. Diurnal cycles in near-surface-ocean stratification impact regional Sea Surface Temperature(SST) patterns, winds, and the development and propagation of the MJO and MISO, that in turn influence monsoon rainfall and global hydroclimate (Chapters 13, 14). Hot spots of this fine-scale vertical variability occur in regions of upwelling at the eastern equatorial boundary near Sumatra, in the southeastern Arabian Sea, and in the Seychelles-Chagos Thermocline Ridge, as well as in the salinity-stratified Bay of Bengal. These are also regions of high variability in air-sea fluxes of CO_2 and in primary productivity. **We recommend enhanced vertical and temporal resolution of upper-ocean measurements in these regions and the addition of near-surface biogeochemical observations.**

Recent studies suggest that the Indian Ocean has stored an astounding 30% of the global oceanic heat uptake from the atmosphere over the last two decades. This heat uptake has strongly contributed to the temporary slowdown in global surface atmosphere temperature warming often referred to as the climate change “hiatus”. The heat is thought to have largely entered the basin from the Pacific via the Indonesian Throughflow, yet its relationship to warming in the southern subtropics and to regional sea level rise is unclear. And its ultimate fate, regarding a possible return to the atmosphere to contribute to a future acceleration in global warming, is unknown. This motivates the need for observations that can monitor the dominant oceanic fluxes of mass and heat (Chapter 23) and ultimately constrain basin-scale budgets associated with decadal variability and change. **We recommend the establishment of boundary flux arrays in the Agulhas and Leeuwin Currents, an enhancement of Indonesian Throughflow monitoring, and an increase in observations of the deep ocean below 2000 m.**

There is an overarching need for sustained biogeochemical measurements as an integral part of the IndOOS. De-oxygenation and acidification trends, the marine carbon cycle, primary productivity variability, and ecosystem changes are largely unconstrained throughout the Indian Ocean. Management of the Indian Ocean’s natural resources, including coral reefs and wild-catch fisheries, under a changing climate will require a step-change in the amount of biogeochemical data collected. **We recommend an increase in biogeochemical measurements throughout the basin, initially targeted to regions of high variability and change, such as the Arabian Sea, Bay of Bengal, and eastern equatorial Indian Ocean.**

In addition to *in situ* observing system needs, there are three additional ingredients necessary for the future advancement and success of the IndOOS. First, **satellite measurements are central to the IndOOS**, providing the only basin-wide view of the ocean and of air-sea fluxes. Continuous, overlapping satellite missions are vital, as are the *in situ* observations that calibrate and validate these missions. Second, **there is urgent need for advancements in data assemblage and coupled data assimilation techniques**. Quality control, archiving, inter-calibration, and mapping of oceanographic datasets can be fragmented and uneven and need to be improved if these data are to connect with end-users and decision-makers. There is a need for an efficient data management system for all observing platforms that follows international best practices (metadata reporting, community accepted standards for quality assurance and control (QA/QC)), and data publication that enables interoperable discovery and

free, open access. Advancements in assimilation techniques are needed to better leverage the potential of the IndOOS observations in products, state estimations, and predictions. Finally, **there is a necessity for increased engagement and partnerships among Indian Ocean rim countries**. Much of the expansion of the IndOOS into coastal and upwelling regions will be reliant on increased involvement and cooperation of regional countries and agencies, along with their commitment to observing best-practices, and to data sharing and dissemination. Collaboration, resource sharing, and capacity building between nations are essential in this. These challenges are not new to ocean observing and the Framework for Ocean Observing, GOOS, GOOS partners, and the GOOS regional alliances provide the tools and models for success (www.goosocean.org). For the Indian Ocean, a pro-active and inclusive IORP, IO-GOOS, and Indian Ocean Resources Forum (IRF) are essential to entrain, guide, facilitate, support, collaborate with, and provide resources for new IndOOS partners and components. These bodies will require ongoing and recommitted support via the WCRP from the World Meteorological Organization, the International Council for Science, and the Intergovernmental Oceanographic Commission of UNESCO. These recommendations are summarized in Figure ES.1, which shows all the observing system components for the next phase of IndOOS.

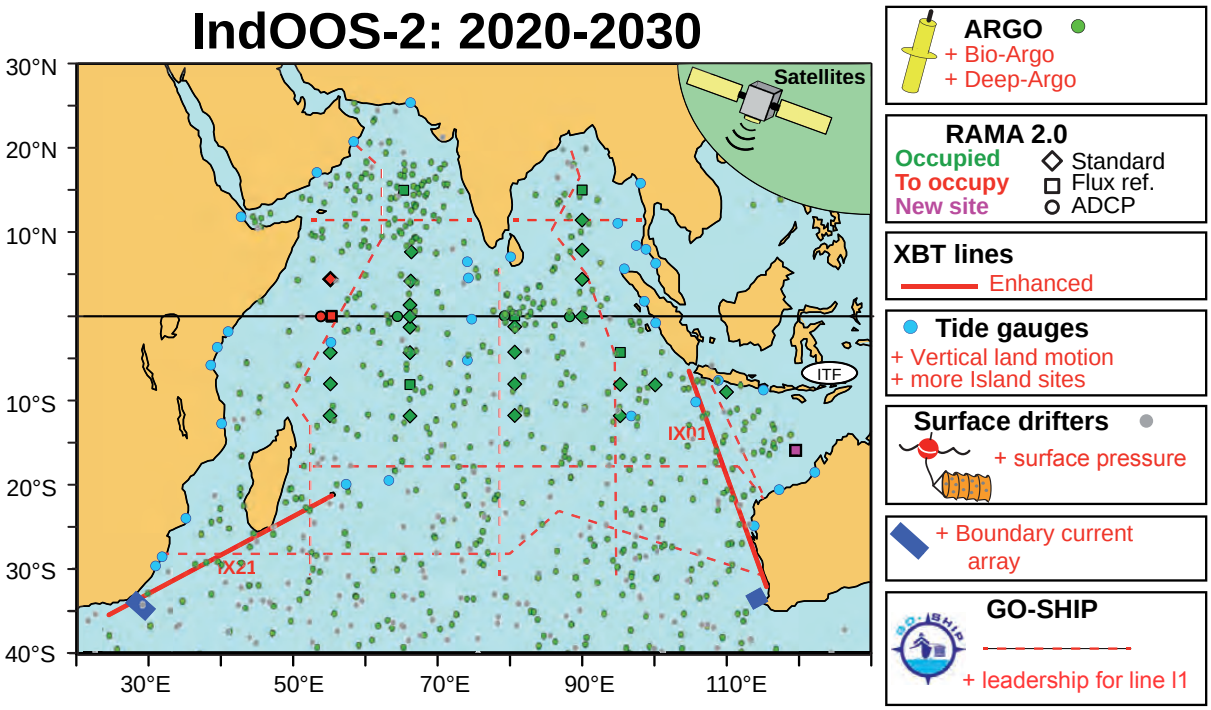

Figure ES.1 IndOOS-2: 2020-2030. **Argo**: Maintain the core 3° x 3° array; add 200 Biogeochemical (BGC)-Argo floats; develop a Deep-Argo program. **RAMA**: Consolidate to RAMA-2.0, occupying 3 remaining sites in Arabian Sea; increase resolution of upper-ocean measurements and add biogeochemical measurements at flux reference sites; add new site off Northwestern Australia. **XBT**: Maintain IX01 and IX21 lines; install auto-launchers and increase near-coastal resolution on IX01. **Tide gauges**: Add colocated measurements of land motion; add sites in Southwest Indian Ocean and on islands. **Surface drifters**: Maintain core 5° x 5° array, evaluate addition of barometric pressure measurements. **Boundary current arrays**: Add measurements of mass, heat, and freshwater fluxes of the Agulhas and Leeuwin Currents, including hydrographic end-point moorings to capture basin-scale overturning. **GO-SHIP**: Find national commitment for section I01; add measurements of phytoplankton community structure. **Satellites**: Maintain overlapping, inter-calibrated missions; enhance spatial resolution of Sea Surface Height (SSH) or currents directly.

Following is a list of actionable recommendations, prioritized based on their number of applications and/or unique importance. For instance, the Argo program is of highest priority, being cited in 13 of the 17 chapters herein on science drivers, while development of SOOP-CO_2 measurements are a high priority because there are no long-term records of surface carbon flux in the Indian Ocean, an important climate parameter. A full justification of these recommendations and their ranking is provided in the Synthesis at the end of this review.

Actionable Recommendations

Tier I: Maintain and consolidate essential capacities, while better considering practicalities.

The most essential observing networks of the IndOOS are: Argo, RAMA, satellite missions, tide gauges, XBT lines, and surface drifters and GO-SHIP. These networks have supported, and should continue to support, understanding and prediction of many important phenomena, including the monsoons (Chapter 14), tropical cyclones and rainfall variability (Chapters 12, 13, 15), heat and freshwater cycles (Chapters 15, 17, 23, 25), regional sea level change (Chapter 21), and tropical modes of sub-seasonal to decadal climate variability (Chapters 13, 19, 22) in the Indian Ocean. The continuation of these networks is essential for the future detection and attribution of anthropogenic changes in the Indian Ocean (Chapter 25).

A. The Argo program is extraordinarily successful (Chapter 1) and should be maintained at highest priority. We recommend enhancement with biogeochemical- and Deep-Argo programs, as itemized in Tier II below.

B. We recommend RAMA be consolidated to a new design — **RAMA-2.0 — reducing the original plan from 46 sites to 33** in consideration of issues such as vandalism and available ship time (Chapter 2). **Three western equatorial sites (55°E) need to be occupied at highest priority to complete RAMA-2.0.** Scientific capacity will be largely maintained with fewer moorings while also providing more opportunity and flexibility to add new sites, upgrade technology, and add new sensors. **Coordination between RAMA and the Indian array OMNI is a priority** and will improve operational efficiency as well as data accessibility and standards.

C. The tide gauge network will continue to grow in importance as more regional climate predictions are demanded. The network should be consolidated with **more colocated GNSS (land motion) stations**, prioritizing sites where records are longest (Chapter 5), and with **more island stations** (in particular in the southwestern tropical Indian Ocean), which are highly effective for comparisons with satellite data and for combined reconstructions of long-term regional sea level changes.

D. Satellite missions provide the only spatially coherent view of the ocean, albeit only at the surface. Continuous, inter-calibrated surface winds at diurnal timescale, all-weather sea surface temperature, as well as sea surface height, sea surface salinity, and ocean color are of highest priority (Chapter 6). **Space-based capabilities for measuring meso- and sub-mesoscale variability should be enhanced.**

E. Much of the XBT network has been superseded by Argo (Chapter 3). However, Argo does not capture regions of high variability, intense narrow flows, or shallow water. **The outstanding priority is to maintain IX01**, which captures the interannual variability of geostrophic Indonesian Throughflow (ITF) transport over the upper 700 m. To consolidate IX01 **we recommend installation of automated launchers** to increase data resolution and return, denser profiling over the shelf/slope regions, plus a **regional enhancement**

of Argo to provide more measures of salinity. **IX21 should be enhanced with collection of pCO_2** (Chapter 24) and its potential for capturing changes in the Agulhas Current investigated. **Data from IX14 across the Bay of Bengal should be shared and made accessible.**

F. The surface drifter program should be maintained at current design density **and enhanced with more barometric pressure observations, with the optimal density of pressure observations to be evaluated at highest priority (Tier I)** (Chapters 4, 12, 15).

G. The GO-SHIP provides the only means to collect a comprehensive suite of colocated hydrographic, biogeochemical, and tracer measurements, through shipboard water sample collection and laboratory analysis (Chapter 7). These occupations should continue at decadal interval and it is **a priority to identify national or multi-national support for the occupation of I01E and I01W sections across the Bay of Bengal and Arabian Sea.**

Tier II: Extend IndOOS capacities to better address scientific and operational drivers.

Enhancements of the IndOOS are necessary to meet growing societal needs for data, forecasting, and prediction at a time when extreme events, such as cyclones and heatwaves, are intensifying, when floods and droughts are growing in number, and when marine ecosystem changes and their impacts on fisheries are becoming evident. Climate and climate variability are changing fast and a global climate observing system, with a fit-for-purpose IndOOS component, will provide our only means of mapping those changes and predicting what may happen next.

A. Foremost, we recommend **development of sustained measurements towards understanding the carbon cycle and ecosystem variability and change** in the Indian Ocean. Until now, these measurements are extremely sparse. For example, not one of the 1698 stations of primary productivity used to develop the satellite ocean color algorithm for estimating ocean primary productivity globally, comes from the Indian Ocean. Of particular importance are observations in the Arabian Sea, where profound biogeochemical and ecosystem changes may have already occurred (Chapters 16, 20, 24). These observations must be made alongside physical measurements.

(A1) **A suite of 200 biogeochemical-Argo floats** (measuring nutrients, bio-optics, and oxygen in addition to temperature and salinity) in the Indian Ocean, as part of the global biogeochemical-Argo implementation plan (Chapters 1, 16, 18, 20, 24, 25). Floats should be targeted to regions with strongest de-oxygenation trends, upwelling zones, high primary productivity variability, and regions important for the marine nitrogen cycle. These include the Arabian Sea and Bay of Bengal oxygen minimum zones, the Seychelles-Chagos Thermocline Ridge (SCTR), and the eastern equatorial region. (A2) **$MAPCO_2$ systems and biogeochemical measurements at RAMA Flux Reference sites**, targeting regions with high variability in CO_2 fluxes and/or primary productivity, and/or rapidly decreasing pH, with the Arabian Sea and SCTR highest priority (Chapters 24,25). (A3) **Establish SOOP-CO_2 measurements in the southern Indian Ocean (IX21)**, and in the northern Arabian Sea and Bay of Bengal. (A4) **Add observations of chlorophyll concentration and phytoplankton community structure on key GO-SHIP lines and RAMA maintenance voyages** to validate ocean color satellite data and track changes in productivity and the biological carbon pump. (A5) **Establish a Continuous (video) Plankton Recorder survey** for the Indian Ocean to measure zooplankton community composition variability and change (Chapter 16).

B. **Key processes of the near-surface ocean, including diurnal mixed layer and barrier layer variability, need to be better measured** to meet the need for improved subseasonal to seasonal forecasting and surface flux products (Chapters 9, 10). In particular, these measurements will refine our understanding of the MJO and MISO and their influence on monsoon rainfall and hydro-climate (Chapters 13, 14, 15), while direct measures of surface fluxes are needed to validate bulk algorithmic estimates (Chapter 2, 10, 14).

(B1) **A new RAMA flux reference site between Australia and Indonesia** in the outflow of the ITF (14°S, 115°E), where tropical SST and rainfall intraseasonal variability are highest. (B2) **Direct flux measurements and increased vertical resolution of temperature and salinity (T/S) sensors** (0.5 m, 1 m, 2 m, 3 m, 5 m, 7 m, 10 m, and every 5 m down to 50 m) at RAMA flux reference sites on the equator and in the Arabian Sea, Bay of Bengal, and SCTR.

C. **The IndOOS must be expanded into shelf/slope regions, with an emphasis on the subtropics**, where swift boundary currents and their fluxes dominate basin-wide heat, freshwater, and nutrient budgets (Chapters 11, 21, 23, 25) and where coastal upwelling systems influence primary productivity, air-sea fluxes, and climate variability (Chapters 9, 18, 19, 20). In particular, key climate modes in the subtropics, such as Subtropical Dipole and Ningaloo Niño (Chapters 12, 19), as well as the gyre and overturning cell which carry and store anthropogenic heat and other properties (Chapters 23, 25), need to be constrained with boundary flux measurements.

(C1) **Re-establish an Agulhas Current volume, heat, and freshwater transport array** at the western boundary near 34°S, colocated with altimeter ground track and including an “end-point” mooring to measure basin-wide geostrophic overturning down to 2000 m. Measure full-depth T/S, oxygen, and core nutrients during maintenance cruises and, ideally, combine with periodic glider surveys to capture small scale flows over the shelf and slope. (C2) **Enhance the Leeuwin Current array** to measure full-depth volume, heat, and freshwater fluxes through combined mooring and glider observations at the eastern boundary, including an“end-point” mooring down to 2000 m to measure basin-wide geostrophic overturning when paired with the Agulhas Current “end-point” mooring. (C3) Monitor T/S fluxes, dissolved oxygen, and core nutrients with **gliders or autonomous underwater vehicles in the Sumatra-Java upwelling region and South Java Current**, the eastern pole of the IOD. (C4) Monitor T/S fluxes, dissolved oxygen, and core nutrients with **gliders or AUVs along the west coast of India** where monsoon currents, upwelling, and the Arabian Sea oxygen minimum zone intersect and societal implications are greatest.

D. We recommend that the IndOOS be expanded into the deep ocean below 2000 m. Here circulation and thermohaline changes affect sea level change and decadal-to-multidecadal variability. Coupled climate models and their projections rely on ocean data assimilation products that remain almost entirely unconstrained in the deep ocean (Chapters 11, 21, 25).

(D1) A suite of **Deep-Argo floats**, with priority in the southern subtropical Indian Ocean where deep heat content change is largest.

Tier III: Pilot projects to investigate efficacy, sustainability, and potential for integration into the IndOOS.

In some cases, where observing technology needs further advancement, where scientific understanding is too limited to yet design effective monitoring programs, or where the efficacy or

feasibility of additional measurements is uncertain, initial pilot studies are needed.

A. A pilot study within the **Somali Current and upwelling system** in the western Arabian Sea. Potentially a surface flux buoy (with turbulence measurements) and/or wave glider, biogeochemical-Argo deployments with specialized missions, such as shallower profiling and higher temporal sampling, and/or glider sections. This study should include a capacity development component (Chapters 17, 18).

B. A pilot project to **double the number of Argo profiles in the tropics** in order to capture upper-ocean, intra-seasonal variability of MJO and MISO. The number of Argo floats could be enhanced or floats programmed for shallower, higher frequency profiling while within 10° of the equator (Chapter 1).

C. A pilot study of **air-sea interaction and carbon uptake in the southeast subtropical Indian Ocean** subduction zone, potentially utilizing new sensor technologies.

D. **Continued exploration of the Indian Ocean with new autonomous and expendable platforms and new sensor technologies** that may improve or revolutionize the IndOOS in the future, including directional wave spectra drifters (with SST and GPS sensors), χ-SOLO floats (turbulence), X-Spar floats, Saildrones, Wave Gliders, and Minimets (Chapter 8).

Applications: Validation and Improvement of Data Products, Models, and Predictions

In addition to actionable recommendations for the observing system, this review has highlighted a number of other priorities for the Indian Ocean community that involve **data-mining, analyses, and collaborations towards the validation and improvement of the products, models, and predictions** that derive from the IndOOS. These include:

A. Find and digitize historic sea level data.

B. Analyze existing observations to determine the locations of largest productivity variability and prioritize these locations for biogeochemical observations.

C. Compare *in situ* chlorophyll and productivity observations to collocated satellite ocean color to quantify the accuracy of satellite algorithms and develop regionally tuned algorithms, if necessary.

D. Engage with the atmospheric reanalysis community to help evaluate and guide future improvement of tropical convective parameterizations.

E. Speed development of coupled ocean-atmosphere data assimilation techniques.

F. Improve capabilities for reanalysis, prediction, and observing system evaluation through stronger collaborations among data assimilators, modelers, and observationalists.

G. Develop collaborations with the paleo-proxy community to provide long records of surface temperature variability in the IOD eastern pole and of sea level variability near the west coast of Australia, in the Chagos archipelago, and Mascarene Islands.

Table of Contents

Executive Summary I

Table of Contents i

Introduction 1

1 Argo Profiling Floats 9

2 RAMA-2.0 14

3 XBT Network 22

4 Surface Drifter Observations 27

5 Tide Gauges 31

6 Past, Present, and Future Satellite Missions 35

7 The Global Ocean Ship-Based Hydrographic Investigations Program (GO-SHIP) 39

8 New Technologies for *In Situ* Measurements 44

9 Operational Subseasonal-to-Seasonal (S2S) Forecasting 49

10 Improvement of Surface Fluxes 53

11 Ocean Data Assimilation Systems 58

12 Extreme Events 63

13 Intra-seasonal Air-sea Coupling: Madden-Julian Oscillation and Monsoon Intra-seasonal Oscillation 68

14 South-Asian Monsoons: Upper-ocean Processes that Influence the Monsoon Annual Cycle 73

15 Regional Hydroclimate 78

16 Ocean Primary Productivity: Variability and Change 83

17 Boundary Currents and Exchanges with Other Basins 89

18 Upwelling, Coastal-open Ocean Interactions, and Ecosystems 95

19 Interannual Variability and Predictability 99

20 Oxygen Variability and Change, Oxygen Minimum Zones **103**

21 Regional Sea-level Variability and Change **108**

22 Decadal Variability and Predictability **113**

23 Heat Content and its Major Flux Components **118**

24 Carbon Cycle, Acidification, and Ecological Impacts **122**

25 Anthropogenic Climate Change **128**

Synthesis **135**

Acknowledgements **146**

References **147**

Appendix A: List of Acronyms **197**

Appendix B: List of Contributors **204**

Introduction

Jérôme Vialard, Lisa M. Beal, and Mathew K. Roxy

The Review Process Behind this Roadmap

In 2016, the Ocean Observations Panel for Climate (OOPC), an expert panel of GOOS who provide advice on scientific requirements to JCOMM (the Joint WMO-IOC Technical Commission for Oceanography and Marine Meteorology), tasked the CLIVAR/IOC-GOOS Indian Ocean Region Panel (IORP) to perform an evaluation of the Indian Ocean Observing System (IndOOS) and make recommendations for a fit-for-purpose IndOOS moving forward. The IORP has led this task in collaboration with the IMBeR/IOGOOS SIBER panel (Sustained Indian Ocean Biogeochemistry and Ecosystem Research), recognizing from the outset the potential and importance of integrating biogeochemistry measurements into the IndOOS over the upcoming decade. The entire review effort, including three international workshops, sixty authors, and an expert review panel of six, has been sponsored by WCRP, IOGOOS, IOC-UNESCO, US NOAA, and IUGG. A full list of the acronyms used throughout this document can be found in Appendix A.

The first IndOOS decadal review workshop took place in February 2017 in Perth, Australia, alongside the IORP, SIBER, IOGOOS, and IRF annual meetings, as well as the Second International Indian Ocean Expedition (IIOE-2) steering committee and science meetings. The review talks and discussions of the workshop were open to all these groups. Experts were invited, many from the IORP and SIBER panels, to give broad review talks on the essential science questions and societal needs for Indian Ocean observations and to provide background on the past and present observing components of IndOOS, as well as a look forward to new observing platforms and sensor technologies. Following these talks, breakout groups were tasked to discuss: (1) What scientific and operational outcomes should IndOOS achieve? And (2) How do (can) the components of IndOOS serve these scientific and operational goals?
From these discussions the terms of reference for the IndOOS-2 roadmap were defined as:

- ***Make actionable recommendations for priority observing system components*** *going forward, including pilot studies with new technologies*
- Provide justification for these recommendations by:
    - *Reviewing the current status of IndOOS and its past successes and failures.*
    - *Articulating the scientific and operational drivers of IndOOS and their societal impacts.*
    - *Identifying the essential ocean variables (EOVs) that address these drivers, their geographic coverage and spatio-temporal resolution.*

Twenty-five chapters were outlined, each addressing the above terms of reference with respect to the various observing components (Chapters 1-8), operational drivers (Chapters 9-11), and scientific drivers (Chapters 12-25) of the IndOOS. A full list of contributors can be found in Appendix B.

A first draft of this document was produced in December 2017 and submitted for public comment and for assessment by an expert review board of six jointly appointed by CLIVAR, the OOPC, IO-GOOS, the IOC, and IMBER (for names see Appendix B and Synthesis). The review board provided written feedback, as well as face-to-face comments and discussion with chapter authors at the second IndOOS decadal review workshop held in Jakarta, Indonesia in

March 2018. The workshop was once again organized alongside IORP, SIBER, IOGOOS, IRF and IIOE-2 meetings and open to these groups. All 25 chapters of the roadmap were presented and discussed and the terms of reference were refined as follows:

- *Develop strong statements for the continuation of the Indian Ocean observing system in terms of the important climate questions and climate variables to be measured.*
- *Evaluate the design of the observing system in terms of the identified climate questions and essential ocean variables and provide* ***actionable recommendations*** *for its future evolution.*

A framework for prioritization of the more than one hundred actionable recommendations arising from the review was also defined during the second workshop and is articulated in the Synthesis at the end of this document.

A revised version of this roadmap was produced in February 2019, following major revision of all the chapters, the collation and prioritization of the 136 actionable recommendations therein, and subsequent development of the Executive Summary, Introduction, and Synthesis. These last sections were submitted for final comment from the CLIVAR community and from the expert review board during March and April 2019. The major outcomes of the review were discussed among IORP, SIBER, and other members of the Indian Ocean community at the final IndOOS decadal review workshop in Port Elizabeth, South Africa in March 2019. Presentation of actionable recommendations for the observing system was followed by discussions on how to disseminate and implement them. Publication and dissemination of this document to relevant agencies and stakeholders in the Indian Ocean region followed in December 2019.

Societal Needs for the IndOOS

The Indian Ocean is the smallest of the four major oceanic basins, but close to one third of humankind lives in the 22 countries that border its rim. Many of these countries have developing or emerging economies, which are vulnerable to extreme weather events and to changes in the monsoon cycles, as well as to climate variations and climate change. There is also rapid growth in their blue economies, related to new opportunities to exploit oceanic resources and services (Llewelyn et al., 2016). As a result, societal demands for information about the ocean and its ecosystems, and for the sub-seasonal to seasonal forecasts and climate predictions that depend on such information, are growing in this region, driving the need for sustained and improved observations of the Indian Ocean.

Many Indian Ocean rim countries depend on rain-fed agriculture. In India, for instance, 60% of jobs are in agriculture, which accounts for 20% of GDP, and there is a tight link between grain production and monsoon rainfall (Gadgil and Gadgil, 2006). Indian Ocean sea surface temperatures influence monsoon rains (Ashok et al., 2001, Annamalai et al., 2005; Chapters 14 and 15), as well as flooding in east African countries (Webster et al., 1999) and droughts and wildfires in Indonesia (Abram et al., 2003, D'Arrigo and Wilson 2008) and Australia (Ashok et al., 2003, Ummenhofer et al., 2009a). Recently, the Indian Ocean has been warming faster than any other basin in response to climate change (Chapter 25, Roxy et al., 2015) and, as a result, decreasing rainfall over eastern Africa is predicted to increase the number of undernourished people in this region by 50% by 2030 (Funk et al., 2008).

The Indian Ocean hosts many countries dependent on fisheries and whose fisheries have poor adaptive capacity, including India, Indonesia, Sri Lanka, Pakistan, Thailand, Madagascar, Mozambique, and Tanzania (Allison et al., 2009). Climate change is predicted to induce a

decline of fish catches for most of these nations (Barange et al., 2014). More generally, the intense marine productivity of the northern Indian Ocean is under threat (Chapter 16, Bopp et al., 2013, Roxy et al., 2015). This strong vulnerability arises because of increased thermal stratification due to surface warming and because the monsoon winds, that drive upwelling and support high productivity, are changing. Moreover, the Arabian Sea hosts one of the largest zones of subsurface oxygen-depleted waters in the world ocean and it is expanding (Chapter 20). Oxygen-depleted waters are predicted to reach the surface more frequently, causing an increasing number of fish mortality events (Naqvi et al., 2009).

Population density around the Indian Ocean rim is projected to become the largest in the world by 2030, with 340 million people exposed to coastal hazards (Neumann et al., 2015). This rapid population growth will conflate with climate change induced sea level rise (Han et al., 2010) and with higher tropical cyclone intensity to increase vulnerability (Elsner et al., 2008; Rajeevan et al., 2013). Already, the Bay of Bengal region witnesses more than 80% of the total fatalities due to tropical cyclones (Chapter 12), while only accounting for 5% of these storms globally (Paul, 2009).

Beyond its direct impact on rim countries, the Indian Ocean influences climate globally. As a whole, the basin accounts for about one fifth of the global oceanic uptake of anthropogenic CO_2 (Chapter 24; Takahashi et al., 2002), helping to buffer the effects of global warming. It is the breeding ground for the Madden Julian Oscillation (Chapter 13), an atmospheric phenomenon that modulates rainfall and tropical cyclone activity across most of the tropics worldwide (Zhang et al., 2005). Year-to-year temperature variations associated with intrinsic Indian Ocean climate variability (Chapter 19) influence the evolution of the El Niño Southern Oscillation in the neighboring Pacific Ocean (Clarke and Van Gorder, 2003; Luo et al., 2010; Izumo et al., 2010), the leading mode of year-to-year climate variability globally. The Indian Ocean is also a tropical-subtropical gateway from the Pacific to the Atlantic, as part of the global oceanic "conveyor belt" (Chapters 17 and 23; Broecker et al., 1991) that drives climate variability at multidecadal and longer timescales. A redistribution of heat from the Pacific to the Indian Ocean over the last decade is thought to have played a key-role in regulating global mean surface temperatures (Tokinaga and Xie, 2012; Liu et al., 2016), with rapid warming of the Indian Ocean representing about one third of global ocean heat gain since 1990 (Chapters 21, 22 and 23; Lee et al., 2015; Nieves et al., 2015). The longer term Indian Ocean surface warming trend induced by climate change is also having far-reaching impacts (Chapter 25), modulating Pacific (Luo et al., 2012, Han et al., 2014, Hamlingon et al., 2014) and North Atlantic climate (e.g., Hoerling et al., 2004) and causing droughts in the West Sahel and Mediterranean (Giannini et al., 2003; Hoerling et al., 2012).

The role of the Indian Ocean in regional and global climate variability and change and the vulnerability of its rim populations articulate the need to better observe, understand and model this ocean, with the ultimate goal of being able to serve societal demand for quantitative predictions of future weather and climate.

Scientific Drivers and New Frontiers for the IndOOS

Scientific interest in the Indian Ocean is not new and was initially fostered by its unique features. One of these is its geography. A low-latitude throughflow from the Pacific via the Indonesian Seas (Gordon et al., 2010) and the Asian landmass to the north (Figure 0.1) bring about unusual features, such as the reversing monsoon currents, upwelling along the western boundary off Somalia and Oman, a shallow cross-equatorial overturning cell, the semiannual equatorial Wyrtki jets, and the uniquely poleward Leeuwin Current at the eastern boundary in the subtrop-

ics (Schott et al., 2001).

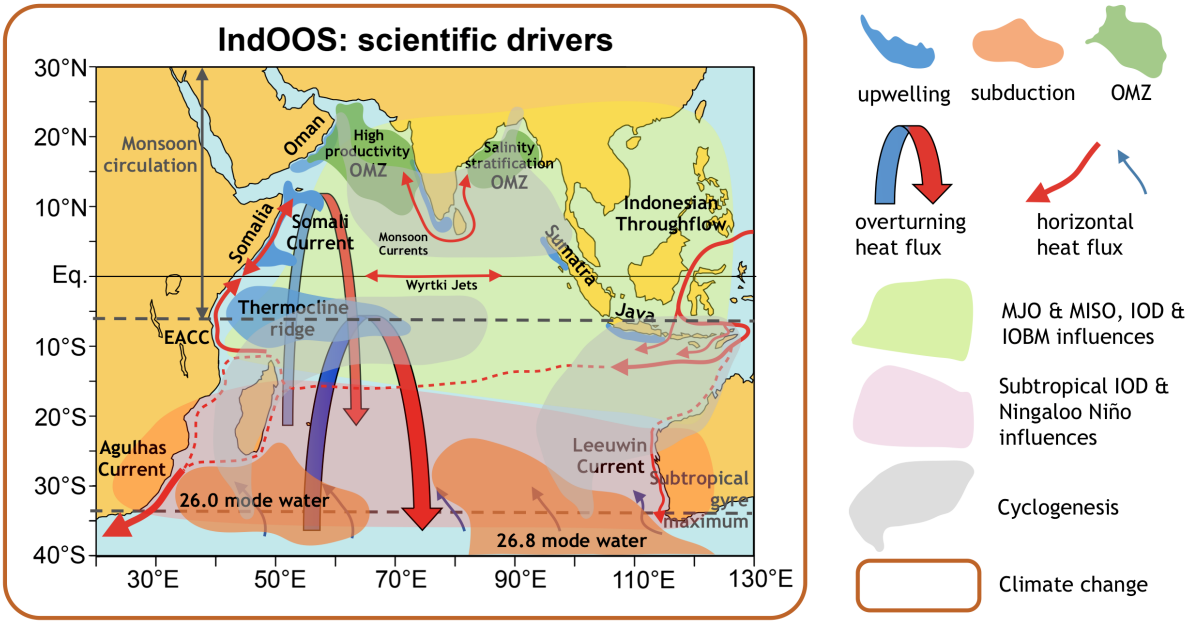

Figure 0.1 The main scientific drivers of the Indian Ocean Observing System, including the Oxygen Minimum Zones (OMZs), upwelling and subduction zones, major heat flux components, the tropical modes of the Madden-Julian Oscillation (MJO), the Monsoon Intra-Seasonal Oscillation (MISO), the Indian Ocean Dipole (IOD) and Indian Ocean Basin Mode (IOBM), the subtropical modes of Ningaloo Niño and subtropical IOD, cyclogenesis, and climate change.

Cut off from cold northern latitudes by the Asian landmass, the Indian Ocean receives excess heat from the atmosphere as well as an influx of heat from the Pacific via the Indonesian throughflow. This excess heat is largely exported at the open southern boundary (Chapters 17, 23). Within the Indian Ocean heat is transported southward across the equator by the upper branches of the tropical and subtropical overturning cells (Schott et al., 2002), which are linked to off-equatorial upwelling zones and to subduction in the subtropics (Figure 0.1). The Indian Ocean heat budget affects basin-wide climate, as well as patterns of sea surface temperature and sea surface height across the basin; however its variability is poorly understood. It is thought to be strongly constrained by the Agulhas Current at the western boundary (Chapters 17 & 23, Bryden and Beal, 2001) and by the Indonesian Throughflow (Sprintall et al., 2014), with recent evidence that the poleward Leeuwin Current, although small, may play a significant role at interannual time scales (Zhang et al., 2018).

The presence of the Asian landmass induces a complete reversal of the winds across the northern Indian Ocean: the northeast and southwest monsoons (Schott et al., 2001). These winds drive a complex reversal of the Indian Ocean circulation north of 10°S (Figure 0.1), including the Somali Current at the western boundary and the semi-annual Wyrtki jets along the equator that carry heat eastward during the inter-monsoon periods. Many of these oceanic processes are not well reproduced by state-of-the-art climate models, adversely impacting predictability of the monsoons (Annamalai et al., 2016, Chapter 14). The strong southwest monsoon winds yield unique upwelling at the western boundary of the Arabian Sea (Figure 0.1, Chapter 18), modulating evaporation and moisture transport towards India (Chapters 14, 15, Izumo et al., 2008), providing a globally significant source of atmospheric CO_2 (Chapter 24), and fostering intense oceanic productivity (Chapter 16). High productivity, together with low ventilation, leads to a subsurface depletion of oxygen (Chapter 20), and this oxygen minimum zone is now expanding and has already led to a dramatic shift in the Arabian Sea ecosystem (Gomes et al., 2014). In

the Bay of Bengal, saline stratification creates a very different environment, with excess freshwater input from monsoon rain and river runoff strongly inhibiting the vertical mixing of both heat and nutrients. This salinity-related "barrier layer" is thought to regulate regional monsoon rainfall (Shenoi et al., 2002), oceanic productivity (Prasanna Kumar et al., 2002), wet/dry spells of the monsoon (Chapter 13), and cyclogenesis (Chapter 12, Sengupta et al., 2008, Neetu et al., 2019).

While the powerful ENSO climate mode focused the attention of the international climate community during the 1980s, the last two decades have witnessed rising awareness of the importance of coupled climate variations in the Indian Ocean (Schott et al., 2009). The tropical Indian ocean has a large warm pool (surface temperature $>$ 27.5°C), common to the neighboring Pacific, that maintains atmospheric convection (Graham and Barnett, 1987) and energizes the largest global atmospheric circulation cell, the Walker circulation. The Indian Ocean warm pool is coupled at the 30-90 day timescale with the Madden-Julian Oscillation (MJO) in boreal winter and with the monsoon intraseasonal oscillation (MISO) in summer (Figure 0.1, Chapter 13), each influencing rainfall and cyclogenesis regionally. If simulated correctly, the influence of oceanic processes on these coupled modes could yield enhanced seasonal climate predictability throughout the tropics (De Mott et al., 2015; Chapter 9). The southwestern tropical Indian Ocean, around 5-10°S, is also strongly coupled with the atmosphere. The tropical gyre brings cool thermocline water close to the surface in the Seychelles-Chagos thermocline ridge (Figure 0.1) so that sea surface temperatures are highly sensitive to atmospheric anomalies and can feedback on cyclogenesis and MJO development (Vialard et al., 2009a).

At interannual time scales the tropical Indian ocean is strongly influenced by ENSO, warming uniformly during El Niño events (Chapter 19) and remaining warm through the following spring (Xie et al., 2009), a response known as the Indian Ocean Basin Mode (IOBM). The Indian Ocean also has interannual climate modes of its own, such as the Indian Ocean Dipole (IOD, Saji et al., 1999; Webster et al., 1999, Chapter 19). In its positive phase, cold surface temperatures near Java-Sumatra (Figure 0.1), warm temperatures in the western tropical Indian Ocean thermocline ridge, and anomalous easterly winds near the equator induce various impacts like droughts in Indonesia and Australia and floods over eastern Africa (Yamagata et al., 2004). The IOD develops through the Bjerknes feedback, similar to ENSO (Saji et al., 1999; Webster et al., 1999), with equatorial wave processes playing a central role in its evolution (Nagura and McPhaden, 2010; McPhaden et al., 2015), and often co-occurs with ENSO (Yamagata et al., 2004). The Indian Ocean also hosts interannual climate modes in the subtropics (Chapter 19). Subtropical Indian Ocean Dipole events are large-scale sea surface temperature anomalies that have a strong influence on South African rainfall (Reason, 2001). Ningaloo Niño events are marine heatwaves off western Australia, which can affect fisheries and lead to increased Australian rainfall. In 2011 a strong Ningaloo Niño (Chapter 12) caused the first recorded bleaching of the pristine Ningaloo reef (Feng et al., 2013). Some Ningaloo Niño events may be predictable due to their association with ENSO (Doi et al., 2016).

Of all these science drivers, the urgent need for sustained and enhanced observations of the Indian Ocean is perhaps most potently demonstrated by its enormous intake of heat over the last decade, accounting for no less than 30% of the global oceanic heat gain (Chapters 21, 22, 23; Lee et al., 2015; Vialard et al., 2015; Nieves et al., 2015; Liu et al., 2016). Will the Indian Ocean continue to warm more rapidly than the rest of the world ocean? What effects will this have on the Walker circulation? On upwelling, ecosystems, and fisheries? On the monsoon wet/dry spells (MISOs)? On carbon uptake and vertical mixing? On cyclone activity and storm surges? On regional sea level rise? When and where will the excess heat be released back to the atmosphere? Will it accelerate future global warming? Answering these questions and de-

veloping skilful predictions requires carefully designed oceanic measurements sustained over many decades.

There are few multi-decadal observational records in the Indian Ocean and this is a serious problem when it comes to distinguishing climate change trends from patterns of natural variability (Carson et al., 2015). The longest records are sea level from the Fremantle tide gauge at the Australian west coast, and upper ocean transport of the Indonesian Throughflow from the IX01 XBT line (Figure 0.1). These datasets suggest that decadal variations in the Throughflow (Wainwright et al., 2008) and Leeuwin Current (Feng et al., 2004) since the 1980's are linked to Indian Ocean heat content and to Pacific Ocean decadal variability. Aside from these records, the relative paucity of observations prior to the advent of the IndOOS ten years ago means little is known about multi-decadal variability in the Indian Ocean in comparison with our understanding of the Pacific Decadal Oscillation and North Atlantic Oscillation (Han et al., 2014; Chapter 22). Even less is known about the changing biogeochemistry of the Indian Ocean (Chapters 16, 20, 24).

There is no doubt that the Indian Ocean, as other basins, is responding to anthropogenic climate change, with evidence of increasing surface temperatures and heat content, rising sea level, increased carbon uptake, and an intensified water cycle (Chapter 25, IPCC 2013). The biogeochemical consequences of these changes are serious, with warming, acidification, and an expansion of oxygen minimum zones all putting increasing stress on marine ecosystems (Bopp et al., 2013). Understanding regional patterns of change within the Indian Ocean (Han et al., 2010), attributing them to either natural variability or anthropogenic forcing, and being able to project them into future decades is an ongoing challenge. Only a well-planned and internationally-supported Indian Ocean Observing System can provide the necessary observations.

IndOOS Components and Achievements

The IndOOS is currently comprised of five *in situ* observing networks (Figure 0.2): Profiling floats (Argo, Chapter 1), a moored tropical array (RAMA, Chapter 2), repeat lines of temperature profiles (XBT network, Chapter 3), surface drifters (GDP, Chapter 4), and tide gauges (Chapter 5). Augmenting these networks are remotely-sensed observations, in particular of surface winds, sea level, SST and salinity, rainfall, and ocean color (Chapter 6), as well as decadal surveys of a wide range of full-depth water properties (nutrients, CFCs etc) via the GO-SHIP program (Chapter 7).

The Argo network is global, with a target of one autonomous profiler per 3° x 3° region, each profiling the ocean every ten days to measure temperature, salinity, and pressure down to 2000 m, and lasting about 3 years (Chapter 1, Gould et al., 2004). Full coverage of the Indian Ocean north of 40°S requires about 450 floats and was first achieved in 2008. There are currently 576 active floats providing over 20,000 profiles per year. Argo data have captured the seasonal-to-interannual variability of the subtropical circulation and thermohaline structure in the Indian Ocean for the first time and were instrumental in tracking the enormous oceanic heat uptake - 30% of the global uptake since 1990 - during the "hiatus" decade (Chapters 1, 21 to 23). Argo has become a primary data source for operational oceanography and for validating and initializing numerical models of the ocean and climate (Chapters 9, 11). A growing number of profilers (currently 48) are equipped with biogeochemical sensors to measure key processes related to plankton blooms, OMZs, and fisheries, to name a few, particularly in the Arabian Sea, and Bay of Bengal regions.

The Research Moored Array for African-Asian-Australian Monsoon Analysis and Prediction

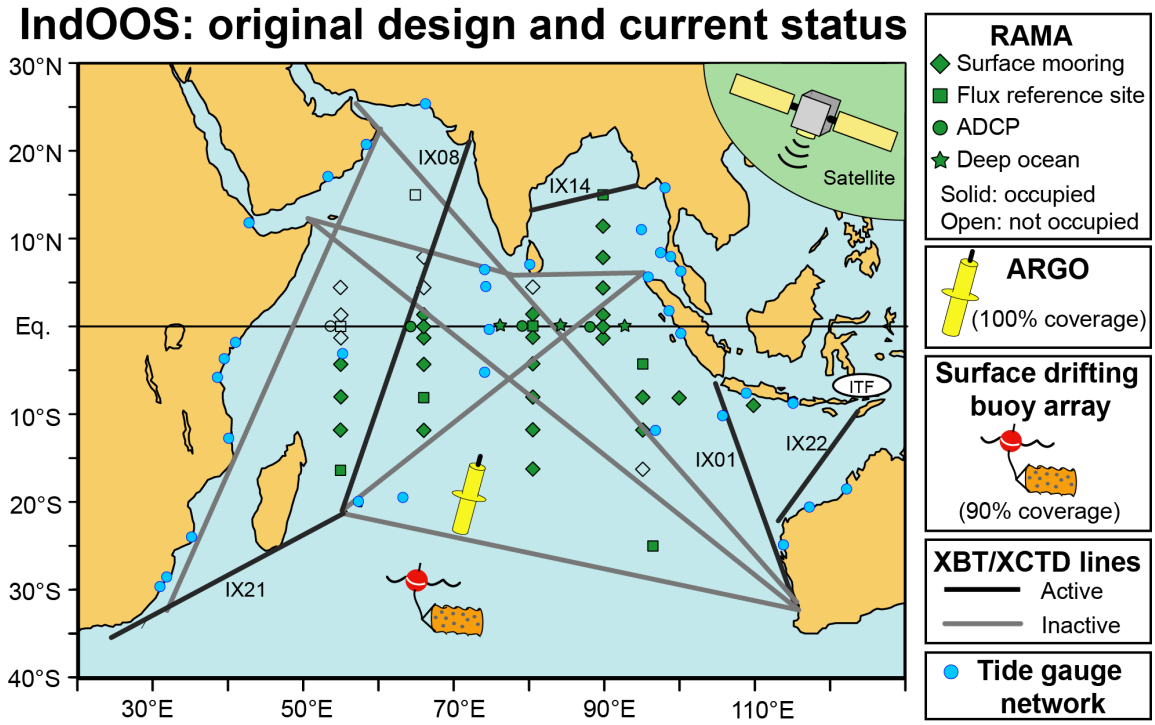

Figure 0.2 Status of the IndOOS in 2018. The original IndOOS design comprises the Argo (Chapter 1), RAMA (Chapter 2), XBT/XCTD (Chapter 3), surface drifting buoy (Chapter 4) and tide gauge (Chapter 5) networks. It is supported by satellite observations (Chapter 6) and the GO-SHIP program (Chapter 7). The empty symbols indicate RAMA sites that were not implemented due to logistical constraints (see Chapter 2 for details).

(RAMA, Chapter 2, McPhaden et al., 2009) was arguably the observing network that launched IndOOS. It followed the implementation of tropical arrays in the Pacific and Atlantic Oceans, which together comprise the Global Tropical Moored Buoy Array (McPhaden et al., 2010). RAMA provides sub-daily time series of key oceanographic and surface meteorological variables in real-time (https://www.pmel.noaa.gov/gtmba/) in a region where the oceanic response to atmospheric forcing is rapid and coupled feedbacks are critical. All RAMA moorings measure meteorological surface parameters and oceanic temperature and salinity down to 500 m. Some also make direct measurements of velocity, while others are “flux reference sites” with additional measurements for computation of air-sea momentum, heat, and freshwater fluxes (Chapter 10). A very few sites have biogeochemical sensors (Chapter 24). RAMA data have enabled the study of tropical modes of variability in the Indian Ocean, such as the MJO, MISO, and IOD, as well as the equatorial circulation and some biophysical interactions. RAMA data feed important operational applications, such as numerical weather and seasonal forecasts, gridded continuous estimates of air-sea fluxes, ocean re-analyses, and inter-calibration of successive satellite missions (Chapters 2, 9, 10, 11).

The voluntary observing ship eXpendable Bathy Thermograph (XBT) network collects temperature observations over the upper $\sim$1 km of the ocean along regular commercial shipping routes. Prior to the advent of Argo, XBTs provided more than 50% of all subsurface temperature observations (Chapter 3). The XBT network remains important for monitoring phenomena poorly sampled by Argo, such as boundary currents and oceanic fronts, mesoscale variability, and volume and heat transports. For instance, the IX01 XBT line between Indonesia and Australia is critical for quantifying the interannual-to-decadal variability of the Indonesian throughflow (Meyer et al., 1995; Sprintall et al., 2002; Wijffels et al., 2008; Wainwright et al., 2008) and was

able to capture its strengthening trend during 1984-2013 (Liu et al., 2015).

The Global Drifter program (GDP, Chapter 4) consists of surface drifters drogued to follow ocean currents at 15 m, at a nominal density of one drifter per 5° x 5° region. All drifters also measure temperature and about half now measure sea level pressure, which has been shown to significantly improve numerical weather prediction in other basins (Centurioni et al., 2016). Coverage in the Indian Ocean has been about 70% since 1996 and about 90% since 2014. Surface drifters have allowed the seasonal mapping of the reversing monsoon circulation in the Arabian Sea (Beal et al., 2013).

The tide-gauge network around the Indian Ocean rim (Chapter 5) provides measurements of sea-level which are needed for Tsunami warnings, the monitoring and prediction of tides, the study of cyclone-induced storm surges (Chapter 12), and for the understanding of basin-scale variations and trends in sea level rise (Chapters 21, 22, 25). Tide gauges can also provide proxies for dynamical changes, such as coastally-trapped waves with Pacific origins along the west coast of Australia (Chapter 17). Only a subset of tide gauges also monitor land motion, a necessary condition for a precise quantification of long term trends in sea level.

The observing networks that make up IndOOS are most effective in combination, and when used alongside data from, in particular the global satellite missions (Chapter 6). For example, Vialard et al., (2008) used a combination of RAMA, Argo, and satellite data to study air-sea interactions associated with the Madden-Julian Oscillation. Satellite data are the only source of basin-scale, high frequency measurements. Satellite measurements of SST, sea surface height (from which surface currents can be derived), ocean color (that can be used as a proxy for chlorophyll concentration), Sea Surface Salinity (SSS), significant wave height, and ocean mass provide key measurements of the state of the Indian Ocean. Atmospheric variables such as surface wind and wind stress, surface shortwave radiation, precipitation and outgoing long-wave radiation are also extremely important to characterize forcing on the ocean, coupled climate processes, and air-sea fluxes.

GO-SHIP is an internationally-coordinated program of multi-disciplinary, trans-basin hydrographic surveys which are repeated decadally (Chapter 7). GO-SHIP collects a wide variety of measurements unobtainable through automated means, including physical, geochemical and trace properties of seawater to full ocean depth that can be used to constrain ocean circulation and water mass changes to long time scales. Given the magnitude of decadal and multidecadal climate variability and change in the Indian Ocean, and the dearth of geochemical measurements, GO-SHIP is an increasingly important component of the IndOOS.

Looking forward, innovative instrumentation and platform technologies are likely to transform the IndOOS in the future (Chapter 8). Some of these technologies, such as gliders, are well-established research tools with immediate potential for IndOOS pilot programs in difficult-to-measure regions, such as upwelling zones and currents close to the boundaries.

In the following 25 chapters the current status of the these IndOOS components are reviewed, including past successes and failures (Chapters 1 - 8), the demands that operational products and forecasts place on the IndOOS is assessed (Chapters 9, 10, 11), and the oceanic and climatic phenomena that the observing system must capture are articulated (Chapters 12 - 25). Each chapter also identifies a set of essential ocean variables (EOVs) that must be observed and a list of Actionable Recommendations for adjustments and enhancements to the observing system that will provide much-needed improvements to the scientific outcomes, operational products, and societal benefits of the IndOOS over the next decade.

1. Argo Profiling Floats

Muthalagu Ravichandran[1,2], T V S Udaya Bhaskar[2], and Nicholas J. Hardman-Mountford[3]

[1]National Centre for Polar and Ocean Research (NCPOR), Goa, India, [2]Indian National Centre for Ocean Information Services (INCOIS), Hyderabad, India, [3]Oceans and Natural Resources Directorate, Commonwealth Secretariat, London, UK

Argo is a global array of profiling floats that measure temperature and salinity over the upper 2000 m of the Ocean every 10 days. Here we present the status of Argo floats in the Indian Ocean and their applications, both operational and scientific. We also recommend future directions for Argo, like development of an array of floats with biogeochemical sensors (BGC-Argo) to measure and understand biogeochemical processes, increasing the number of floats in the equatorial Indian Ocean to better capture intraseasonal-to-interannual variability, and implementation of a Deep-Argo array to map heat and mass below 2000 m.

1.1 Introduction

Ocean and climate have a symbiotic connection through the complex processes of heat and mass transfer. To understand climate there is a need for enhancing ocean predictability through a well-designed and sustained operational ocean observing system. In an internationally coordinated effort, a goal was established to deploy a global array of 3000 profiling floats to map the heat and mass of the global ocean and the Argo program was realized.

The Argo program is an important component of the Global Ocean Observing System (GOOS), designed to measure temperature and salinity (T/S) of the upper 2000 m of the ice-free ocean (Riser et al., 2016). T/S are essential ocean and climate variables (EOVs and ECVs) of GOOS and the Global Climate Observing System (GCOS). Once deployed, Argo floats descend to a parking depth of 1000 m, drift at that depth for nearly 10 days and then descend to a profiling depth of 2000 m before acquiring T/S data while ascending to the surface. At the surface, data are transmitted to via satellite for real-time availability. Iridium has replaced ARGOS for communication, providing much higher data transmission rates and allowing higher vertical sampling resolution and two-way communication.

The National Argo Data Assembly Centers make data available to the global community on the global telecommunication system within 24 hours of collection for operational forecasts. Quality-controlled data sets are made available by the Regional Argo Data Centers within 6 months. The regional Argo Data Center for the Indian Ocean is maintained at INCOIS (http://www.incois.gov.in/argo/ARDCenter.jsp) and provides a range of derived Argo products, such as objectively analyzed gridded data, status of floats, yearly float deployments and profiles, age of floats, etc. Global data sets are available from (http://www.coriolis.eu.org/Observing-the-Ocean/ARGO). Many operational centers (http://www.argo.ucsd.edu) use Argo data to provide real time ocean analysis.

1.2 Present status of Argo floats in the Indian Ocean

To meet the global Argo design density of one float per 3° x 3°, the Indian Ocean requires 450 floats north of 40°S. In 2017 there were 576 active floats (Figure 1.1a) with 48 of these BGC-Argo floats, which measure dissolved oxygen (DO), chlorophyll fluorescence, backscattering of light by particles, light attenuation, and in some cases nitrate concentration and pH. Deployment

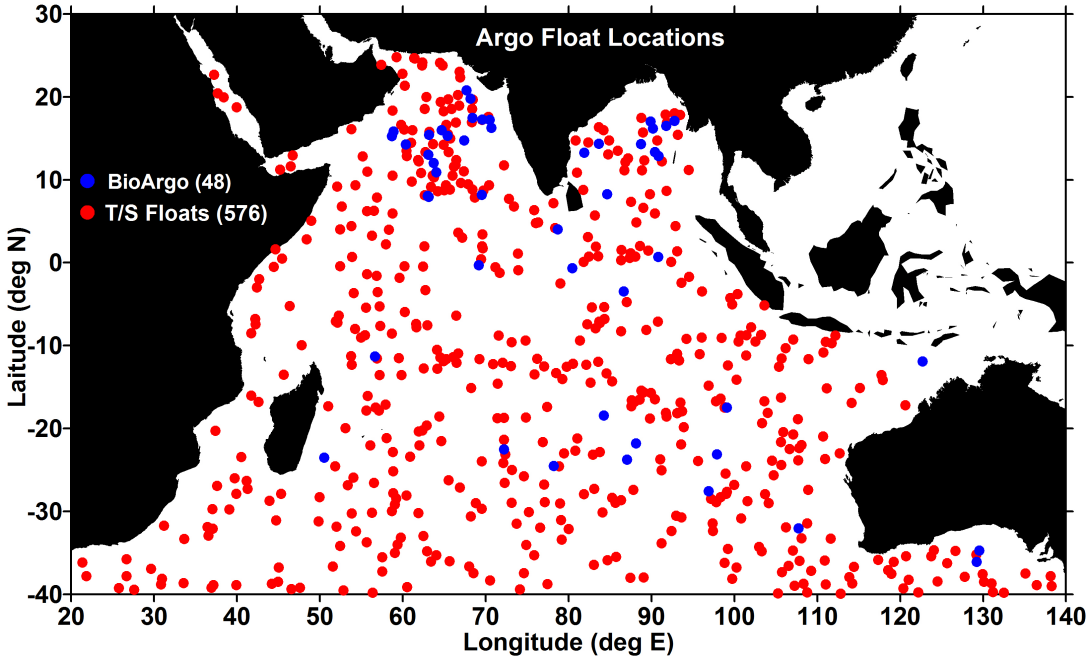

(a)

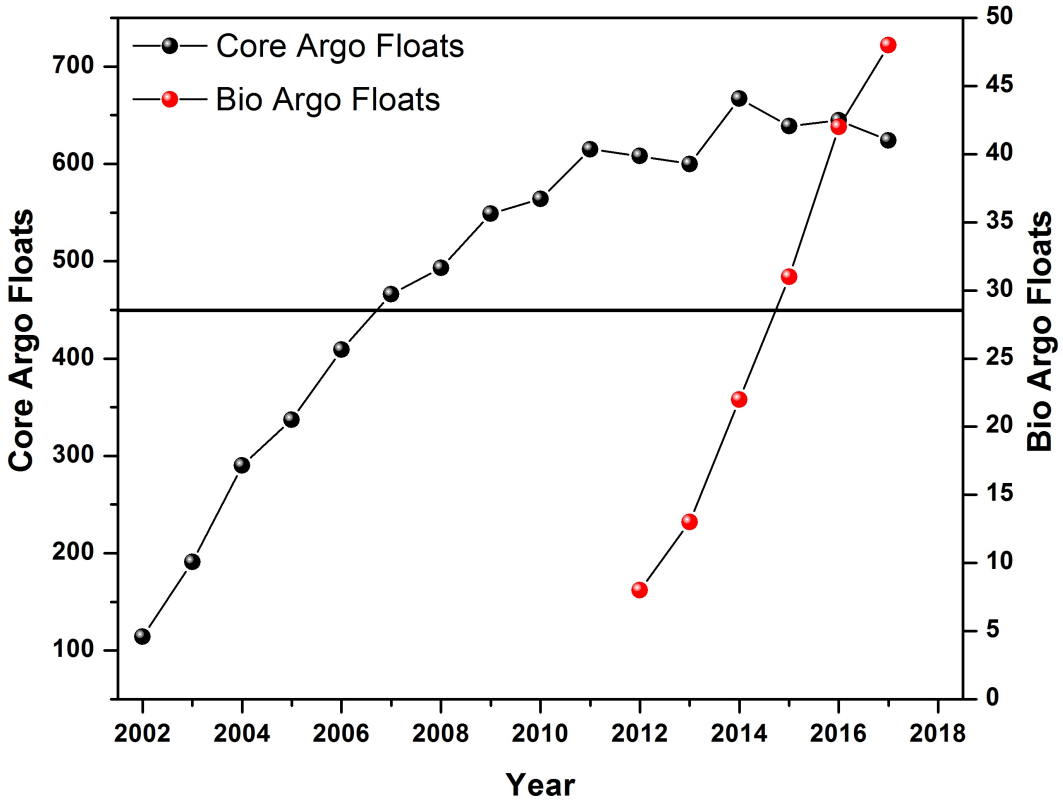

(b)

Figure 1.1 (a) Number of Argo profiling floats in the Indian Ocean as of 2017. Red dots are core Argo floats, measuring temperature and salinity. Blue dots are BGC-Argo floats. (b) Growth of active Argo floats in the Indian Ocean. Horizontal line is the design density, indicating full coverage. Note different axes for core and BGC-Argo floats.

of Argo floats with oxygen sensors began in 2006 and with biogeochemical sensors in 2012. Although the target number of Argo floats is achieved in the Indian ocean, there are persistent gaps in the central Indian Ocean, northern Bay of Bengal, and Andaman Sea. Most of the Bay

of Bengal floats are configured for 5-day profiling, to better capture intraseasonal variations.

The Argo program commenced in 1999 and the build-up of floats in the Indian Ocean began in 2001. Full coverage in the Indian Ocean was achieved in 2008 (Figure 1.1b) and the number has increased to more than 600 floats since that time. Australia, China, France, Germany, India, Japan, Korea, U.K, South Africa, and the U.S have contributed to the growth of Argo in the Indian Ocean, through both ship time and instruments. The Argo Information Center and Regional Argo data center coordinate ships of opportunity to deploy floats in the Indian Ocean. Deployment in the Arabian Sea was initially hindered due to piracy. There are less opportunities to deploy floats in the southern Indian ocean. RAMA cruises provide opportunities for Argo deployments, a synergistic interaction in the implementation of these two IndOOS programs.

1.3 Argo applications

Data from the Argo program, together with satellite remote sensing and other *in situ* observations, are enhancing our understanding of ocean circulation and its influence on global climate variability. Argo has revealed the local balances of evaporation minus precipitation in the salinity structure of the upper ocean (Durack et al., 2012, Helm et al., 2010, Hosoda et al., 2009), as well as longer term changes in subsurface water masses brought about by climate change (Zhang et al., 2008, Downes et al., 2009).

Many operational centers are assimilating Argo data for seasonal predictions of the monsoon, El Niño, and the Indian Ocean Dipole mode (Oke and Schiller, 2007, Agarwal et al., 2008, Krishnamurti et al., 2007, Huang et al., 2008, Reddy et al., 2017). Though Argo observations are primarily intended to study seasonal-to-climate scale phenomena, the data are also used for other areas of research, such as cyclones and intra-seasonal variability. For instance, assimilation of Argo data revealed that subsurface ocean temperatures carry signatures of the passage of intraseasonal waves (Krishnamurti et.al, 2007). On the technology front, Riser et al., (2008) demonstrated float-based three hourly measurements of wind speed and rainfall in the Bay of Bengal and Ravichandran et al., (2012) demonstrated the importance of BGC-Argo floats deployed in the Arabian Sea. A full publication list is available at http://www.argo.ucsd.edu/Bibliography.html.

1.4 Future directions

It is imperative to enhance observations in the Indian Ocean to improve the spatio-temporal resolution and deep coverage of data, as well as to increase the number of BGC-Argo floats to capture missing ecosystem and climate links.

Deep Ocean Argo: The current Argo array provides T/S of the upper ocean down to 2000 m, which is half of the mean ocean depth. Observations of the deep ocean are needed to constrain the ocean's role in Earth's energy budget, to understand the deep ocean circulation and its variability, and to study transient climate sensitivity. Signals below 2000 m significantly contribute to both heat content and sea level variability and change (Zilberman et al., 2017). Deep Argo floats profile down to 4000 or 6000 m, and several countries have conducted pilot studies to demonstrate the technical capability of such floats and the scientific value of the data. More efforts are needed to deploy deep Argo in the Indian Ocean to observe the thermohaline changes below 2000 m. The global deep Argo design density is one float per 5° x 5°, at least 250 floats north of 40° S in the Indian Ocean. In the near future at least one float should be deployed in the Arabian Sea, Bay of Bengal, eastern equatorial Indian Ocean, western equato-

rial Indian Ocean, and thermocline ridge region, plus at least four in the southern Indian Ocean.

Enhancement of BGC-Argo: BGC-Argo is an extension of the standard Argo array to include biogeochemical sensors. Measures of dissolved oxygen can be used to understand marine photosynthesis and respiration, and exchange with the atmosphere. Chlorophyll a from fluorescence is a proxy for phytoplankton biomass. Nitrate can provide an understanding of new production. Backscatter can be used as a proxy for particulate organic carbon. Acidity (pH) provides important constraints on net photosynthesis and respiration, as well as the long-term trend associated with increasing atmospheric carbon dioxide. Additionally, colored dissolved organic matter (CDOM) and downwelling irradiance can be inferred and measured using a radiometer. These parameters can be used to understand carbon uptake, oxygen minimum zones, nitrate cycling, ocean acidification, the biological carbon pump, and primary productivity(biogeochemical-argo.org).

The few BGC-Argo floats deployed in the Indian Ocean thus far have already provided many new insights, such as oxycline depth in the Arabian Sea OMZ (Prakash et al., 2012), chlorophyll distributions in eddies (Dufois et al., 2017), and chlorophyll variability in the southeastern Arabian Sea (Ravichandran et al., 2012). A Global BGC-Argo group are calling for a design density of 1000 floats globally, that is at least 200 in the Indian Ocean. Until now the Australia-India joint Indian Ocean Bio-Argo project have achieved 48 active floats with sensors to measure oxygen, chlorophyll, and particle backscattering at 700 nm. It is imperative to increase the number of BGC-Argo floats and their capabilities.

Enhancement of equatorial floats: With enhanced spatial resolution from additional Argo floats in the equatorial Pacific, Gasparin et al., (2015) find that Argo is able to represent around 70–80% of the variance at intraseasonal time scales and more than 90% of the variance for the seasonal to long term variability in the Pacific Ocean. The higher spatial resolution of the Argo array compared with the moored array makes it better suited for capturing spatial patterns of variability and propagation on intraseasonal and longer periods.

From the above study, it is clear that IndOOS can also benefit by deploying double the number of floats - or by doubling the profiling frequency of the floats - within a few degrees of the equator (10°S to 10°N), to better capture the MJO and MISO.

1.5 EOVs

Argo floats measure the EOVs of temperature and salinity over the upper 2000 m of the ocean. Data from these floats have revolutionized our understanding of ocean circulation and oceanic heat content and their variability. With advancement of sensor technology and the proven stability of the float platform, biogeochemical EOVs are being added to Argo floats. Measures such as oxygen, nutrients, chlorophyll, backscatter, pH, and CDOM are essential to the study of primary productivity, carbon uptake, and ecosystem change.

1.6 Actionable recommendations

A. Maintain core Argo of at least 450 floats north of 45°S.

B. Double the number of floats/profiles in the equatorial Indian Ocean in order to capture intraseasonal to interannual variabilities of MJO and MISO.

C. Deploy more BGC-Argo floats to address carbon uptake, OMZs, nitrate cycling, acidification, the biological carbon pump, and phytoplankton communities.

D. Deploy deep Argo floats to map circulation, heat and salt content below 2000 m.

E. Conduct Observing System Experiments (OSEs) and Observing System Simulation Experiments (OSSEs) to evaluate the required spatio-temporal resolutions of the array in light of developing scientific and societal need.

2. RAMA-2.0

Michael J. McPhaden[1], Muthalagu Ravichandran[2,3], Ken Ando[4], Weidong Yu[5], and Eric Schulz[6]

[1]NOAA/Pacific Marine Environmental Laboratory (PMEL), Seattle, WA, [2]Indian National Center for Ocean Information Service (INCOIS), Hyderabad, India, [3]National Centre for Polar and Ocean Research (NCPOR), Goa, India, [4]Japan Agency for Marine-Earth Science and Technology (JAMSTEC), Yokosuka, Japan, [5]School of Atmospheric Sciences, Sun Yat-Sen University, Zhuhai, China, [6]Bureau of Meteorology (BOM), Melbourne, Australia

2.1 Introduction

RAMA—The Research Moored Array for African-Asian-Australian Monsoon Analysis and Prediction—was originally designed by the CLIVAR/GOOS Indian Ocean Region Panel (IORP) to address fundamental questions related to the ocean's role in monsoon dynamics. RAMA was established in 2004 as the moored buoy component of the IndOOS (Masumoto et al., 2010). It is the Indian Ocean complement to the TAO/TRITON array in the Pacific and the PIRATA array in the Atlantic Ocean, which together comprise the Global Tropical Moored Buoy Array Program (McPhaden et al., 2010). Surface moorings provide high-resolution time series in real-time for studies of ocean-atmosphere interactions and ocean dynamics. They are especially valuable in the tropics where there is a broad spectrum of energetic variations in both the ocean and the atmosphere and where the oceanic response to atmospheric forcing is rapid. Moorings can also serve as platforms for a host of other sensors, including for marine biogeochemistry, ecosystem dynamics, and biodiversity.

There are four types of moorings in RAMA (Figure 2.1). These are (1) functionally equivalent ATLAS, m-TRITON and Bailong moorings, (2) more heavily instrumented Flux Reference Sites for comprehensive air-sea flux determination, (3) Acoustic Doppler current profiler (ADCP) sites for direct measurement of velocity in the upper ocean, and (4) Deep Ocean sites along the equator equipped with current meters at selected depths down to 4000 m. The EOVs that these moorings measure are summarized in Table 2.1 and given in full detail in McPhaden et al., (2009). All the surface moorings transmit data in real-time to shore for use in weather, ocean, and climate forecasting. Quality controlled data are available in delayed mode via the World Wide Web from PMEL (USA), JAMSTEC (Japan), and INCOIS (India) as well as from World Data Centers.

The ships that service RAMA have collected a variety of measurements that contribute to the ocean and climate data record. These include underway measurements from hull-mounted ADCP and surface thermosalinograph, Conductivity-Temperature-Depth (CTD) stations that allow water sampling in support of biogeochemical research, marine meteorological measurements and atmospheric radiosonde launches, and deployment of Argo floats, surface drifters, and expendable bathythermographs (XBTs). Moored arrays are thus a vital element in a network of satellite and *in situ* platforms that deliver essential ocean variables and essential climate variables (ECVs) as part of the Global Ocean Observing System (GOOS) and the Global Climate Observing System (GCOS).

Table 2.1 Essential Ocean Variables (EOVs) Measured by RAMA moorings

	SST	T(z)	SSS	S(z)	U(10m)	U(z)	Wind Stress	Surface Heat Flux
Flux Ref. Site	X	X	X	X	X#		X‡	X*
Surface Mooring	X	X	X	X	X		X‡	X**
ADCP	X	X	X	X	X	X†		
Deep Ocean		X		X	X	X@		

Table 2.1 EOVs measured by RAMA moorings. In addition to these EOVs some RAMA moorings measure biogeochemical parameters such as pCO_2 and pH at 15°N, 90°E. Notes: #Flux reference sites may have additional point current meters in the upper 40 m. †Acoustic Doppler Current Profiler (ADCP) moorings have an upward looking ADCP mounted at 250-400 m depth. @Deep Ocean sites have point current meters mounted at several depths over 4000 m and later deployments include an upward-looking ADCP mounted nominally at 100 m depth. ‡Supporting variables needed to compute wind stress from bulk formulae are measured: Near surface humidity and air temperature, sea surface temperature, vector wind, near surface current and, on flux reference sites, air pressure. *On all surface moorings, supporting variables needed to compute surface turbulent fluxes are measured: SST, wind speed, near surface air temperature and humidity, and surface current. On all surface moorings, downwelling shortwave radiation is also measured. **In addition to the meteorological measurements made on surface moorings, flux reference site moorings measure surface air pressure and downwelling longwave radiation. Note that Deep Ocean sites will be discontinued in RAMA-2.0.

RAMA has enabled many scientific advances since inception and is a valuable source of data for ocean, weather, and climate forecasting. An open data policy and easy access to data (https://www.pmel.noaa.gov/gtmba/) have facilitated collaborations across national boundaries. Some of these collaborations have been interdisciplinary in nature, involving studies of biogeochemistry and biophysical interactions unique to the Indian Ocean (Strutton et al., 2015; Sutton et al., 2014). The original RAMA publication (McPhaden et al., 2009) has been cited nearly 300 times as of August 2019 and an extensive and growing bibliography of RAMA-related refereed journal publications further attests to the array's success (https://www.pmel.noaa.gov/gtmba/rama-journal-publications).

New partnerships have been formed between institutions within and outside the Indian Ocean region to build RAMA and to promote joint research efforts. Specific examples include high level agreements between NOAA and the Indian Ministry of Earth Sciences (MoES) and between NOAA and the Indonesian Agency for Meteorology, Climatology and Geophysics (BMKG). To implement the array, RAMA partners have conducted 88 cruises on 22 different ships from 11 different nations, using 2116 days of ship time to deploy and recover 342 moorings in the 15 years since September 2004.

From the very beginning stages of RAMA design and implementation, capacity development efforts have been undertaken to strengthen scientific and technical capabilities in Indian Ocean rim nations so that they can more fully participate in building the observing system as well

as reap the scientific and societal benefits from it. Approximately twenty capacity development workshops focused on IndOOS and RAMA have taken place across the basin since the early 2000s. These include NOAA-sponsored training conferences held annually since 2006 in Indonesia that attract participation from multiple US research institutions and workshops sponsored by JCOMM's Data Buoy Cooperation Panel (DBCP) Task Team for Capacity Building to provide training on the implementation of ocean observations and their applications for societal benefit. There have also been several exchange visits between RAMA partner institutions for transfer of technical information and standardization of best practices (e.g., Freitag et al., 2016).

Next we summarize the current status of RAMA and the challenges involved in sustaining it. Based on the past decade or so of experience, we propose adjustments that will result in a more robust and cost-effective array that meets scientific and societal need. We also describe opportunities to enhance the array to improve understanding of physical oceanographic and climate variability, marine biogeochemistry, and ecosystem dynamics. Finally, a protocol is suggested for establishing new sites in the array.

2.2 Current Implementation Challenges

The original RAMA design (Figure 2.1) consists of 46 moorings (McPhaden et al., 2009). In August 2018 the array was 85% complete, thanks to the efforts of many institutions in countries committed to advancing Indian Ocean science: India, Indonesia, Japan, China, the United States, Australia, the 13 African nations that comprise the Agulhas and Somali Current Large Marine Ecosystem program and the 8 Asian countries that comprise the Bay of Bengal Large Marine Ecosystem.

There are a variety of challenges to fully implementing RAMA. Piracy has long prevented the establishment of planned sites in the Arabian Sea. Fortunately, through naval interventions of many nations and the introduction of best practices for ship operations, piracy has now been essentially eradicated in the Arabian Sea. In December 2015 Lloyds of London significantly reduced the so-called piracy "high risk area" and in June 2018, the NOAA Ship Ronald H. Brown ventured into the Arabian Sea to occupy three new RAMA sites. Thus, we are cautiously optimistic that piracy will no longer stand in the way of completing and sustaining the array.

Another significant challenge is ship time. Surface moorings have a design lifetime of one year and require servicing from specialized vessels capable of deep sea mooring operations. Securing adequate ship time is an ongoing challenge. Over the period 2014-16 for example, only 94 sea days per year were available to service sites maintained with PMEL equipment, well short of the estimated 145 sea days that were needed. Several sites, including two flux reference sites at 25°S, 100°E and 16°S, 55°E (Table 2.2), have not been serviced in the past 3-5 years because of this lack of ship time (McPhaden et al., 2016).

A third significant challenge is fishing vandalism. Some RAMA sites, though regularly maintained, have poor data return because equipment is damaged or lost due to fishing interference. The most extreme example of vandalism is the mooring at 1.5°N, 80.5°E where data return has been only $\sim$50% over the past 12 years and less than half of the 11 moorings deployed there have been recovered. This site is relatively close to land, which is a major factor in the prevalence of fishing damage. The site at 4°N, 80.5°E is even closer to land, within the Sri Lankan Exclusive Economic Zone (EEZ), and has never been occupied (Figure 2.1, left). The severity of damage from fishing vandalism farther south now convinces us that this site is not viable. Vandalism has also increased at 1.5°N, 90°E and 1.5°S, 95°E, possibly due to an increase in purse seine fishing, for which gear conflict leads to more severe mooring damage than does

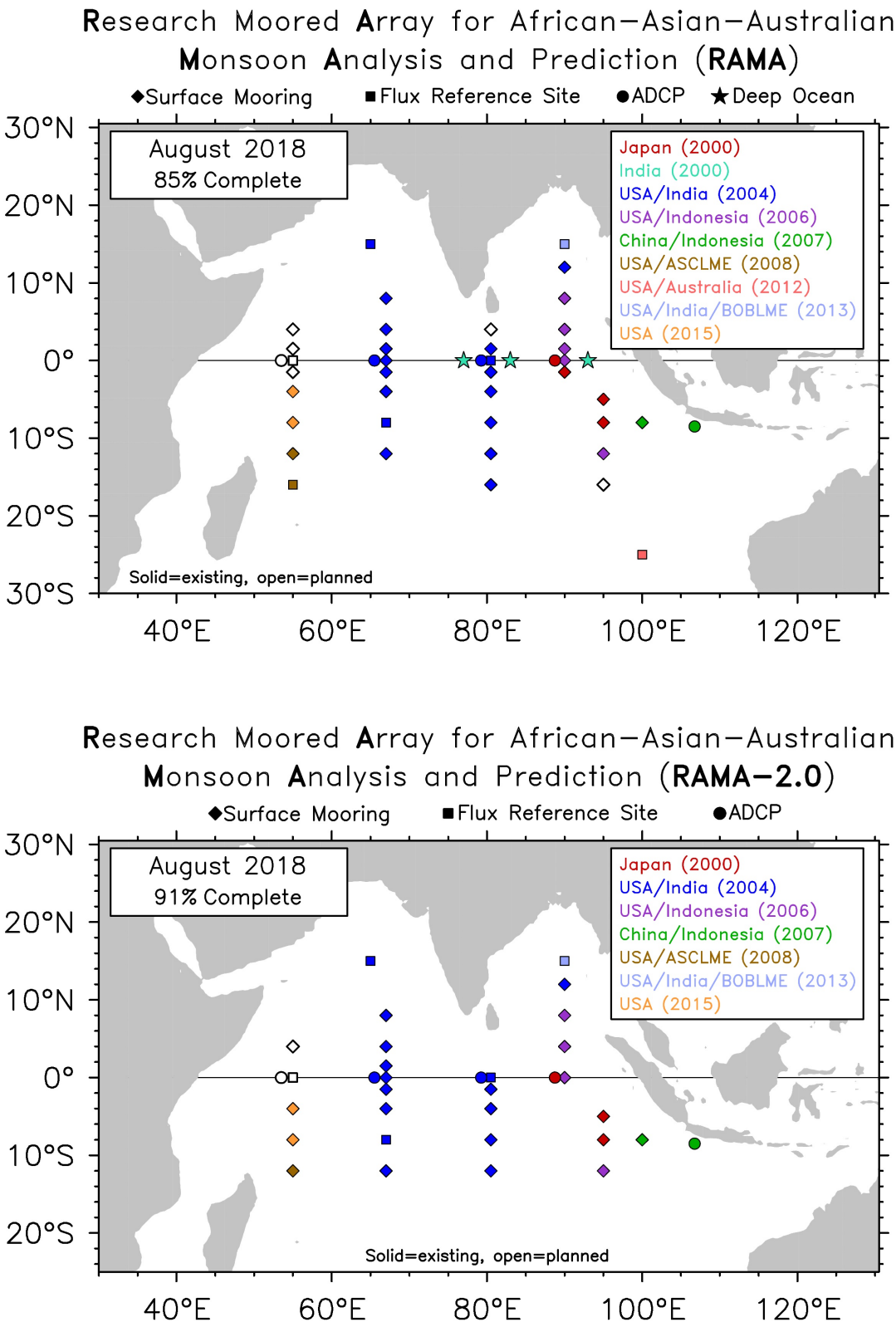

Figure 2.1 Top: Original design of RAMA. Sponsoring nations/programs are color coded by site with the first year of engagement shown in parentheses. Bottom: Proposed configuration for RAMA-2.0.

long line fishing.

Some mooring sites have been terminated because of programmatic changes. For instance, maintenance of the deep-sea mooring at 0°, 93°E by India's National Institute of Oceanography ended in late 2014 and the NIO equatorial deep ocean moorings at 77°E and 83°E were recovered in November/December 2016. No future deployments are planned at these locations.

Budgetary issues are also a concern for RAMA. PMEL's annual operating budgets have been flat for many years, translating to decreased funding with respect to inflation. JAMSTEC has faced a 5% annual budget cut for all activities recently, creating shortfalls for ship operations, buoy equipment acquisition, and other critical functions. At the same time, costs for PMEL moorings have increased. The new T-Flex mooring system is more expensive than the old ATLAS system because it uses commercially available off-the-shelf components. T-Flex is more capable, more vandal-resistant, and will provide much higher data throughput and reduced data loss by using Iridium. JAMSTEC has also redesigned m-TRITON to be more vandal-resistant, with stronger wire and a tower to protect meteorological sensors.

2.3 A Sustainable Mooring Array

Given budgetary pressures, ship time limitations, fishing vandalism, and the reality that some sites are already decommissioned, we propose a reduced RAMA design that still meets most of the original scientific objectives (McPhaden et al., 2009). RAMA-2.0 is optimized for long-term viability and sustainability and contains 33 rather than 46 sites (Figure 2.1). Table 2.1 lists those sites to be decommissioned and the primary reasoning, above and beyond aggregate budgetary constraints.

Even with fewer moorings, key regions such as the equatorial waveguide, the Seychelles-Chagos Thermocline Ridge, Bay of Bengal, Arabian Sea, and the eastern and western poles of the Indian Ocean Dipole are well sampled. This modified design, embedded in the full multi-platform IndOOS, allows a concentration of effort on maintaining sites that have produced good data, are logistically accessible, and still meet most of the original objectives of RAMA. With fewer moorings in RAMA-2.0 the total ship time requirement is lowered to an estimated 160 days per year and the transition from PMEL's legacy ATLAS system to the new more capable T-Flex mooring system can be accelerated.

Table 2.2 RAMA sites to be decommissioned and the primary reason

SITE	REASON
1.5°N, 90°E	Vandalism
1.5°S, 90°E	Vandalism
16°S, 95°E	Ship Time
25°S, 100°E	Ship Time
4°N, 80.5°E	Vandalism
1.5°N, 80.5°E	Vandalism
16°S, 80.5°E	Ship Time
0°, 77°E	Program Termination
0°, 83°E	Program Termination
0°, 93°E	Program Termination
1.5°N, 55°E	Ship Time
1.5°S, 55°E	Ship Time
16°S, 55°E	Ship Time

2.4 Potential New Measurements

RAMA moorings can be platforms for a wide variety of additional sensors that fulfil IndOOS requirements, or for specialized studies. There is a history of such enhancements in TAO/TRITON and PIRATA going back more than 20 years. The primary requirements for adding new instrumentation are that sensor payloads be compatible with the mooring design and that there are sponsors to purchase and integrate sensors into the mooring system and to process and disseminate the new data streams.

It is straightforward to add more temperature/conductivity sensors and current meters to increase vertical resolution in and below the surface mixed layer. For example, compared to the standard suite of six T/C sensors in RAMA (McPhaden et al., 2009), Flux Reference Site moorings are equipped with 2-3 more T/C sensors in the upper 140 m and have downwelling longwave radiation and atmospheric pressure sensors on the surface buoy to complement the standard suite of meteorological sensors (wind velocity, air temperature, relative humidity, rain, short wave radiation). These additional sensors help advance understanding of processes affecting transfers of momentum, heat, and fresh water across the air-sea interface. Likewise 41 ocean turbulence sensors have been deployed on RAMA moorings since 2011, with support from Oregon State University (Pujiana et al., 2018; Pujiana and McPhaden, 2018), to measure vertical mixing and its effects on the evolution of the Madden-Julian Oscillation and on Monsoon Intra-Seasonal Oscillations. Similarly, for the past several years PMEL and FIO have deployed Ocean Tracking Network sound receivers on all RAMA moorings supplied by Dalhousie University to support marine ecosystem and biodiversity studies. There is an opportunity to add atmospheric pressure measurements, valuable for monitoring and predicting tropical cyclones, at sites in the southern hemisphere, Bay of Bengal, and Arabian Sea.

Automated biogeochemical measurements are also possible at RAMA moorings. A 6-month long deployment of a near surface fluorometer in 2010 at 0°, 80.5°E (Strutton et al., 2015) revealed intraseasonal phytoplankton blooms along the equator in an otherwise biological desert. Since 2013 a Moored Autonomous pCO_2 ($MAPCO_2$) system deployed on the RAMA mooring at 15°N, 90°E has provided surface pCO_2 and pH measurements to estimate air-sea carbon dioxide fluxes and acidification. There is opportunity to deploy dissolved O_2 sensors in the oxygen minimum zones of the Arabian Sea and Bay of Bengal. These sensors have been deployed for several years in the OMZ of the North Atlantic on PIRATA moorings, with some on T-Flex moorings that transmit their O_2 data in real-time from 300-500 m below the surface (Bourles et al., 2019).

There is a clear need for expanded biogeochemical measurements to address many of the societal drivers of the IndOOS (Chapters 16, 18, 20, 24). The Sustained Indian Ocean Biogeochemistry and Ecosystem Research community (SIBER, Hood et al., 2012) and the Second International Indian Ocean Expedition (IIOE-2, Hood et al., 2015) science plans identify RAMA Flux Reference sites as platforms for future sustained biogeochemical time series measurements using automated sensors. It is a matter now of identifying the necessary resources to support instrument procurement, data acquisition, and scientific analysis.

2.5 Potential New Sites

In addition to abandoning sites that are unsustainable or enhancing sites with additional sensors to meet broader IndOOS objectives, there are compelling reasons to add new sites to RAMA-2.0. One addition that has been discussed over the past few years is a Flux Reference Site in the Timor Sea (14°S, 115°E) where intraseasonal SST variability associated with the

MJO is largest and where air-sea interactions affect tropical storm formation and rainfall across southern and eastern Australia. The Timor Sea is a heavily fished region however, so feasibility of maintaining a surface mooring in the region needs to be demonstrated.

In June 2018, the Secretary of MoES announced that data collected outside the EEZ of India from its Ocean Moored buoy Network in the northern Indian ocean (OMNI) would henceforth be freely and openly available. As a result, NOAA and MoES are undertaking an effort to more closely coordinate RAMA and OMNI in terms of data quality standards, sampling strategies, data display and dissemination, and field work. This coordinated activity will enhance the scientific impact of RAMA and OMNI while at the same time improving operational efficiencies of both.

To accommodate evolving scientific priorities and new opportunities like that presented by OMNI, we propose a protocol for RAMA expansions following that devised by the Tropical Moored Buoy Implementation Panel (TIP), an Action Group of the Data Buoy Cooperation Panel, and successfully adopted by PIRATA (Bourles et al., 2008). Parties interested in establishing a new site or sites will formulate a proposal defining the scientific objectives and how they are consistent with the mission of RAMA, how the sites would be funded, and how they would be maintained, specifically with regard to ship time. These proposals will be submitted to the CLIVAR/IOC-GOOS Indian Ocean Region Panel (IORP) for review and approval. Approved expansions, if they have no prior record of success, will be given a three-year pilot phase to demonstrate feasibility, namely that the site can be maintained, not suffer grievously from fishing vandalism, produce good data, and stimulate new scientific progress. At the end of the three years, the parties will submit a report to the IORP describing outcomes in relation to objectives. The IORP then assesses whether the expansion should become a permanent part of the array. This proposal-driven process ensures a scientifically sound approach to new sites and a constituency committed to finding resources to establish and maintain them.

2.6 Actionable Recommendations

RAMA was established in 2004 through partnerships involving several nations with a commitment to advancing Indian Ocean science and has proven to be a highly successful venture in sustained ocean observing, enabling many new scientific discoveries and contributing to capacity building in the region. However, after 15 years, the array is not yet complete and there is a need for a more cost-effective and sustainable design that preserves its core scientific value, namely RAMA-2.0 (Figure 2.1, bottom panel).

We have highlighted opportunities to enhance RAMA with additional physical and biogeochemical sensors, both as part of the sustained ocean observing system and for short term intensive process studies. We also envision that it may be desirable to add new, appropriately justified sites to RAMA-2.0 in the future and have described a mechanism to accomplish this. In summary, this document provides a basis for how to move forward on a robust and sustainable moored buoy component to IndOOS that addresses ocean, weather, climate, biogeochemistry, and ecosystem research imperatives for the next decade.

Finally, although it has not been possible to maintain the original RAMA site at 25°S, 100°E as part of the sustained observing system for lack of regular and reliable ship time, there has been discussion in the community about the need, nevertheless, to accurately quantify the air-sea heat, moisture and momentum fluxes in the southeastern subtropical Indian Ocean. This is a subduction region where source waters supply the northward flowing branch of the subtropical and cross-equatorial cells (Schott et al., 2009) and where carbon uptake and sequestration

are important for understanding the global carbon balance (Valsala et al., 2012). Thus, it may be appropriate to consider a pilot study in this region to test new technologies for sustainable solutions.

Our specific, actionable recommendations are:

A. RAMA-2.0: Reduce RAMA sites from 46 to 33, based on pragmatics of piracy, vandalism, ship time, and costs.

B. Consider adding a new Flux Reference Site in Timor Sea (14°S, 115°E), region of highest tropical SST variability, beginning with 3-year feasibility assessment.

C. Add O_2 sensors on Arabian Sea and Bay of Bengal moorings to measure OMZs.

D. Add BGC sensors in regions where variability and long term change in primary productivity and biogeochemistry is pronounced.

E. Undertake a pilot project to develop sustainable observations of air-sea interaction and carbon uptake in the subduction zone of the southeast subtropical Indian Ocean.

3. XBT Network

Ming Feng[1], Janet Sprintall[2], and Rebecca Cowley[3]

[1]CSIRO Oceans and Atmosphere, Perth, Western Australia, Australia, [2]Scripps Institution of Oceanography, La Jolla, California, USA, [3]CSIRO Ocean and Atmosphere, Hobart, Tasmania, Australia

3.1 Background

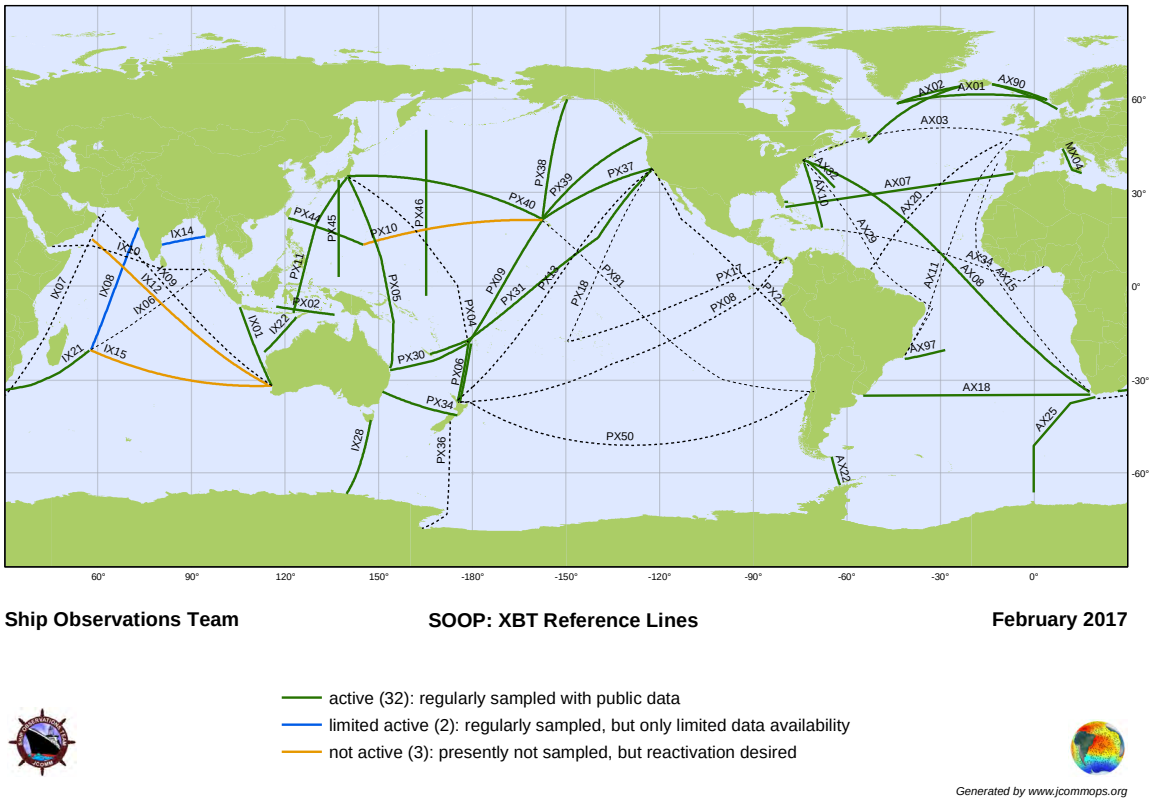

Figure 3.1 Global XBT network. Numbers in brackets refer to global totals.

The eXpendable BathyThermograph (XBT) network consists of transects across the Indian Ocean and marginal seas along which XBTs are deployed to collect temperature profiles over the upper 1 km of the ocean. High Resolution (HR) transects are occupied ∼4 times per year along near-exactly repeating lines, with XBTs deployed every 20 to 30 km to resolve mesoscale eddies and fronts. Frequently Repeated (FR) transects are occupied ∼12 times per year, with deployments every 100 to 150 km in regions where temporal variability is strong. The XBT network is shown in Figure 3.1.

FR IX01 monitors the Indonesian Throughflow (ITF) and the Java/Sumatra upwelling zone and began sampling in 1983. FR IX22 samples through the Banda Sea of Indonesia to the North-west Australian shelf and began sampling in 1987. FR PX02 is a valuable source of real-time data from the internal Indonesian seas and began in 1983. FR IX12 samples the thermocline

ridge in the central Indian Ocean and the Arabian Sea boundary currents and began in 1983. FR IX14 crosses the Bay of Bengal monthly since 1991. Finally, HR IX15 and IX21 together close the southern limit of the subtropical Indian Ocean and began in 1994 (Table 3.1). Many of these XBT transects have been in operation for over 30 years. There have also been some shorter term transects which are no longer a priority (Table 3.1).

XBTs are mainly deployed via the ships of opportunity program (SOOP). XBT lines, combined with Argo floats, are highly effective for quantifying upper ocean heat budgets, where the net transport in or out of the region, along with estimates of interior heat and freshwater storage and surface fluxes, provide a method for understanding the role of ocean dynamics in climate variations (International CLIVAR Project Office, 2006). In particular, XBT transects have proven critical for monitoring changes of the Indonesian Throughflow (ITF), as well as for studies of basin-wide meridional heat transport. XBT transect data have been used for model testing, climate prediction, tropical ocean variability and prediction, and heat content and climate change estimates (Smith et al., 2001). Repeat XBT transects also monitor changes in specific Indian Ocean phenomena that affect climate, such as the upwelling zones of Java, Somalia, and the Lakshadweep Dome, mesoscale variability in the southeast Indian Ocean, and the thermocline ridge near 10°S.

Table 3.1 Summary of status and sampling strategy for XBT transects in the Indian Ocean. FR: frequently repeated; HR: high resolution; LD: low density.

Line	**Status**	**Data years**	**Number of transects per year**	**Operator**
IX01	Active	1983-present	FR and HR, $>$12	Australia
IX06	Ceased	Infrequent	-	USA
IX07	Ceased	Infrequent	-	France
IX08	Data unavailable	Unknown	-	India
IX09	Ceased	1990-1998	LD	-
IX10	Ceased	1990-1998	LD	-
IX12	Inactive	1986-2015	FR and HR, Up to 20	Australia
IX14	Data unavailable	Unknown	-	India
IX15	Inactive	1994-2013	HR, 4	USA
IX21	Active	1994-present	HR, 4	USA
PX11/ IX22	Active	1986-present	FR, Up to 20	Australia
PX02	Active	1983-present	FR	Australia

An implementation plan for the XBT network of the Indian Ocean was originally developed in 2006 (International CLIVAR Project Office) and more recently the network has been prioritized as part of the 2017 JCOMM SOT-9 panel. As of 2017, transects PX02, IX01, IX08, IX14, IX21, and IX22 remain in operation. The vessels that sampled along IX12 went offline in 2015, but

the XBT community is actively seeking a replacement vessel to continue this important time series. Transect IX15 is not currently operable due to a lack of shipping traffic along this route.

XBT profile data from all lines, with the exception of IX08 and IX14 run by Indian agencies, are publicly available through NCEI (https://www.nodc.noaa.gov), as well as in transect mode from IMOS and SIO (imos.org.au; http://www-hrx.ucsd.edu).

3.2 What have we learned from XBT observations?

XBT observations provided more than 50% of the total available data of subsurface thermal structure and variations prior to the arrival of the Argo data stream in 2003. As such, they have enabled quantification of long-term oceanic heat content change under the influence of anthropogenic warming (e.g. Domingues et al., 2008). They have also helped characterize the Indian Ocean response and feedback to the climate change hiatus period in recent decades (Drijfhout et al., 2014; Dong and McPhaden, 2016), as well as decadal variations in the Indian Ocean(Han et al., 2014a; Chapter 22).

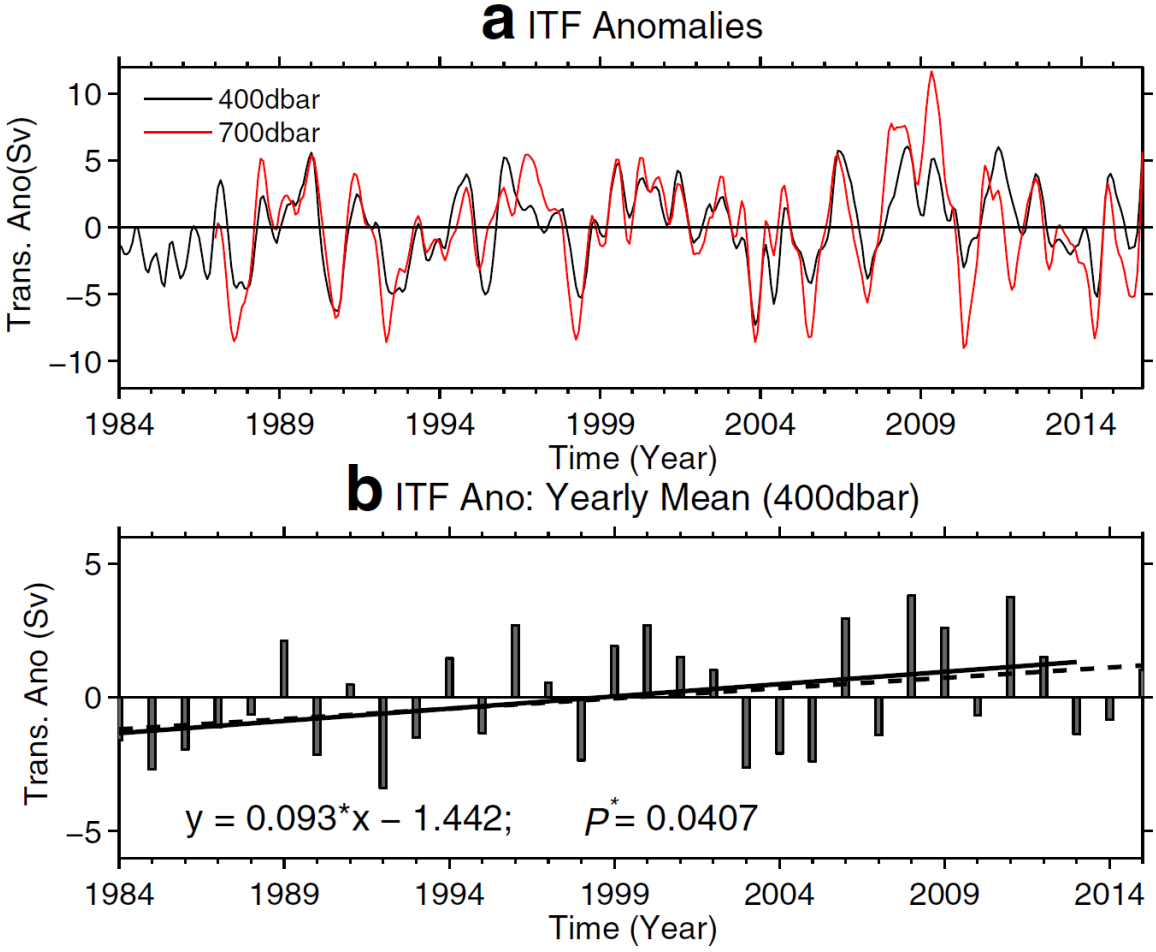

Figure 3.2: a. The ITF transport anomalies estimated by IX01 XBT data. A monthly time series of the ITF transport anomalies estimated by IX01 XBT temperature records and monthly T-S relationship with reference depths of 400 and 700 m from January 1984 to December 2015. b. Annual mean ITF transport anomalies with a reference depth of 400 dbar and their linear trends during 1984-2013 and during 1984-2015 (from Feng et al., 2018, which is updated from Liu et al., 2015). Positive transport anomalies are toward the Indian Ocean.

The XBT network is at present the only element of the Indian Ocean observing system to provide systematically repeating observations that resolve narrow swift boundary currents, including the ITF. Moreover, in the shallow Indonesian Seas, where important signals are carried by the coastal waveguide and the ITF, XBT lines IX01, PX02 and IX22 provide the only real-time profiling data in a region inaccessible to Argo floats. These XBT data are fed into ocean and seasonal weather and regional climate forecasting models and have been used to examine fine-scale mixing critical to water mass transformation within the Indonesian Seas (Ffield and Robertson, 2008). Most importantly, they have been used to quantify the ITF volume and heat transports (Meyer et al., 1995; Sprintall et al., 2002; Wijffels et al., 2008), its interannual and decadal variability (Meyer et al., 1996; Wijffels and Meyers, 2004; McClean et al., 2005; Liu et al., 2015; Feng et al., Chapter 17 of this report; Figure 3.2), and its strengthening trend of up to 1 Sv per decade during the 30-year period from 1984-2013 (Liu et al., 2015; Figure 3.2). As a result, the ITF has been implicated in the large heat transfer from the Pacific to the Indian Ocean over the last decade (Lee et al., 2015, Nieves et al., 2016; Vialard, 2015).

To estimate volume and heat transports across XBT lines, geostrophic velocities are derived by assuming a tight temperature-salinity relationship, obtained using a salinity climatology. However, various studies have shown that interannual-decadal salinity variations are large (Phillips et al., 2005; Feng et al., 2016) and have been shown to influence geostrophic calculations along the IX01 section (Liu et al., 2015). Hence, it is important to monitor upper ocean salinity variability near IX01, potentially through an enhancement of regional Argo coverage, to more accurately capture the transport variability of the ITF in the future.

In the past, the IX01, IX08, and IX12 lines were used to quantify Java-Sumatra upwelling and its interannual variations associated with the Indian Ocean Dipole (Feng and Meyers, 2003), geostrophic transport (Donguy and Meyers, 1995), and Rossby wave propagation in the tropical/subtropical Indian Ocean (Masumoto and Meyers, 1998; Feng and Meyers, 2003). More recently, the IX14 data have revealed interannual variability of the western boundary current in the Bay of Bengal (Sherin et al., 2018) and IX12 data are being used to examine changes in the Arabian Sea boundary current system as part of the U.S. ONR NASCar project. All XBT data are assimilated into numerical models and reanalysis products to constrain interannual and decadal variability in the Indian Ocean (e.g. Good et al., 2013; Zhuang et al., 2013).

The XBT network has excellent synergy with other components of the IndOOS. For instance, combining repeat XBT lines across intense, narrow boundary currents with remotely-sensed altimetry data and with Argo profiles in the interior has proven an effective technique to provide information on the spatial and temporal variability of trans-basin volume and heat fluxes (Zilberman et al., 2018). Such case studies are presently being undertaken for the Somali Current system in the Arabian Sea measured by IX12 and the Agulhas measured by IX21.

3.3 Essential Ocean Variables

XBTs measure the EOV of temperature over the upper 1 km of the ocean. Although the function of the XBT network for broad scale upper ocean heat storage monitoring has been largely superceded by the Argo program, XBTs still provide the only observations in shallow marginal seas and that resolve boundary currents and exchange flows. In particular, XBT lines across the ITF and Agulhas Current are the only long term observations of these major fluxes that are crucial for the Indian Ocean basin scale heat and freshwater balances. Thus, it is important to maintain XBT transect sampling of the Indian Ocean boundary currents (IX21, IX12, IX14, IX08), as well as the Indonesian seas (IX01, IX22, PX02). Salinity measurements near the IX01 section are also a crucial EOV for accurate geostrophic flux estimations.

3.4 Actionable recommendations

In line with XBT community recommendations made as part of the 2017 JCOMM SOT panel, overall, PX02, IX01, IX21, and IX22 are the most critical transects, and salinity measurements along IX01 would be a critical enhancement:

A. Continue $>$30 year record of IX01, IX22, and PX02, providing geostrophic volume and heat transports of the ITF. Better target the 200 m isobaths to improve monitoring of swift currents along the shelf.

B. Enhance Argo deployment density along IX01 to better resolve salinity variability related to the ITF.

C. Maintain the 16-year time series along the High Resolution IX21 line to potentially capture long term changes of the Agulhas Current.

D. Reactivate IX12 to detect long term changes in the tropical thermocline ridge as well as in the boundary current system of the Arabian Sea.

E. Encourage the public release of IX08 and IX14 data, maintained by India.

F. Implement automatic XBT launchers on IX01 as priority and on all Indian Ocean SOOP vessels (Chapter 8), as already used on IX21. Auto-launchers (routinely used in the Pacific and Atlantic) provide higher resolution data and improved data return with minimal crew labour efforts.

G. Installation of hull-mounted ADCPs on SOOP vessels to provide absolute upper ocean heat transport.

4. Surface Drifter Observations

Rick Lumpkin[1] and Luca Centurioni[2]

[1]NOAA/Atlantic Oceanographic and Meteorological Laboratory, Miami, FL, USA, [2]Scripps Institution of Oceanography, La Jolla, CA, USA

4.1 Overview

A satellite-tracked Surface Velocity Program (SVP) drifter (hereafter "drifter") of NOAA's Global Drifter Program (GDP) is a Lagrangian instrument drogued to follow horizontal currents at a depth of 15m with an accuracy better than 1 cms^{-1} per 10 ms^{-1} wind (Niiler et al., 1995, 1987). Many other drifter designs have been exploited for various regional studies and operational purposes (for recent reviews, see Lumpkin et al., 2016 and Centurioni et al., 2018).

Drifters observe several key EOVs, principally surface currents, SST and sea-level atmospheric pressure (SLP). Drifter observations provide the largest quantity of SST observations from the *in-situ* observing system, and are used for satellite SST calibration and validation (e.g. Xu and Ignatov, 2010). While drifters are designed to measure currents at 15 m, their trajectories can also be used to infer windage and upper ocean velocity shear after they have lost their drogues. Approximately half of the drifters also measure surface barometric pressure which has been shown to improve numerical weather prediction (Centurioni et al., 2016, Horányi et al., 2017) and has other applications including inverse-barometer-effect correction of satellite altimetry data and computation of climate indices (Woodruff et al., 2011). This upgrade costs 1200 US dollars per drifter and can be supported by collaboration between the GDP and regional partners via the DBCP Barometer Upgrade Program. Less than 1% of the drifters measure upper-ocean temperature (to a depth of 150m), surface wind velocity, SSS (Centurioni et al., 2018), and/or surface waves (Centurioni et al., 2017).

4.2 History

Overviews of the purpose and history of the GDP are given by Niiler (2001), Lumpkin and Pazos (2007), and Maximenko et al., (2014). Large-scale deployments of GDP drifters in the Indian Ocean (25°E–125°E, 30°N–32°S, excluding the region northeast of Indonesia and Malaysia) started in 1995. Figure 4.1 shows a time series of the number of Indian Ocean drifters since that time, and also of the fraction of 5°×5° bins occupied by at least one drifter (the Global Ocean Observing System requirements, Needler et al., 1999). Since 1996, around 60–80% of the region is sampled; this coverage has increased to 80–95% in the last three years thanks to several research initiatives sponsored by the US Office of Naval Research and to partnerships with RAMA (see Chapter 2).

Molinari et al., (1990) conducted one of the earliest studies of Indian Ocean surface circulation using drifters, mapping the large-scale seasonal changes of the monsoon-driven circulation. Subsequent studies including Michida and Yoritaka (1996), Shennoi et al., (1999), Grodsky et al., (2001), and Beal et al., (2013), have refined these maps and improved our understanding of scientific drivers such as boundary currents and exchanges with other basins (Chapter 17), interannual variability (Chapter 19), and heat and freshwater transport (Chapter 23). In 2015, 36 high-temporal-resolution (5 min) salinity drifters designed by the Lagrangian Drifter Laboratory (LDL) at the Scripps Institution of Oceanography (SIO), were deployed in the Bay of Bengal as a part of the ONR Air-Sea Interactions Regional Initiative (ASIRI) and revealed salinity patches

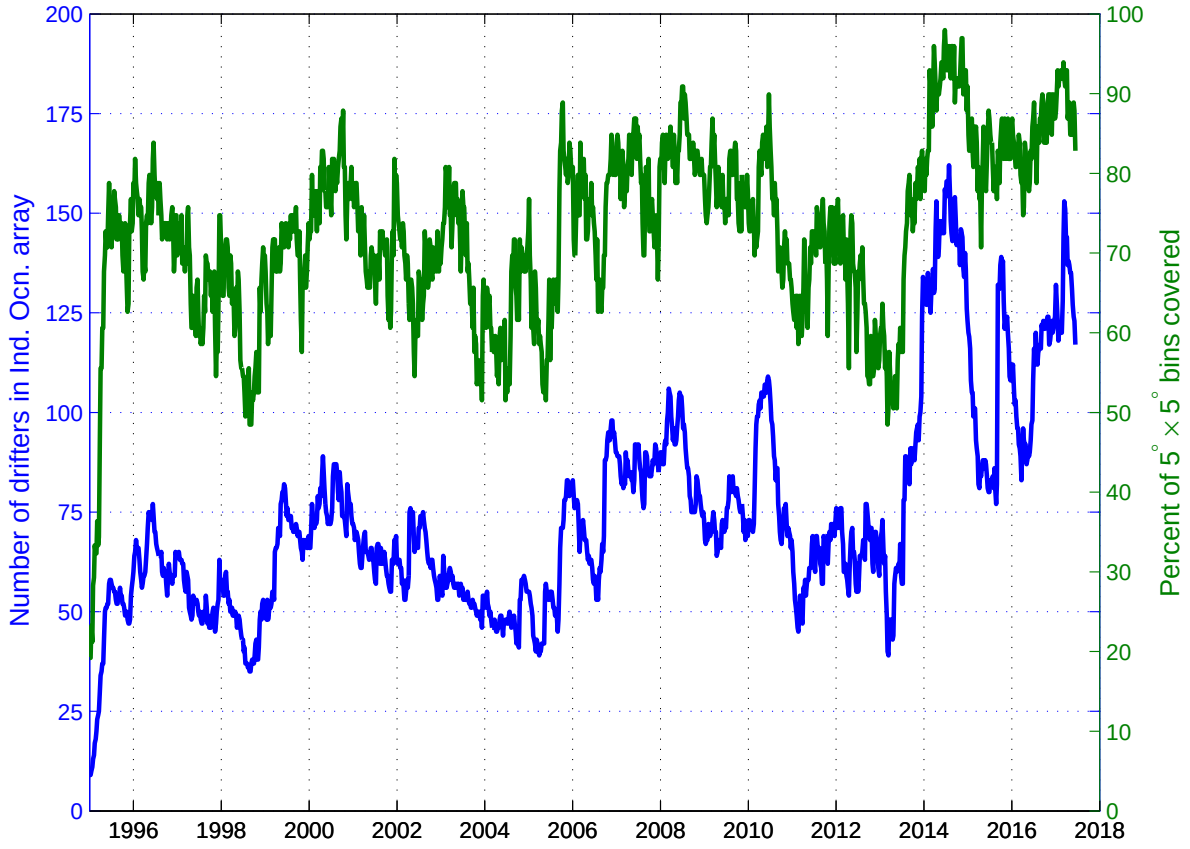

Figure 4.1 Number of GDP drifters in the Indian Ocean (blue) and percent of 5°×5° bins sampled by the drifters (green).

with anomalies $>$1.5 psu at spatial scales of $<$5 km and temporal scales of only a few hours (Hormann et al., 2016).

4.3 Current status

Figure 4.2 shows the density of GDP Indian Ocean observations in the historical database, in drifter days per square degree. Historically undersampled regions include the western equatorial region, the central and northern Somali Current and Great Whirl, and the region of the inflowing Indonesian Throughflow between Australia and Indonesia. To achieve 100% coverage, deployment opportunities must be increased in these regions. The Somali Current, Great Whirl, and Seychelles-Chagos Thermocline Ridge are persistently under-sampled largely because drifters moving westward in the South Equatorial Current upstream of these features tend to run aground at the East African coast.

A number of active partnerships enable drifter deployments in the Indian Ocean. The Australian Bureau of Meteorology arranges the deployment of nearly 40 drifters equipped with barometers every year in the equatorial and South Indian Ocean. GO-SHIP lines, such as I05, I06S and I07N, provide a platform in years that they are occupied. Through collaboration with NOAA/PMEL, drifters are deployed during RAMA mooring cruises originating from Indonesia, India, Korea, and others (see Chapter 2). It is desirable to increase deployment efforts and collaboration with Indonesia to improve coverage in the eastern tropics. Through ongoing collaborations with the Kenyan Meteorological Agency, the US Naval Oceanographic Office, and

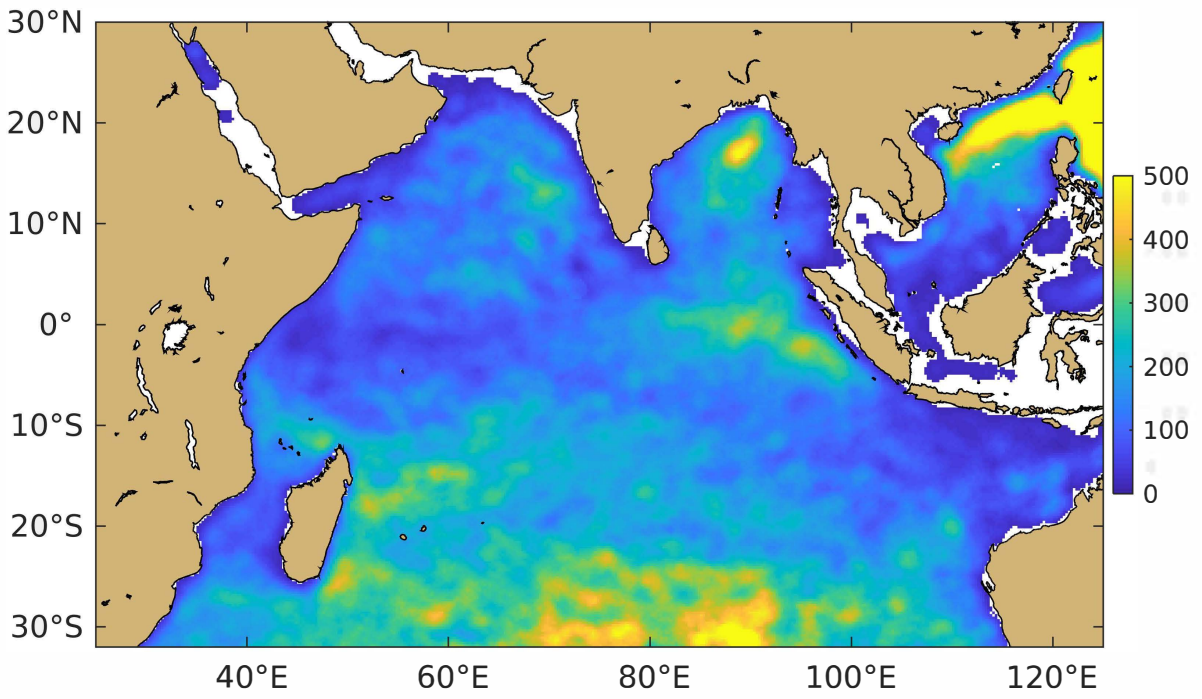

Figure 4.2 Density of drifter observations (drifter days per square degree) in the Indian Ocean, in the quality-controlled GDP database (observations through 30 June 2017).

the Royal Australian Navy, over 50 GDP NOAA and ONR funded drifters are currently being deployed each year in the western and northern Arabian Sea.

4.4 Data policy compliance

Drifter data are made available in near-real time for operational purposes through ftp and web application services by the LDL, Collecte Localisation Satellites (CLS), and MeteoFrance on the Global Telecommunications System and in delayed mode, after approximately two months for quality control and interpolation, at the GDP web page (www.aoml.noaa.gov/phod/dac). Work is underway to archive the delayed mode data at NOAA's National Center for Environmental Information (NCEI) (real-time data is already archived there) and assign them a digital object identifier. The drifter data management plan is described in the OceanObs'09 Community White Paper "Data Management System for Drifting Buoys" (Keely et al., 2009).

4.5 Actionable Recommendations:

A. Deploy more drifters in persistently undersampled regions such as the Somali Current, Great Whirl, Seychelles-Chagos Thermocline Ridge, and in the inflowing ITF between Australia and Indonesia west of the Timor Sea.

B. Sustain the array via international partnerships coordinated through the Data Buoy Co-operation Panel.

C. Re-evaluate the GOOS/GCOS sampling requirements in light of the scales of motion in the basin. For example, 5°×5° bins are very coarse compared to equatorial and boundary flows.

D. Evaluate the value of barometric pressure observations for numerical weather forecasting and recommend what percentage of the IndOOS drifters should collect these observations.

5. Tide Gauges

Alakkat S. Unnikrishnan[1], Andrew Matthews[2], Médéric Gravelle[3], Laurent Testut[4,3], Thorkild Aarup[5] Philip L. Woodworth[2], and B. Ajay Kumar[6]

[1]CSIR-National Institute of Oceanography, Goa, India, [2]National Oceanography Centre, Liverpool, U.K., [3]LIENSs, CNRS/Université de La Rochelle, La Rochelle, France, [4]LEGOS, Toulouse, France, [5]GLOSS/IOC, UNESCO, Paris, France, [6]ESSO-INCOIS, Hyderabad, India

5.1 Introduction

Tide gauge measurements provide data for routine tidal predictions in ports as well as for extreme events such as storm surges and tsunamis. Along with satellite altimeter measurements, tide gauges also provide measurements used for sea-level rise estimates. This is particularly important for impact assessment in low-lying coastlines of south Asia as well as islands such as the Maldives in the Indian Ocean.

5.1.1 Current status of the network

Figure 5.1 shows a map of active tide gauge stations in the Indian Ocean, including those that supply quality-controlled monthly-mean sea level data to the Permanent Service for Mean Sea Level (PSMSL, http://www.psmsl.org) and those that supply real-time data to the Intergovernmental Oceanographic Commission's Sea Level Station Monitoring Facility(http://www.ioc-sealevelmonitoring.org), operated by the Flanders Marine Institute (VLIZ, Belgium). The stations shown as 'PSMSL only' include records without complete datum control, known as non-Revised Local Reference (non-RLR) stations, and many records of only short duration. Real-time stations have increased in number since the 2004 tsunami. There are 20 stations that have datum-controlled records (RLR) longer than 40 years that can be used for estimating long-term changes in sea level (shown in green). Unfortunately, most of them are in the northern hemisphere. Only two stations, namely Mumbai on the west coast of India and Fremantle on the west coast of Australia, have more than 100 years of data.

The spatial coverage of the Indian Ocean tide-gauge network is not as good as in the Atlantic and Pacific. Due to inadequacies in coverage, particularly in the southern Indian Ocean, long-term trends and variability at decadal and longer time scales are less well resolved.

Figure 5.2 shows the network of Global Navigation Satellite System (GNSS) stations co-located with tide gauges in the Indian Ocean, as stored at the SONEL (Service d'Observation du Niveau des Eaux Littorales) data center (http://www.sonel.org). GNSS measurements monitor changes in the level of the land on which the gauges are located and are necessary to place sea level measurements from tide gauges in an absolute, geocentric reference frame. Hence, there is a requirement for GNSS equipment to be co-located at GLOSS core network tide gauge stations (IOC, 2012). The Indian Ocean is particularly deficient in this respect. King et al.,(2014) has highlighted several sites as priorities for GNSS stations near to Indian Ocean tide gauges. Priority stations include Karachi, Aden, and stations along the Thailand coast, such as Ko Taphao Noi, where the tide gauge records are longer than 40 years but there is no GNSS station in the vicinity. In parallel to new installations, an effort should be made in making the data of the existing GNSS stations publicly available (the stations in red in Figure 5.2 are co-located GNSS stations for which no data are available on SONEL, mainly along the Indian, Indonesian and Australian coasts). There is also a particular need for long-term datum control within the tide

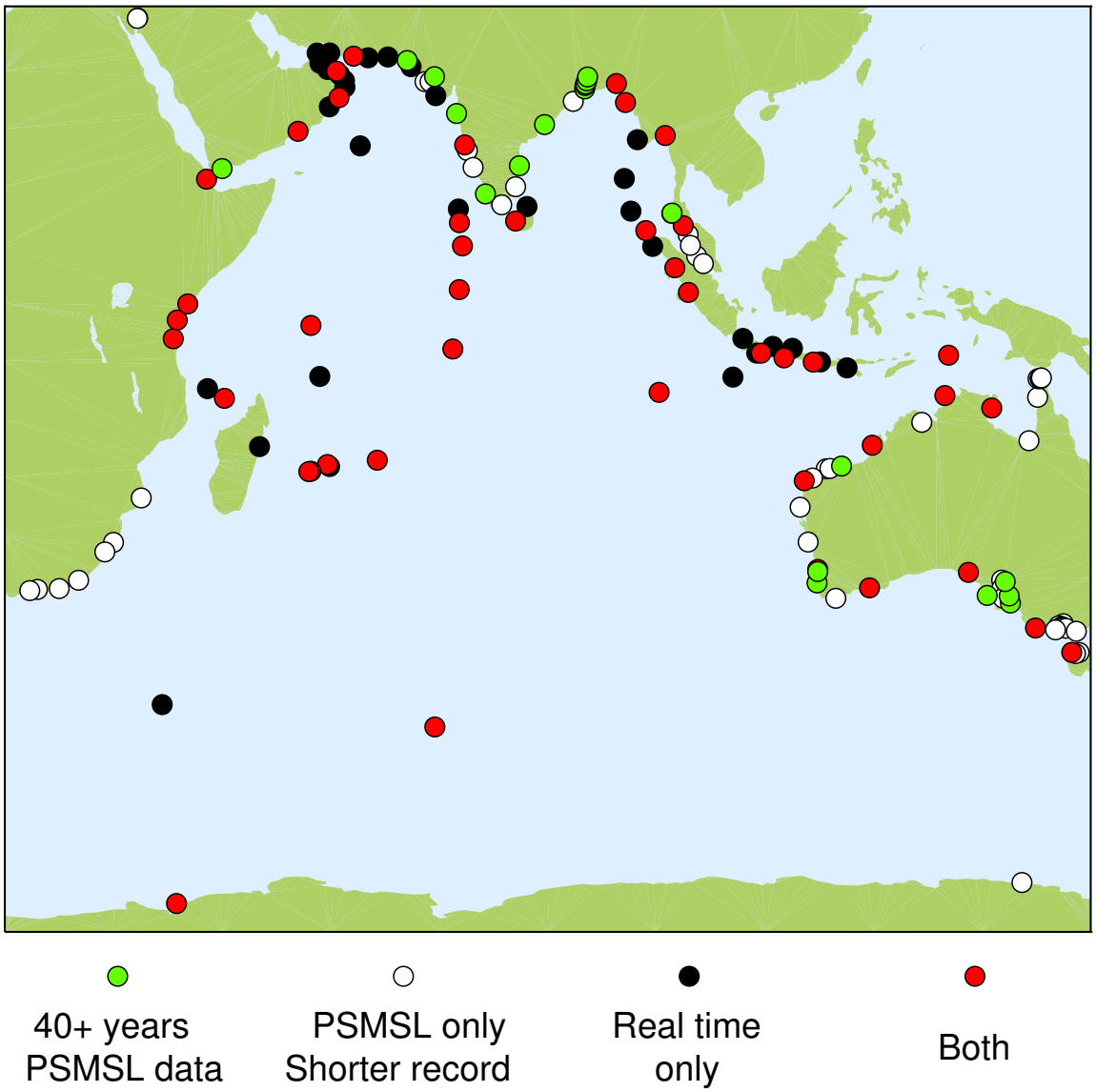

Figure 5.1 Active tide gauge stations in the Indian Ocean. PSMSL stations are considered active if data are available for 2011 or later. Real-time stations are considered active if they have supplied data in 2017.

gauge network and for ties between the tide gauges and GNSS equipment (Woodworth et al., 2017).

5.1.2 High-frequency data

The Indian Ocean tide-gauge network has been extended since the commencement of the Indian Ocean Tsunami Warning and Mitigation System (IOTWMS) following the 2004 Indian Ocean tsunami. This was achieved by upgrading some stations and with the installation of some new stations. There are now more than 100 tide gauges in the Indian Ocean (Global Sea Level Observing System (GLOSS) and non-GLOSS) that provide sea level data in real time (not quality controlled) via the IOC Sea Level Station Monitoring Facility. Higher-frequency, quality-controlled data (hourly values and similar) are available from the University of Hawaii Sea Level Center (http://uhslc.soest.hawaii.edu/). Tide gauge hardware with real time transmission has

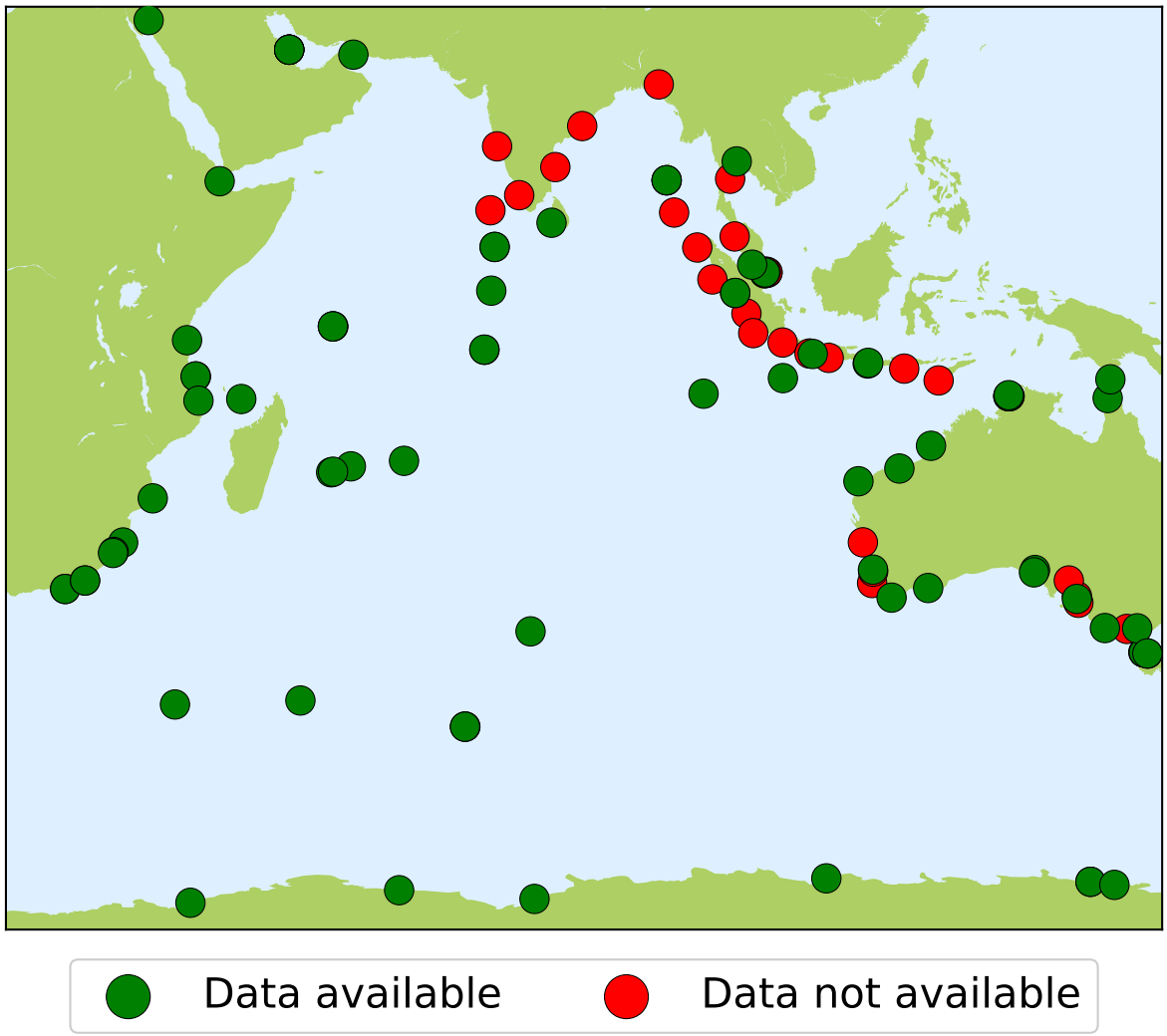

Figure 5.2 Current status (August, 2018) of the GNSS network co-located with tide gauges in the Indian Ocean.

declined in price and as a result we expect the density of the network can be increased over the coming years.

5.1.3 Data Usage and Comparison with Altimeter Data

Monthly and annual mean sea level data have been used for estimation of long-term trends in the northern Indian Ocean (e.g., Unnikrishnan and Shankar, 2007). The Indian Tsunami Early Warning Centre (ITEWC), at INCOIS, Hyderabad, India makes use of tide-gauge data as well as bottom pressure recorder data for detection of tsunamis in the Indian Ocean (Srinivasa Kumar et al., 2012, Ch. Patanjali Kumar et al., 2015). Church et al., (2006) found good correlations between tide gauge data and altimeter data at island stations in the Indian Ocean using approximately 10 years of altimeter data. Altimeter and tide gauge data comparison has also been undertaken using selected long records along the Indian coast (e.g., Kochi and Diamond Harbour, Unnikrishnan et al., 2015) and reasonable correlations reported. However, inconsistencies have been found across different sea-level reconstruction products used to determine regional decadal variability (Nidheesh et al., 2017) and more direct measurements are needed.

5.2 Actionable Recommendations

A. Enhance the tide-gauge network along the coasts of Thailand and Africa, in the equatorial Indian Ocean (Chapter 10.4) and Seychelles-Chagos thermocline ridge region (Chapter 14.3). Improve the network of island stations, which are highly effective for comparisons to satellite altimeter data and for combined 'reconstructions' of long-term regional sea level change.

B. Enhance and consolidate existing networks in the Southern Ocean and around Antarctica on a long-term basis through cooperation of their countries (namely Australia, France, Japan, Russia, South Africa and the UK).

C. Sustain the core tide gauge network for GLOSS and for tsunami monitoring (IOC, 2015). CLIVAR linkage and support in this respect is beneficial.

D. Digitize historical sea level data not already archived in several countries.

E. Increase number of tide gauge stations with colocated GNSS stations (land movement) and strengthen coordination between national operators of these stations.

6. Past, Present, and Future Satellite Missions

Tong Lee[1,2]

[1]NASA Jet Propulsion Laboratory (JPL), [2]California Institute of Technology, USA

6.1 Past and current contributions of satellites to Indian Ocean research

Satellites are an integral component of the IndOOS. Oceanographic satellite missions provide a suite of oceanographic variables, such as sea surface temperature (SST), salinity (SSS), and height (SSH), as well as significant wave height (SWH), ocean surface wind speed and wind stress, precipitation, ocean mass, and variables related to ocean color (e.g., chlorophyll concentration). Combinations of satellite measurements also provide estimates of ocean surface currents and surface heat fluxes. Even before the major elements of the *in situ* component of IndOOS were developed in the 2000s, ocean observing satellites have been providing routine measurements of some oceanic variables, including SST from Advanced Very High Resolution Radiometers (AVHRRs) since 1981 and SSH anomalies from TOPEX/Poseidon from 1992-2006.

Satellites can provide more uniform spatiotemporal sampling of the surface ocean than *in situ* systems. The extensive spatial sampling of satellite observations enables the calculation of spatial derivative fields that are important for the study of oceanic and atmospheric circulation and air-sea interaction. Such derivative fields include SST and SSS gradients, surface geostrophic currents (from horizontal gradients of SSH), and ocean surface wind stress curl and divergence. Satellite data help capture spatiotemporal variations at scales not resolved or inadequately captured by *in situ* data. Many satellites provide more measurements in the coastal ocean than can *in situ* platforms. The extensive, often global, coverage of satellites facilitates studies of large-scale teleconnections and impacts over and beyond the Indian Ocean.

Satellite observations are complementary to *in situ* observations in the Indian Ocean, such as those from RAMA moorings, the Argo array, XBT network, and GO-SHIP. Satellite altimetry data, in some cases together with gravimetry data from GRACE (Gravity Recovery and Climate Experiment), in combination with Argo observations since the mid 2000s, have enabled a comprehensive study of sea level and the relative contributions of thermosteric, halosteric, and mass contributions (Fukumori and Wang, 2013; Llovel and Lee, 2015). Satellites and mooring data together have greatly facilitated the studies of upper-ocean processes such as mixed-layer heat balance (Foltz et al., 2010) and the dynamics of equatorial Indian Ocean currents (Nagura and McPhaden, 2012).

At the same time, *in situ* data help interpret surface observations from satellites by providing information about vertical structure below the sea surface (Llovel and Lee, 2015). *In situ* data also provide independent measurements that are critical to the calibration and validation of many satellite measurements (Ebuchi et al., 2012; Lee et al., 2016). High-frequency measurements from moorings can help de-alias signals that are not resolved by satellites, such as diurnal variability (Gille et al., 2003). Sustained *in situ* measurements are critical to the intercalibration of an observed variable from different satellite missions (Wentz et al., 2017).

Satellite observations have provided many fundamental contributions to Indian Ocean research and a comprehensive review is not possible within this chapter. The following provides some

examples on various time scales. On intraseasonal time scales, satellite observations have been used to study Kelvin and Rossby waves, basin modes (resonance), wind-thermocline-SST coupling, the response to MJO, and effects of mesoscale eddies (Han et al., 2001; Han et al., 2005; Fu et al., 2007; Zhou and Murtugudde, 2010; Nagura and McPhaden, 2012; Grunseich et al., 2013; Gaube et al., 2013; Suresh et al., 2013; Girish Kumar et al., 2013; Guan et al., 2014). On seasonal time scales, satellite data have been used to understand the dynamics of the Indian Ocean, in particular, the role of Rossby waves driven by seasonal winds and radiated from the eastern boundary (Fu and Smith, 1996; Eigenheer and Quadfasel, 2000; Yang et al., 2001; Wang et al., 2001; Brandt et al., 2002), and the different signatures of annual Rossby waves from SSH and SSS (Menezes et al., 2014a). On interannual time scales, satellite data revealed the variations associated with Indian Ocean Dipole (IOD) and the basin-scale warming in the Indian Ocean associated with the 1997-98 El Nino (Yu and Reinecker, 1999; Webster et al., 1999), the interpretation of IOD in terms of Recharge Oscillator theory (McPhaden and Nagura, 2014), and the relationships of the IOD with variability in the southern tropical Indian Ocean (Rao et al., 2002; Han and Webster, 2002; Xie et al., 2002; Rao and Behera, 2005). On decadal time scales, satellite observations have illustrated relationships between SSH and local and remote forcings, the influence of decadal variability from the Pacific sector, and changes of the shallow meridional overturning circulation (Lee et al., 2004; Lee and McPhaden, 2008; Llovel and Lee, 2015; Wang et al., 2015; Srinivasu et al., 2017) e.g., Figure 6.1.

Satellite ocean color measurements have been fundamental to the research of Indian Ocean primary productivity and the linkages to ocean and climate processes (Chapter 12). Satellite radiation measurements, including those for the incoming and reflected solar radiation as well as the outgoing longwave radiation, are critical for estimating basin-scale air-sea heat fluxes (Chapter 16). Precipitation measuring satellites, such as the Tropical Rainfall Measuring Mission (TRMM) and the Global Precipitation Measurement (GMP) core satellite, provide the backbone of observations necessary to study the linkage of the Indian Ocean with the water cycle and to estimate net surface freshwater flux and evaporation at the air-sea interface (Hoyos and Webster, 2007; Yu et al., 2017).

6.2 Continuity and enhancement of satellite observing capability for the future IndOOS

While satellite observations have made enormous contributions to Indian Ocean research over the past few decades, several improvements are required to meet a fit-for-purpose IndOOS and the future continuity of satellite missions is not ensured.

Of particular importance is the need to enhance the temporal sampling of satellite-derived wind and wind stress measurements. Wind forcing plays a dominant role in oceanic variability over a broad range of time scales. In the equatorial Indian Ocean and near the Maritime Continent strong diurnal variability in the winds is important to MJO and MISO development. Currently, there are only two continuity series of satellite scatterometers: the MetOp series by the European Space Agency (ESA) and EUMETSAT, and the Oceansat series by the Indian Space Research Organization (ISRO). These two scatterometers provide approximately 60% coverage of the ocean at the 6-hourly interval, the de-correlation time scale of the diurnal cycle. Wind measurements from additional scatterometers and passive microwave radiometers are needed to reduce the aliasing of diurnal variations into lower frequencies.

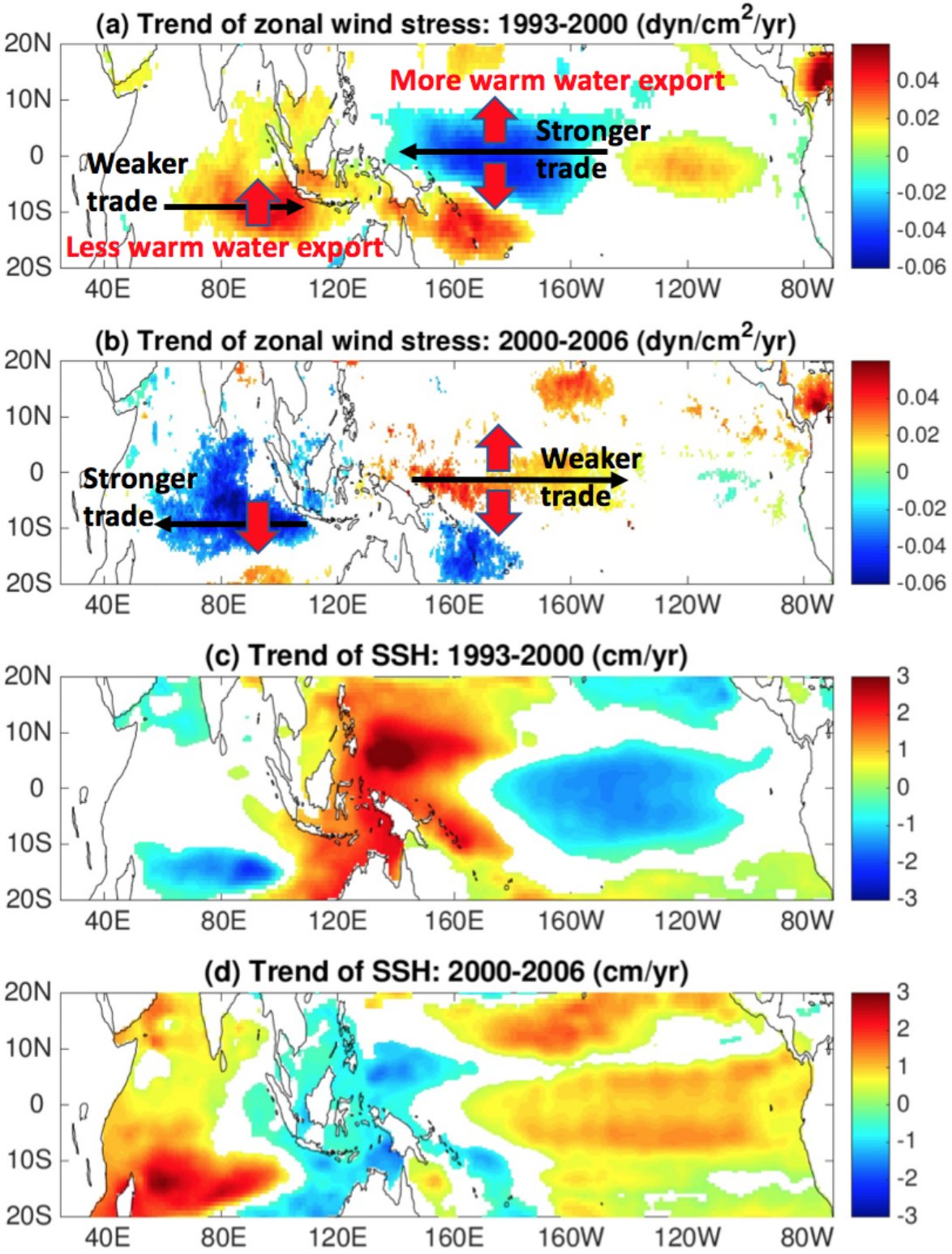

Figure 6.1 Trends of zonal wind stress during 1993-2000 estimated from ERS scatteromer data (a) and those during 2000-2006 estimated from QuikScat scatterometer data. SSH trends for the 1993-2000 (a) and 2000-2006 (b) periods estimated from altimeter data. These observations were also used to infer changes in the upper and lower branches of the shallow overturning circulations in the Pacific and Indian Oceans and their linkages as described in Indo-Pacific linkage subsection. After Lee et al., (2010). Adapted from Lee and McPhaden, (2008).

Enhancement of spatiotemporal sampling to monitor sub-mesoscale variability is also important, especially in the Bay of Bengal where abundant sub-mesoscale variability is believed to affect the horizontal dispersion of freshwater and the vertical mixing of heat and nutrients (e.g., Ramachandran et al., 2017). The Surface Water Ocean Topography (SWOT) satellite, scheduled to be launched in 2021, is expected to provide important observations of these sub-mesoscale processes. There are also ongoing concept studies and development of technology for space-based measurements that resolve sub-mesoscale currents, such as the ESA's Sea Surface Kinematics Multiscale (SKIM) and NASA's Wind and Current Mission (WaCM). The BoB is also home to narrow and coastal freshwater plumes that have significant implications for biogeochemistry and cyclogenesis. The current $\sim$40-km resolution of SSS from SMOS and SMAP (Reul et al., 2013, Fore et al., 2016) is marginal to study these features and hence future increases in spatial resolution of satellite SSS are necessary.

The continuity of satellite observations of Essential Ocean Variables (EOVs) is a critical issue for the future IndOOS. SSH measurements from nadir altimetry missions are reasonably ensured to 2030 and beyond. There are also operational commitments for infrared (IR) SST, both polar-orbiting (the NOAA series) and geostationary (the Himawari series), and various missions already planned for ocean color measurements in the foreseeable future. However, the continuity of passive microwave radiometer (PMW) SST (for the 6.9 GHz channel) is not currently ensured and these measurements are needed in regions of strong atmospheric convection, such as the equatorial and southern subtropical Indian Ocean, where clouds often obscure IR SST. The continuity of satellite missions for SSS is also a critical issue. The Indian Ocean has the most dynamic variability of SSS globally, with strong linkages to river run-off. Sustaining satellite SSS measurements is thus necessary to further the understanding of the dynamics of the Indian Ocean and its linkages with climate variability and the regional terrestrial water cycle.

In situ measurements are necessary for the calibration and validation of various satellite measurements, as well as for inter-calibrating measurements from different satellite missions. This is particularly true for SST, SSS, and ocean surface winds. Therefore, sustaining the related *in situ* measurements in support of the satellite observing system is a vital element of IndOOS.

6.3 Actionable recommendations

Based on the discussion above, a list of actionable recommendations is provided towards a fit-for-purpose satellite observing system for the IndOOS, focusing on satellite observations that are currently not ensured for the next decade and beyond.

A. Ensure three satellite scatterometers in coordinated orbits to sample diurnal winds, with near real-time public data access.

B. Sustain passive microwave radiometer all-weather SST mission(s).

C. Continue satellite SSS and improve their accuracy and spatial resolution.

D. Enhance space-based capability to monitor sub-mesoscale variability (e.g., for sea level and ocean surface currents).

E. Sustain *in situ* measurements for satellite calibration and validation, particularly from high-frequency moorings.

7. The Global Ocean Ship-Based Hydrographic Investigations Program (GO-SHIP)

Bernadette M. Sloyan[1,2,4] and Rik Wanninkhof[3,4]

[1]CSIRO, Oceans and Atmosphere, Hobart Australia, [2]Centre for Southern Hemisphere Oceans Research, Hobart, Tasmania, Australia, [3]NOAA Atlantic Oceanographic and Meteorological Laboratory Miami USA, [4]Co-Chair GO-SHIP

7.1 Introduction

GO-SHIP is the systematic and global survey of select hydrographic sections carried out by an international consortium of countries and laboratories (Figure 7.1). The sections span all the major ocean basins, including the Indian Ocean, and the full-depth water column with a suite of accurate measurements for climate studies.

Global hydrographic surveys have been carried out approximately every decade since the 1950s through research programs such as IGY, IIOE , GEOSECS, WOCE/JGOFS , and CLIVAR. In 2009 the Global Ocean Ship-based Hydrographic Program (GO-SHIP, http://www.go-ship.org) was established as a component of the Global Ocean Observing System (GOOS) to provide international coordination and scientific oversight of the decadal global ocean survey. The international hydrographic surveys of the 1960s, 1990s (WOCE) and 2000s (CLIVAR Repeat Hydrography and GO-SHIP) answered many first-order questions about large-scale ocean circulation and carbon inventories. They also raised many new questions concerning ocean variability and trends, circulation, and biogeochemical controls on carbon and tracer inventories, distributions, and long-term secular trends associated with climate change and ocean acidification (Talley et al., 2016). These observations showed that the full-depth ocean exhibits significant interannual variability, on top of the expected decadal trends, as part of patterns of global change, complicating efforts to detect and attribute human influences on the ocean (Talley et al., 2016).

GO-SHIP will continue to build a time-series of full-depth repeat ocean measurements capable of resolving decadal and longer-term changes in the circulation and property storage (including heat, freshwater, oxygen, and carbon) of the global oceans. Future directions include a greater focus on biological measurements, including bio-optics, to assess ocean health, and validating measurements obtained from remote sensing and the new generation of robotic sensors such as profiling floats.

7.2 GO-SHIP Objectives

The GO-SHIP principal scientific objectives are:

1. Understanding and documenting the large-scale ocean water property distributions, their changes, and drivers of those changes, and,

2. Addressing questions of the large physical, biogeochemical, and biological changes anticipated for the future ocean. Specific questions concern increasing dissolved inorganic carbon, warming, acidification, and stratification changes resulting from atmospheric CO_2 increases and associated changes in the Earth's radiation balance.

The observations will aid understanding of interaction and feedbacks of anthropogenic perturbations with natural cycles of water and sea-ice and with changes in circulation and ventilation processes.

In addition to addressing these scientific objectives, GO-SHIP provides deployment opportunities and the high-quality reference observations needed for autonomous observing platforms (e.g. Argo, BGC-Argo) and their delayed mode quality control and inter-calibration procedures. GO-SHIP research vessels also collect underway meteorological and surface ocean observations as part of the Ship Observation Team (SOT), and support the testing of new ocean observing technologies and sensors.

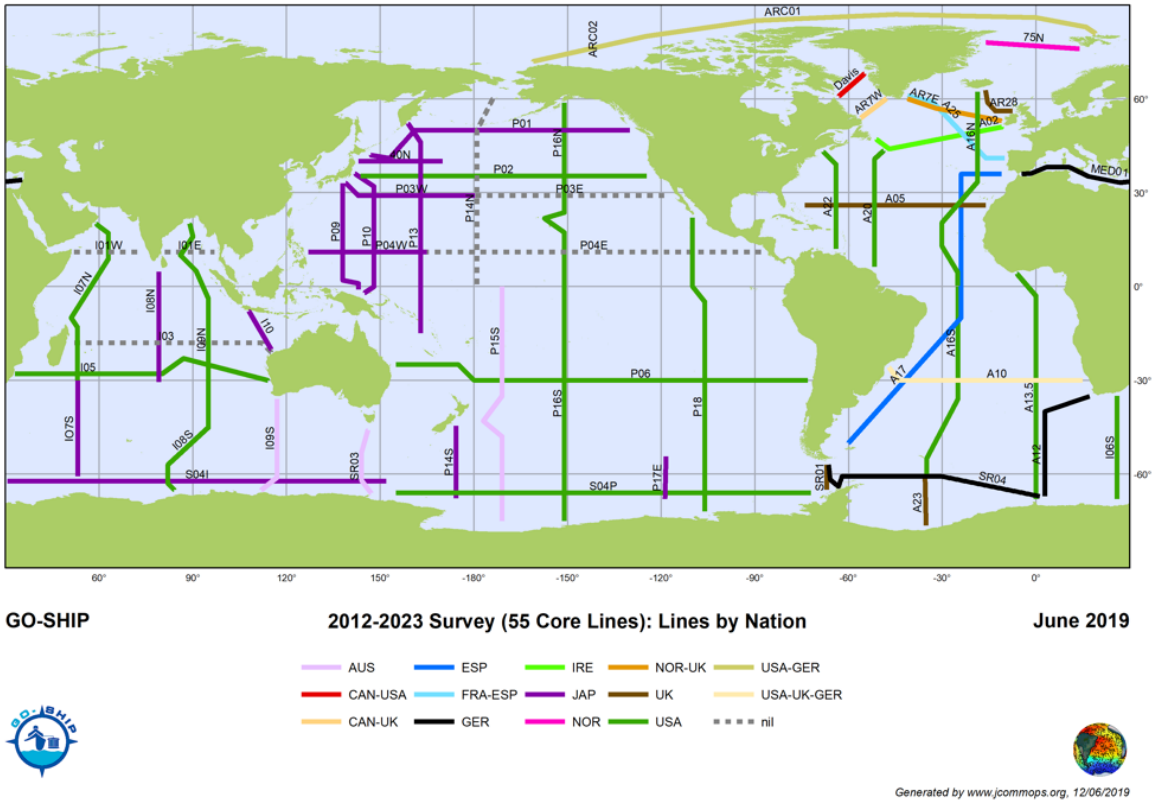

Figure 7.1 Hydrographic sections of GO-SHIP (2012-2023), color-coded by country. Section currently without (national) support are shown as gray dashed lines.

7.3 GO-SHIP: Indian Ocean

GO-SHIP has a number of sections in the Indian Ocean that are part of the global decadal survey. Of note is the newly established I7S line, under the auspices of JAMSTEC, Japan, that fills a critical gap in the southwestern Indian Ocean (Figure 7.1)

Two zonal sections in the northern Indian Ocean - I01E and I01W - remain uncommitted (Figure 7.2) and have not been occupied since approximately 1998. These sections remain on the GO-SHIP survey plan due to their scientific importance, particularly in light of deoxygenation in the Northern Indian Ocean. Also, I03 in the extra-tropics was last completed in 2003 and a study on the value of retaining this section is warranted.

Collaboration between GO-SHIP and the CLIVAR/IOC-GOOS Indian Ocean Region panel provides a unique opportunity for (1) leveraging national support to complete the Indian Ocean survey; (2) increasing high quality observations of a suite of ocean measurements; (3) building a sustained program for ship-based observations of the Indian Ocean and; (4) providing further opportunities for full interpretation of the rich datasets.

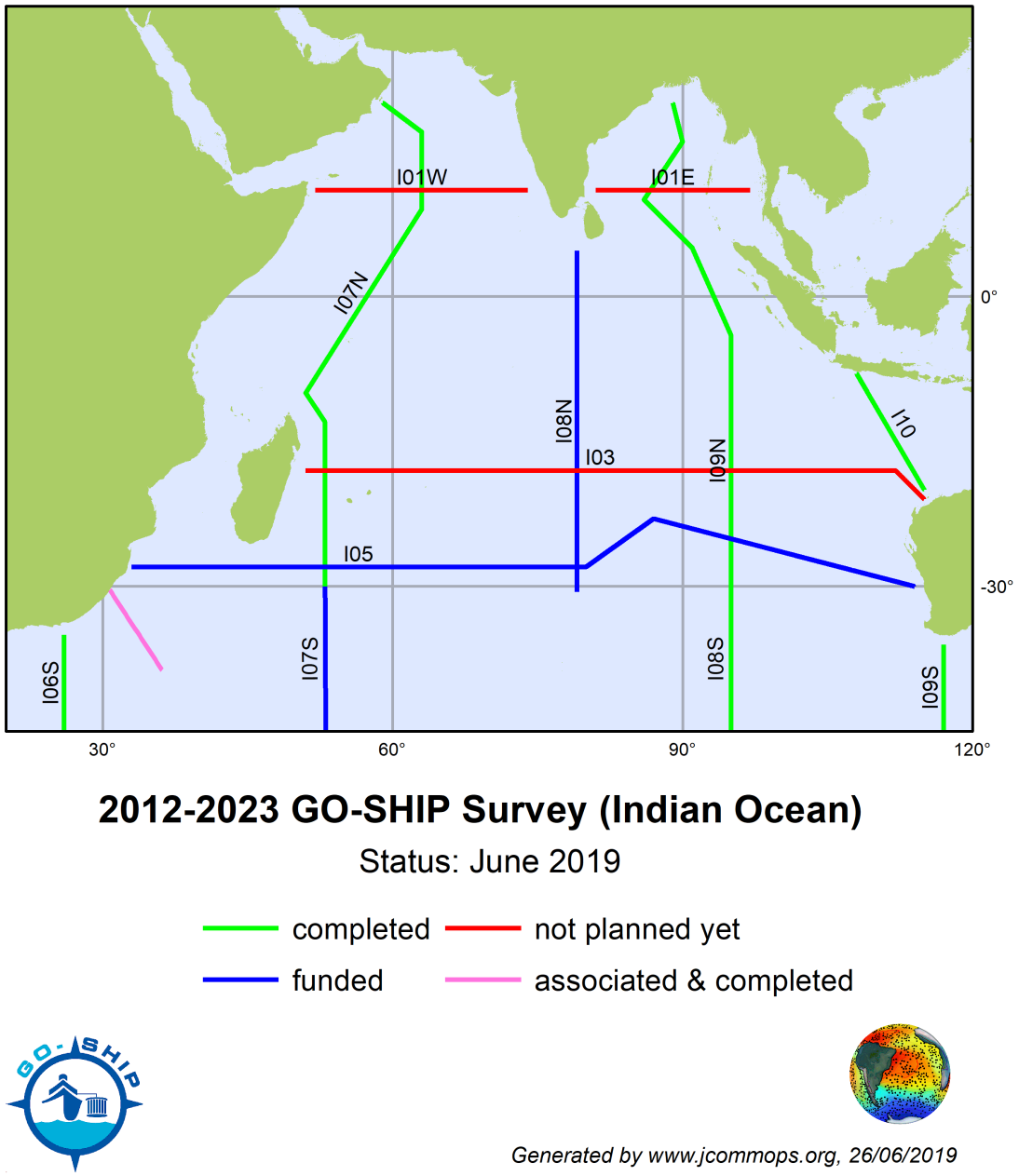

Figure 7.2 GO-SHIP Indian Ocean sections

7.4 GO-SHIP Variables and Data Time Line Policy

The GO-SHIP measurement suite is endorsed by all international participating nations and is divided into three levels of priority: Level 1, Level 2, and Level 3 (Table 7.1). Best practices and

standards of accuracy for all Level 1 and 2 measurements should adhere to, or be higher than, those set by the GO-SHIP repeat hydrography manual (Hood et al., 2010b, www.go-ship.org).

Level 1 core measurements are mandatory on all cruises, and include standard hydrographic and tracer profiling, and velocity profiling. These measurements are required to directly quantify change in ocean carbon inventory, estimate anthropogenic CO_2 empirically, characterize large-scale water mass ventilation rates, constrain horizontal heat, freshwater, carbon, nitrogen, and oxygen transports and/or net divergence, and provide a basis for model evaluation.

Level 2 measurements are highly desirable to the scientific objectives of GO-SHIP cruises. GO-SHIP recommends that level 2 data should be collected when possible.

Level 3 ancillary measurements are done according to opportunity and space available. They should not significantly interfere with Level 1 or 2 efforts, and may be parameters of regional interest or specific to an individual cruise. They include new technologies and measurement techniques. For example, in the northern Indian Ocean ∂^{15}N of NO_3 measurement as an indicator of denitrification is of high interest.

Table 7.1 GO-SHIP Measurement and Data Release Schedules. Notes: (1) Available daily during cruise. (2) Released to relevant data management structure within 5 weeks of cruise; (2P) in preliminary form. (3) Released within 6 months of shore-based analysis. (4) Released within 15 months of sample collection.

Level 1: (*All data are to be released in final form 6 months after the cruise except where noted*) Inorganic carbon system parameters: Dissolved inorganic carbon (DIC); Total Alkalinity (TAlk); pH (two of three) (2P); CTD pressure, temperature, conductivity (salinity) (1,2); CTD oxygen (sensor) (2P); Bottle salinity (2); Nutrients by standard auto analyzer (NO_3/NO_2, PO_4, SiO_3) (2); Dissolved oxygen (2P); Chlorofluorocarbons (CFC-11, CFC-12) and SF_6 (2P); Surface underway parameters (T, S, pCO_2) (1); ADCP shipboard (2P); ADCP lowered (2P); Underway navigation and bathymetry (2); Meteorological data (1).
Level 2: (*All data are to be released in final form 6 months after the cruise except where noted*) Examples include discrete pCO_2 (2); N_2O (2); ^{14}C (3); CCl_4 (2); ∂^{13}C of DIC (3); Dissolved organic carbon; dissolved organic nitrogen; ^{3}H/^{3}He (4); Fe/trace metals; CTD Transmissometer; Surface underway measurements (nutrients, O_2, Chl, pH, DIC, TAlk, skin temperature).
Level 3: (*All data are to be released in final form within 2 years of analysis*) Examples include, but are not limited to, microstructure/turbulence; chlorophyll; Primary production; HPLC pigments; Experimental continuous analyzers; ∂^{15}N of NO_3; ^{32}Si; ∂^{18}O of H_2O; NH_4; Low level nutrients; Total organic phosphorus; Upper ocean optical; isotopes of O_2; N_2, Ar, O_2; Methyl halides; DMS.

7.5 Data policies

The GO-SHIP data policy is stringent and geared toward rapid, open dissemination, with a clear structure for all data to undergo quality control, and to be sent to and made available from recognized data centers. The policy includes:

1. All Level 1 and 2 observations, cruise reports, and metadata are made public in preliminary form through a specified data center soon after collection (“early release”), with final calibrated data provided six months after the cruise, with the exception of those data requiring on-shore analyses (see Table 7.1).

2. All data collected as part of the program are submitted to a designated data management structure for quality control and dissemination for synthesis.

7.6 Conclusion

GO-SHIP builds on previous global-scale hydrography efforts. The program evolves based on the findings of the previous work and emerging science requirements and technological developments. A future development will include additional biogeochemistry and biology measurements to enable GO-SHIP to determine trends and variability in marine biogeochemistry and ecosystems. These objectives will be incorporated into the sustained primary objectives of GO-SHIP.

GO-SHIP will continue to provide and expand its capacity for testing and validating new autonomous sensors and serve as a reference/calibration dataset for other observing systems (See Chapter 25). As biogeochemical and biological sensors are added to these autonomous platforms, the GO-SHIP data will be invaluable for validating and calibrating these new sensors (See Chapter 16 and 25). In addition, the global hydrographic survey provides access to remote ocean areas for the deployment of all autonomous observing platforms in support of the IndOOS (e.g., Chapters 16, 24, 25).

7.7 Actionable Recommendations

A. Review the GO-SHIP Indian Ocean plan and advise whether section I03 or I05 should be considered a full GO-SHIP reference section in future.

B. Identify national or multi-national support for the I01E and I01W sections.

C. Increase participation in the GO-SHIP program, with a focus on Indian Ocean rim countries.

D. Recommend regions where specific Level 2 and 3 measurements are of highest priority.

E. Promote a strong collaboration between GO-SHIP and IndOOS to optimise GO-SHIP research vessels in support of other components of the IndOOS, where feasible.

8. New Technologies for *In Situ* Measurements

Magdalena Andres[1], Craig M. Lee[2], Emily L. Shroyer[3], and Luca Centurioni[4]

[1]Woods Hole Oceanographic Institution, Woods Hole, MA, USA, [2]Applied Physics Laboratory, University of Washington, Seattle, Washington, USA, [3]Oregon State University, Corvallis, Oregon, USA; [4]Scripps Institution of Oceanography, La Jolla, CA, USA.

Observational strategies that cleverly leverage a combination of time-tested and cutting-edge technologies are required to achieve the goals of the Indian Ocean Observing System (IndOOS) for the benefit of society. Modern capabilities—which include autonomous systems, real-time data delivery, and new sensors—provide access to regions of the spatiotemporal sampling spectrum that have previously been unachievable. Integrated systems that employ complementary platforms, exploiting each for their particular strengths and assuaging weaknesses, are the way forward. Recent technological advances include both new types of platforms that provide autonomy (e.g. REMUS), reduced-power consumption (e.g. Wirewalker), or a combination of these strengths (e.g. Wave Gliders), and new sensor designs that have been made possible through advances in low-power, small-footprint computing and electronics. Advances in adaptive sampling strategies have been achieved in part through expanded global networks that allow for data exchange at increasing speeds. The list of sampling technologies and approaches is extensive and cannot be fully covered here. Instead, we provide selected examples below and consider them in the framework of the IndOOS.

8.1 Revisiting an Established Technology

Targeted subsurface temperature observations from expendable bathythermographs (XBTs) have been important for documenting changes in ocean heat content and will continue to play an important role in the IndOOS, particularly when combined with the Argo array (Cheng et al., 2016; Feng et al., Chapter 3). One way to improve sustainability of repeated XBT lines is through the use automatic launchers that require no rider on the Voluntary Observing Ships (VOS) and little intervention from the ship's crew. At the same time, providing an Iridium satellite link enables remote data retrieval and mission setup. One such system, AXIS – the Automated eXpendable Instrument System (Fratantoni et al., 2017), has been part of an Atlantic Meridional Overturning Circulation (AMOC) observing system since 2011. VOSs might also be equipped with hull-mounted acoustic Doppler current profilers (ADCPs). Collectively, these data provide a powerful way to measure upper-ocean heat transport (Rossby et al., 2017). The 10,000 km long southern boundary of the Indian Ocean (e.g. between Durban and Fremantle) could be a valuable repeat-line for an AXIS system (or other auto-launcher) in combination with a hull-mounted ADCP, as would regions in the northern Arabian Sea, which are difficult to access via international research vessels, but which support high commercial vessel traffic.

8.2 Integrating Platforms: Boundary Current Observations with CPIESs and Underwater Gliders

Current and pressure-sensor-equipped inverted echo sounders (CPIESs) can be used to obtain long-duration, high temporal resolution time series of boundary current transport and velocity structure. CPIESs have been deployed as 'transport lines'—e.g., as part of the ACT time series, OKTV Line, PN Line and ASUKA Line (Beal and Elipot, 2015; Andres et al., 2015), in 'dynamics arrays'—e.g., KESS, CDRAKE, SYNOP, SK-II and FLEAT (Donohue et al., 2010; 2016) and in various 'niche' applications such as the study of non-linear internal waves in the South China

Sea (Li et al., 2009).

CPIESs are deployed on the seafloor in a rigid anchor stand for durations ranging from one to five years. Each CPIES measures the round-trip surface-to-bottom acoustic travel time, near-bottom pressure and temperature, and the horizontal currents 50 m above the seabed. These measures can be used together with a region's hydrography – from shipboard casts, Argo floats, or gliders – to obtain time series of absolute geostrophic velocity profiles from the surface to the bottom and their corresponding transports. Several technological advances are under development at the University of Rhode Island to enhance the capabilities of CPIESs. These include (1) the capability for remote retrievals of data batches (via a popup data shuttle which rises to the surface at a prescribed time and links to the satellite Iridium network) and (2) incorporation of a Doppler current profiler instead of the current sensor (DCPS-PIES).

Gliders have seen widespread success for scientific (Rudnick et al., 2016) and operational missions, and could contribute to IndOOS. Underwater gliders are small (50-kg mass, 2-m length), buoyancy-driven vehicles optimized for extended endurance. Gliders propel themselves by changing buoyancy, sinking or rising through the water column and adjusting attitude to use lift from the hull and wings to project vertical motion into the horizontal. This allows the vehicles to navigate from point to point while they profile vertically through the water column. At the surface between dives, gliders geolocate using GPS, upload data, and download new commands via Iridium satellite modem. Gliders carry flexible payloads that can include sensors for temperature, conductivity (for salinity), velocity profiles, dissolved oxygen, chlorophyll and CDOM fluorescence, optical backscatter, temperature and shear microstructure, nitrate, spectral irradiance, PAR, nitrate, zooplankton and marine mammals.

Gliders are well-suited for quantifying boundary current variability. Gliders move slowly (20 km/day) to provide finely-spaced profiles, with the capability to maintain continuous sampling for periods typically lasting up to half a year. They can thus resolve scales of a few kilometers and weeks over sections of hundreds of kilometers length, while maintaining sampling over seasons to years – scales that are well-matched to resolving long-term variability in boundary flows. Geostrophic transports can be reliably calculated from density sections using the thermal wind relationship (e.g. Lien et al., 2014) referenced to the depth-average current calculated as the difference between observed and modeled glider displacement over a dive (Eriksen et al., 2001; Rudnick and Cole, 2011). Or direct transports can be measured using glider-mounted ADCPs (Todd et al., 2017). Gliders have been successfully used for sustained, multi-year quantification of eastern (California Current; Todd et al., 2011; Zaba and Rudnick, 2016) and western (Kuroshio Current; Lien et al., 2014 and Gulf Stream; Todd et al., 2016) boundary currents. Similar approaches, using logistics local to target regions in the Indian Ocean, could be applied to sustain measurements for the IndOOS, building on existing glider sections across the boundary current off Sri Lanka.

Recent use of moorings and CPIESs in tandem with gliders has been highly successful. Gliders can resolve water mass changes that CPIESs or moorings alone could not detect (Andres et al., 2017). The combination of fixed and mobile platforms resolves a broader range of scales than could be achieved by one of these platforms alone, allowing investigations of the interactions between scales. In the Indian Ocean, integrated glider/CPIESs arrays are being used to study the undercurrent off Sri Lanka (Anutaliya et al., 2017) and could also contribute significantly to studies of other surface boundary currents and their undercurrents (e.g., the Agulhas, Somali, and Leeuwin Currents) and of the currents along the equator. They could be used to investigate the flows' interactions with topography at the many dramatic ridges in the Indian Ocean and the interactions of mesoscale eddies with these ridges and the western boundary

currents. In addition, CPIESs would be well suited to study thermocline movement (and the bottom pressure signals) at the Seychelles-Chagos Thermocline Ridge.

Other promising unmanned platforms include the Saildrone and the Wave Glider that are being used in experimental mode to obtain momentum and flux measurements, as well as other sea surface and meteorological observations.

8.3 Moored Profilers for High-Current Regimes

In some cases it is desirable to resolve subtle changes in water properties at a fixed location (like within a boundary current) or to resolve transport variability in density space rather than depth space. Moored profilers, which can sample temperature, salinity, and velocity at high vertical resolution as they ride up and down a mooring line, are particularly suitable for such studies and have been used as part of the AMOC observing system in a 10-year study of the Deep Western Boundary Current south of Cape Cod (Line W, Toole et. al., 2017). Two important enhancements to the basic moored profiler technology are underway at the Woods Hole Oceanographic Institution (WHOI) and are important innovations for long-endurance observing systems. The first is an Articulating Profiler which minimizes drag, and thereby power consumption, by aligning the profiler body with the relative 3-D flow. The sensors are mounted at the leading end of the body to sample undisturbed water, reducing measurement noise. The second development leverages hydrodynamic lift from the incident ocean currents. A LAMP (Lift-Assisted Moored Profiler) will improve reliability in strong currents, where the present traction drive wheel can stall. This may make moored profiler measurements of strong currents like the Agulhas feasible. Other profiling systems, in particular the Wirewalker developed at Scripps Institution of Oceanography, harness surface wave motion for profiling where moored or drifting buoys experience sufficient wave pumping (Lucas et al., 2016).

8.4 Capitalizing on Expendable Platforms

The operational Global Drifter Program provides 15-m ocean currents, *in situ* SST, and sea-level pressure data, as detailed in Chapter 4. Emerging technologies have the potential to further the impact of surface drifters. Low-cost, expendable, undrogued drifters equipped with SST and GPS sensors capable of measuring the directional spectra of surface gravity waves have been developed by the Lagrangian Drifter Laboratory (LDL) at the Scripps Institution of Oceanography (Centurioni et al., 2017). The Directional Wave Spectra (DWS) drifter samples the vertical, zonal, and meridional velocity components of the GPS antenna and computes the power spectral density, co-spectra, and quadrature-spectra parameters of the wave spectra at a minimum interval of 30 min, relaying them to the LDL data server in real-time through the Iridium satellite system. Commands sent over two-way Iridium communication can modify power consumption and telemetry cost while the DWS drifter mission is underway. All of the transmitted wave data, as well DWS drifter status are accessible in real time on a dedicated website as wells as through the Global Telecommunication System of the World Weather Watch. The first open ocean array of 22 DWS drifters was deployed in the tropical North Pacific Ocean in winter 2016.

Surface Lagrangian drifters equipped with salinity sensors were deployed in the Bay of Bengal in 2015 as part of the Office of Naval Research (ONR) funded program ASIRI (Hormann et al., 2016), but cost prevents basin-wide implementation. New low-cost sensors are currently being tested for long-term stability and may offer a viable solution for the calibration and validation of satellite salinity observations in the future.

Expendable Lagrangian drifters equipped with sonic anemometers and configurable for air or ship deployment could also represent a valuable addition to the IndOOS and the global array. Such drifters, termed Minimets (https://gdp.ucsd.edu/ldl_drifter/instruments/minimet.html), have been used for over a decade to measure sea-level wind within hurricanes and typhoons. An inexpensive (and hence expendable) freely-drifting spar buoy instrument system (X-Spar) that could provide cost-effective, distributed measurements of meteorological variables is under development at WHOI. It will return near-surface meteorological and oceanographic observations for periods of a year or longer. Since data are recovered remotely via Iridium satellite link, it will be particularly suitable to use in regions where regular shipboard mooring servicing is not feasible.

8.5 Augmenting the Capabilities of Existing Assets

Integration of new sensors on existing IndOOS platforms, such as Argo and the RAMA array, offers added value and can target specific science needs. For example, the shallow stratification in the Bay of Bengal necessitates clean near-surface measurements of both temperature and salinity. Modifications to the standard Argo float by including a secondary, unpumped conductivity-temperature sensor has provided near-surface profiling without lowering the quality of deep measurements by the primary sensor (Anderson and Riser, 2014). Similarly, subsurface temperature sensors could be added to SVP drifters to resolve the diurnal cycle of the temperature stratification in the upper 12 m. Furthermore, addition of optical and chemical sensors to Argo floats provides the potential to greatly enhance our understanding of the biogeochemistry and biophysical connections in this historically undersampled region (Chapter 1). Supported through ONR's DYNAMO program (Moum et al., 2013a) and continuing with the ASIRI and MISO-BOB initiatives (Wijesekera et al., 2016), turbulent mixing sensors (χ-pods) have been added to RAMA moorings along the Equatorial Indian Ocean and within the Bay of Bengal along 90°E (e.g., Warner et al., 2016). χ-pods provide a direct measure of temperature, velocity, and temperature variance dissipation at each deployment location (Moum and Nash, 2009). The resultant multi-year time series of turbulent mixing has led to an understanding of the role of subsurface fluxes in modulation of the upper ocean structure (Moum et al., 2013a; Warner et al., 2016). χ-pods are also being integrated on the SOLO II floats with the long-term goal of including this capability within the Argo program (Shroyer et al., 2016).χ-SOLO floats were first tested in the Bay of Bengal in 2015, yielding both upper ocean turbulent flux information as well as clean *in situ* measurements of temperature within a few centimeters of the ocean's surface.

8.6 Concluding Remarks

The above examples highlight recent approaches that have increased our physical sampling capabilities by adapting time-tested technology, integrating platforms, leveraging the strengths of expendable systems, and developing new sensing capabilities. In addition, novel remote sensing products will undoubtedly play a fundamental role in IndOOS (Chapter 6), as well as key advances in biogeochemical sensing technologies which can take advantage of existing and new platforms.

Continued advancements in technology and analysis techniques will be critical to achieving the IndOOS goals. To support these advancements, partnerships are critical, through which interested groups and countries buy into existing infrastructures under the GOOS umbrella and

add sensors as needed, such as successfully done through RAMA. This same model could be applied to an IndOOS glider and mooring infrastructure.

8.7 Actionable Recommendations

Future efforts to sustain and improve the capabilities of the IndOOS should look to novel approaches that integrate complementary combinations of platforms. Key components of the observing system where recent technological advancements and synergies between platforms could be leveraged include the following:

A. Monitoring boundary currents with arrays comprising CPIES, gliders, and moorings, possibly with Articulating Profilers or LAMPs in the future, in regions like the Somali, Leeuwin, and Agulhas Currents.

B. Investigating the remote Indian Ocean interior with autonomous or expendable platforms that incorporate traditional and new sensor technologies including DWS drifters (with SST and GPS sensors), χ-SOLO floats, X-Spar floats, Saildrones, Wave Gliders, and Minimets.

C. Continued integration of χ-pods on RAMA moorings to examine seasonal transitions within the equatorial wave guide and the accompanying atmospheric and oceanic variability.

D. Auto-launchers to enable doubling of XBT sampling on some key lines like IX01, that monitors exchanges between the Pacific and Indian Oceans.

E. Outfitting commercial vessels with hull-mounted ADCPs to provide a measure of the heat flux across key lines like the southern boundary of the Indian Ocean.

9. Operational Subseasonal-to-Seasonal (S2S) Forecasting

Aneesh C. Subramanian[1], Frederic Vitart[2], Chidong Zhang[3], Arun Kumar[4] and Magdalena A. Balmaseda[2]

[1]University of Colorado, Boulder, USA, [2]European Centre for Medium-Range Weather Forecasts (ECMWF), UK, [3]PMEL/NOAA,USA, [4]NOAA, USA

9.1 Introduction

Modes of intraseasonal to seasonal variability (ISV) in the tropical Indian ocean-atmosphere system form a bridge between weather systems and longer term interannual and decadal modes of variability which are the source of important climate anomalies throughout the globe (Chapters 13 and 14). The eastward propagating Madden–Julian Oscillation (MJO) is the most common and energetic mode of ISV in the tropics (Madden and Julian, 1972, 1994; Wheeler and Kiladis, 1999; Zhang et al., 2005; Lau and Waliser, 2011). The MJO is a planetary scale convectively coupled eastward propagating disturbance of 30–60 day periodicity. The monsoon intraseasonal oscillation (MISO) is another important ISV in the Indian Ocean, a quasi-oscillatory mode manifesting as eastward and northward propagating convective rainbands that modulate the Asian summer monsoon in the region (Goswami et al., 2005; Waliser et al., 2006a, b). The processes behind MISO, such as moisture sensitivity and surface-feedbacks, are not well understood and are likely different from those that govern the MJO dynamics (Goswami et al., 2005 and references therein). Global climate models (GCM) have problems simulating and predicting the salient features of MISO and the MJO. Major deficiencies are observed in forecasting their spatial structure and northward propagation (Sperber et al., 2001; Kang et al., 2002; Waliser et al., 2003; Sperber and Annamalai, 2008; Lin et al., 2008; Sperber et al., 2013; Sabeerali et al., 2013).

On seasonal timescales, contemporary dynamical forecast systems have little forecast skill beyond two months. Predictions of tropical SST variations are no better than persistence (e.g. Stockdale et al., 2006) due to a combination of model error, bias in the mean state, and deficient oceanic initial conditions (Wajsowicz, 2007; Luo et al., 2007). Seasonal variations in Indian Ocean SST are influenced by the Australian–Asian monsoon and by chaotic forcing from intraseasonal oscillations in both the atmosphere and ocean. At the same time subsurface dynamics, including tropical ocean waves and coastal currents, govern some of the memory in the system (Schott et al., 2009) and can act as a source of predictability. Hence, while forecast skill of SST in this region is limited, it can be improved by improving oceanic initial conditions.

9.2 Modeling, Observation, and Prediction

The current generation of climate and weather forecasting models have limited prediction skill compared to the potential predictability of the MISO events (Lee et al., 2015; Neena et al., 2015). The fidelity of simulated MISOs in GCMs depends on the representation of air-sea interaction over the tropical Indian Ocean (Wang and Schlesinger, 1999; Lin et al., 2006; Zhou et al., 2012).

Recent international field campaigns in the central equatorial Indian Ocean and Bay of Bengal (BoB) are leading to a better understanding of the coupled atmosphere-ocean dynamics in the region. The Dynamics of the MJO (DYNAMO) field campaign in 2011-12 (Yoneyama et al.,

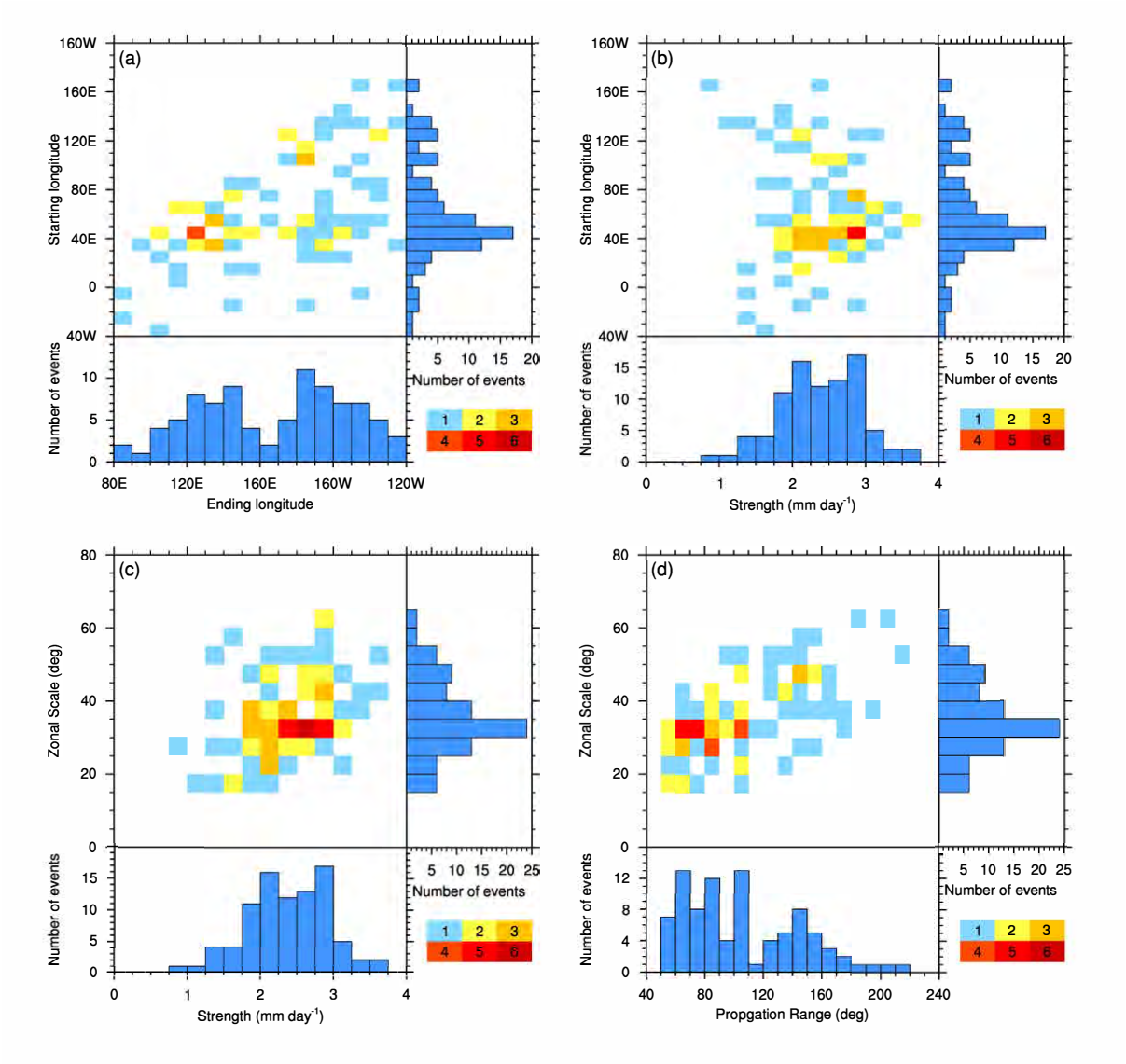

Figure 9.1 Distributions of tracked MJO events using the TRMM precipitation data. (a) starting vs ending longitudes, (b) starting longitudes vs mean strength, (c) mean zonal scales vs mean strength, and (d) mean zonal scales vs propagation ranges. Colors of the joint distributions represent the number of events. Source: Zhang and Ling (2017)

2013) and the Air-Sea Interactions in the Northern Indian Ocean (ASIRI) in 2013-2017 combined mature and new observational platforms to study multiscale dynamics, thermodynamics, and air-sea interaction. Observations revealed rich frontal features, sub-mesoscale variability, shallow barrier layers that reduce mixing, strong wind-forced surface currents, and significant diurnal modes of air-sea interaction all of which affect SST variability, MJO, and MISO.

Most MJOs, when tracked using precipitation signals, are now seen to form over the Indian Ocean (Figure 9.1a; Ling et al., 2012; Zhang and Ling, 2017) with a peak near the Seychelles-Chagos Thermocline Ridge, while previous results, derived from the Rainfall Measuring Mission (RMM) index, suggested genesis over the entire tropics (Matthews et al., 2008). Dissipation occurs preferentially over the Maritime Continent, which is a barrier to MJO propagation, or over the central Pacific once it reaches the cold SSTs east of the western Pacific warm pool (Figure 9.1a).

The role of coupled processes in the MJO has been investigated in the European Centre for Medium-Range Weather Forecasts Extended-Range Forecasting System. A series of subseasonal (extended range) forecasts were initialized daily over a time period coincident with Tropical mooring (TOGA-COARE) observations. Forecasts were performed with SSTs provided by persistence of initial conditions, with observed SSTs, and with SSTs simulated through coupling to a full dynamical ocean model. The subseasonal experiment with the full dynamical ocean model showed the most forecast skill for the MJO, indicating a significant role for coupled processes (Figure 9.2). Sensitivity experiments performed in this context further showed that simulation of the diurnal cycle, requiring 10 m vertical resolution in the upper ocean, is a significant factor in improving the forecast skill (Woolnough et al., 2007; Ge et al., 2017). Other work with the ECMWF extended-range and seasonal systems shows that the oceanic initial conditions influence the amplitude of the spread, and therefore the potential predictability, of SST in the Eastern Indian Ocean, a key region influencing the MJO, ENSO, and Indian Ocean Dipole .

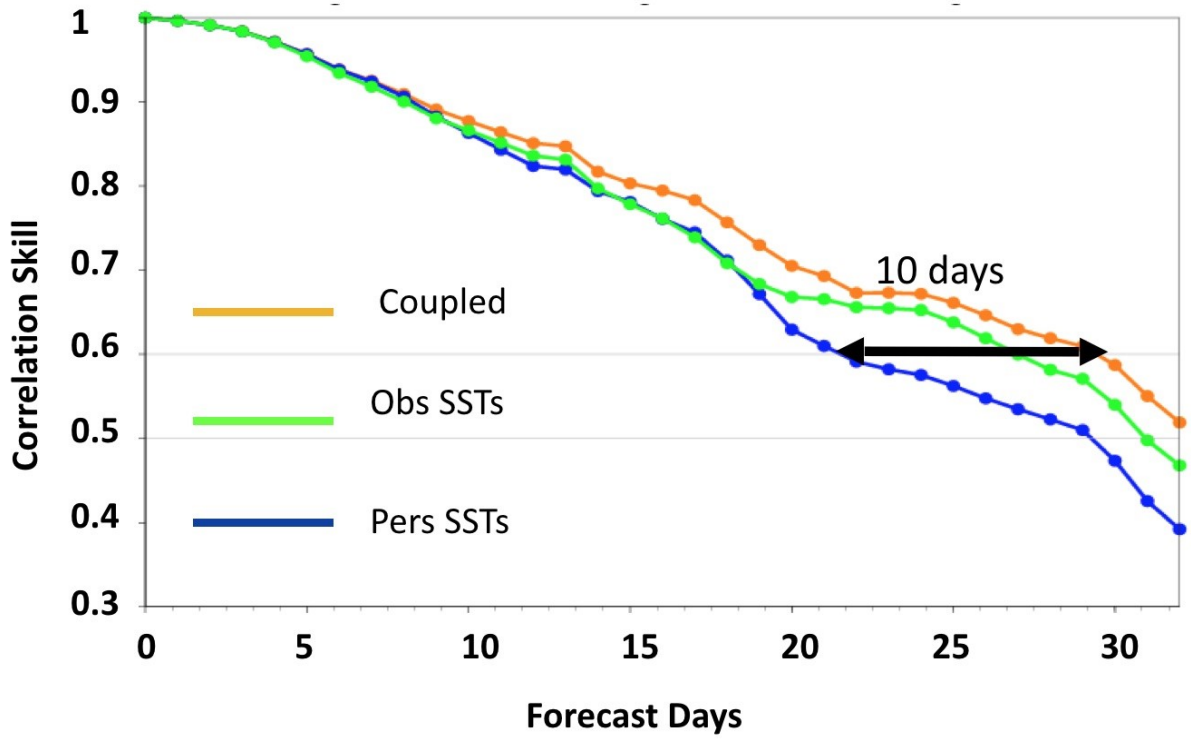

Figure 9.2 Correlation of the observed RMM rainfall times series with the ensemble mean forecast time series for experiments initiated with observed SSTs (green line), coupled ocean SSTs (orange line), and persistent SSTs (blue line). Observations and inclusion of air-sea coupling improves predictions.

ENSO is a major source of predictability of SST and climate variability in the tropical Indian Ocean. The Indian Ocean also supports its own interannual mode of coupled ocean-atmosphere variability, the IOD (Saji et al., 1999; Webster et al., 1999). The IOD develops independently, but interacts strongly with ENSO (e.g. Lau and Nath, 2004; Behera et al., 2006) and generates low-frequency variations in rainfall anomalies over southeast Asia, Africa, and Australia (Clark et al., 2003; Saji et al., 2006; Meyers et al., 2007). Hence IOD acts as a source of climate predictability over the region and globally, beyond that of ENSO.

IOD predictions show skill for up to one season, with a boreal spring prediction barrier (Wajsowicz et al., 2007; Luo et al., 2007). Forecast skill is limited by model mean-state biases and

model physics errors, as well as limitations in the number of observations and in assimilation methods that provide initial conditions. Current generation ocean models have large-scale, mean-state biases over the Indian Ocean, in particular the mean east–west gradients of thermocline depth and SST (Cai et al., 2005; Saji et al., 2006). Improved understanding and model representation of sub-grid-scale processes, like upper ocean diapycnal mixing, can help reduce these mean state biases and improve IOD prediction skill.

In summary, with an increasing need for subseasonal to seasonal (S2S) forecasting, these recent results show that sustained, colocated observations of the ocean and atmosphere that resolve diurnal time scales and small-scale upper-ocean processes, are required in key regions across the tropical Indian Ocean. These observations, as part of IndOOS, are vital for improving model representations and parameterizations of ISV and for providing real-time data of oceanic initial conditions for S2S forecasts. The development of improved coupled data assimilation methods that can maximize the efficacy of such observations for initialization of extended range forecasts and for reanalyses applications is also a necessity.

9.3 Essential Ocean Variables (EOV)

Observations of surface heat fluxes, temperature, salinity, and upper ocean mixing at diurnal time scales in the tropical Indian Ocean are crucial for improving S2S forecasts in the region, due to their key role in the evolution of MJO and MISO events. Observations in the eastern tropical Indian Ocean and the Bay of Bengal are of particular importance. Required EOVs are temperature, salinity, velocity at the surface of the ocean and over the upper 50 m, plus 10 m winds, 2m air temperature and humidity, precipitation, shortwave and longwave radiation every hour (minimum 3 hours) to resolve the diurnal cycle. The spatial resolution of these measurements needs to be 5° in longitude ($\sim$1110 km) and 1° in latitude ($\sim$111 km) near the equator to resolve the equatorial wave guide.

9.4 Actionable Recommendations

Maintaining the core networks of IndOOS, especially the RAMA array, Argo program, and suite of satellite measurements, is the first priority. Recommendations for future enhancements that can improve S2S forecasting are:

A. Increase the vertical resolution of upper ocean sensors on RAMA buoys to better resolve the shallow diurnal warm layer and night time mixed layer deepening. Suggested depths of temperature and conductivity sensors are: 0.5 m, 1 m, 2 m, 3 m, 5 m, 7 m, 10 m, and every 5 m down to 50 m

B. Add a new RAMA site in the eastern Indian Ocean off the northwest coast of Australia, with upper ocean temperature/salinity sensors and a meteorological station.

C. Add surface flux reference sites in the western Indian Ocean (equatorial and Arabian Sea).

D. Enhance some of the existing upper ocean measurements at RAMA sites with concurrent high frequency meteorological measurements.

E. Increase observations in coastal regions, especially near the Maritime Continent.

10. Improvement of Surface Fluxes

Lisan Yu[1], and Michael J. McPhaden[2]

[1]Woods Hole Oceanographic Institution, Woods Hole, MA, USA, [2]NOAA/Pacific Marine Environmental Laboratory, Seattle, WA

10.1 Ten years of progress in air-sea flux climatologies

When designing RAMA 10 years ago (McPhaden et al., 2009), there was strong consensus on the need for sites with enhanced measurement capabilities for comprehensive air–sea fluxes (i.e., "flux reference site" moorings) in key dynamical regimes. The rationale was plain and clear: Better surface heat and moisture flux climatologies are highly desirable in regions where surface fluxes dominate mixed-layer temperature and salinity variability over diurnal to intraseasonal and longer timescales (e.g. Yaremchuk et al., 2006; Yu et al., 2007). Better surface fluxes are essential for improving numerical weather prediction and climate forecast skills, and for understanding the mechanisms responsible for frontal-scale air-sea interaction over western boundary currents (Chapter 23). During the RAMA design phase, the six surface-flux climatologies available at that time were examined to determine their quality and to help develop strategies for air-sea measurements (Yu et al., 2007). The six flux products showed large discrepancies over the Indian Ocean (Figure 10.1). The standard deviation (STD) in the long-term mean net heat flux (Q_{net}) exceeded 25 Wm^{-2} over almost the entire basin north of 20°S, with the maximum difference of 40 Wm^{-2} occurring in the vicinity of the Somali Current.

The Q_{net} going into the ocean is the sum of a number of heat exchange processes at the air-sea interface. These processes include incoming and reflected solar radiation, outgoing and re-emitted longwave radiation, sensible heat (SH) transfer by conduction and convection, and latent heat (LH) release by evaporation of sea surface water. In general, these heat flux components are computed from parameterizations using surface meteorological variables obtained from numerical weather prediction (NWP) reanalysis, ship reports from the Comprehensive Ocean-Atmosphere Data Set (COADS), and satellite retrievals. These data sources have different biases that result from sampling frequency, coverage, and statistical and/or dynamical interpolation frameworks. Moreover, different flux algorithms incorporate different physical and/or statistical approaches. These factors could account for the significant differences among the surface flux products.

During the past 10 years, significant progress has been made in surface flux estimates, from both satellite analyses and atmospheric reanalyses, due largely to two factors. The first factor is the ever-advancing satellite technology for retrieving flux-related variables, such as SST and near-surface wind, and, most significantly, surface radiation products. The CERES instrument onboard the polar-orbiting Aqua satellite and follow-on missions since 2000 provided the first-ever complete coverage of an accurate energy budget and cloud observations over the Indian basin, from which the surface radiative budget can be computed using an energy balanced and filled (EBAF) approach (Kato et al., 2013). Previous surface radiation products, such as ISCCP and GEWEX SRB, were constructed from geostationary satellites, which have a broad gap in coverage over the Indian Ocean (Zhang et al., 2004). This gap has been a major obstacle for estimating basin-scale spatial and temporal variability and trends of Q_{net} in recent decades, coincident with a period of unprecedented rise in SST and heat content (Roxy et al., 2014; Lee et al., 2015). The second factor is successive generations of atmospheric reanalyses that have improved in quality as a result of better physical models, more observations to constrain the

models, and better assimilation methods. There has been a wave of updated versions of global reanalyses from NCEP (Saha et al., 2010), JMA (Kobayashi et al., 2015), NASA (Rienecker et al., 2011), and ECMWF (Dee et al., 2011).

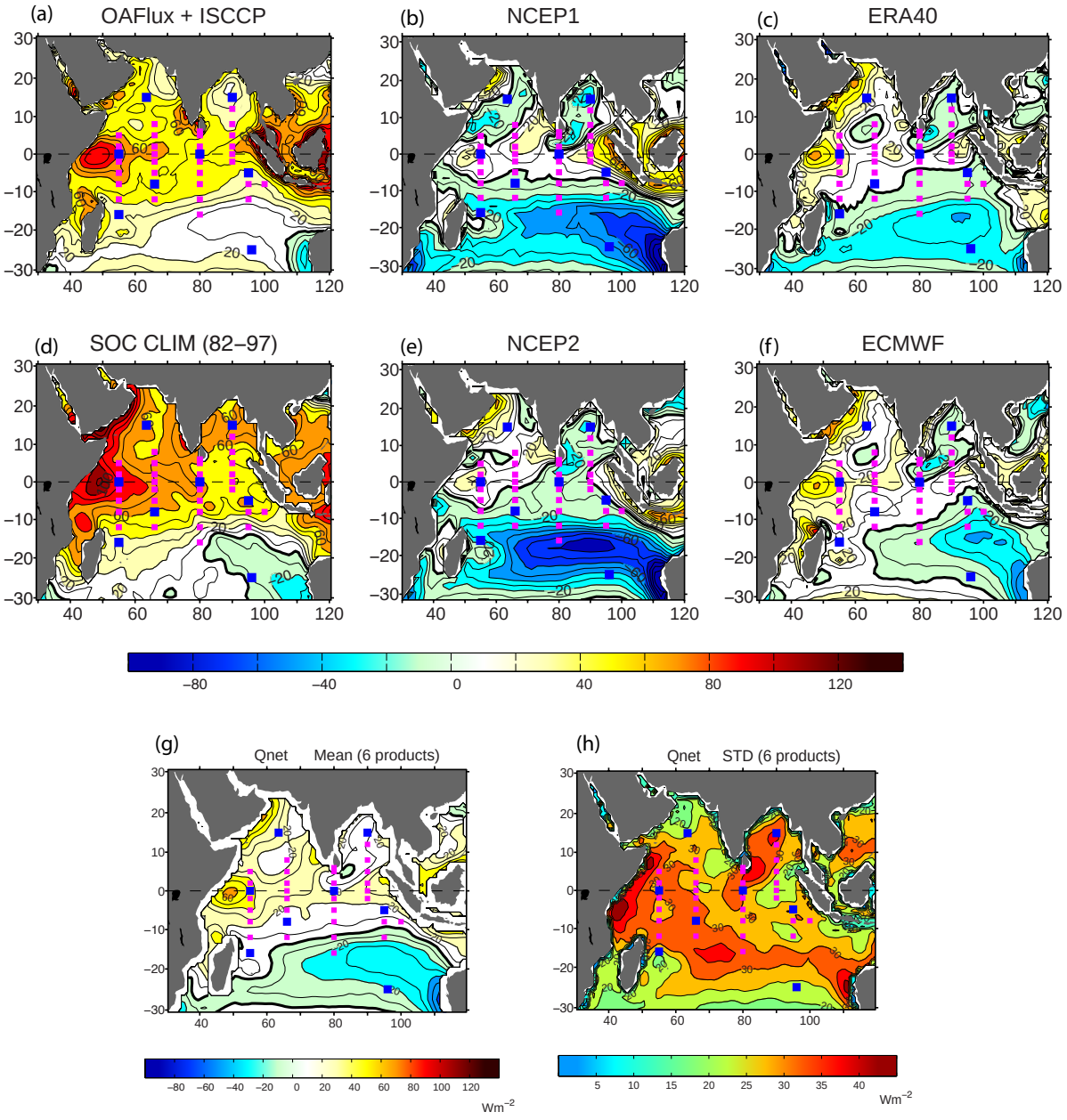

Figure 10.1 Time-mean Q_{net} from (a) OAFlux+ISCCP, (b) NCEP1, (c) ERA40, (d) SOC, (e) NCEP2, and (f) ECMWF for the period 1988-2000. (g) ensemble mean and (h) STD spread of these 6 Q_{net} products (adapted from Yu et al., 2007). The designed RAMA buoy locations are superimposed, and those marked by blue squares denote flux reference sites.

To examine the degree of improvement over the past 10 years, we evaluate Q_{net} using 6 of the latest products (Figures 10.2a-f), constructing their ensemble mean (Figure 10.2g) and STD (Figure 10.2h) for the period 2001-2010. Compared to the Q_{net} ensemble mean of 10 years ago (Figure 10.1), the present Q_{net} shows a similar spatial pattern but with enhanced magnitude in both maximum net heat gain ($Q_{net}>0$) and maximum net heat loss ($Q_{net}<0$) regimes.

The maximum oceanic net heat gain occurs in the western equatorial region off the coast of Somalia and is enhanced by about 10 Wm^{-2}. The maximum net heat loss occurs over the southeastern subtropical basin and is also enhanced by about 10 Wm^{-2}. Compared to the Q_{net} ensemble spread of 10 years ago (Figure 10.1h versus Figure 10.2h), the spread in the 6 recent Q_{net}products is 50% less, with the STD difference of 25 Wm^{-2} confined mostly to the equatorial region and the Somali and Agulhas Current regions.

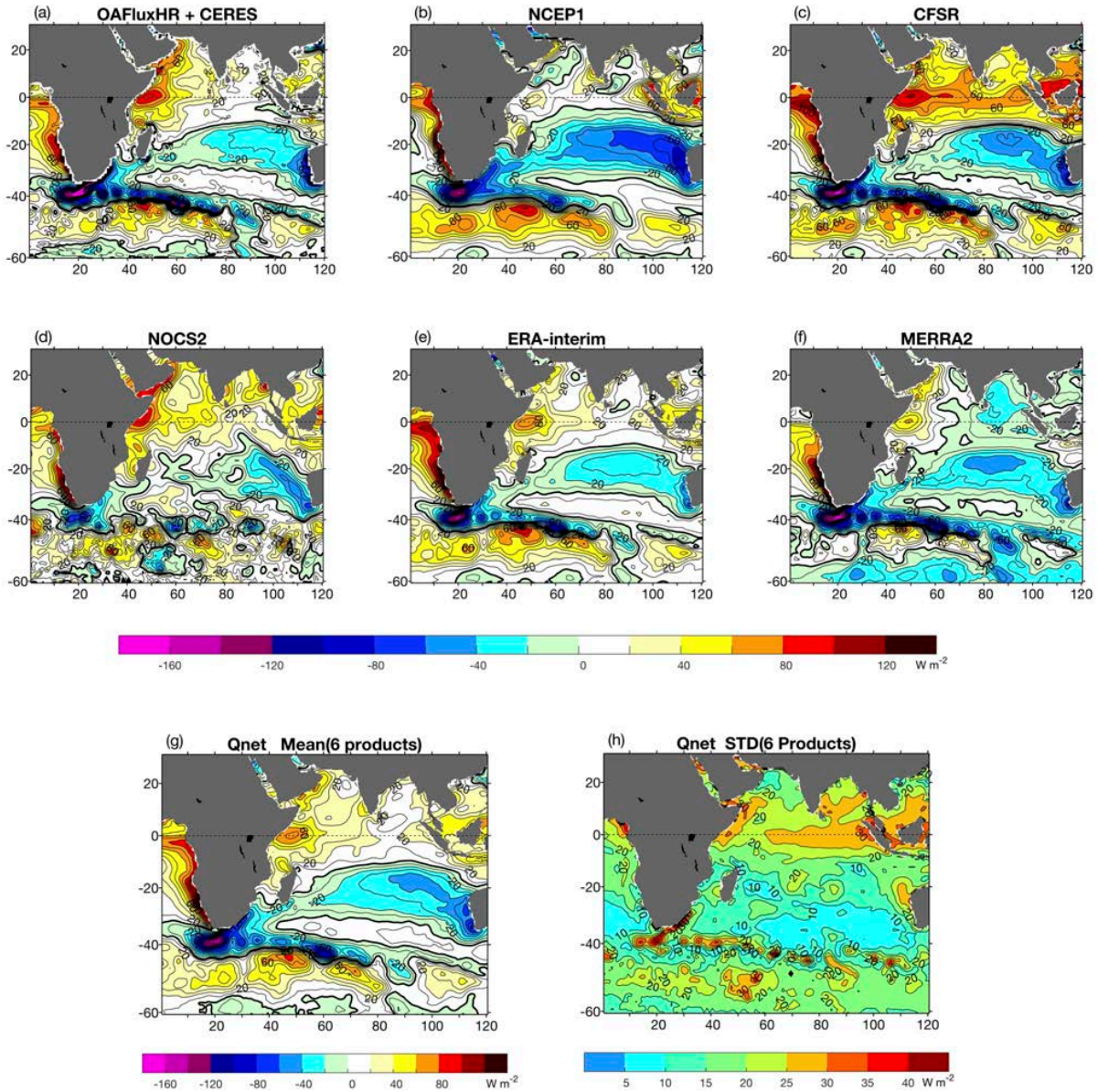

Figure 10.2 Time-mean Q_{net} from (a) OAFluxHR+CERES, (b) NCEP1, (c) CFSR, (d) NOCS2, (e) ERA-interim, and (f) MERRA2 for the period 2001-2010. (g) ensemble mean and (h) STD spread of these 6 Q_{net} products.

Reduction in the mean Q_{net} is most evident in the CERES EBAF and the newly developed satellite-only, high-resolution OAFlux (OAFlux-HR) data sets (Figure 10.2a). This combined satellite Q_{net} captures net heat loss over the subtropical Indian Ocean, a major correction to the basin-wide warm bias in OAFlux+ISCCP. The correction can be attributed to better surface radiation products from CERES (Kato et al., 2013) and to an improved turbulent bulk flux algorithm (Jim Edson et al., 2017 personal communication) in the OAFlux-HR computation. Q_{net} is

also reduced in NOC2.0 (previously SOC) using ICOAD ship reports (Figure 10.2d; Berry and Kent 2009), possibly due to increased sampling in the region. On the other hand, the agreement between the four reanalyses of Q_{net} is still poor. CFSR has an excessive net heat gain (+80 Wm^{-2}) in the equatorial region, and MERRA2 has an excessive net heat loss (-30 Wm^{-2}) in the Bay of Bengal and eastern tropics (Figures 10.2c and 10.2f). The differences in these two products account for a large portion of the STD between all products (Figure 10.1e). Significantly, despite the fact that ERA-interim and OAFlux-HR + CERES are independent, with one produced by a reanalysis system and the other constructed from satellite retrievals, the two exhibit broad-scale consistency both in spatial pattern and magnitude.

10.2 Sources of uncertainty and the role of RAMA reference sites

Despite significant progress over the past decade, the spread in Q_{net} mean values remains large (20 Wm^{-2}) over the tropical Indian Ocean north of 10°S (Figure 10.1e). Yu et al., (2017) point out that reanalysis models balance total energy at the top of the atmosphere, rather than at the surface. Without an energy balance constraint at the ocean surface the errors in each flux component add up and give rise to large biases in mean Q_{net} (Figure 10.3). Given this, improving model parameterizations of surface flux processes might be the only way to improve mean Q_{net} from reanalyses.

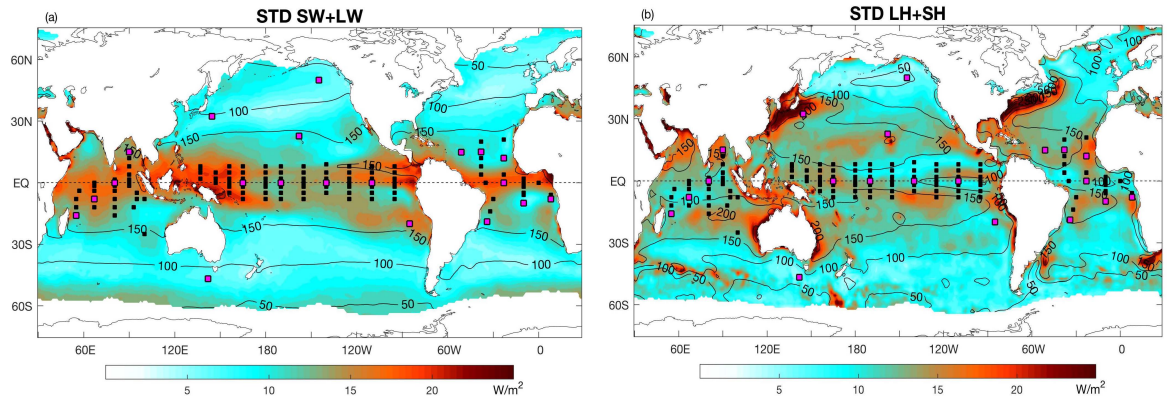

Figure 10.3 Standard deviations (STD) of the means based on 14 products for (a) SW+LW and (b) LH+SH. Black contours denote the ensemble mean patterns. The location of the global tropical moored buoy array is superimposed, with pink squares indicating flux reference sites.

To illustrate the leading sources of uncertainty in mean Q_{net}, 14 products are compared, including 9 reanalyses (NCEP1, NCEP2, CFSR, ERA-interim, ERA-20C, MERRA, MERRA-2, JRA55, 20CR), 4 satellite products (ISCCP, SRB, CERES, OAFlux-HR), and 1 ship-based product (NOC), over the 10-year period from 2001-2010. The standard deviations of the mean surface radiation (net shortwave plus longwave (SW+LW)) and turbulent latent and sensible heat fluxes (LH+SH) show that the uncertainty in SW+LW dominates the uncertainty in Q_{net} in the tropical Indian Ocean (Figures 10.3a,b). Net freshwater flux (evaporation-minus-precipitation) products show a similar spread and pattern in the mean precipitation (Yu et al., 2017). These uncertainties are not unique to the Indian Ocean, but are common to reanalyses in all tropical warm pool waters and indicate that the long-standing problem of tropical convective cloud parameterizations impacting the surface radiative budget and leading to major errors in the net heat balance at the tropical ocean surface.

10.3 Air-sea flux EOVs

Ocean-surface wind stress is a flux EOV. It has been recommended that turbulent latent and sensible heat fluxes also be designated as flux EOVs. Since energy and freshwater budgets do not close at the ocean surface in the reanalysis systems, use of reanalysis products for flux estimates in the near future is not promising. One exception is the ERA-interim product, for which the mean Q_{net} is more consistent with satellite-based products and buoys than other reanalyses. However, the time series of ERA-interim has spurious trends, induced by the injection of new SST datasets (e.g. Liang and Yu 2016). Improvement of parameterizations of tropical convective clouds, as a first priority, will improve reanalysis products.

Satellite products are promising for providing high quality, gridded flux estimates into the future. However, none of the surface heat flux components are directly retrieved by remote sensing. Surface radiation is computed from the radiation observed at the top of the atmosphere using an energy balanced and filled approach (Kato et al., 2013). Surface moisture and heat fluxes are computed from bulk flux parameterization which require surface meteorological observations (SST, wind, near-surface air temperature and humidity). Retrieving near-surface air temperature and humidity from satellite scanners and sounders remains difficult (Yu and Jin 2018) and the uncertainty in bulk flux algorithms is not negligible (Brunke et al., 2002). Thus, we need flux reference sites at the ocean surface to validate improvements and new developments of satellite retrieval algorithms and flux products. Sustained observations, as part of the Global Tropical Moored Buoy Array (McPhaden et al., 2010) and the OceanSites program (Send et al., 2010), are also vital constraints for atmospheric analyses and reanalyses.

10.4 Actionable Recommendations

A. Implement unoccupied flux reference sites in Arabian Sea and western Indian Ocean and maintain established flux reference sites in the revised RAMA-2.0 design (Chapter 2).

B. Re-establish a flux reference site in the eastern subtropical gyre subduction region.

C. Enhance a subset of the flux reference sites with direct flux measurements to validate bulk algorithm flux computations.

D. Engage with the atmospheric reanalysis community to evaluate and guide the future improvement of tropical convective parameterizations.

E. Engage with the satellite surface radiation producers to diagnose and validate surface radiative products.

11. Ocean Data Assimilation Systems

Tong Lee[1,2]

[1]NASA Jet Propulsion Laboratory (JPL), [2]California Institute of Technology, USA

11.1 Ocean state estimation as a driver of IndOOS

Ocean data assimilation (ODA) systems are important tools for characterizing and understanding ocean variability, evaluating observing system impacts, initializing climate prediction, and driving biogeochemistry models. One of the priorities for the IndOOS is to provide quality data across many spatio-temporal scales to improve the ODA products.

Prior to the mid 2000s, ODA systems were primarily constrained by satellite-derived SST and SSH data augmented by sparse *in situ* measurements from the XBT network. The lack of *in situ* data limited the constraints and evaluation of subsurface ocean structure from ODA products, especially currents and salinity. The development of IndOOS since the mid 2000s has already led to improvements in ODA products. The assimilation of Argo salinity data into NOAA's National Center for Environmental Prediction (NCEP) Global Ocean Data Assimilation System (GODAS) significantly reduced regional salinity biases, including the thickness of the barrier layer (Huang et al., 2008) (Figure 11.1), and representations of zonal currents and SSH in the tropical Indian Ocean. IndOOS *in situ* data have also led to the evaluation and improvement of subsurface temperature and salinity, surface and subsurface currents, and SSH in the ODA system of the Indian National Centre for Ocean Information Services (INCOIS), which is developed from NCEP's GODAS system in collaboration with NCEP (Rahaman et al., 2016).

In the past decade there has been significant progress in the development of ODA systems and their use for operational oceanography, for initialization of seasonal-to-interannual prediction, and for analyses of seasonal-to-decadal variability of ocean circulation (Dombrowsky et al., 2009; Lee et al., 2009; Fujii et al., 2015). IndOOS observations, from both *in situ* and satellite platforms, have provided the backbone for this progress (https://www.godae-oceanview.org/science/ocean-forecasting-systems/assimilation-characteristics/). IndOOS data are fundamental, not only for the improvement of individual ODA systems, but for assessing consistency and fidelity among ODA systems. For instance, as part of GOOS, IndOOS data have been integral to the evaluation and intercomparison of ODA systems under the Ocean ReAnalysis Intercomparison Project (ORA-IP, Balmaseda et al., 2015) and its extension, the CREATE project (Collaborative REAnalysis Technical Environment, https://esgf.nccs.nasa.gov/projects/create-ip/data_description#OceanRe), which have shown that consistency among an ensemble of multi-decadal ODA products mapped onto a common grid has improved markedly since the development of the IndOOS in the 2000s (Figure 11.2).

11.2 Future observational needs and recommendations

Despite the encouraging improvements brought by the establishment of IndOOS there remain significant discrepancies among ODA products and between ODA products and observations. These arise from limitations in forward ocean models and data assimilation schemes, as well as from remaining gaps in observations. Improving ocean models and data assimilation methods is a long-term effort requiring many decades of sustained observing through the IndOOS. For instance, testing the impacts of ODA on initializing seasonal-to-decadal predictions requires observations over many realizations of interannual and decadal events.

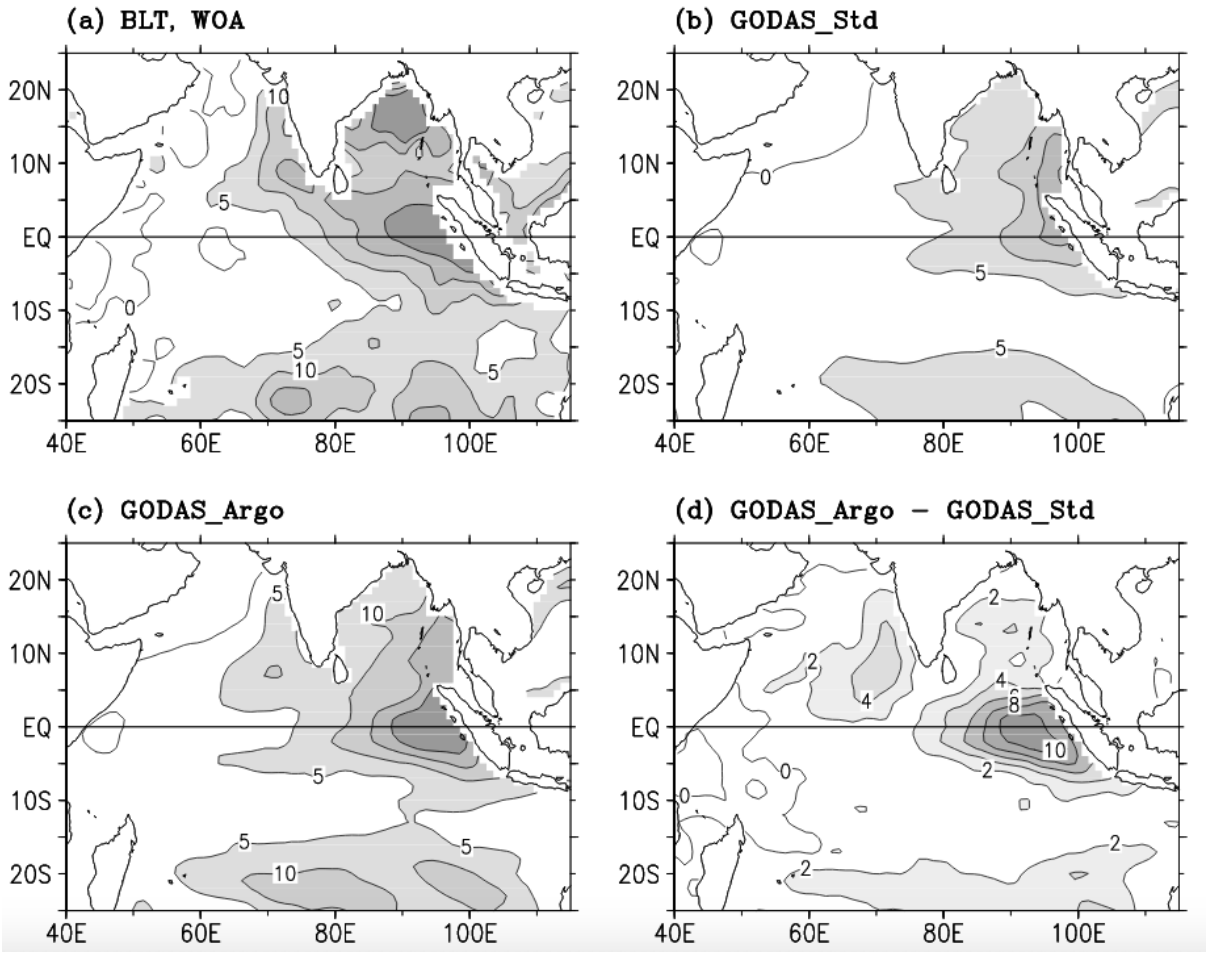

Figure 11.1 Barrier-layer thickness inferred from (a) observations from the World Ocean Atlas, (b) GODAS assimilation without Argo data, (c) GODAS assimilation with Argo data, and (d) the difference between (c) and (b). After Huang et al. (2008).

Enhancements of IndOOS are also necessary. For example, the role of the deep ocean below 2000 m - the maximum profiling depth of the current Argo array - will become important at multi-decadal time scales, yet the deep ocean is currently ill constrained in ODA products (Palmer et al., 2017, Storto et al., 2017) prompting for new deep-Argo profiles. Coastal regions, where boundary currents carry important meridional fluxes of heat, freshwater, and nutrients, are not sampled, or are poorly sampled, by IndOOS (Chapters 17, 23). Continuity and enhancement of satellite measurements (Chapter 6) are also needed. In particular, improved temporal sampling of wind stress to capture the diurnal cycle, and improved spatial resolution and quality of SSS data, which dominates stratification over much of the Bay of Bengal and eastern tropical Indian Ocean.

Observing the Indonesian Throughflow (ITF) is of particular importance to the Indian Ocean heat and nutrient budgets, yet it is currently not monitored adequately. The data from the IX1 XBT line provides estimates of its geostrophic transport only down to 750 m (e.g. Wijffels et al., 2008) and salinity, and therefore density, must be inferred from a climatological temperature-salinity relationship. Water mass changes and transport deeper than 750 m are not accounted for. ODA products have significant discrepancies in their representation of the heat and freshwater fluxes of the ITF (Lee et al., 2010), which have ramifications on the state of the Indian Ocean. An improved sustained observing system for the ITF is a priority.

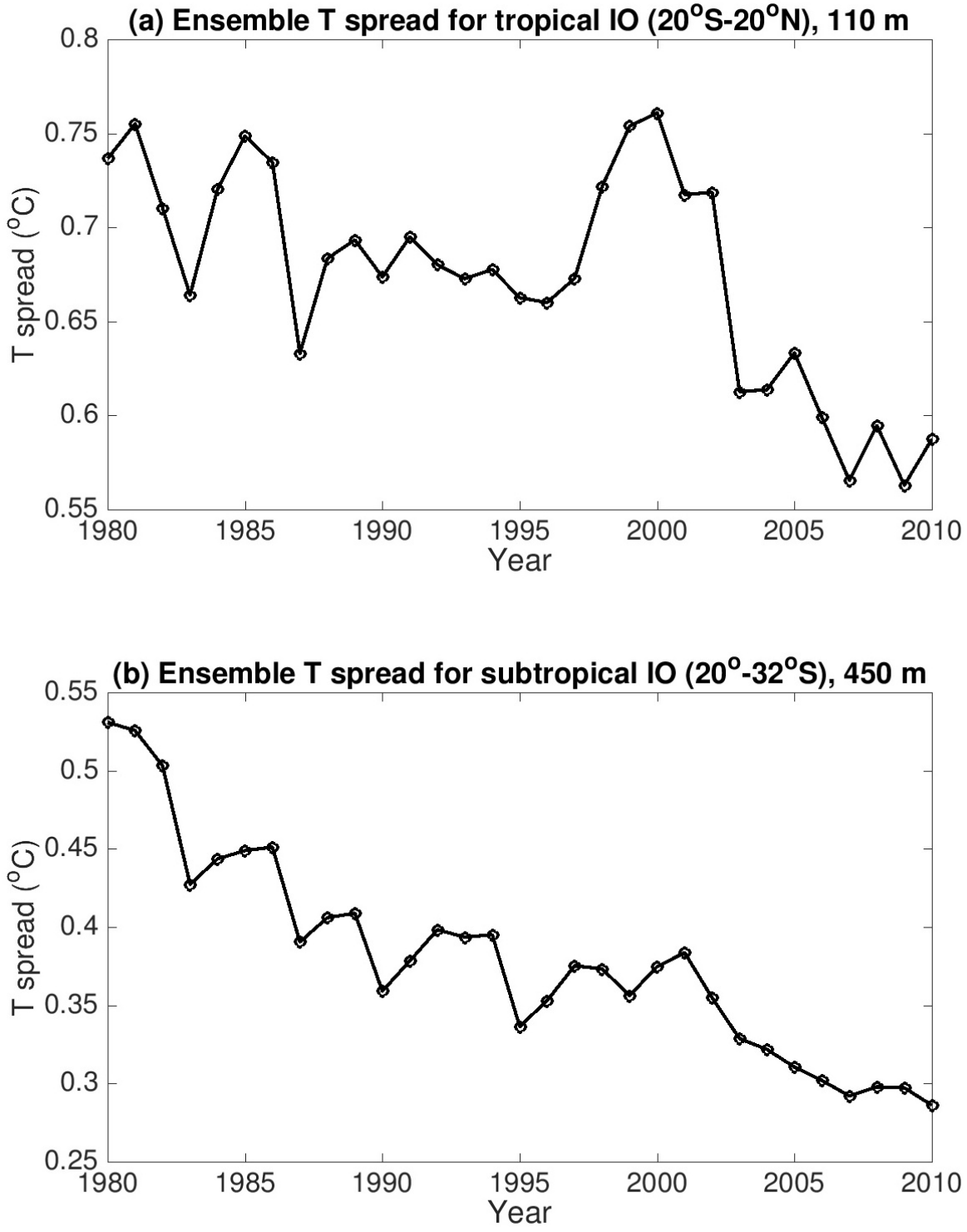

Figure 11.2 Ensemble spread of subsurface temperature near the thermocline in (a) the tropical and (b) the subtropical Indian Ocean among eight multi-decadal ocean state estimation products. The consistency is significantly better since the mid 2000s and the development of the IndOOS, as indicated by reduced spread.

While the ITF dominates exchanges between the Indian Ocean and the Pacific in the trop-

ics, the Agulhas Current and the circulation across the southern boundary of the Indian Ocean (near 34°S) are critical to understanding subtropical climate in the basin and to monitoring exchanges with the Atlantic and Southern Oceans (Biastoch et al., 2009, Beal and Elipot, 2016). No effort has been made to examine the consistency of ODA products in characterizing these inter-ocean exchanges. However, due to the lack of sustained measurements of the Agulhas Current and the meridional transports across the southern boundary, it is likely that ODA systems are under-constrained with respect to these inter-ocean exchanges. Long-term monitoring of the Agulhas Current (Morris et al., 2017) and the meridional transports across the basin (e.g., McDonagh et al., 2005) must be a priority for the IndOOS.

Currently, most ODA systems do not assimilate surface meteorology measurements from IndOOS. However, coupled ocean-atmosphere data assimilation is emerging (Saha et al., 2010) and more measurements of the ocean-atmosphere boundary layer will be needed to ensure consistency between state estimates of the ocean and atmosphere with regard to air-sea fluxes as well as climate predictions across different time scales (Penny and Hamill, 2017). Necessary observations include not only the air-sea fluxes of momentum, heat, and freshwater, but also observations of upper-ocean stratification and currents that influence these interactions. Enhancement of these measurements will be important for the future generation of coupled assimilation systems.

ODAs and coupled assimilation systems can also be used to evaluate the relative impact of observing system elements on state estimates and climate predictions through Observing System Experiments (OSE) for existing observations and through Observing System Simulation Experiments (OSSE) for future observations (Fujii et al., 2015, Penny and Hamill, 2017). Such experiments have the potential to provide guidance on how to prioritize observations for IndOOS and its future enhancement. However, the results from OSE and OSSE are system dependent and are affected by the limitations in the forward models and data assimilation schemes and hence it is difficult to objectively measure their success. We recommend coordinated efforts, based on multiple ODAs and with close interactions among modelers, data assimilators, and observationalists to maximize the effectiveness of OSE and OSSE efforts in observing system evaluation and design for the IndOOS.

Based on the above discussion, the recommended actions to improve the consistency and fidelity of ODA products, in support of the science and operational drivers of IndOOS as outlined at the beginning of this review, are provided below.

11.3 EOVs

EOVs required to constrain and improve ODA systems in the context of IndOOS include sea surface temperature and salinity, subsurface temperature and salinity, sea surface height, ocean surface and subsurface currents, ocean surface (wind) stress and heat flux. Although most ODA systems do not assimilate ocean surface stress and ocean surface heat flux these two EOVs directly influence the fidelity of ocean state estimates based on the ODA systems. For systems that use the four-dimensional variational or adjoint method, such as that employed by the Estimating the Circulation and Climate of the Ocean group (ECCO, ecco-group.org), these two EOVs are used to constrain the ocean state estimation (Forget et al., 2015). The same is true for emerging coupled ocean-atmosphere data assimilation systems, such as NOAA's Climate Forecast System Reanalysis (CFSR) (Saha et al., 2010). Similarly, many ODA systems do not assimilate sparse subsurface velocity measurements, however, they are important to the evaluation of ocean state estimates as independent observations.

11.4 Actionable recommendations

A. Augment deep ocean measurements such as deep Argo.

B. Develop a comprehensive monitoring system for the Indonesian Throughflow.

C. Enhance capabilities to monitor subtropical fluxes, in particular the dominant Agulhas Current, at the southern boundary of the basin.

D. Continue development of coupled ocean-atmosphere data assimilation systems.

E. Strengthen collaborations among data assimilators, modelers, and observationalists to improve capabilities for reanalysis, prediction, and observing system evaluation.

12. Extreme Events

Matthieu Lengaigne[1], Ming Feng[2], Satheesh Neetu[3], David Barbary[4], Hamish A. Ramsay[5], Jérôme Vialard[1], and Kevin Walsh[6]

[1]LOCEAN-IPSL, Sorbonne Universités (UPMC, Univ. Paris 06)-CNRS-IRD-MNHN, Paris, France, [2]CSIRO Oceans and Atmosphere, Perth, Western Australia, Australia, [3]CSIR-National Institute of Oceanography (NIO), Goa, India, [4]Equipe cyclone, Laboratoire de l'Atmosphère et des Cyclones (UMR 8105, Meteo-France, CNRS, Reunion University), Saint-Denis de La Réunion, France, [5]CSIRO, Oceans and Atmosphere, Aspendale, Victoria, Australia, [6]School of Earth Sciences, University of Melbourne, Parkville, Victoria, Australia

12.1 Tropical Cyclones

Tropical Cyclone (TC) track prediction has improved dramatically over the last decades, but intensity forecast improvements have comparatively stalled (DeMaria et al., 2013). Various environmental atmospheric conditions influence TC intensification, such as strong vertical wind shear and high mid-tropospheric humidity. Yet, TCs primarily draw their energy from evaporation at the ocean surface, and hence enthalpy flux at the air–sea interface plays an essential role in maintaining and intensifying TCs.

SST has a strong control on the enthalpy flux and hence on TC intensity. Under the TC, kinetic energy dissipated by friction and vertical mixing (Price et al., 1981; Vincent et al., 2012a) at the air-sea interface can cause cooling of SST (Figure 12.1b) and limit TC intensification (Cione and Uhlhorn, 2003). The order of magnitude of this cooling is modulated by oceanic subsurface stratification (Vincent et al., 2012b), with larger cooling in regions with a shallow thermocline, and hence a larger negative feedback on TC intensification. This sensitivity has motivated the need for metrics of oceanic subsurface stratification in statistical forecasts of TC intensity (DeMaria et al., 2005)

The IO is home to $\sim$25% of global TC activity. In the northern IO, TCs are prevalent in the western and central part of the Bay of Bengal (BoB; Figure 12.1a) and exhibit a bimodal seasonal distribution, occurring mostly during the pre- and post-monsoon seasons (Figure 12.1d). In the southern IO TCs occur across the basin, centred at 15°S, from November to April (Figure 12.1a,c), and particularly over the southwestern IO and the islands of Mauritius, La Reunion, and Madagascar (Figure 12.1a). TC characteristics are strongly affected by air-sea coupling processes (Lengaigne et al., 2018) and by climate variability, such as the Madden-Julian Oscillation at intraseasonal timescales (Bessafi and Wheeler, 2006) and El Niño at interannual timescales (Kuleshov et al., 2008). Climate change appears to have increased the intensity of major TCs during the post-monsoon period in the Bay of Bengal (Balaguru et al., 2014) and the pre-monsoon period in the Arabian Sea (Evan and Camargo, 2011). Future projections suggest an increase in the number of the most intense TCs (Knutson et al., 2015), while frequency changes remain uncertain (Murakami et al., 2012).

Unique characteristics of upper ocean thermohaline structure in the IO may result in different ocean-atmosphere coupling compared to other basins and therefore different TC sensitivity. For instance, there can be strong haline stratification in the Bay of Bengal that causes a barrier to mixing and cooling (Thadathil et al., 2016), while the Seychelles-Chagos Thermocline Ridge (SCTR) in the southwestern tropical Indian Ocean is one of the rare oceanic regions where warm SSTs coexist with a shallow thermocline, which can enhance cooling under a TC (Lengaigne et al., 2018).

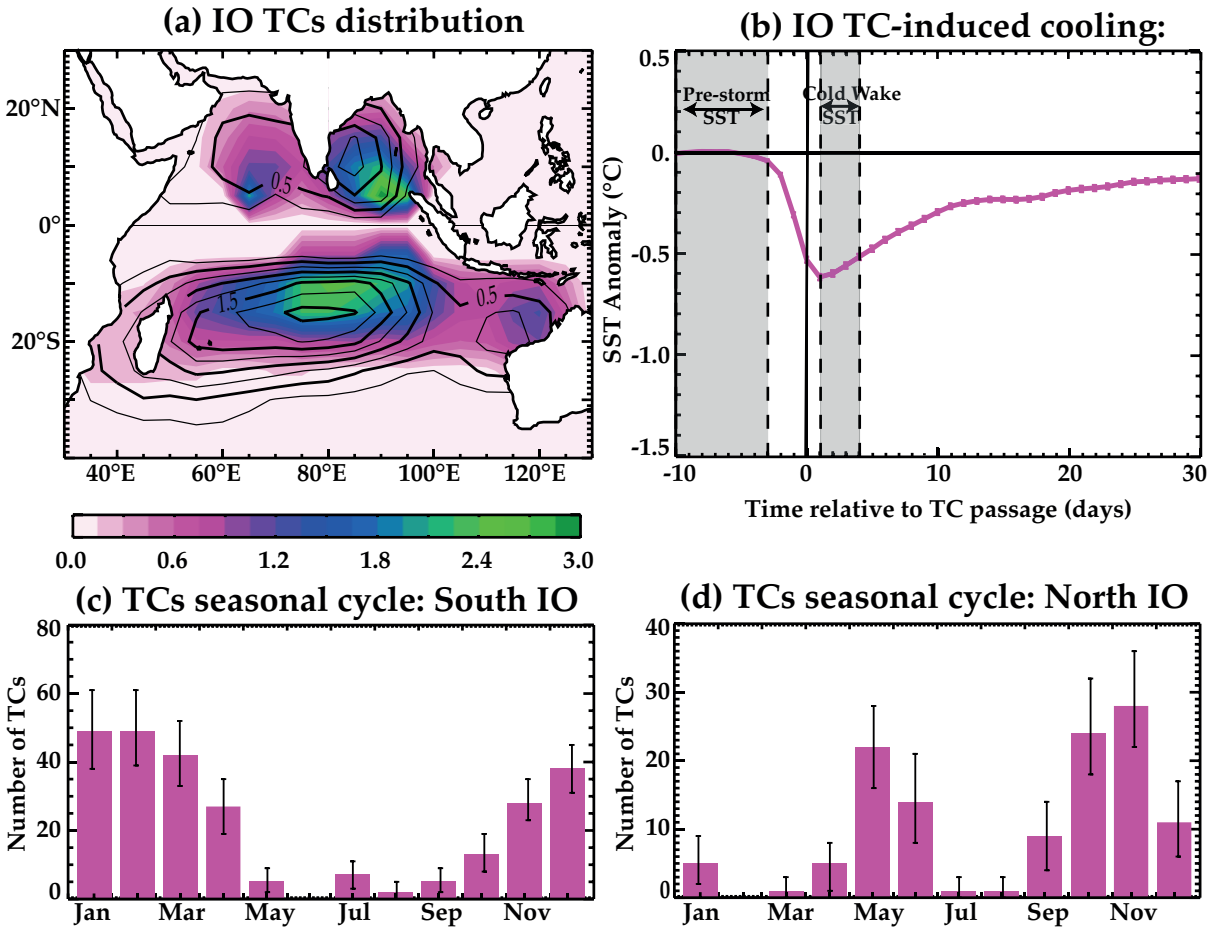

Figure 12.1 (a) Observed climatological distribution of normalized cyclogenesis (color) and TC density (contour) in the IO. (b) Composite evolution of the TC-induced SST cooling within 200 km of all TC-tracks in the IO (°C). Percentage of TCs occurring each calendar month in the (c) southern and (d) northern IO. Observed TC positions and magnitudes are derived from the International Best Track Archive for Climate Stewardship (IBTrACS) (Knapp et al., 2010) over the 1989-2009 period. Observed SST response under TCs is characterized using a blend of satellite SST data (http://www.remss.com/measurements/sea-surface-temperature/oisst-description/). Whiskers on panels b,c,d indicate the 90% confidence level from a bootstrap method. Adapted from (Lengaigne et al., 2018)

RAMA moored buoy data in the BoB have shown that a warm subsurface layer and strong salinity stratification played essential roles in the rapid intensification of Nargis TC (Lin et al., 2009; Yu and McPhaden, 2011). At seasonal timescales, these data demonstrated that thick barrier layers are induced by stronger haline stratification and a deeper thermocline during the post-monsoon season (Thadathil et al., 2016). These thick barrier layers contribute to much weaker TC-induced oceanic cooling as compared to the pre-monsoon period (Neetu et al., 2012, Neetu et al., 2019), fostering post-monsoon TC intensification (Balaguru et al., 2012). At interannual timescales, the probability of TCs in the BoB appears to decrease during El Niño events (Felton et al., 2013) and positive Indian Ocean Dipole events (Yuan and Cao, 2012).

In the SCTR, TC activity decreases dramatically during strong El Niño events (Astier et al., 2015). Large-scale variations of the atmospheric environment (Felton et al., 2013; Astier et al., 2015) and of oceanic stratification (Xie et al., 2002; Vincent et al., 2014; Burns et al., 2016) associated with these events have been implicated. TCs in the northwest Australia basin have also been related to ENSO (Ramsay et al., 2011), and more recently to IOD-like SST variability

(Ramsay et al., 2017), but the role of subsurface oceanic conditions is less clear and likely less prominent in this region (Vialard et al., 2013).

Over the long term, surface and subsurface warming trends appear related to an increasing trend in TC intensity (Elsner et al., 2008; Rajeevan et al., 2013; Malan et al., 2013; Balaguru et al., 2014). Yet, the IO region poses a particular challenge for quantifying long-term TC intensity trends because of the large discontinuity in satellite viewing angle when Meteosat-5 was introduced in 1998 (Kossin et al., 2013).

12.2 Marine heat waves (MHW)

MHWs are episodic warm SST extremes that persist for days to months (Hobday et al., 2016). These extreme events cause extensive coral bleaching (Moore et al., 2012; Perry and Morgan, 2017; Monroe et al., 2018) and can alter the ecosystem (Wernberg et al., 2013; 2016). In the Indian Ocean, these extreme events are often related to strong, large-scale climate variations associated with ENSO and the Indian Ocean Dipole.

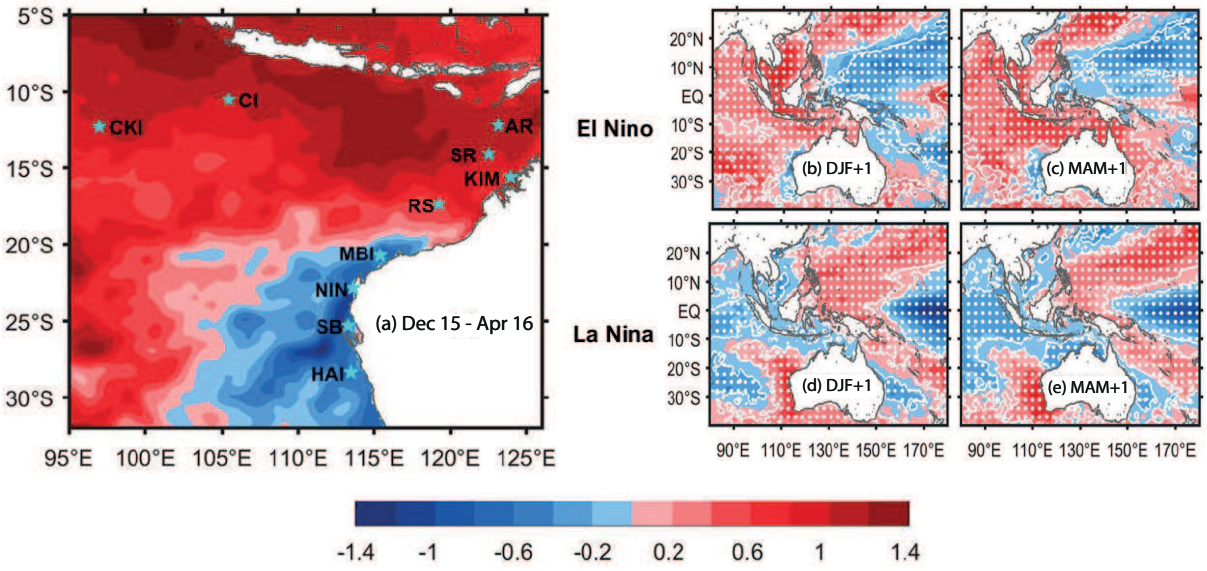

Figure 12.2 (a) Averaged SST anomalies in the southeastern IO during December 2015- April 2016. Stars denote locations of reef systems. Composited SST anomalies for El Niño events in (b) DJF+1 and (c) MAM+1 during January 1982- April 2015. (d,e):Same but for La Niña. The white contours and dots indicate anomalies exceeding the 95% significance level based on a two-tailed Student's t test. Adapted from Zhang et al. (2017)

The subtropical coast of west Australia has witnessed major MHWs during the past decades, such as in 2010-2011 (Feng et al., 2013), resulting in massive coral bleaching and decimation of economically important fish species (Wernberg et al., 2013). These MHWs are generally instigated by an anomalous strengthening of the Leeuwin Current during strong La Niña events (Figure 12.2d, e) and further facilitated by local air-sea-land coupling and the Madden-Julian Oscillation (Kataoka et al., 2018; Marshall et al., 2015). The negative phase of the Interdecadal Pacific Oscillation since the late 1990s also appears to have contributed to an increase in the number of MHWs in this region (Feng et al., 2015a).

Farther north, MHWs have also led to massive coral bleaching in the equatorial eastern Indian Ocean, the tropical oceans near the maritime continent, and off the coast of northwest Australia

(Zhang et al., 2017), such as in early 2016 (Figure 12.2.a). These events generally occur during or after the peak of strong El Niño events (Figure 12.2b,c), in response to reduced cloud coverage and Australian monsoon weakening (Benthuysen et al., 2018). Major coral bleaching events have also been observed in other regions of the tropical IO, particularly in 1998, 2010 and 2016, including the Maldives archipelago (Perry and Morgan, 2017), the southwestern IO and Mozambique channel (Gudka et al., 2018), the Bay of Bengal (Lix et al., 2016; Edward et al., 2018), and the Red Sea (Monroe et al., 2018). These events also occurred following major El Niño events, when the IO experiences a delayed basin-wide warming (Du et al., 2009).

ENSO-related MHWs have occurred more frequently in recent decades, as a combined result of natural decadal variability and global warming (Zinke et al., 2014; Feng et al., 2015; Zhang et al., 2017; Oliver et al., 2018). With unabated global warming, MHWs and related coral bleaching events will become more frequent in the future (Lough et al., 2018; Heron et al., 2016).

12.3 Extreme Events as drivers of IndOOS

In situ measurements as part of IndOOS are essential for providing measurements of the subsurface oceanic conditions important to TC intensification, particularly since cooling under the TC is not well observed by satellite remote sensing, even by microwave radiometers, due to strong precipitation. The RAMA and Argo arrays contribute to these. Enhancement of surface barometric measurements from drifters will improve initial conditions for TC forecasting. Coastal tide gauges are needed to measure storm surge. Sustained satellite observations are also essential for measurements of surface currents and surge in the wake of TCs. In particular, complementing the Jason-2 mission, the recent SARAL altimetry mission should improve vital near-coastal observations and the new proposed SWOT (Surface Water Ocean Topography) mission will provide finer spatial coverage and high resolution. Also, the MEGHA-TROPIQUES satellite will provide repeated scanning over the tropical regions of sea surface winds, clouds, humidity, temperature, rainfall and radiation. More intercalibration-work is necessary to develop basin-scale wind and SST records reliable in rainy/cloudy regions. An additional RAMA site off the northwest coast of Australia could provide better observations of both TCs and MHWs, while enhanced monitoring of the Leeuwin Current would improve understanding of MHWs off west Australia.

12.4 EOVs

TC intensification is influenced by SST and upper ocean stratification, while MHWs are influenced by air-sea flux and boundary current variability. Therefore, to better monitor, understand, and predict these extreme events requires accurate observations of: (1) Heat and momentum fluxes, sea level pressure, sea-level, and waves, both in regions of cyclogenesis and along cyclone tracks, at hourly resolution. (2) *In situ* measurements of SST and upper-ocean (0-200m) temperature, salinity, and velocity (hourly) in the contrasting TC prone regions, BoB and southern extra-tropical IO. (3) Temperature and velocity in the Leeuwin Current. (4) Upper ocean temperature, salinity, velocity, and turbulence, as well as air-sea fluxes in the MHW hotspots, such as off the tropical coast of northwest Australia and in the southwest tropical IO.

12.5 Actionable recommendations

A. New (and sustained) satellite technology and intercalibration-work to (i) develop continuous, basin-scale wind and SST records reliable in rainy/cloudy regions, (ii) increase resolution of altimetry for oceanic currents and surge response to TCs.

B. Maintain the Argo network in TC-prone regions.

C. Sustain RAMA-2.0 and enhance air-sea flux measurements at sites in the BoB (meridional section at 90°E from 5°N) and southwestern IO (between 55°E and 80°E from 5°S).

D. Maintain coastal tide-gauge measurements, particularly around the BoB and along the west coast of Australia. Enhance along east African coast.

E. Enhance glider observations along the west coast of Australia and across the Leeuwin Current.

F. Establish a RAMA flux mooring site in the northwestern Australian basin (15°S; 120°E) to capture TC and MHW signals.

G. Enhance barometric measurements from surface drifters and encourage pilot study in BoB using drifters that make more measurements: atmospheric pressure, wind speed and direction, air and sea temperature, salinity, humidity and waves.

H. Enhance glider observations of oceanic response to TCs in the BoB. This could become the BoB counterpart of the Hurricane Underwater Gliders program led by NOAA/AOML-CARICOOS in the Caribbean Sea and southwestern tropical North Atlantic Ocean.

13. Intra-seasonal Air-sea Coupling: Madden-Julian Oscillation and Monsoon Intra-seasonal Oscillation

Toshiaki Shinoda

Texas A&M University-Corpus Christi, USA

13.1 Introduction

The Madden-Julian Oscillation (MJO; Madden and Julian, 1972) and the monsoon intra-seasonal oscillation (MISO; Yasunari 1980, Krishnamurti and Subrahmanyam 1982) are major sources of intra-seasonal variability in the tropics. Here we discuss the role of the ocean and of air-sea interaction in the initiation and propagation of the MJO and MISO over the Indian Ocean. The predictability and forecasting of intra-seasonal variability are discussed in Chapter 9.

The MJO is associated with large-scale atmospheric circulation and deep convection. It propagates eastward around the globe on an approximate timescale of 30-60 days. The MJO impacts the onsets and breaks of Indian and Australian monsoons (e.g., Yasunari et al., 1979; Hendon and Liebmann, 1990), tropical cyclone activity (e.g., Liebmann et al., 1994, Maloney and Hartman, 2000a, b), climate variability in the extra-tropics through teleconnection (e.g., Weickmann et al., 1985), and interannual variability such as ENSO (e.g., Kessler and Kleeman, 2000; McPhaden et al., 1999) and the Indian Ocean dipole (e.g., Han et al., 2006, Shinoda and Han, 2005).

The MISO is a dominant mode of intra-seasonal variability in the tropical troposphere during boreal summer over the Asian Monsoon region. It is characterized by 30–60 day variations of convection and low-level winds, propagating northward from the equator towards South and Southeast Asia. The MISO causes fluctuations in rainfall during the Indian summer monsoon and plays an important role in triggering the monsoon onset (e.g., Goswami and Ajaya Mohan, 2001; Webster et al., 2002, Lau and Yang, 1996; Annamalai and Slingo, 2001; Hoyos and Webster, 2007).

There are many important scientific issues on this subject that cannot be covered in this short chapter. DeMott et al., (2015) provide an extensive review, covering many aspects of tropical intra-seasonal air-sea interaction.

13.2 Air-sea coupled processes in the MJO and MISO

a. Madden-Julian Oscillation (MJO)

The MJO drives significant fluxes of momentum and heat into the tropical western Pacific and Indian Oceans (Shinoda et al. 1998), causing large upper ocean responses, including strong equatorial currents, fluctuations of mixed layer temperature, and changes of thermocline depth (e.g., Krishnamurti et al., 1988, Kessler et al., 1995, Shinoda and Hendon, 1998; McPhaden et al., 2002, Waliser et al., 2003; Moum et al., 2013b). The importance of air-sea interaction for MJO development and propagation has been widely debated since an international field campaign in the early 1990's (Webster and Lukas, 1992), during which significant SST variations associated with the MJO were observed (e.g., Weller and Anderson, 1996). A comparison of many coupled and uncoupled numerical model experiments suggests that including air-sea

feedbacks improves simulations of MJO's amplitude, period, and propagation (e.g., Kemball-Cook et al., 2002; Sperber et al., 2004; Zhang et al., 2006; Woolnough et al., 2007; Kim et al., 2008).

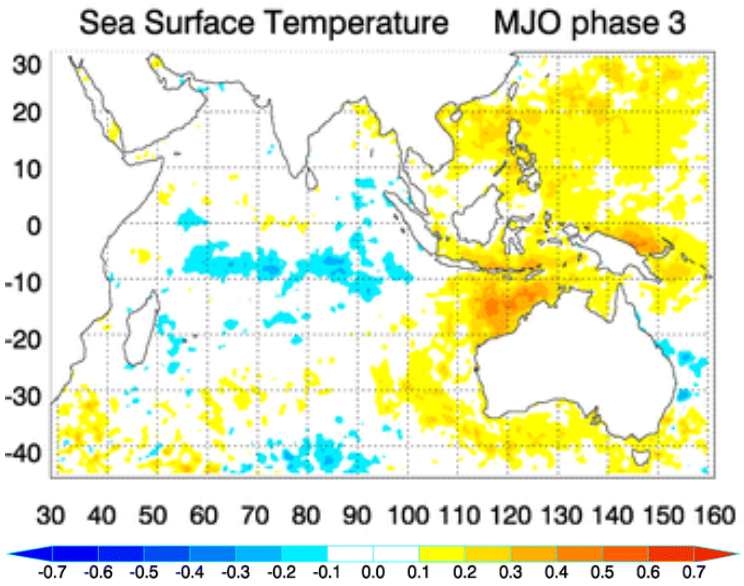

Figure 13.1 Composite SST anomalies (°C) for phase 3 of the MJO (based on Wheeler and Hendon 2004) over the November–April season calculated from POAMA (Predictive Ocean Atmosphere Model for Australia) Ensemble Ocean Data Assimilation System. Adapted from Marshall and Hendon, (2014).

Processes controlling intra-seasonal SST: While surface shortwave radiation and latent heat flux are the primary controllers of intra-seasonal variation of SST (Shinoda and Hendon, 1998), the contribution of ocean dynamical processes can be significant over the Indian Ocean. One such location is the Seychelles-Chagos thermocline ridge (SCTR, McCreary et al., 1993; Xie et al., 2002; Hermes and Reason, 2008) where the main thermocline is very shallow. Intra-seasonal SST variability is much larger in the SCTR region than most other areas in the tropical Indian and western Pacific Oceans.

The relative importance of surface heat fluxes and ocean dynamics in controlling intra-seasonal SST in the SCTR region remains unclear (e.g., Duvel et al., 2004; Han et al., 2007; Vinayachandran and Saji, 2008; Jayakumar et al., 2011, Drushka et al., 2012, DeMott et al., 2015). Recent studies (e.g., Halkides et al., 2015; Li et al., 2014) demonstrate the large spatial and temporal variability of processes controlling SST, suggesting that previous discrepancies are due to regional differences, interannual variability, and event-to-event variability. Also, significant uncertainties in the mixed layer heat budget still exist, due partly to the uncertainty of surface heat fluxes and the difficulty of quantifying vertical mixing processes including entrainment and vertical advection.

Another area of large SST variability associated with the MJO is the Timor Sea off the northwest coast of Australia (e.g., Duvel and Vialard, 2007; Vialard et al., 2008; Vialard et al., 2013; Marshall and Hendon, 2014) where SST anomalies induced by the MJO exceed 0.5°C (Figure 13.1). It appears that SST warming (cooling) in this region is driven by surface heat fluxes and coastal downwelling (upwelling) generated by easterly (westerly) wind anomalies during

the supressed (active) phase of the MJO (Marshall and Hendon, 2014). However, quantitative clarification requires better spatial and temporal data coverage, including *in-situ* observations.

Impact of diurnal cycle: SST warming during the suppressed phase of the MJO is enhanced by the diurnal cycle of shortwave radiation (e.g., Shinoda and Hendon, 1998; Shinoda et al., 2005; Li et al., 2013). This effect could play an important role in the initiation of the MJO, since warm SSTs can enhance moisture accumulation in the troposphere, stimulating the initiation of atmospheric convection. Regional coupled model simulations have demonstrated the importance of the diurnal cycle for the initiation of MJO convection during the event observed by the international field campaign of 2011/2012 (Seo et al., 2015). Further experiments, as well as observations of many different events, are necessary to confirm the role of diurnal warming.

MJO propagation through the Maritime Continent: Eastward MJO propagation often weakens over the Maritime Continent (MC), known as the "MJO propagation barrier". The failure of propagation occurs more often in numerical model simulations (e.g., Inness and Slingo, 2006), known as the "MC prediction barrier". Several mechanisms for the MJO propagation barrier have been suggested, including a reduced surface moisture source over the islands (Sobel et al., 2008), disruption of low-level winds by the island topography (Inness and Slingo, 2006), and the pronounced diurnal cycle in precipitation over the islands (Neale and Slingo, 2003). The resolution of most numerical prediction models may not be sufficient to resolve these processes and this could cause the MC prediction barrier. Many oceanic processes relevant to air-sea interaction in this region are still not well understood. Salinity stratification caused by a strong diurnal cycle of precipitation may also potentially influence SST and heat fluxes in this region. Accordingly, understanding oceanic processes in the MC region may help improve the MJO prediction.

MJO diversity: During the intensive observation period of a recent international field campaign in October-December 2011 (Yoneyama et al., 2013), three active episodes of large-scale convection associated with the MJO propagated eastward across the tropical Indian Ocean. While the strength of atmospheric convection was similar for the three MJO events, the oceanic response was strong for the second event (e.g., Moum et al., 2013b) but much weaker for the first event. This difference suggests that the role of air-sea coupling in the MJO varies substantially from event to event (MJO diversity; e.g., Fu et al., 2015). Hence, it is crucial to maintain and enhance long-term measurements that cover many MJO events to advance our understanding of air-sea coupled processes associated with the MJO.

b. Northward propagating monsoon intra-seasonal oscillation (MISO)

Air-sea coupling is thought to be important for MISO development and propagation (e.g., Webster et al., 1998; Vecchi and Harrison, 2002; Rajendran and Kitoh, 2006; Roxy and Tanimoto, 2007; Achuthavarier and Krishnamurthy, 2011). In particular, coupled and uncoupled numerical model experiments demonstrate that the inclusion of air-sea interaction leads to more realistic simulation and better prediction skills of the MISO (e.g., Kemball-Cook and Wang, Fu et al., 2003, Seo et al., 2007; Bellon et al., 2008; Wang et al., 2009). However, it is still unclear to what extent oceanic processes influence the MISO dynamics.

As the MISO propagates from the equator to Southeast Asia, it appears to be influenced by underlying SSTs in the Bay of Bengal. Processes that control intra-seasonal SST variability in the Bay of Bengal have been investigated by many observational and modeling studies (e.g., Sengupta et al., 2001a; Waliser et al., 2004, Duvel and Vialard, 2007, Vialard et al., 2012). While these studies indicate that shortwave radiation, latent heat flux, and ocean dynamics are all important, the relative contribution of these processes varies among the studies. The discrepancies could be due to the different time periods of the analyses as well as to methodology

and data sources. For example, there are significant year-to-year MISO variations associated with interannual or longer term climate variability such as the Indian Ocean Dipole (e.g., Ajayamohan et al. 2008, Sabeerali et al. 2014, Karmakar et al 2015, Jongaramrungruang et al., 2017), and such variations could influence the characteristics of MISO and thus the associated ocean variability.

The Bay of Bengal receives a substantial amount of freshwater through precipitation and river runoff, creating a complex upper ocean stratification including a strong halocline and temperature inversion. The strong salinity stratification causes a thin mixed layer and thick barrier (the isothermal layer below the mixed layer) which prohibits vertical mixing, reduces the entrainment heat flux, and hence affects intra-seasonal SST variability (Vinayachandran et al., 2002a; Rao and Sivakumar, 2003; Sengupta et al., 2016). Recent studies suggest that SST variability caused by strong salinity stratification significantly influences atmospheric convection over the Bay of Bengal associated with the MISO (Li et al., 2017a, 2017b).

Despite recent advances in understanding the ocean's role in the MISO, it is still difficult for models to accurately simulate upper ocean structure and variability in the Bay of Bengal. Realistic simulations are severely hampered by uncertainties in estimates of river discharge which directly influence salinity variability in the northern Bay of Bengal. Long-term measurements in the northern bay, such as a surface mooring at 18°N, 90°E (Weller et al., 2016), would be very useful for understanding the overall impacts of salinity stratification on the MISO intensity and propagation.

13.3 Essential Ocean Variables (EOV)

The atmospheric forcing associated with the MJO generates equatorial jets and waves which in turn feedback on the MJO, hence monitoring near-equatorial upper ocean variability is crucial. Off the equator, the upper ocean stratification in the Bay of Bengal should be monitored, where air-sea coupling plays an important role in the MISO development and propagation. In addition, diurnal variability in the near-surface layer needs to be resolved, given its importance for MJO initiation. Sustained observation within the Indonesian Seas is desirable, since air-sea interaction processes in the MC region may play an important role in the MJO propagation.

Variables: Equatorial (10°N-10°S) and Bay of Bengal temperature, salinity, velocity, SST, SSS, near-surface wind, air temperature and humidity, precipitation, shortwave and longwave radiation.

Resolutions: Temporal: One hour to resolve a diurnal cycle. Zonal: At least 10° in longitude ($\sim$1110 km). Meridional: 1° in latitude ($\sim$111 km) near the equator to resolve equatorial wave guide.

13.4 Actionable Recommendations

Sustained measurements are crucial for the study of intra-seasonal air-sea coupling over the Indian Ocean, and thus sustaining the IndOOS, especially the RAMA array and Argo program, is the first priority. Although the meridional resolution of the current RAMA buoy network is coarser than the desirable resolution specified in the EOVs above, with the additional coverage of satellite and Argo data it may be acceptable. Thus, adding new RAMA sites in key areas for the MJO and MISO is the higher priority.

A. **Increased vertical resolution in the upper 10 m of RAMA buoy**. Suggested depths of T/S sensors are: 0.5 m, 1.0 m, 2.0 m, 3 m, 5 m, 7 m, 10 m, to monitor the diurnal cycle in the near-surface layer. The enhancement of vertical resolution would be particularly useful at flux reference sites (Chapter 10) and in the key regions listed below.

B. **New RAMA site off northwestern Australia in the Timor Sea at 14°S, 115°E**. The largest SST anomalies associated with the MJO are found here. Measurements can lead to improvements in MJO prediction, as well as marine heat waves (Chapter 12), and variability of the Australian monsoon .

C. **Continuation of surface buoy measurements at 18°N, 90°E in the northern Bay of Bengal**. Upper ocean and SST variability in this region plays an important role in the MISO development and propagation, and thus the continuation of the buoy at this location is crucial.

D. **Enhancement of the RAMA buoy in the SCTR (4°S, 65°E)**. Inclusion of velocity (ADCP) measurements will constrain vertical mixing processes and thus the mixed layer heat budget.

E. **Additional buoy measurements in the Indonesian Seas**. At present, long-term measurements within the Indonesian Seas exist only at the Makassar Strait. A buoy in the southern part of the Banda Sea would capture the largest intra-seasonal SST anomalies found within the Indonesian Seas (Napitu et al., 2015).

14. South-Asian Monsoons: Upper-ocean Processes that Influence the Monsoon Annual Cycle

Hariharasubramanian Annamalai[1], Motoki Nagura[2], and Kelvin Richards[1]

[1]International Pacific Research Center/Dept. of Oceanography, University of Hawaii, USA,
[2]JAMSTEC, Japan

The seasonal-mean monsoon rainfall largely dictates the socio-economic conditions of small-scale farming communities in South and Southeast Asia, which has a direct impact on world rice production. Furthermore, diabatic heating associated with the monsoon influences the global atmospheric circulation. Given the global manifestation of the monsoon, understanding and modeling the processes responsible for its variability remains a grand challenge of the World Climate Research Program.

Over the past few decades, research has elucidated some of the complex interactions among the ocean, atmosphere, and land components of the climate system that influence the South-Asian monsoon. At the same time, progress in improving the coupled models used to simulate and predict the monsoon has been slow (Delsole and Shukla, 2002; Turner and Annamalai, 2012; Zhao et al., 2018), despite an increase in data from multiple observing platforms. Due to the complexity of the monsoon, identifying specific causes for the slow progress is difficult but major challenges are: (i) persistent model errors, not due to limitations in one particular parameterization (e.g., convection) but in multiple processes and their interactions, and (ii) inadequacies of the existing suite of observations for understanding monsoon systems and to constrain model physics (Annamalai et al., 2015, 2017).

Here we focus on upper-ocean physics, arguing that in order to improve our understanding of coupled processes and constrain model physics, new and sustained observations in the tropical Indian Ocean (TIO) are needed.

14.1 Scientific Background

Upper-ocean processes strongly influence the monsoon annual cycle (Shenoi et al., 2002; Schott et al., 2009; Seo et al., 2009; Thadathil et al., 2016; Nagura et al., 2015). Here, we review those regions and processes that link most strongly to the monsoons.

ITCZ/Indo-Pacific warm pool relationship: In conjunction with land surface heating, the monsoon annual cycle is driven by the displacement of the Intertropical Convergence Zone (ITCZ), which is anchored by the north-south migration of the Indo-Pacific warm pool, where SST is $>$28°C (Shukla and Fennessy, 1994). During both seasons (Figs. 14.1 a-b) there is intense rainfall ($>$8 mm/day) only in regions where SST is high, suggesting strong dependence. Despite the seasonal displacement of the thermal equator, SST over the equatorial Indian Ocean remains warm during summer, and over the Bay of Bengal during winter, suggesting that oceanic processes have a leading influence on SST in these regions.

Upwelling: In the northern Indian Ocean there is a remarkable east-west asymmetry in SST and precipitation during the monsoon (Figure 14.1a), which largely results from oceanic processes. During summer there is intense upwelling of cold water along the Somali and Omani coasts, driven by the cross-equatorial low-level atmospheric jet, where SST drops to about 23$-$24°C. Also, horizontal advection by ocean currents in conjunction with evaporative cooling

and mechanical mixing results in cold SST in the central Arabian Sea (McCreary et al., 1993), weakening rainfall there. In contrast, SST over the Bay of Bengal is everywhere above 28°C during summer and rainfall is intense resulting in strong upper-ocean stratification (Shenoi et al., 2002; Thadathil et al., 2008). During winter the lack of coastal upwelling results in SST being warmer in the western Arabian Sea than during the summer (Figure 14.1b; Schott and McCreary, 2001).

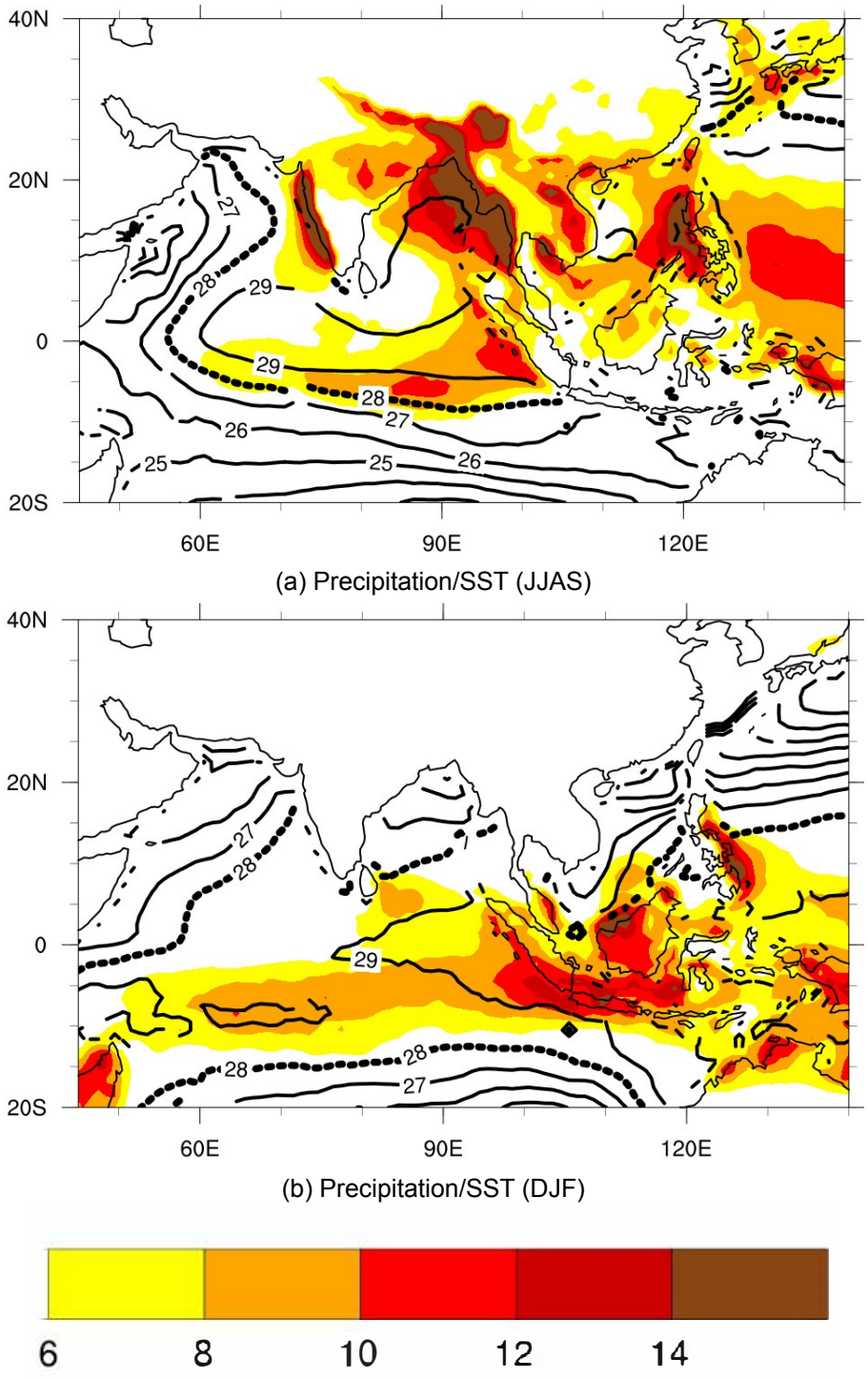

Figure 14.1 (a) Boreal summer (June-September) climatology of precipitation (shaded; mm/day) and SST (contours; °C) constructed from TRMM/TMI products (1998-2015) and (b) same as (a) but for boreal winter (December-February).

Salinity impacts on upper-ocean stratification: In the Bay of Bengal (Howden and Murtugudde, 2001; Thadathil et al., 2008, 2016) and in the Arabian-Sea mini-warm pool (Durand et al., 2004) near-surface stratification is impacted locally by precipitation and river run-off and remotely through advection. The freshwater thins the surface mixed layer and generates a barrier layer that prevents entrainment of cold subsurface waters (Lukas and Lindstorm et al., 1991). Furthermore, solar radiation can penetrate the mixed layer to warm the barrier layer, generating temperature inversions (Sengupta and Ravichandran, 2001b).

In the Bay of Bengal the fresh-water flux has roughly equal contributions from precipitation and river-runoff (Dai et al., 2009; Anderson and Riser, 2014; Thadathil et al., 2016) and the barrier layer is thickest during November-December (Thadathil et al., 2007), supporting temperature inversions in the upper ocean and helping sustain warm SSTs during winter (Figure 14.1b, Shenoi et al., 2002). High-resolution observations from multiple instruments collected during ASIRI (An Ocean-Atmosphere Initiative for Bay of Bengal; 2013-17) identified shallow, salinity-controlled mixed layers of $\sim$20 m depth resulting from high river runoff and heavy rainfall (Wijesekera et al., 2016) and modified by lateral mixing due to mesoscale features (Mahadevan et al., 2016b). Barrier layers are spread southward and into the interior by the East India Coastal Current (Akhil et al., 2014) and the wintertime anticyclonic circulation (Thadathil et al., 2007).

The onset of the monsoon normally occurs during late May to early June and in some years an "onset vortex" forms over the southern Arabian Sea that leads to the development of cyclonic storms. The vortex is fueled by the very warm SSTs of the Arabian Sea mini-warm pool ($68°-77°$E, $6°-15°$N). Based on limited observations and simulations, the advection of low-saline waters from the Bay of Bengal appears to promote salinity stratification and temperature inversions in the mini-warm pool (Durand et al., 2004; Vinaychandran et al., 2007; Mason et al., 2005; Nyadijo et al., 2012).

Equatorial Indian Ocean: The equatorial Indian Ocean lacks the persistent trade winds of the other equatorial oceans, owing to strong atmospheric convection over the Maritime Continent (Figs. 14.1a-b). Instead there are westerly winds during the intermonsoon periods that help drive eastward-flowing Wyrtki Jets (Wyrtki et al., 1973). Modeling studies suggest that freshwater-induced barrier layers intensify the jets by trapping wind momentum in a thinner-mixed layer (Han et al., 1999; Masson et al., 2003). The Wyrtki Jets are an important component of the Bjerknes' feedback (Annamalai et al., 2017), carrying mass and heat from the west and helping maintain the eastern equatorial warm pool, which in turn promotes local precipitation and upper-ocean stratification, which feeds back to intensify the Wyrtki Jets.

Seychelles-Chagos thermocline ridge: Interannual variations in the timing of monsoon onset are linked to SST variations over the SCTR during boreal spring, through their impact on the poleward migration of the ITCZ (Annamalai et al., 2005a). The linkage is particularly strong during years after the peak phase of El Niño, when fluctuations in thermocline depth and SST are most strongly coupled (Xie et al., 2002). There is evidence for the formation of salinity stratification at intraseasonal timescales (Vialard et al., 2009a), but data scarcity means the dynamical impact remains unclear.

Systematic errors in climate models: Analyses of several generations of climate models indicate that model biases in precipitation (Sperber et al., 2013) are coupled to biases in thermocline depth (Nagura et al., 2013), both of which persist throughout the annual cycle. Model errors are prominent over regions where upper-ocean stratification is expected to impact air-sea interaction (Annamalai et al., 2017). Figure 14.2a shows that barrier layer thickness during

boreal winter is biased over the central-northern Bay of Bengal, Arabian Sea mini-warm pool, and eastern equatorial regions, where models also depict a cold SST bias (Levine et al., 2013). Nagura et al., (2018) note that systematic errors in Bay-of-Bengal precipitation and associated salinity are linked to model biases in mixed-layer thicknesses and thermocline depths in the northern Arabian Sea.

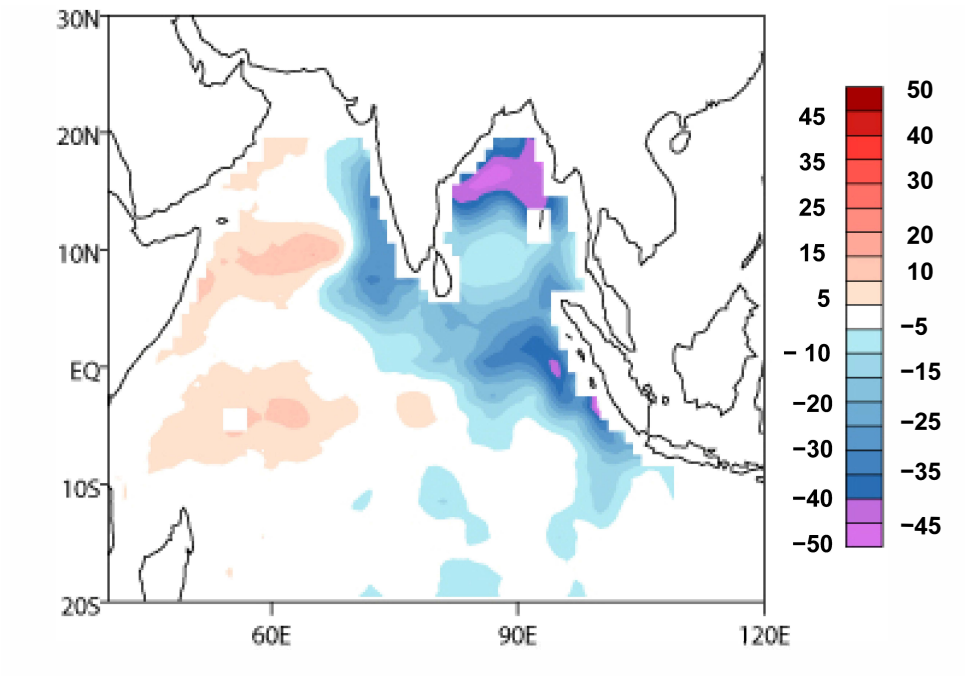

(a)

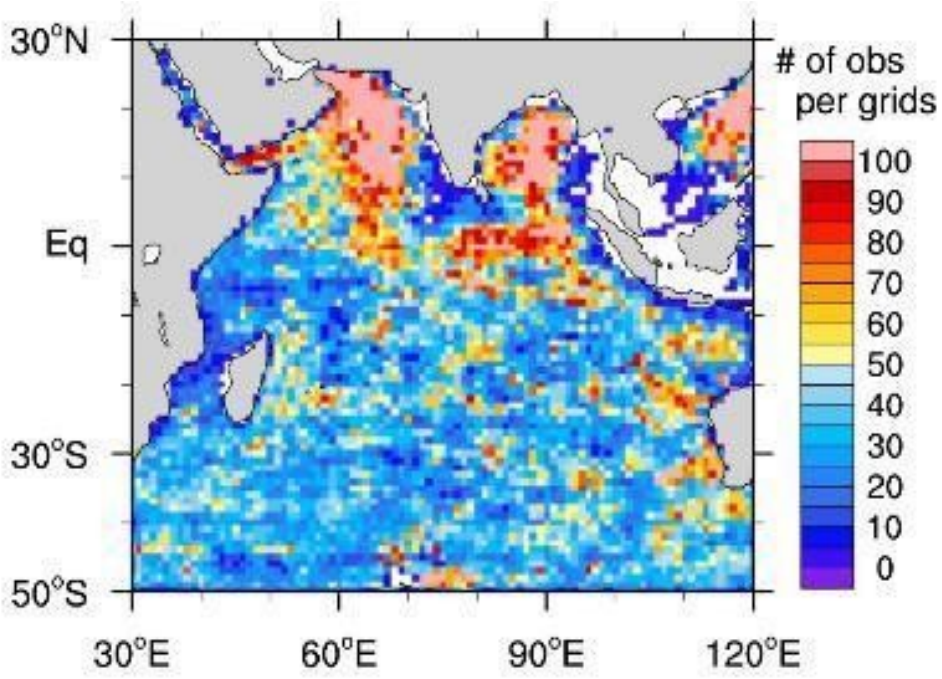

(b)

Figure 14.2 (a) CMIP5 multi-model-mean bias in barrier-layer thickness (m) during boreal winter and (b) Number of *in situ* observations (CTD and Argo since 1961).

14.2 Monsoons as a driver of IndOOS

To capture important barrier and mixed layer processes that influence the monsoons observations are needed over the shallow shelf/slope regions of the northern BoB, near the mouth of the Ganges/Brahmaputra rivers, where barrier layers and temperature inversions form, yet Argo floats cannot enter (Figure 14.2). We recommend a surface flux buoy poleward of 14°N. Also, more Argo floats equipped with auxiliary surface temperature-salinity (STS) sensors ($\sim$10 cm vertical resolution in the top 2$-$4 m) similar to those implemented by Anderson and Riser (2014). Deployment of Argo floats with auxiliary STS sensors are also recommended in the Arabian Sea mini-warm pool (68°$-$77°E, 6°$-$15°N).

It is critical to quantify key processes of the Bjerknes feedback, which includes Wrytki Jet transports and structure along the equator and the accumulation and discharge of heat in both the east and west. An ADCP network in the central basin is recommended, along with observations of upper-ocean salinity and temperature in the eastern (100°E and 110°E) and western (45°E, 50°E, 55°E, 60°E and 65°E) equatorial region. Over the central-eastern equatorial region high vertical resolution (10 cm) is needed to capture mixed-layer depth.

Large data gaps hamper the construction of a reliable climatology for the SCTR (Figure 14.2). and currently there are no sustained observations of salinity distribution in the upper-ocean. A feasible approach is to introduce auxiliary STS sensors on Argo floats and extend the RAMA array to a few more locations along 65°E and 75°E, and between 12°S and the equator.

14.3 Essential Ocean Variables

Our limited knowledge of the important oceanic processes that influence the monsoons suggest key regions where sustained observations of upper-ocean ($\sim$150 m) salinity, temperature, and velocity, preferably with 10 cm resolution over the top 5 m, are needed to improve our understanding of regional barrier and mixed layer physics and of the Bjerknes feedback. These observations are needed to improve models and predictions. In particular, temperature and salinity in the northern Bay of Bengal, the northeastern Arabian Sea, the Seychelles-Chagos Thermocline Ridge, and the eastern and western equatorial region, plus velocity at the equator.

14.4 Actionable recommendations

A. Argo floats equipped with auxiliary surface temperature and salinity (STS) sensors in the Bay of Bengal, Arabian Sea warm pool, and SCTR to capture fine-scale upper-ocean thermohaline stratification.

B. Surface buoys in the BoB (poleward of 14°N) and Arabian Sea that measure meteorological parameters as well as high-resolution upper-ocean (150 m) temperature and salinity.

C. Enhance RAMA sites with ADCPs in the central basin (65°-85°E) and with high resolution (10 cm) temperature and salinity measurements in the eastern (100°E and 110°E) and western (45°E, 50°E, 55°E, 60°E and 65°E) regions.

D. Additional RAMA sites within the SCTR, along 65°E and 75°E and between 12°S and the equator.

15. Regional Hydroclimate

Caroline C. Ummenhofer

Woods Hole Oceanographic Institution (WHOI)

15.1 Introduction

Upper-ocean conditions in the Indian Ocean influence regional hydroclimate across a range of timescales, from sub-seasonal to decadal and beyond. On sub-seasonal timescales, both northward and eastward propagating ISOs are active in the Indian Ocean (Chapter 13; Schott et al., 2009). The MJO (Zhang et al., 2005, 2013) is associated with eastward propagating, large-scale atmospheric circulation and deep convection that interact with warm underlying SST over the Indian Ocean and Maritime Continent. Several major flooding events in Indonesia and Malaysia have been associated with the MJO. Strong easterly winds over the eastern Indian Ocean near Java, associated with a Rossby wave-type response to the MJO, allowed for anomalous southward penetration of northeasterly winds from the South China Sea and strong low-level convergence over the region (Aldrian et al., 2008; Tangang et al., 2008). Observing these convectively coupled waves, especially during the convectively active MJO phase, is therefore important. The limited number of soundings in the tropics is thought to have adverse effects on estimated rainfall rates and on heat and moisture budgets (Katsumata et al., 2011). Representation and prediction of ISOs is better in ocean-atmosphere coupled models compared to stand-alone atmospheric models, highlighting the importance of the feedback between the atmosphere and the upper-ocean on intraseasonal timescales (Mahadevan et al., 2016a).

Northward propagating ISOs over the Indian Ocean are associated with active and break periods in monsoon rainfall from India to the Philippines (Chapter 14; Annamalai and Sperber, 2005; Schott et al., 2009). Equatorial SSTs centered on 70-90°E interact with northward-propagating mesoscale instabilities in the atmosphere to affect Indian summer monsoon precipitation (Zhou et al., 2017). A persistence of warm SST anomalies over the shallow thermocline region of the SCTR can delay the north-northwest migration of the intertropical convergence zone into the northern Indian Ocean and thus postpone the monsoon onset over southern India (Vecchi and Harrison, 2004; Annamalai et al., 2005a, Vialard et al., 2009a). Strong intraseasonal SST signals in the SCTR were linked to active phases of the MJO in 2007/2008 (Vialard et al., 2008).

The Bay of Bengal is an area of particularly active northward propagating ISOs, as reflected in strong coupling between SST and intraseasonal summer monsoon rainfall variability (Wijsekera et al., 2016 and references therein), with SST warming in the northern Bay of Bengal leading the onset of intraseasonal rainfall by 5 days. This rainfall-SST relationship is strengthened in years with anomalously warm SSTs, resulting in stronger low-level moisture convergence, as occurs during the negative phase of the Indian Ocean Dipole (Ajayamohan et al., 2008, Jongaramrungruang et al., 2017).

The IOD (Chapter 19; Saji et al., 1999, Webster et al., 1999) is the Indian Ocean's leading mode of variability on interannual timescales and widely impacts hydroclimate in surrounding countries (Saji and Yamagata, 2003), including rainfall and flooding in East Africa (Behera et al., 1999, Birkett et al., 1999, Webster et al., 1999, Black et al., 2003, Ummenhofer et al., 2009b, Manatsa et al., 2012; Manatsa and Behera 2013), droughts, wildfires, and streamflow in Indonesia (Abram et al., 2003; Hendon et al., 2003; D'Arrigo and Wilson, 2008; D'Arrigo

et al., 2011), and Australian rainfall and droughts (Ashok et al., 2003; Cai et al., 2009a, b; Ummenhofer et al., 2008, 2009a, c, 2011b). The IOD also modulates the well-known teleconnection between ENSO and the Asian monsoon systems (Ashok et al., 2001, 2004; Gadgil et al., 2004; Ummenhofer et al., 2011a). The Indian Ocean Subtropical Dipole (Chapter 19) also affects continental hydroclimate. Warm SST in the west and cool SST in the east is associated with enhanced low-level moisture advection onto southern Africa and increased rainfall during austral summer (Behera et al., 2001; Reason et al., 2001, 2002).

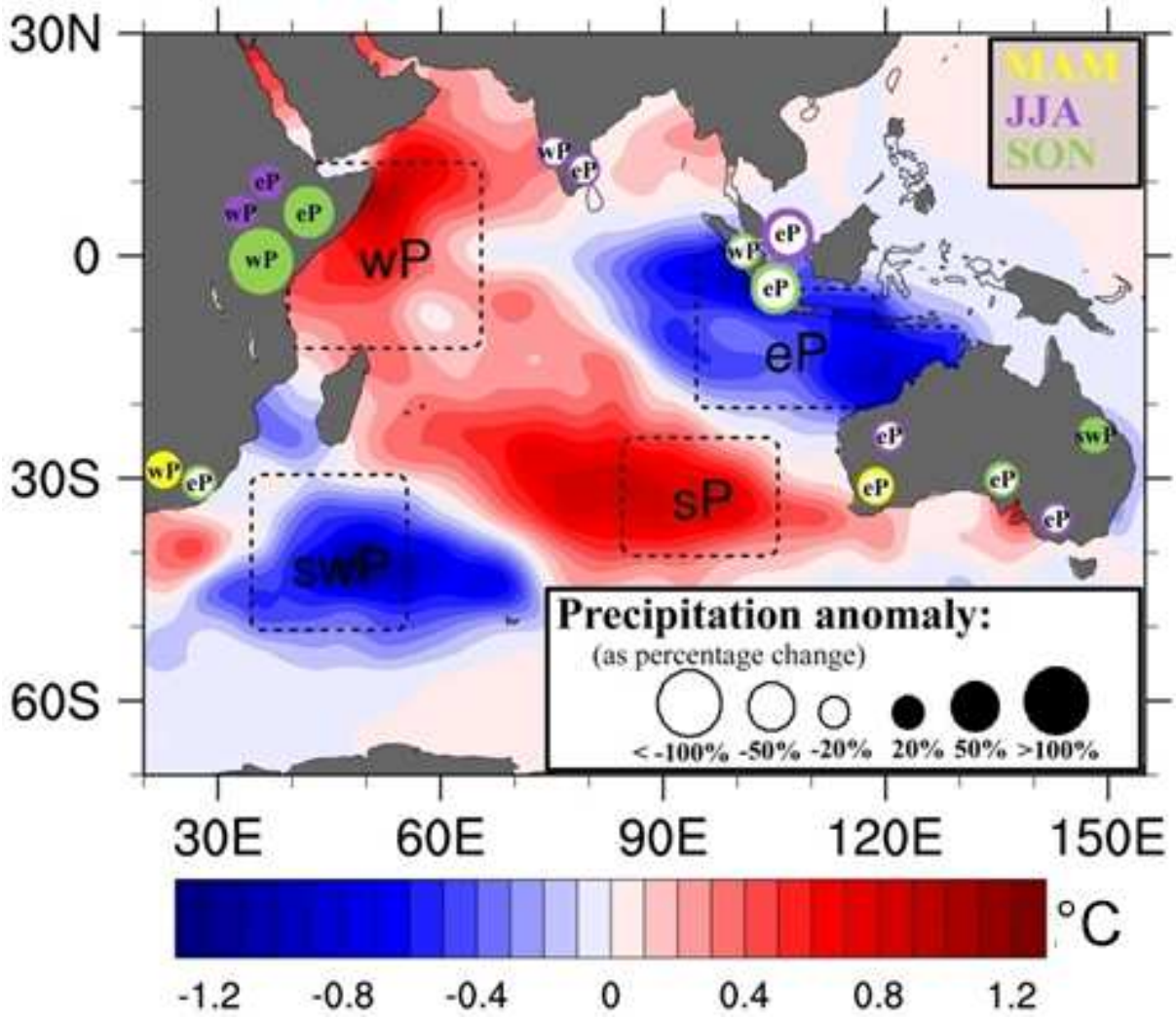

Figure 15.1 Schematic of the influence of Indian Ocean SST anomalies on regional rainfall for March-May (MAM), June-Aug. (JJA), and Sep.-Nov. (SON), from atmospheric general circulation model simulations. SST anomalies averaged during March-Nov. Regions with SST anomalies characteristic of tropical and subtropical Indian Ocean dipoles are employed in the simulations and indicated by dashed boxes. Anomalous rainfall associated with these regional SST anomalies are shown by circles over Indian Ocean rim countries. Filled (empty) circles denote rainfall increase (decrease), with circle size reflecting the magnitude of change and color the season. (Adapted from Ummenhofer et al., 2009d).

In a series of atmospheric general circulation model experiments, SST anomalies were linked to precipitation over Indian Ocean-rim countries (Ummenhofer et al., 2008, 2009b,c). SST anomalies closely resembling both tropical and subtropical Indian Ocean dipoles induce a basin-wide re-organization of the atmospheric circulation, resulting in significant rainfall changes over the surrounding landmasses (Figure 15.1). Precipitation over southwestern Australia is modulated by variations of the meridional temperature gradient in the eastern Indian Ocean, which af-

fects thermal winds, moisture flux, and baroclinicity over the region (Ummenhofer et al., 2008, 2009c). Over East Africa, years with an anomalously wet 'short rain' season (September-November) were found to be more closely linked to increased convergence of onshore moisture transport driven by warm SST in the western Indian Ocean (Ummenhofer et al., 2009b), than to a strengthened zonal SST gradient associated with the IOD (Saji et al., 1999, Webster et al., 1999, Black et al., 2003).

The Indian Ocean is particularly influential for regional hydroclimate on decadal timescales, as found for droughts and wet spells in Australia and East Africa (Ummenhofer et al., 2009a, 2011b, 2018). Changes in the tropical atmospheric circulation across the Indo-Pacific on multi-decadal timescales (Vecchi and Soden, 2007; L'Heureux et al., 2013) modulate the relationship between Indian Ocean SST and regional rainfall. After 1961 when the Pacific Walker cell weakened, the Indian Ocean cell strengthened and the East African short rains became more variable and wetter (Nicholson et al., 2015). Similarly, there was a strengthening in the relationship between the IOD and East African rainfall post-1961, with 73% of short rain variability in East Africa explained by the IOD, up from 50% in previous decades (Manatsa and Behera, 2013). After 1997, the correlation increased to 82%, explaining spatially coherent rainfall extremes across the region (Manatsa and Behera, 2013). Williams and Funk (2011) argue that warming Indian Ocean SST in recent decades is associated with reduced long rains for the March-June season in Ethiopia and Kenya. In contrast, warming trends in the western Indian Ocean have been related to increasingly wetter short rain seasons in East Africa (Liebmann et al., 2014).

Changes in the eastern Indian Ocean thermocline depth on decadal timescales can potentially impact the frequency and strength of the IOD (Annamalai et al., 2005b). Investigating the rare occurrence of three consecutive positive IOD events in 2006–2008, Cai et al., (2009c) found that subsurface oceanic conditions may have been key. An anthropogenic contribution was also proposed, since positive IOD events became more frequent over the period 1950–1999 in the CMIP5 models, which also project an increase in extreme positive IOD events (Cai et al., 2014b). Some decadal IOD variability has been linked to the Pacific Decadal Oscillation (Krishnamurthy and Krishnamurthy, 2016). Low-frequency changes in the eastern Indian Ocean thermocline depth (0-10°S, 90-100°E), in response to multi-decadal variations in Pacific wind forcing, appears to lead to decadal variations in the frequency of IOD events (Ummenhofer et al., 2017). Positive IOD events were unusually common in the 1960s and 1990s when the thermocline was shallower, while deeper thermocline depth in the 1970s and 1980s was associated with frequent negative IOD and rare positive IOD events (Ummenhofer et al., 2017). Hence it is important to better understand how slowly evolving upper-ocean thermal properties at multi-decadal time scales can affect IOD events that influence regional hydroclimate. This understanding could help decadal forecasting capabilities for the Indian Ocean region, which stands out globally as an area with the highest predictive skill in the 2–9yr range (Guemas et al., 2013).

The eastern Indian Ocean has exhibited considerable changes in SSS in recent decades, driving halosteric impacts on SSH (Vargas-Hernandez et al., 2014, Llovel and Lee, 2015). Hu and Sprintall (2016) found that the halosteric component of the ITF drives 35% of interannual ITF variability. Over the past decade enhanced rainfall over the Maritime Continent, potentially a manifestation of decadal trends in the Walker Circulation (Du et al., 2015) and strengthening Indo-Pacific equatorial winds, is thought to have contributed to an increase in ITF transport (Feng et al., 2015a, Hu and Sprintall, 2017) and a global redistribution of oceanic freshwater and heat (Chapters 22, 23). Sustained *in situ* observations of the ITF, as provided by the long-standing IX01 line (e.g., Liu et al., 2015) and augmented by the Argo program, need to be maintained to assess variability and change in the upper-ocean properties of importance to the

Indian Ocean hydrological cycle (Chapters 1, 3).

To better understand the hydrological cycle over the Indian Ocean region more broadly, observations of precipitation, riverine input (runoff), and evaporation at daily resolution are warranted. Focus areas for these measurements include the Maritime Continent and the northwest shelf off Australia given the large decadal signal there (Feng et al., 2015a, Hu and Sprintall, 2016, 2017), as well as the Bay of Bengal where high riverine input and rainfall make surface waters the freshest of any tropical ocean (Mahadevan et al., 2016a). In the Bay of Bengal, in particular, uncertainty in the freshwater distribution and mixing pathways for riverine input is high, and shallow, salinity-controlled mixed layers significantly affect upper-ocean heat content and SST (Wijsekera et al., 2016).

Since 2010, the Soil Moisture and Ocean Salinity (SMOS) satellite has provided SSS measurements consistent with *in situ* observations from RAMA in the equatorial and southern Indian Ocean, but exhibits large errors in the Bay of Bengal and Arabian Sea. This problem is likely due to errors from land contamination and strong winds (Ratheesh et al., 2013, Sharma et al., 2016), making it difficult to capture large SSS gradients in the Bay of Bengal (Mahadevan et al., 2016b). With new satellite missions (Chapter 6), such as Soil Moisture Active Passive (SMAP), remotely sensed SSS measurements will hopefully improve in marginal seas and coastal regions (Sharma et al., 2016). Satellite remote sensing of surface ocean and atmospheric variables necessary to track the hydrological cycle crucially depends on *in situ* observations for calibration (Chapter 6). In addition to the upper-ocean and marine meteorological observations from RAMA (Chapter 2), the Argo (Chapter 1) and surface drifter programs (Chapter 4) are essential. Undersampled regions in the equatorial eastern Indian Ocean, off the northwest shelf of Australia, the Andaman Sea, and in the Bay of Bengal (Chapter 4) are all regions of importance for the Indian Ocean hydrological cycle.

15.2 Essential Ocean Variables

To understand how Indian Ocean conditions modulate regional hydroclimate and to ultimately improve rainfall predictions for Indian Ocean rim countries, sustained measurements of EOVs are required. They include:

1. SST, SSS, atmospheric pressure, winds, and fluxes at 3-hourly to daily time scale across the entire Indo-Pacific region.

2. Precipitation, riverine input/runoff, and evaporation at daily resolution (higher frequency for precipitation), especially over the Maritime Continent region, northwest shelf of Australia, and the Bay of Bengal.

3. Some key sites where surface meteorology and atmospheric pressure measurements are colocated with surface heat, freshwater, and momentum fluxes, as well as near-surface ocean temperature, salinity, and velocity at sub-daily timescales in locations that influence regional rainfall, such as the SCTR, Arabian Sea, Bay of Bengal, eastern and western equatorial Indian Ocean, and northwest shelf off Australia.

4. Temperature and salinity over the top 150 m at daily-to-weekly resolution, with a focus on the SCTR, Arabian Sea, Bay of Bengal, the eastern equatorial upwelling region off Sumatra and Java, the western equatorial Indian Ocean, as well as the northwest shelf off Australia.

15.3 Actionable Recommendations

Given the EOVs highlighted above, recommendations for IndOOS are:

A. Maintain existing satellite observations for relevant variables at the air-sea interface, with basin-scale coverage over the Indo-Pacific region.

B. Improve SSS-sensing satellite capabilities over marginal seas and coastal regions.

C. Maintain and improve river gauge network to observe runoff from Indian Ocean rim countries.

D. Maintain surface drifter network and enhance with more surface barometric pressure sensors and increase coverage in eastern equatorial Indian Ocean and off northwestern Australia.

E. Maintain surface meteorological measurements and ocean observations from commercial shipping, as part of the VOS programme.

F. Complete and maintain RAMA-2.0, especially for 90°E into the Bay of Bengal, 55°E and 67°E for the SCTR, and in the eastern Indian Ocean (95-107°E).

G. Establish a RAMA surface mooring and flux reference site off northwestern Australia.

H. Maintain XBT lines IX01 and IX22, more regularly sample IX08 and IX14, and reactivate IX12.

I. Maintain the current Argo network and increase coverage in undersampled regions like the northern Bay of Bengal and central equatorial Indian Ocean).

16. Ocean Primary Productivity: Variability and Change

Peter G. Strutton[1] and Raleigh Hood[2]

[1]Institute for Marine and Antarctic Studies, University of Tasmania, and Australian Research Council Centre of Excellence for Climate Extremes, [2]University of Maryland, USA.

16.1 Introduction

Primary productivity is highly variable in the Indian Ocean, with unique features in both space and time. The western boundary currents support fisheries of local and global importance (Lee et al., 2005). The Leeuwin Current in the east is moderately productive and spawns eddies that travel west, some maintaining signatures of elevated productivity as far as Madagascar (Gaube et al., 2013). The Arabian Sea upwelling system, despite high biological productivity, is a strong source of CO_2 to the atmosphere, while the southern Indian Ocean is a weak sink (Takahashi et al., 2009). Productivity in the equatorial band, the Arabian Sea, and Bay of Bengal are all strongly modulated by annual monsoon wind reversals (Hood et al., 2017; Strutton et al., 2015).

The Indian Ocean Dipole mode and El Niño Southern Oscillation also impact primary productivity in the basin (Currie et al., 2013; Keerthi et al., 2016; McCreary et al., 2009; Wiggert et al., 2009a. See also Wiggert and Resplandy, Chapter 20). A positive IOD increases productivity in the eastern tropical Indian Ocean around the Sumatra upwelling system, and slightly decreases productivity in the central tropical Indian Ocean. The Somali upwelling system in the west appears more sensitive to El Niño, which can suppress upwelling and reduce productivity there. The Indian Ocean is rapidly warming (Roxy et al., 2014) and there is evidence for concomitant changes in the productivity of the basin, particularly in the west (Roxy et al., 2016) where there has been a shift to more harmful algal blooms in the northeastern Arabian Sea (Gomes et al., 2014). The Indian Ocean's role in ecologically and economically important fisheries, air-sea CO_2 exchange, and its emerging sensitivity to climate change call for sustained observations that can lead to a better understanding of primary productivity and its drivers.

Compared to the Pacific and Atlantic, the Indian Ocean is poorly sampled with respect to biogeochemistry and ocean productivity. For example, the Vertically Generalized Productivity Model (VGPM; Behrenfeld and Falkowski, 1997) was developed using a global database of 1698 primary productivity stations. None of these data are from the Indian Ocean. This satellite productivity algorithm has become the gold standard for estimating ocean primary productivity and its change over time globally, yet the complete lack of validation data in the Indian Ocean raises doubts about its accuracy. The chronic dearth of measurements presents both a problem and an opportunity for the future of the IndOOS. The opportunity is obvious. The problem is deciding how best to distribute platforms and sensors when there are insufficient observations to inform an observing system design. Here we tackle this problem by reviewing some of the existing knowledge, suggesting regions that are obvious candidates for future attention, and recommending an approach to instrument these regions.

16.2 Seasonal cycle and primary productivity

Basin scale patterns: Patterns of primary productivity in the Indian Ocean are strongly tied to the monsoons, the equatorial jets, and the stratification of the south Indian Ocean Gyre (Figure 16.1). From June through September (Figure 16.1a) the southwest monsoon drives upwelling off the coasts of Somalia and Oman, as well as a southeastward monsoon current off India,

leading to maximum productivity in the northwestern Arabian Sea and along the west coast and southern tip of India and around Sri Lanka. Equatorial productivity is low, but the spatial extent of the lowest chlorophyll there is reduced by the expansion of high chlorophyll in the Arabian Sea. At the same time, deeper winter mixing in the southern hemisphere appears to enhance productivity in the subtropical gyre, shrinking the size of this chlorophyll desert to its annual minimum.

During the inter-monsoon lull in the winds in October-November (Figure 16.1b) productivity in the Arabian Sea declines, while the eastward Wyrtki Jet may help generate high productivity along the equator. During the northeast monsoon of December through March (Figure 16.1c) productivity in the central Arabian Sea peaks again, related to deepening mixed layer depths, while chlorophyll along the Somali coast is at its annual minimum. In the southern hemisphere the oligotrophic subtropical gyre is at its summer maximum spatial extent. Finally, in April-May (Figure 16.1d) basin-wide productivity is lowest.

The limited available data on higher trophic level (zooplankton and planktivorous fish) responses to these spatial and temporal changes in productivity suggest patterns that tend to mirror or follow them (Hood et al., 2017). Next we describe some regional features in more detail.

Bay of Bengal: There are three important annual blooms in the Bay of Bengal (Vinayachandran et al., 2009). Blooms along the coast coincide with the seasonal maximum in river discharge in August and September (Yaremchuk et al., 2005). The bloom at the tip of India during the southwest monsoon reaches to the east of Sri Lanka and into the Bay of Bengal also in August-September and a bloom appears in the southwestern bay during northern hemisphere autumn. In addition to these seasonal features, cyclones can generate nutrient mixing and elevated chlorophyll, although in the northern part of the bay the strong halocline inhibits mixing. It has been shown that these blooms are associated with changes in copepod abundance and zooplankton community structure (Hood et al., 2017).

Arabian Sea: Productivity in the Arabian Sea is driven by two different processes (McCreary et al., 2009). Textbook seasonal upwelling during the southwest monsoon, from about July through September, drives blooms along the coast of Somalia, Oman, and western India (Barber et al., 2001). While in the northern and central Arabian Sea blooms are semi-annual, driven by entrainment of subsurface chlorophyll into the thickening mixed layers during both monsoons and also by subsequent detrainment. Higher trophic level species in this region have evolved behavioral responses to the strong seasonally and spatially changing conditions that include vertical feeding migrations of a copepod (Calanoides carinatus) and the reproductive cycle of a large pelagic fish (Scomberomorus commerson) (Hood et al., 2017). While productivity in this region is in some ways better studied than others, questions remain regarding the role of zooplankton grazing, potential iron limitation and the importance of nitrogen fixation.

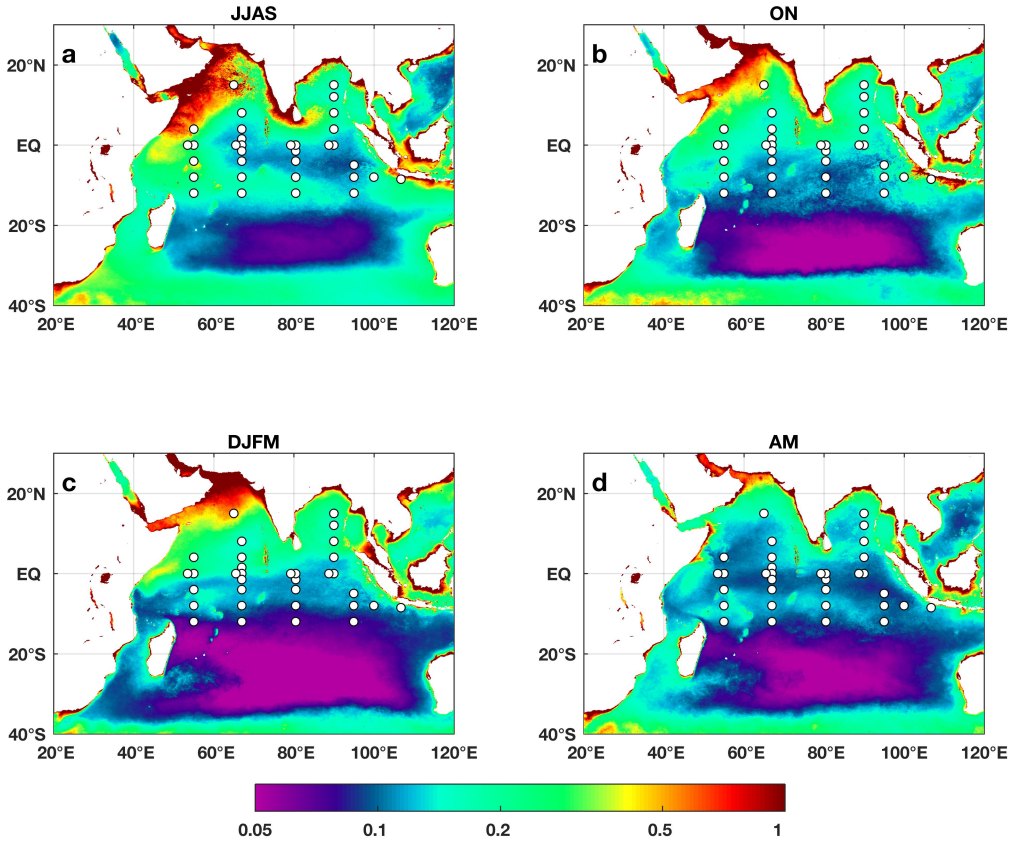

Figure 16.1 Seasonal variability in SeaWiFS satellite chlorophyll [mg m^{-3}]. (a) June-September, (b) October-November, (c) December-March and (d) April-May. Circles are the RAMA-2.0 sites (McPhaden et al., chapter 2).

Equatorial Indian Ocean: Productivity is low on the equator during the boreal spring intermonsoon period (March to May, Figure 16.1c, d), increasing dramatically in the west during the southwest monsoon, but remaining less than 0.5 mg m^{-3} in the central equatorial region, despite high concentrations just to the north off southern India and Sri Lanka. In boreal autumn, high productivity in the wake of islands is advected eastward along the equator from the Chagos-Laccadive Ridge at 73°E (Figure 16.1b), reversing and sweeping westward in late winter (Figure 16.1c). Intermittent bursts of chlorophyll have been observed at the equator at 80°E in this season (Strutton et al., 2015) and attributed to both local entrainment of nutrients and/or chlorophyll, and to southward advection of the island wake band of high chlorophyll by undulating Wyrtki jets. Higher trophic level responses to changes in productivity along the equator have not been studied.

Southwest Indian Ocean: South of Madagascar in late Austral summer, a large bloom develops that covers up to 1% of the global ocean surface (Figure 16.1c and d). Srokosz et al., (2015) suggested that the bloom is fertilized by iron that originates from the island of Madagascar and is advected eastward in the eddying South Indian Counter Current. Considerable interannual variability in the extent of the bloom was linked to variability in the number of eddies. Recently, Ramanantsoa et al., (2018) examined the structure of the upwelling in this region, finding it linked to separation of the East Madagascar Current and upwelling favorable winds. Nothing is known about higher trophic level responses to these blooms.

16.3 Observing productivity

Sustained observations of productivity in the Indian Ocean have been limited to one very important data stream: Satellite ocean color. Since the launch of SeaWiFS in 1997 the data set is continuous and robust, except for areas of persistent clouds, and has been used to document a long term decrease in Indian Ocean productivity (Roxy et al., 2016).

Historical ship-based productivity measurements do exist (Zeitzschel et al., 1973). These data cover not only phytoplankton primary productivity, but also abundance and rate observations for bacteria and grazers. These data serve as historical baselines as well as indicators of regions that merit closer monitoring, such as the Arabian Sea where the balance of nutrient limitation versus grazing remains unclear. There has been no coordinated program for sustained bio-optical and nutrient sampling at RAMA sites, but ad hoc deployments have revealed dynamics associated with seasonal and shorter time scale processes (Strutton et al., 2015).

Biogeochemical sensors mounted on Argo floats have the potential to answer questions regarding both large scale patterns of primary productivity at seasonal to long-time scales, as well as mesoscale features, such as the role of eddies in nutrient fluxes and sub-surface chlorophyll patterns (Dufois et al., 2017; Gaube et al., 2013). The number of BGC-Argo deployments in the Indian Ocean is growing rapidly (chapter 1) and an implementation plan for a global BGC-Argo program exists (Johnson and Claustre, 2016; http://biogeochemical-argo.org/).

To monitor changes in plankton biodiversity it is desirable to establish a Continuous Plankton Recorder (CPR) and/or video plankton recorder (VPR) Survey in the Indian Ocean, for example, along a basin-wide section to be repeated seasonally, annually, or biannually, similar to that conducted in the Atlantic by the Sir Alister Hardy Foundation for Ocean Sciences in Plymouth, UK. The CPR filters water continuously through a 270 micrometer mesh, thus sampling large phytoplankton and zooplankton. On return to the laboratory, the mesh is removed from the mechanism and divided into samples, each representing 10 nautical miles (19 km) of tow. The CPR works best on long tows of 500 nm or more and is equipped with an internal cassette that can be changed multiple times, making it ideal for trans-oceanic sections. Both the CPR and VPR can be equipped with sensors that measure salinity, temperature and chlorophyll fluorescence.

16.4 Essential Ocean Variables

The Global Ocean Observing System defines nutrients, ocean color, and phytoplankton biomass and diversity as the relevant EOVs for ocean primary productivity (http://www.goosocean.org).

Measuring some of these EOVS at RAMA sites could provide data in a few of the regions of greatest variability of primary productivity. However, planning of appropriate depths and sufficient vertical resolution for nutrient and chlorophyll measurements is a challenge without prior knowledge of the vertical scales of the features, which we do not have for the Indian Ocean. A similar statement could be made for dissolved oxygen: Mapping features such as oxygen minimum zones (OMZs) from moorings would require large numbers of sensors located at depths we can only guess at. For these reasons, oxygen, nutrient, and bio-optical measurements on Argo floats seem the best way to obtain the data needed to better understand biogeochemical processes and primary productivity in the Indian Ocean, and this view is shared by Wiggert and Resplandy (Chapter 20) in their discussion of oxygen minimum zones.

Autonomous nutrient sensors are currently limited to nitrate. Hence, to obtain the full suite

of nutrients - nitrate, phosphate, silicic acid, and ammonium - requires ship-based sampling along the established decadal GO-SHIP lines. These voyages also represent an opportunity to collect vital data on phytoplankton community structure, as do RAMA maintenance voyages. Establishing a CPR or VPR survey for the Indian Ocean, towed from ships of opportunity, would provide quantitative information on phytoplankton biomass (chlorophyll) and higher trophic level species composition, capturing variability and trends at basin-wide spatial scale.

16.5 Actionable Recommendations

Satellite ocean color provides the only broad scale information on variability of primary productivity, and hence these missions must be sustained. The important regional productivity features that an *in situ* observing system must quantify are: (1) The intensity and spatial extent of the Arabian Sea coastal upwelling blooms during the southwest monsoon, particularly along the Somali coast; (2) The central Arabian Sea, where there are semi-annual peaks in productivity; (3) The equator, linked to the seasonal variability of the Wyrtki jets; (4) The Bay of Bengal, coastal India and Sri Lanka; and (5) The spatial extent of the oligotrophic gyre.

Some RAMA-2.0 sites could be enhanced to host sensors that capture some of these regions. Candidate locations include the northern-most mooring in the Arabian Sea (65°E, 15°N), the three moorings in the Bay of Bengal (90°E line), the southernmost mooring of the 80.5°E line for the gyre, plus moorings on the equator for the Wyrtki Jets. However, as mentioned above, capturing the vertical scales of variability will require large numbers of well-placed sensors. For this reason autonomous platforms such as Argo are most promising for the near future.

A ship of opportunity CPR survey in the Indian Ocean would provide the only measure of phytoplankton and plankton community structure variability and change. Given the dynamic nature of the Arabian Sea, a CPR route between India and the Gulf of Oman and perhaps beyond into the Persian Gulf would capture important features. The merchant ships that ply such routes operate 12 months of the year and are relatively immune from the sea states generated by the summer monsoon, a season when there are very few samples collected from research ships. Such a survey could characterize monsoon-driven seasonal changes in plankton community composition. Other trans-oceanic routes, such as from Perth in Western Australia to South Africa or to the Red Sea, would be unique, sampling the biodiversity in waters about which little is known.

The prioritized **actionable recommendations** for implementation of sustained productivity measurements as part of IndOOS are:

A. Analyze existing observations and model outputs to better determine the locations of largest productivity variability. These areas should be prioritized for biogeochemical observations.

B. Consult with the global BGC-Argo community, to plan observations of nutrients, bio-optics, and oxygen on Argo floats in regions of high primary productivity variability (Recommendation A), as well as OMZs and areas important for the marine nitrogen cycle.

C. Add observations of phytoplankton community structure and chlorophyll concentration on key GO-SHIP lines and RAMA maintenance voyages to track changes in phytoplankton abundance, provide validation data for ocean color satellites and, when coupled with particle and nutrient measurements from BGC-Argo floats, help to understand changes in the strength of the biological carbon pump.

D. Compare *in situ* chlorophyll and productivity observations to colocated satellite ocean color to quantify the accuracy of satellite algorithms from SeaWiFS and develop regionally tuned algorithms, if necessary.

E. Sustain satellite ocean color missions.

F. Implement a ship of opportunity Continuous and/or Video Plankton Recorder survey in the Indian Ocean to capture variability and change in plankton community composition.

17. Boundary Currents and Exchanges with Other Basins

Ming Feng[1], Raden D. Susanto[2], Helen Phillips[3], and Lisa Beal[4]

[1]CSIRO Oceans and Atmosphere, Perth, Western Australia, Australia, [2]University of Maryland, Maryland, USA, & Bandung Institute of Technology, Indonesia, [3]University of Tasmania, Hobart, Tasmania, Australia, [4]University of Miami, Florida, USA

17.1 Motivation

Ocean boundary currents are narrow, fast-flowing currents that are important for heat transport, nutrient distribution, marine productivity, and ocean climate at regional and basin set al.cales. The low-latitude northern boundary of the Indian Ocean, the seasonally-reversing monsoonal forcing, and the connection with the Pacific engender some unique boundary current systems (Figure 17.1). The Indonesian Throughflow (ITF) drains some of the Western Pacific warm pool into the tropical Indian Ocean. The ITF and the Agulhas Current form the warm return route of the global overturning circulation, which regulates global climate on multi-decadal and centennial time scales. The reversing Somali Current is part of the shallow overturning circulation of the Indian Ocean, supplying southern hemisphere waters to upwelling cells along the western boundary of the Arabian Sea and compensating cross-equatorial Ekman transport. At the subtropical eastern boundary, the uniquely poleward-flowing Leeuwin Current instigates marine heatwaves.

The ITF is observed to have strengthened during the climate change hiatus in recent decades (Liu et al., 2015), reversing a previous declining trend (Wainwright et al., 2008). Over the long term it is projected to weaken under the influence of human-induced climate change, associated with weakening of the deep upwelling in the Pacific and a slowdown of the global overturning circulation (sen Gupta et al., 2016; Feng et al., 2017). On the other hand, the Agulhas leakage is expected to increase with climate change (Biastoch et al., 2013) and could bolster the Atlantic Meridional Overturning Circulation (AMOC; Weijer et al., 2002; Beal et al., 2011) at a time when Greenland ice melt is expected to weaken it. Western boundary currents are strengthening with climate change in reanalyses models (Wu et al., 2012), yet direct observations point to a potential increase in their eddy kinetic energy instead (Beal and Elipot, 2016). Sustained observations of these boundary currents are crucial to measure and attribute changes, and quantify the effect of these changes on basin scale and regional heat, freshwater, and nutrient budgets. With the increase in the intensity of ENSO variability under a warming climate (Cai et al., 2014a; 2015), interannual variability in the Indian Ocean may also intensify.

Boundary currents have not been well observed by the IndOOS, partially due to lack of resources and capacity of bordering countries, and partially to cost and logistics. The narrow, intense nature of boundary currents requires finely spaced instrumentation to observe their structure and variability. The environment is challenging because the instruments are susceptible to human interference and require robust engineering to manage long-term deep deployments. Proximity to coasts raises the need for diplomacy and regional collaborations.

17.2 Background and historical observations

Indonesian Throughflow: The ITF (Figure 17.1) conveys volume, heat, and freshwater fluxes from the tropical Pacific into the eastern Indian Ocean through the complex topography and

narrow passages of the Indonesian Seas. Tidal mixing and air-sea interaction in the Indonesian Seas strongly modify the water properties (Ffield and Gordon, 1996; Alford et al., 1999; Hatayama et al., 2004; Koch-Larrouy et al., 2007; 2010; 2015; Nagai and Hibiya, 2015; Ray and Susanto, 2016). The ITF exits into the Indian Ocean mainly through the Timor passage, Ombai Strait, Lombok Strait, and the Sunda Strait, with an average transport of 15 Sv (Figure 17.1; Sprintall et al., 2009; Susanto et al., 2016).

Sustaining direct *in situ* measurements of the ITF within the passages is logistically challenging and expensive. However, there is a 30 year time series from the IX1 XBT line between Fremantle, Australia and Sunda Strait, Indonesia, currently occupied bi-weekly (Chapter 3). This line captures the upper ocean geostrophic structure of the ITF outflow as it first enters the Indian Ocean (Meyers et al., 1995, Wijffels et al., 2008). Measurements in all major ITF passages were taken simultaneously for the first time from 2003 to 2007 (Gordon et al., 2010; Sprintall et al., 2009; Susanto et al., 2012; Van Aken et al., 2009), revealing a total ITF transport of 15 Sv. Subsequently, the South China Sea throughflow in the Karimata and Sunda Straits was measured (Fang et al., 2010; Susanto et al., 2010; 2013; Wei et al., 2015). Observations show that the ITF has maximum velocities near 100 m depth and intense vertical mixing produces upwelling and cooling of surface waters in the Indonesian Seas that affects regional precipitation and wind patterns (Sprintall et al., 2014). The ITF is influenced by ENSO, El Nino causes a shoaling and slowing of the ITF, and by the Inter-decadal Pacific Oscillation (IPO) and the Indian Ocean Dipole mode (Meyers et al., 1996; Deckker et al., 2016; Lee et al., 2015; Sprintall et al., 2014; Liu et al., 2015). IPO anomalies transmitted through the Pacific-Indian waveguide and ITF have been suggested to influence decadal variations of Indian Ocean thermocline depth (Han et al., 2014) and the shallow overturning circulation (e.g. Zhuang et al., 2013). There has been an increasing trend in the ITF of 1 Sv per decade over the past 30 years (Liu et al., 2015).

Proxies, such as from satellite sea surface height observations, appear to work well for the case where ITF transport is concentrated only in the upper layer (Potemra et al., 1997; Potemra et al. 2005; Sprintall and Revelard, 2014; Susanto et al., 2007; van Aken et al., 2009). A combined geostrophic-hydraulic proxy to estimate the full-depth ITF transport draws upon altimetry sea surface height for the surface layer (geostrophic balance) and ocean bottom pressure for the deeper-layer (hydraulic control) (Susanto and Song, 2015). Nevertheless, proxies assume a fixed stratification making *in situ* observations necessary to capture varying vertical structure associated with thermohaline changes, as well as heat and freshwater transports.

Eastern boundary currents: The meridional pressure gradient in the southeast Indian Ocean provides the driving force for the poleward Leeuwin Current, and also supports shallow, broad eastward currents that feed into it (Figure 17.1; Thompson et al., 1984; McCreary et al., 1986; Furue et al., 2013, 2017; Benthuysen et al., 2014). The Leeuwin Current transports about 3 Sv of warm, fresh tropical waters southwards, influencing the upper ocean heat and freshwater balances in the southeast Indian Ocean (Domingues et al., 2007; Feng et al., 2008). There is broad-scale downwelling (Furue et al., 2017, Liang et al., 2017) of eastward surface currents into the depths of the Leeuwin Undercurrent (200-1000m) to create a zonal overturning cell in the upper 1000m of about 4 Sv (Furue et al., 2017). The Leeuwin Undercurrent also carries waters of Subantarctic origin along the western Australian coast (Woo and Pattiaratchi 2008), leaving the coast near 22°S to contribute to the lower limb of the zonal overturning (Furue et al., 2017). The Leeuwin Current system channels Pacific influences such as ENSO and IPO into the Indian Ocean through the planetary waveguides (Feng et al., 2003; Wijffels and Meyers, 2004). An unseasonably strong Leeuwin Current during the 2010-11 La Nina event in the negative phase of IPO instigated an unprecedented marine heat wave off the west coast of Australia (Feng et al., 2013), causing coral bleaching and damage to the marine ecosystems (Lengaigne et al., chapter 12).

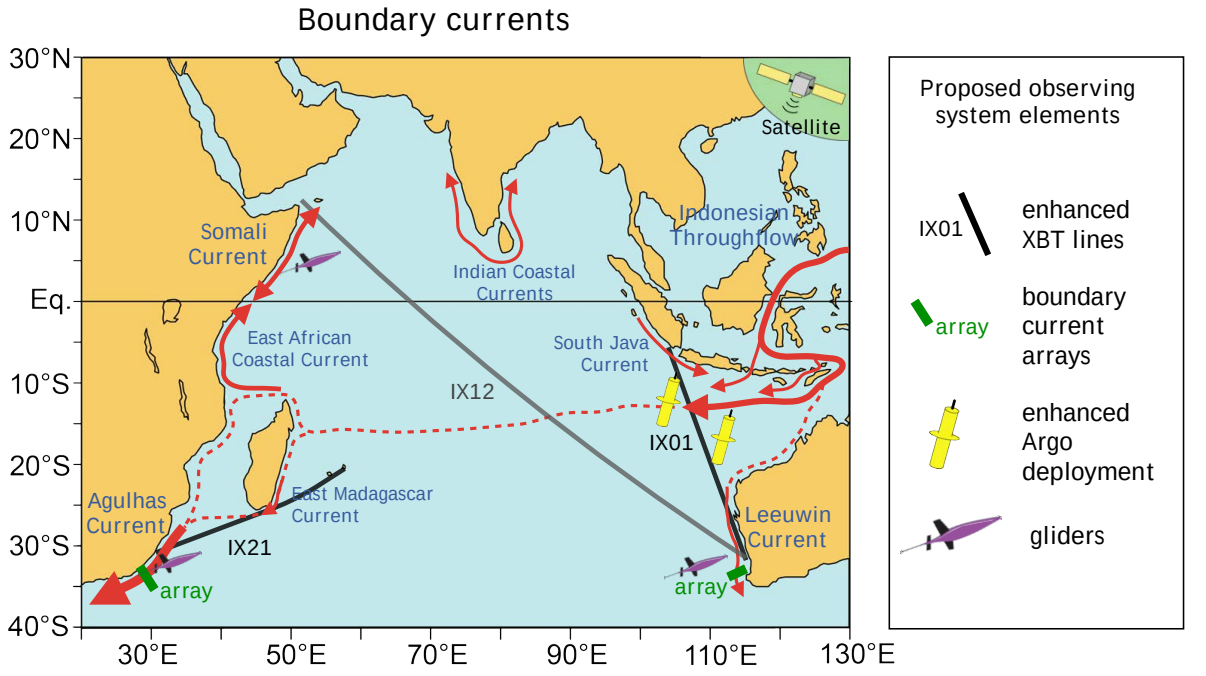

Figure 17.1 Schematic of the ocean boundary currents of the Indian Ocean. Existing and proposed observing system elements are denoted.

Measurements of the Leeuwin Current have been patchy. The southern end of the IX01 XBT line does not provide sufficient resolution to capture the Leeuwin Current. Since 2009, the Australian IMOS program has been monitoring the Leeuwin Current system using ADCP and thermistor moorings and monthly/quarterly glider surveys. However, the mooring observations have been confined to the shelf within the 500 m isobath. Interannual and decadal variations of the Leeuwin Current have been inferred from coastal sea level observations at Fremantle, part of the IndOOS tide gauge network (Feng et al., 2003; Feng et al., 2011).

Close to the equator, the South Java Current system (Figure 17.1) is also an important oceanic waveguide, this time communicating tropical Indian Ocean climate variability eastward into the Indonesian seas (Wijffels and Meyers, 2004; Sprintall et al., 2014). There is strong coastal upwelling (Susanto et al., 2001; Susanto and Marra, 2005) and the cool waters are important to the development of the Indian Ocean Dipole (Vialard et al., chapter 19). The South Java Current is partially surveyed by the IX1 XBT line, as a component of the total ITF transport variability. No designated observing program has been implemented to monitor the South Java Current system, although there are observations of the Java upwelling system (Masumoto et al., chapter 18).

Western boundary currents: The Agulhas Current is the strongest western boundary current in the Southern Hemisphere, carrying an average 85 Sv of warm and salty waters poleward, including 60 Sv of wind-driven subtropical gyre transport and about 25 Sv of ITF and overturning transport. Its seasonal variability is ±10 Sv, with a maximum in austral summer (Beal et al., 2015), opposite to that in the Mozambique Channel. Mesoscale and submesoscale meandering of the Agulhas jet leads to strong episodic exchanges with shelf waters (Leber et al., 2017, Krug et al., 2017) which support high productivity over the eastern Agulhas Bank (Probyn et al., 1994) and may influence the well-known sardine run (Fréon et al., 2010).

The bulk of the ITF waters eventually feed into the Agulhas Current through the Mozambique Channel or via the East Madagascar Current (Figure 17.1; Quartly et al., 2006; Nauw et al., 2008; Ridderinkhof et al., 2013). Flow through the channel is carried by a train of anticyclonic eddies formed at its narrows (Ridderinkhof et al., 2010). A mooring array deployed across the narrows from 2003 to 2012, one of the longest *in situ* records in the Indian Ocean, measured a mean transport of 16.7 Sv, with a maximum in austral winter and IOD-related interannual variability of 8.9 Sv (Ridderinkhof et al., 2010).

The southern Agulhas system is a hotspot for air-sea interaction, pumping moisture into the atmosphere and accelerating winds (Rouault et al., 2003; Small et al., 2008). Rising sea surface temperatures of the Agulhas system (Wu et al., 2012) are expected to alter regional wind and rainfall patterns and may act to dry the adjacent southern African continent (Rouault et al., 2010; Neukom et al., 2014). Ocean reanalyses suggest that warming of the Agulhas system is related to an intensification and poleward shift of the currents (Wu et al., 2012; Yang et al., 2016), driven by changes in the Westerlies which are projected to continue over the twenty-first century under anthropogenic forcing (Cai et al., 2006; Sen Gupta et al., 2009; Biastoch & Boning, 2013). *In situ* observations combined with satellite altimetry point instead to a potential increase in eddy kinetic energy, such that the Agulhas Current has broadened but its transport has not strengthened over the past 25 years (Beal & Elipot, 2016).

The most comprehensive measurements of the Agulhas Current were undertaken during the US Agulhas Current Time-series experiment (Beal et al., 2015; Figure 17.2). An array of current meters and CPIES were deployed along an altimeter ground track for a duration of three years and a 25-year transport proxy estimated. Subsequently, an international partnership was formed between South African, US, and Dutch scientists to establish a sustained observing system that can measure, in addition, the heat and freshwater changes important to climate. The Agulhas System Climate Array was in the water from 2016 to 2018, with sustained deployment dependent on ambitious plans for capacity building and resource sharing among nations which are not yet fulfilled.

At the western boundary of the equatorial gyre the East African Coastal Current overshoots the equator during boreal summer monsoon to supply a northward Somali Current (Schott and McCreary, 2001; Beal et al., 2013) which builds in strength from about 5 Sv in June to 37 Sv in September (Beal and Chereskin, 2003). During boreal winter monsoon, the Somali Current is weaker and flows southward. Roles of the Somali Current in upwelling, monsoon rainfall, and Arabian Sea heat balance are poorly understood, but expected to be important given its large transport (e.g. Beal and Chereskin, 2003). The IX12 XBT line has regularly crossed this region over the past 30 years, but does not resolve the full extent of the Somali Current system (Feng et al., chapter 3).

Boundary currents of the Indian subcontinent: Monsoon currents flow between the Arabian Sea and the Bay of Bengal (BoB) in the northern Indian Ocean: the Southwest Monsoon Current flows eastward during the boreal summer monsoon (May-September) and the Northeast Monsoon Current flows westward during the winter monsoon (November-February) (Figure 17.1). These currents are mainly geostrophic, forced by both local and remote winds, and propagate along the Indian coastal waveguides (Schott and McCreary, 2001; Shankar et al., 2002). They exchange heat and freshwater between the Arabian Sea and the Bay of Bengal and, together with seasonal upwelling, are important for the biogeochemical processes and fisheries off the Indian subcontinent. Intensive observations from the international program ASIRI (Air-Sea Interactions in the Northern Indian Ocean) during 2013-2017, have shown the complex exchanges south and east of Sri Lanka during the northeast monsoon, with the 100-

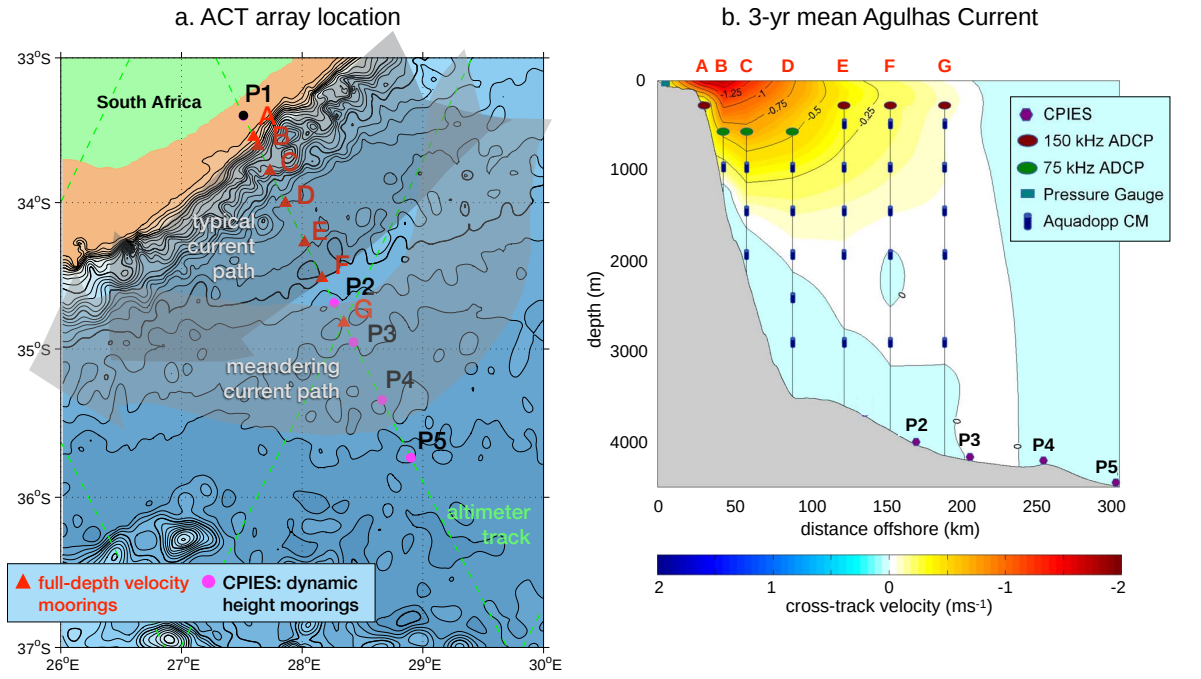

Figure 17.2 Geographical location of ACT mooring array (a) and Vertical section of the mooring array superposed on the 3-year mean cross-track velocity. From Beal and Elipot, 2016.

km-wide East Indian coastal current carrying low-salinity water out of the BoB and an adjacent, broad northward flow (∼300 km wide) that carries high-salinity water into the bay (Wijesekara et al., 2016). Under ASIRI profiling current meter moorings, ocean gliders, and pressure sensor-equipped inverted echo sounders (PIESs) collected time series of the boundary currents, augmented by the nearby surface moorings of RAMA and Indian OMNI (McPhaden et al., chapter 2).

17.3 Essential Ocean Variables

It is essential to capture decadal variations of the Indian Ocean's boundary currents and the ITF in order to understand their roles as carriers of heat, freshwater, nutrients, and carbon, and in driving decadal climate variability and rapid warming trends in the Indian Ocean. Sustained observations of boundary currents have been a priority for international CLIVAR/GOOS for almost a decade, as articulated in an OceanObs09 white paper. Yet currently there is no framework in place for systematic coverage of any of the boundary currents of the Indian Ocean.

Sustained observing of the following EOVs are needed: Velocity, temperature, salinity, and pressure at hourly to monthly temporal resolution, dependent on regional tides and variance, at 5 to 50 km horizontal spacing, dependent on local topography and scales of flow which change across the current, and at vertical resolutions of 10-100 m close to the surface, reducing to 500-1000 m below the thermocline, dependent on local (seasonal) stratification and the depth penetration of the current/undercurrent system. A desirable addition would be to integrate these physical EOVs with nutrient, plankton biomass, and carbon measurements, which are becoming feasible with new automated sensors.

17.4 Actionable recommendations

A. Maintain the frequently repeated IX01 XBT section across the ITF, and enhance with an auto launcher for increased resolution (also of the South Java Current at the northern end) and with Argo float deployments for salinity measurements.

B. Maintain the repeated IX12 XBT section, which crosses the Somali Current and Leeuwin Current systems at its northern and southern ends, respectively, and enhance resolution with an auto launcher.

C. Maintain the existing network of island and coastal sea level stations and ensure open accessibility of these data so that boundary current transports can be estimated using sea level proxies.

D. Maintain satellite altimeter missions to characterize long term variations of mesoscale eddy energetics in ocean boundary currents.

E. Establish an international alliance to measure ITF volume and heat transports, as well as biogeochemical fluxes, in different passages in order to contextualize and constrain the sustained upper-ocean geostrophic estimates from the IX01 XBT section.

F. Re-establish the ASCA mooring array for the Agulhas Current system through regional alliances, combining mooring observations with periodic glider and ship surveys.

G. Enhance the Leeuwin Current array to monitor full-depth volume and heat transports through combined mooring and glider observations.

H. Monitor the Somali Current and the South Java Current using ocean gliders.

I. Sustain observations of the monsoon currents off the Indian subcontinent through regional alliances.

J. Explore the efficacy of IX21 for measuring long-term changes of the Agulhas Current.

18. Upwelling, Coastal-open Ocean Interactions, and Ecosystems

Yukio Masumoto[1], Weidong Yu[2], Raleigh Hood[3], and Michael J. McPhaden[4]

[1]University of Tokyo, Japan, [2]School of Atmospheric Sciences, Sun Yat-Sen University, Zhuhai, China , [3]University of Maryland, USA, [4]PMEL/Tropical Moored Buoy Implementation Panel, NOAA, USA

Upwelling brings cooler and nutrient-rich waters up into the surface layer of the ocean. Cool surface temperatures affect weather and climate over the region, as well as remotely through teleconnection pathways. The nutrient supply can enhance primary productivity (McCreary et al., 2009), thereby influencing the marine food web and commercial fisheries (Hood et al., 2017). At the same time, upwelling brings low oxygen and low pH water up to the surface, with potentially detrimental impacts on marine ecosystems (Feely et al., 2008). Although upwelling zones are regional, they represent ascending branches of basin scale circulation patterns, such as the subtropical cell and cross equatorial cell (e.g., Lee et al., 2004), and thus should be considered in the basin scale context in which they are embedded.

Upwelling systems are an essential component of regional and basin-scale energy transport and material circulations. At the surface they manifest as cooler sea surface temperature (SST), lower sea surface height (SSH), and higher chlorophyll concentration, as readily observed by satellite remote sensing. However, our present understanding of the characteristics and mechanisms of upwelling systems is limited, due mainly to the scarcity of *in situ* observations, both physical and biogeochemical, below the surface. Such observations are necessary to understand the role of upwelling systems in oceanic and climate variability, and their response to this variability and to anthropogenic forcing.

The Indian Ocean is uniquely characterized by seasonally evolving upwelling systems associated with monsoonal winds (Chapter 14). The seasonal development and decay of each upwelling system are not well understood and are further modified by intraseasonal, interannual, and decadal modes of variability (Chapters 13, 19, 22; Vialard et al., 2012; Hood et al., 2015, 2017; Yu et al., 2016). The timing, duration, intensity, and spatial structure of upwelling are determined by the relative contribution from these different modes. The future fate of upwelling, in the context of global warming, is a subject of debate. Several studies have argued that there will be intensification of coastal upwelling in response to the amplified land-sea pressure gradient in the warming world (Bakun et al., 1990; deCastro et al., 2016; Praveen et al., 2016). However, the story in the monsoonal Indian Ocean may be far more complex.

Fisheries and fish products associated with upwelling regions are an important source of protein in developing Indian Ocean rim countries, and provide direct employment to millions of people (FAO, 2004). For example, increases in upwelling in the Java Current are linked to increases in sardine (Sardinella leumuru) catch in Bali Strait (Ghofar et al., 2005). Variations in the strength of the Java Current and the intensity of upwelling are linked to the Indian Ocean Dipole mode and give rise to dramatic interannual variations in sardine catch, which impacts food supply, and therefore market prices and the income of artisanal fishers in Indonesia (Sartimbul et al., 2010). Similar phenomena are observed in other Indian Ocean upwelling systems (Hood et al., 2017). Therefore, there is direct societal benefit in observing and understanding how the timing and intensity of Indian Ocean upwelling systems is modulated by physical processes, and how this modulation might be altered in the future due to climate change.

18.1 Coastal upwelling systems

There are two major coastal upwelling systems in the Indian Ocean, in the east off the islands of Sumatra and Java, and in the west off the coasts of Oman and Somalia (Figure 18.1).

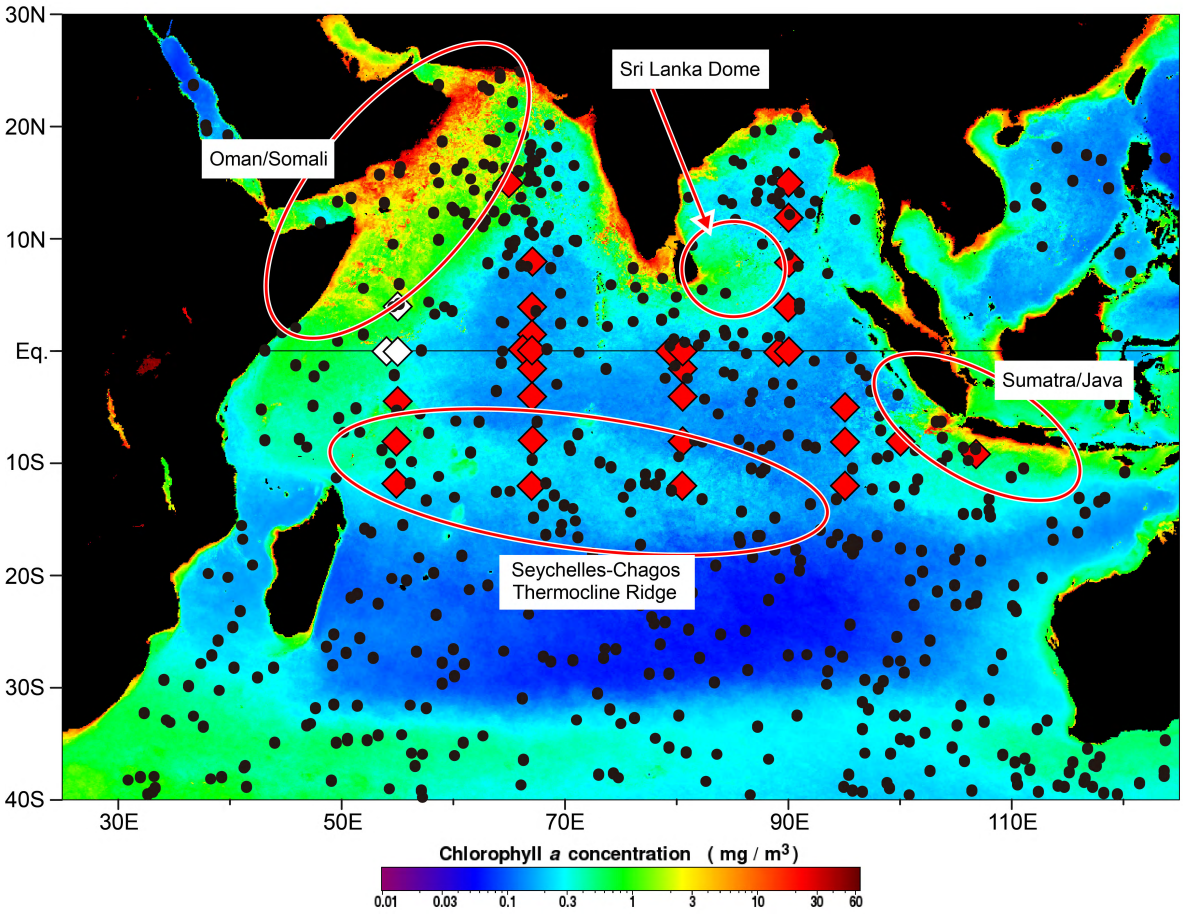

Figure 18.1 Climatological chlorophyll concentration in September from Aqua MODIS. The major upwelling regions are indicated by higher chlorophyll concentration and are highlighted by red ovals. Superposed on the satellite image are locations of Argo floats (black dots) as of March 2018 and of RAMA-2.0 buoys (red (occupied) and white (unoccupied) diamonds).

Upwelling systems are influenced by both regional and remote wind stress and its variability. Fundamental forcing is along-shore monsoonal winds in both regions. The Sumatra/Java upwelling is also affected by remote forcing to the west via the equatorial waveguide (Iskandar et al., 2005; Chen et al., 2016), while the Oman/Somalia upwelling is influenced by wind stress curl in open oceans to the east through westward propagating Rossby waves (Vic et al., 2017). These upwelling systems are also affected by interannual climate modes, such as the Indian Ocean Dipole (Saji et al., 1999; see Chapter 6), which is associated with anomalous primary productivity in the basin (Wiggert et al., 2009b; Currie et al., 2013). Some basic characteristics of seasonal cycle and upwelling strength have been estimated for the Oman/Somalia upwelling (Schott and McCreary, 2001; Schott et al., 2002), yet there is only a qualitative description of the Sumatra/Java upwelling, of which there are few hydrographic observations (Horii et al., 2018). The strongest upwelling signals are concentrated within O(100km) of the coasts, while broader regions of SST cooling and high chlorophyll concentration result from offshore advection and are modified by air-sea heat exchange and by locally and remotely generated mesoscale and

submesoscale variability. Quantitative understanding of these coastal-open ocean interactions need to be improved with temporally and spatially high density data.

There are other coastal upwelling systems of smaller magnitude and spatial extent than those off Sumatra/Java and Oman/Somalia, whose socio-economic impacts may nevertheless be equal to these major systems. Examples are monsoonal-driven upwelling along the southwestern coast of India (Gopalakrishna et al., 2008) and along the northwestern coast of Australia (Rossi et al., 2013) where remote forcing from the Pacific Ocean is transmitted through coastal waveguides (Clarke and Liu, 1994; Meyers et al., 1996; Hood et al., 2017).

18.2 Open ocean upwelling systems

Open ocean upwelling systems, such as the Sri Lanka Dome of the southwest monsoon (Vinayachandran and Yamagata, 1998) and the persistent Seychelles-Chagos thermocline ridge (SCTR; Yokoi et al., 2008; Hermes and Reason, 2009), are associated with cyclonic wind stress curl and modulated by remotely forced Rossby waves (Figure 18.1). Sea surface temperature is very sensitive to variability in the depth of the shallow thermoclines in these upwelling systems, linking them to cyclone activity (Xie et al., 2002), the Asian monsoons (Annamalai et al., 2005; Izumo et al., 2008; Chapter 14), and fisheries (Menard et al., 2007) at seasonal and interannual time-scales.

The SCTR is located in a region of MJO initiation and exhibits the strongest intraseasonal variability of SST in the Indian Ocean (Vialard et al., 2009a; Chapter 13). It also has large interannual variability due to westward propagating Rossby waves triggered by IOD events and the remote influence of ENSO (Xie et al., 2002). Upwelling and strong variability mean the SCTR is more productive than the nearby oligotrophic subtropical ocean. The establishment of the IndOOS, in particular RAMA and the Argo program, have brought much new knowledge about the subsurface structure of the SCTR, including the anomalous oceanic conditions associated with intraseasonal and interannual variations in SST and the seasonal mixed-layer heat budget (Vialard et al., 2009; Foltz et al., 2010). The SCTR attracts a high concentration of tuna fishing activities associated with large tuna schools and is a region of elevated surface phytoplankton levels (Fonteneau et al., 2008). However, the multiscale dynamics and their implications for biochemical processes, linkages between trophic levels, and fisheries resources have yet to explored.

18.3 Physical-biological-biogeochemical interactions

The large variability and diverse physical mechanisms of upwelling systems in the Indian Ocean lead to large uncertainties in the sources and fluxes of major and minor nutrients, limiting our understanding of nutrient delivery and its ecological and biogeochemical implications. These implications include nitrogen fixation, cryptic (i.e. subsurface) plankton blooms, and the oxygen minimum layer (Chapter 20). Fundamental questions remain regarding the impact of upwelling on nutrient stoichiometry (e.g., N, Si, and Fe), associated influence on nutrient limitation controls, and the subsequent species composition of upwelling-induced phytoplankton blooms (Wiggert et al., 2006; Resplandy et al., 2011; Hood et al., 2017). Enhancement and transport of plankton production and distribution and variability of the plankton community are also linked to upwelling systems and have important implications for higher trophic levels and hence artisanal and commercial fisheries (Kaplan et al., 2014).

18.4 Essential Ocean Variables

The mechanisms of variability of upwelling systems in the Indian Ocean, from intraseasonal to decadal to anthropogenic change, are not yet well understood. We need to observe physical, biological, and biogeochemical parameters at several key locations at temporal resolution high enough to resolve intraseasonal variability. Essential Ocean Variables for the upwelling systems are: (1) Temperature and salinity down to 1000 m, resolving the diurnal cycle in several key locations. (2) Satellite data: SST, ocean color, surface winds, and SSH. (3) Biogeochemical and ecological parameters: nutrients, chlorophyll, oxygen, pH, CO_2, and plankton community structures. (4) Microstructure measurements in the upper layer to evaluate vertical mixing processes.

18.5 Actionable Recommendations

The main strength of the IndOOS has been to obtain basin-scale data, away from the boundary areas. For example, the open-ocean upwelling system in the SCTR is observed by RAMA and Argo (Figure 18.1). However, for important coastal upwelling systems *in situ* observations hardly exist. Although these upwelling systems appear regional, they are connected to basin-scale circulation and overturning and can influence basin-scale variability across a broad range of timescales. The IndOOS, therefore, should provide data on background conditions in these upwelling systems, with a focus on intraseasonal to interannual time scales and phenomena responsible for mixed-layer processes and their interactions. Relationships between physical forcing, biogeochemical/ecological responses, and air-sea interactions need to be captured.

The fact that these coastal systems are located within EEZs of Indian Ocean rim countries causes some challenges. Pilot studies are recommended in order to test observing strategies and new observing platforms, and to develop capacity building and resource sharing with scientists, students, and users of the observed data in the rim countries.

We recommend the following actions, though they may involve challenging political and logistical arrangements, to build the IndOOS towards sustained observing of upwelling systems:

A. Maintain RAMA sites along 8°S within the Seychelles-Chagos thermocline ridge and in the equatorial region.

B. Maintain satellite observations of SST, sea level, surface momentum and heat fluxes, and ocean color. Since the satellite based SSH data near the coast is affected by land, tide gauges must also be maintained.

C. Extend the IndOOS into the Sumatra/Java upwelling region, by enhancing deployment of Argo and BGC-Argo floats or adding glider sections.

D. A pilot study of new observing platforms within the Oman/Somalia upwelling region, potentially a RAMA site, BGC-Argo deployment, and/or glider sections. An intensive process study is needed with a capacity development component.

E. A process study to obtain sectional cruise observations across the upwelling regions (Sumatra/Java and/or the Seychelles-Chagos thermocline ridge) during upwelling and non-upwelling seasons to conduct microstructure measurements for evaluation of vertical mixing processes and to obtain water samples for nutrients, chlorophyll, oxygen, pH, CO_2, and plankton community structure analyses.

19. Interannual Variability and Predictability

Tomoki Tozuka[1], Takeshi Doi[2], and Michael J. McPhaden[3]

[1]The University of Tokyo, [2]Application Laboratory, JAMSTEC, [3]NOAA/PMEL

There are four prominent modes of interannual variability in the Indian Ocean, namely the Indian Ocean Dipole (IOD), the Indian Ocean Basin Mode (IOBM), the Indian Ocean Subtropical Dipole (IOSD), and Ningaloo Niño (Figure 19.1). The first two modes have large impacts on both local and remote climate, while the latter two modes strongly influence regional climate. The IOBM is predominantly driven by ENSO and hence is not strictly an independent climate mode and the other three modes are modulated by ENSO. Both IOSD and Ningaloo Niño are associated with modulation of the subtropical high in the southern Indian Ocean.

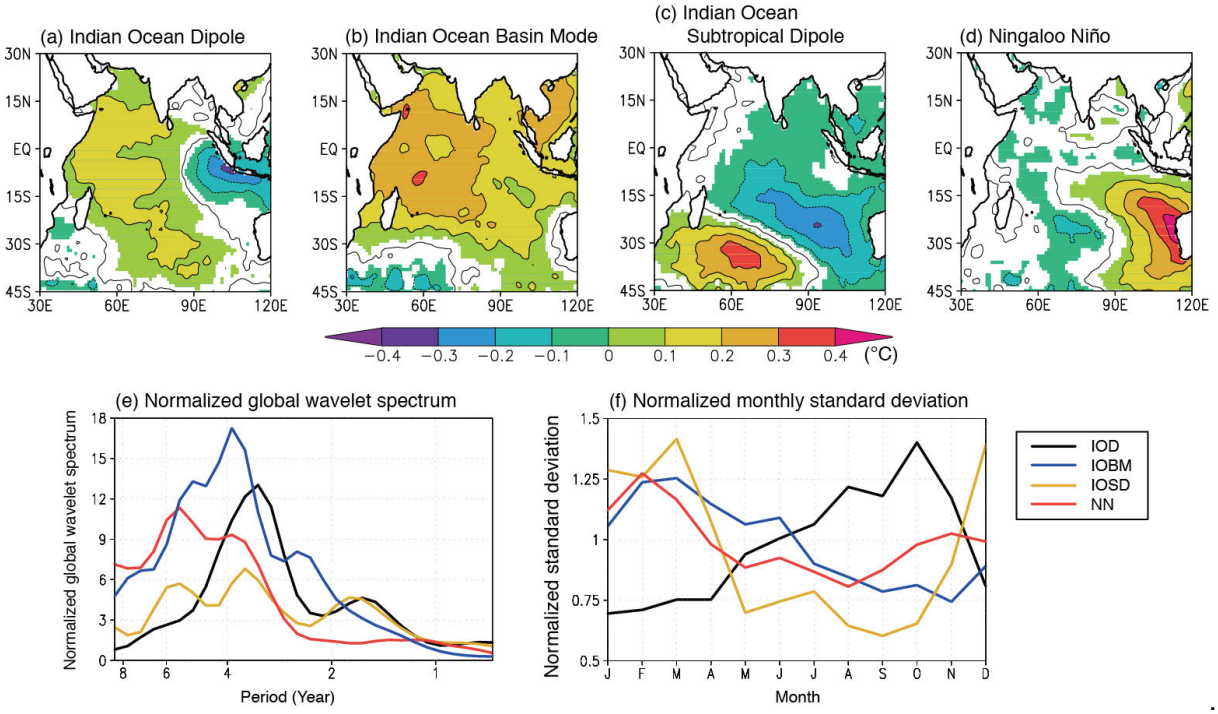

Figure 19.1 Sea surface temperature anomalies (HadISST, Rayner et al., 2003) associated with (a) the Indian Ocean Dipole, (b) the Indian Ocean Basin Mode, (c) the Indian Ocean Subtropical Dipole, and (d) Ningaloo Niño. Detrended SST anomalies (in °C) are regressed against their respective normalized indices. Regression coefficients significant at the 99% confidence level by a two-tailed t-test are shaded and contour intervals are 0.2°C. All months of data are used. (e) Normalized global wavelet spectrum and (f) normalized monthly standard deviation of the four indices (see legend).

19.1 Indian Ocean Dipole

The IOD is an interannual air-sea coupled phenomenon with positive SST anomalies in the western tropics and negative anomalies in the southeastern tropics during its positive phase (Saji et al., 1999; Webster et al., 1999; Figure 19.1a and e). Hence, the Dipole Mode Index is defined as the difference between SST anomalies of the western (50°–70°E, 10°S–10°N) and eastern (90°–110°E, 10°S–Equator) tropics (Saji et al., 1999). Positive IOD is associated with easterly wind anomalies and enhanced convection over the western tropical Indian Ocean

(Reverdin et al., 1987) during boreal fall (Figure 19.1f; Saji et al., 1999). The IOD develops through Bjerknes feedback, similar to ENSO (Saji et al., 1999), and evolves through ocean dynamics, including equatorial wave processes and coastal upwelling (Chapters 18 and 21; Nagura and McPhaden, 2010a; McPhaden et al., 2015). Salinity and barrier-layer variability is significant during IOD events. During a positive IOD, negative sea surface salinity (SSS) anomalies appear in the central-eastern equatorial Indian Ocean, while positive SSS anomalies are observed in the southeastern tropical Indian Ocean (Zhang et al., 2013). Below the surface, near the pycnocline, SSS anomalies of opposite sign occur (Kido and Tozuka, 2017). These salinity anomalies result in barrier layer thickness anomalies and vertical mixing anomalies and may modify the amplitude of negative SST anomalies at the eastern pole (Qiu et al., 2012; Kido and Tozuka, 2017).

The IOD sometimes occurs alongside ENSO, and sometimes independently (Yamagata et al., 2004). Simulation of the IOD has been evaluated by several studies (e.g. Saji et al., 2006; Liu et al., 2014) and, because of its impacts on both local and remote climate (Saji and Yamagata, 2003), many studies have focused on predictability and prediction. Wajsowicz (2005) made the first attempt to assess the skill of a coupled model in predicting SST anomalies over the eastern and western poles of the IOD and Luo et al., (2008) made the first successful real-time prediction of the IOD. ENSO is a major source of predictability for the IOD, through changes in the Walker circulation over the Indo-Pacific region (e.g. Luo et al., 2007; McPhaden and Nagura, 2014; Yang et al., 2015). SST anomalies in the eastern pole show lower prediction skill compared to the western pole (Luo et al., 2007), because the eastern pole is partly driven by local-air sea coupling, whereas the western pole is predominantly controlled by ENSO. Tanizaki et al., (2017) showed that generation mechanisms of negative SST anomalies in the eastern pole are diverse among positive IOD events, and that those events in which vertical processes play an important role tend to be better predicted. Currently, the anomaly correlation coefficient becomes lower than 0.5 after only 3 months (Liu et al., 2017). Under global warming, extreme IOD events are projected to increase (e.g. Cai et al., 2014b) while IOD skewness will decrease (e.g. Zheng et al., 2010; Chapter 25). The RAMA moorings in the tropical Indian Ocean are essential for observing the IOD.

19.2 Indian Ocean Basin Mode

The Indian Ocean Basin mode is associated with positive SST anomalies over the tropical Indian Ocean, typically following an El Niño, and with negative anomalies following La Niña (Yu and Rienecker, 1999; Yang et al., 2007; Figure. 19.1b). This mode is predominantly driven by surface heat fluxes, although ocean dynamics are important in the southwestern tropical Indian Ocean (Klein et al., 1999). The IOBM index is defined by the principal component of the first empirical orthogonal function mode of SST anomalies over the tropical Indian Ocean (40–110°E, 20°S–20°N) (Yang et al., 2007) and explains about 40% of the total SST variability. It is highly correlated with ENSO and with the IOBM index itself with a lag of one season. The interannual frequency band is dominant (Figure 19.1e) and the monthly standard deviation peaks in February-March (Figure 19.1f). The IOBM has been shown to influence climate over the Indo-western Pacific and East Asia in the summer following ENSO events and the effect is known as the “Indian Ocean capacitor effect” (Xie et al., 2009, Annamalai et al., 2005; 2007). About half of the CMIP5 models capture key processes of the IOBM including its strong link with the ENSO (Du et al., 2013). Among the four climate modes of the Indian Ocean, the IOBM has the most predictability because of its strong link with ENSO (Luo et al., 2016a).

19.3 Indian Ocean Subtropical Dipole

The Indian Ocean Subtropical Dipole is a climate mode associated with positive SST anomalies over the western subtropical South Indian Ocean and negative anomalies in the northeastern subtropics during austral summer (Behera and Yamagata, 2001; Figure 19.1c and f). Its index is obtained by subtracting SST anomalies in the northeastern pole (90°–100°E, 18°–28°S) from those in the southwestern pole (55°–65°E, 27°–37°S). It has spectral peaks in the interannual frequency range, but not as sharp as that of the IOD (Figure 19.1e). Mixed layer warming by shortwave radiation is enhanced (suppressed) as a result of negative (positive) mixed layer depth anomalies over the southwestern (northeastern) poles, and these anomalies are induced by anomalous winds associated with changes in the Mascarene High (Morioka et al., 2010). The IOSD has been suggested to influence precipitation over southern Africa (Reason et al., 2001). Although many coupled models simulate the IOSD reasonably well, the location and structure of the SST anomaly vary among models (Kataoka et al., 2012). Prediction skill for IOSD is not much different from persistence, partly because of low predictability of SST anomalies in the southwestern pole (Yuan et al., 2014), although some strong IOSD events are successfully predicted one season ahead. The low prediction skill may be related to difficulty in predicting interannual variability of the Mascarene High and increased observations of upper ocean stratification within the subrtropical gyre may help improve prediction skill.

19.4 Ningaloo Niño

An unprecedented marine heat wave in early 2011 led to the identification of a new climate mode called “Ningaloo Niño” (Feng et al., 2013, 2015b; Chapter 12). This recently-identified phenomenon is associated with positive SST anomalies off the west coast of Australia (Figure 19.1d) and its strength is defined by the Ningaloo Niño Index (area-averaged SST anomalies from 108°E to the coast, and between 28°S and 22°S). Both positive, local ocean-atmosphere feedback and remote forcing from ENSO via atmospheric and oceanic teleconnections contribute to its development (Feng et al., 2013; Kataoka et al., 2014, 2017; Marshall et al., 2015). The mode peaks around austral summer (Figure 19.1f) and has a 4-6 year period (Figure 19.1e). Salinity variability is also linked to Ningaloo Niño (Feng et al., 2015a) with low-salinity anomalies contributing to a $\sim$30% increase in the southward Leeuwin Current which led to the unprecedented warming event in 2010-2011. The increased occurrence of Ningaloo Niño since the late 1990s may be related to the negative phase of the Interdecadal Pacific Oscillation (Feng et al., 2015b). Because of its impacts on local precipitation (Tozuka et al., 2014) and marine ecosystems (Depczynski et al., 2013; Wernberg et al., 2013, 2016), advancing our understanding of this phenomenon is a priority for the coming decade. Improvements in resolving this climate mode are required in many coupled models (Kido et al., 2016).

Ningaloo Niño/Niña events that co-occur with La Niña (El Niño), such as the 2011 event which could be predicted 9 months in advance in hindcast experiments, are relatively predictable owing to the high prediction skill for ENSO (Doi et al., 2013). Events developing independent of ENSO could not be predicted. Measuring the strength of the Leeuwin Current and resolving the flow in the ocean component of coupled models may lead to improved prediction skill (Doi et al., 2016). Also, since mixed layer processes play a key role in the evolution of Ningaloo Niño/Niña, more subsurface observations in the region of maximum SST anomalies will improve understanding and hence prediction.

19.5 Essential Ocean Variables

The IndOOS has played an essential role in our current understanding of interannual climate variability in the Indian Ocean, yet a better understanding and improved predictions are needed. The required EOVs are: Ocean surface wind stress, SSH, SST, SSS, subsurface temperature, salinity, and velocity, and ocean surface heat flux. Considering that coastal currents and upwelling at the eastern boundary play an important role in the development of the IOD (Halkides and Lee, 2009; Tanizaki et al., 2017; Chapter 18) and Ningaloo Niño/Niña (Marshall et al., 2015; Chapter 12), it is desirable to obtain the above EOVs with a horizontal resolution of 0.5° or higher in this region. Sub-daily data are required because intraseasonal variations sensitive to diurnal signals, including the MJO, influence the evolution of these climate modes (Rao and Yamagata, 2004; Marshall and Hendon, 2014; Chapter 13). Subsurface data, for mixed layer and thermocline depth, are valuable for improved prediction of these climate modes (Horii et al., 2008; Doi et al., 2017).

19.6 Actionable Recommendations

Based on the above, and on the current state of the IndOOS, we recommend:

A. Maintain the existing elements of IndOOS, in particular satellite missions and the Argo network.

B. Complete and maintain the RAMA-2.0 buoy network. Tropical sites within the western and eastern poles of the IOD are essential.

C. Enhance near-coastal observations to a horizontal resolution of 0.25° or higher at the tropical eastern boundary.

D. Maintain the IX01 XBT line with a fortnightly resolution to monitor the Pacific influence on Ningaloo Niño/Niña.

20. Oxygen Variability and Change, Oxygen Minimum Zones

Jerry Wiggert[1] and Laure Resplandy[2]

[1]University of Southern Mississippi, USA, [2]Princeton Environmental Institute, USA

20.1 Deoxygenation in the Indian Ocean

Under the influence of anthropogenically driven climate change, the world's oceans are experiencing a clear trend in deoxygenation that is already having profound impacts on ecological function. Oceanic deoxygenation has been slower to gain recognition in the scientific community relative to other high-profile impacts such as warming, sea level rise, and ocean acidification (Gruber et al., 2011). The onset and acceleration of oceanic deoxygenation is driven by global warming through both reduced oxygen solubility as temperatures increase, and reduced ventilation as stratification increases. Ventilation is the process of low O_2 waters within the thermocline outcropping into the mixed layer to allow air-sea exchange. Reduced dissolved oxygen (DO) levels within thermocline waters then result because the oxygen demand associated with heterotrophic remineralization of sinking organic matter is no longer met by the solubility and ventilation-mediated supply of oxygen.

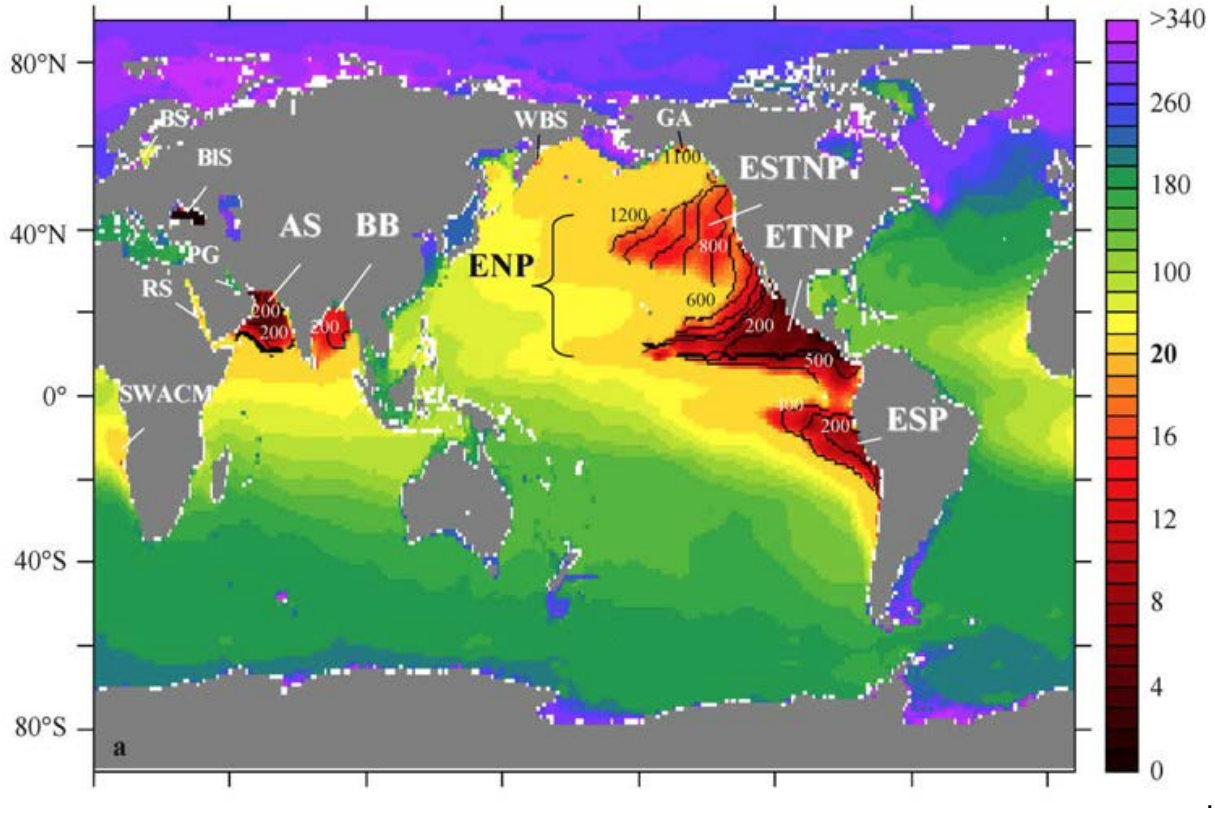

Figure 20.1 Oxygen distribution (μM) at depth where O_2 concentration is minimal, indicating the extent of the OMZs (in red) according to the WOA2005 climatology. Contours indicate the limit of the upper OMZ core depth in meters with a 100-m contour interval. From Paulmier and Ruiz-Pino (2009).

In short, increased flux of export production (higher oxygen demand) and / or reduced ventilation due to stronger stratification (lower oxygen supply) will promote oceanic deoxygenation. In

coastal waters, eutrophication due to increases in nutrient-loading from runoff or riverine input of agricultural fertilizers is a prime example of amplified oxygen demand that has led to coastal hypoxia (Rabalais et al., 2010).

Two of the worlds most severe oxygen minimum zones (OMZs) occur in the northern Indian Ocean (Figure 20.1, Paulmier and Ruiz-Pino, 2009). The Arabian Sea OMZ contributes 20% of the global mesopelagic denitrification budget and has been identified as a hotspot of oceanic efflux of N_2O, which is a greenhouse gas that factors into atmospheric ozone cycling (Bange et al., 2001; Codispoti et al., 2001; Bange et al., 2005; Naqvi et al., 2010). The intensity of the Bay of Bengal OMZ has not reached hypoxic or anoxic conditions and hence its biogeochemical impact is less significant (Bange et al., 2009). However, there has been a systematic deoxygenation of the northern Indian Ocean over the last fifty years (Figure 20.2, Stramma et al., 2010). In the Bay of Bengal this deoxygenation trend may trigger a transition to permanent, wide-spread hypoxia. In the Arabian Sea, where thermocline hypoxia is well-established, this deoxygenation trend is consistent with an estimated 63% expansion of the OMZ since the 1990s (Rixen et al., 2014; Morrison et al., 1999).

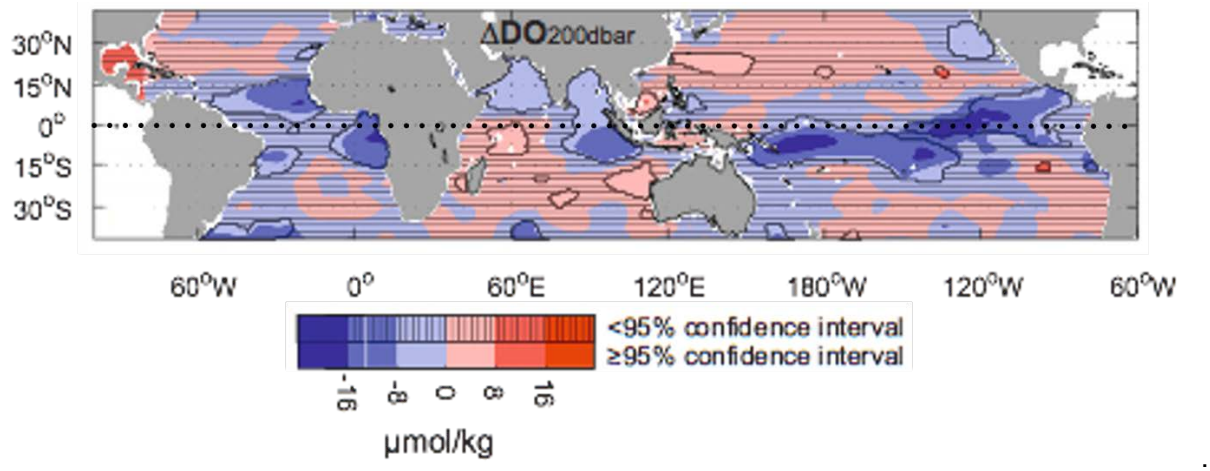

Figure 20.2 Changes in dissolved oxygen (ΔDO) (µmol kg^{-1}) at 200 dbar between 1960–1974 and 1990–2008. Increases (decreases) in DO are indicated in red (blue). Areas with differences below the 95% confidence interval are shaded by black horizontal lines. From Stramma et al., (2010).

In the southern tropical Indian Ocean there is an increase of thermocline DO in the west and a decrease in the east (Figure 20.2, Stramma et al., 2010), suggesting a potential multi-decadal influence exerted by the Indian Ocean Dipole (Saji et al., 1999) on biogeochemical processes. The IOD's influence on cross-basin thermocline dynamics is well-established (Webster et al., 1999), and biophysical responses have been identified across all marine trophic levels (Figure 20.3, Menard et al., 2007; Wiggert et al., 2009). The spatial coherence between long-term DO trends and the IOD signature suggests that these readily observed surface biological responses link to underlying biogeochemical variability that is poorly characterized. This inference is supported by a biophysical model of the Indian Ocean that demonstrates a strong positive correlation between elevated chlorophyll and IOD occurrence in the east during boreal summer and fall, and a strong negative correlation in the west during boreal fall and winter (Currie et al., 2013).

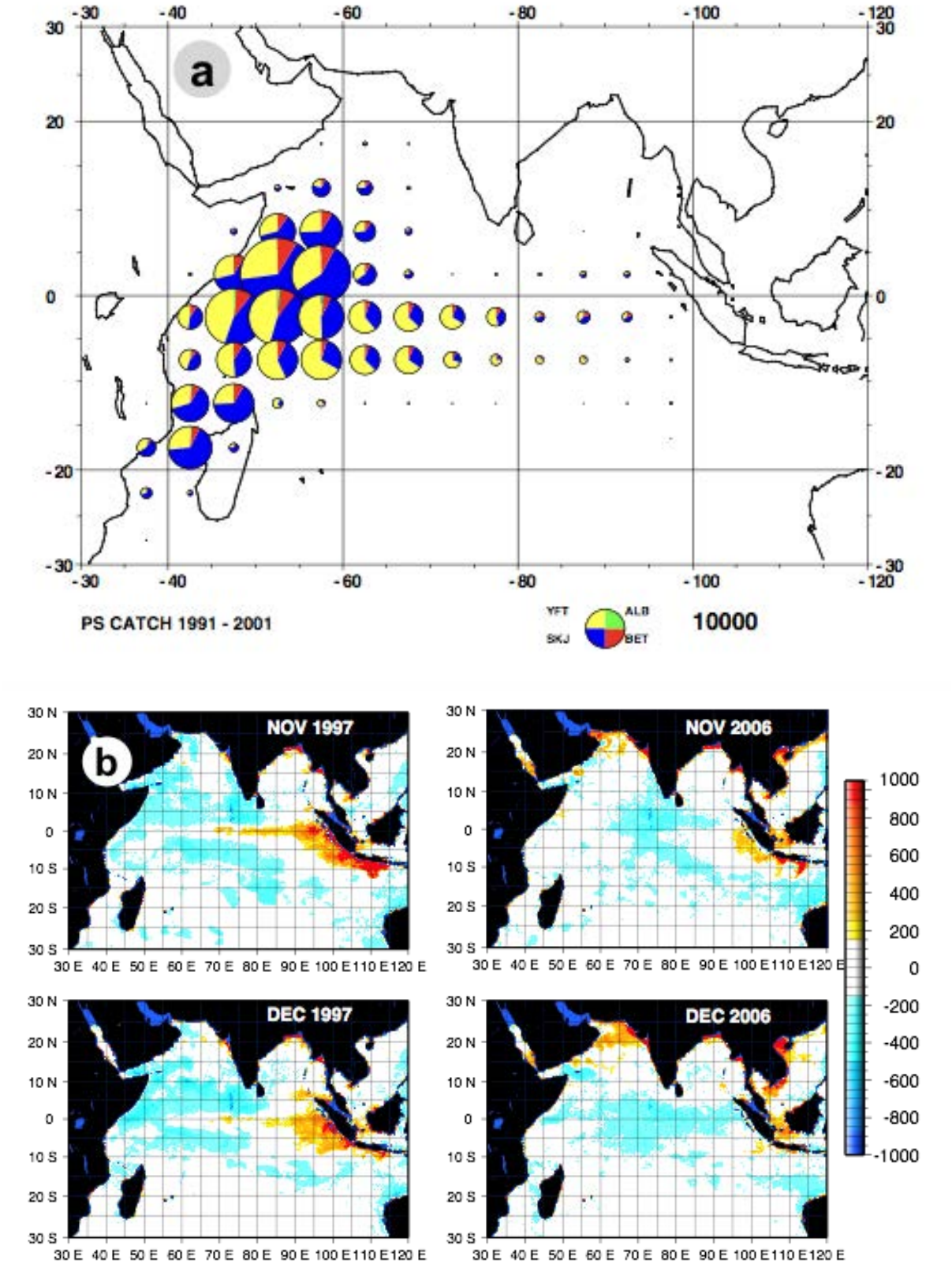

Figure 20.3 a) Average annual purse seine catch per unit effort (CPUE) for tuna (1991 – 2001). During the 97/98 IOD, significant shift of CPUE to eastern Indian Ocean observed (pers comm F. Marsac). Four species are: Yellowfin (YFT), Skipjack (SKJ), Bigeye (BET) and Albacore (ALB). b) Net primary production anomaly (NPPa, mgC m^{-2} d^{-1}) during Nov-Dec period for the IOD manifestations of 1997 and 2006. From Wiggert et al., (2009).

There is also a suggested linkage between IOD and interannual DO variability in the eastern Arabian Sea region, where a model shows suppression of coastal anoxia when the IOD is active (Vallivattathillam et al., 2017). Earth system models consistently project global oceanic de-oxygenation trends, but large uncertainties remain for OMZ regions, including in the Indian Ocean (Bopp et al., 2013). These uncertainties arise from an unknown balance between DO decrease due to warming and an increase due to amplified ventilation, particularly in upwelling regions (Bopp et al., 2017).

20.2 Ecological and societal impacts of oceanic deoxygenation

It is critical that we understand the physical and biogeochemical controls that regulate OMZ severity within the Arabian Sea and Bay of Bengal in order to predict the consequences of anthropogenic climate change. Should the OMZ in the Bay of Bengal transition to widespread hypoxia, as prevails in the Arabian Sea, then profound shifts in nitrogen cycling would result, with globally significant contributions to rates of oceanic denitrification and efflux of nitrous oxide (N_2O), a potent greenhouse gas. Deoxygenation impacts all levels of the marine ecosystem, particularly in combination with global warming. As temperatures in the marine environment increase, the metabolic rates of organisms tend to rise exponentially (e.g., Eppley, 1972), leading to higher production and growth rates that necessitate higher metabolic rates that, in turn, rely on oxygen availability to satisfy increased respiratory demands (Doney et al., 2012). Faced with sub-optimal dissolved oxygen availability, marine organisms will initiate conservation responses, such as reduced activity and cellular function, or avoidance behaviors that may adversely impact growth, reproduction and survival (Ekau et al., 2010). These responses will vary greatly across species. Moreover, as the projected expansion of suboxic waters and associated shoaling of tropical OMZs unfolds, the habitats of planktonic and pelagic species will compress. The foraging efficiency for large fishes, like billfishes and tuna, may improve as a result, while also making them more vulnerable to exploitation by the fisheries industry (Stramma et al., 2010). Deoxygenation can also lead to speciation shifts as trophic niches are impacted through the differential response of taxa to low oxygen conditions, an outcome already observed in the Arabian Sea where specific copepods have increased in the hypoxic water column (Wishner et al., 2008) and *Noctiluca scintillans* now appear during winter and spring (Gomes et al., 2014).

Coastal ocean regions are even more prone to deoxygenation, due to their proximity to human influences, including agricultural activity, sewage outfalls, regulation of riverine inflows, and atmospheric nitrogen deposition. In the eastern Arabian Sea, eutrophication has led to a multi-decadal trend of expanding coastal hypoxia along the west coast of India that has adversely affected coastal fisheries (Naqvi et al., 1998; Ram et al., 2014). The coastal waters of the Bay of Bengal are similarly at risk (Hood et al., 2017). Projections accounting for evolving agricultural practice and human population growth indicate that the northern Indian Ocean, and particularly the Bay of Bengal, is subject to the highest eutrophication potential globally (Seitzinger et al., 2010). The economies of Indian Ocean rim nations, home to approximately 2 billion people, are the most vulnerable to projected climate change impacts on fisheries production (Allison et al., 2009). In conclusion, the potential societal impact of oceanic deoxygenation in the Indian Ocean is acute and far-reaching.

20.3 Essential Ocean Variables

The global database of DO measurements has clear shortcomings in spatial coverage. In fact, there are more observations from the 1960s-1970s baseline period than during the 1990s-2000s (Stramma et al., 2010). A more comprehensive, basinwide dataset of dissolved oxygen

is needed to establish changes since the baseline period. In particular, sampling efforts that better resolve the spatial and temporal variability of the basin's OMZs are crucial. These are regions where hypoxia onset represents a significant elemental cycling transition, and where Earth System Models show the greatest uncertainty. In addition to marginally resolved decadal variability, OMZs likely experience notable variability at seasonal to interannual time scales that impact biogeochemical processes and climate. This variability could be resolved with more observations.

Most important EOVs are: DO and NO_3. Significant deficits of NO_3 within the thermocline serve as an indicator of hypoxia. To more fully ascertain the degree to which an OMZ is hypoxic, and therefore how substantially it is contributing to global N-cycling, a more comprehensive suite of EOVs with greater precision is required: NO_2, NH_4, PO_4, and $\delta^{15}N$. These can provide information about the extent and function of biogeochemical processing within an hypoxic / anoxic OMZ.

The new insight garnered from sustained observations of the spatial and temporal variability of OMZs would allow for the development of more robust biogeochemical models. In turn, these modeling systems can provide insight into the important biophysical processes that control OMZs, and provide more accurate future climate projections.

20.4 Actionable Recommendations

The expansion of the IndOOS to include DO and NO_3 measurements is essential to assess deoxygenation trends across the basin. BGC-Argo floats with sensors for automated observations of these EOVs now exist and a few have already been deployed in the Indian Ocean (Chapter 1). For the full suite of EOVs ship-based observations are necessary.

A. A suite of 200 BGC-Argo floats to cover the Indian Ocean as part of a global implementation plan of 1000 BGC-Argo floats (Chapter 1). *In situ* air calibrations to refine DO measurement precision should be adopted (Bushinsky et al., 2016). Floats should be targeted to regions that exhibit the strongest deoxygenation signals (Figure 20.2).

B. A fleet of gliders or AUVs outfitted to measure dissolved oxygen and core nutrients to sample coastal regions where societal implications are greatest.

C. Leverage ship-based sampling opportunities (GO-SHIP, GEOTRACES) to obtain the full suite of geochemical EOVs (NO_2, NH_4, PO_4, and $\delta^{15}N$) and perform onboard rate experiments within OMZs.

21. Regional Sea-level Variability and Change

Weiqing Han[1], Jérôme Vialard[2], Michael J. McPhaden[3], Mathew K. Roxy[4], Ming Feng[5], Toshiaki Shinoda[6], and Tong Lee[7,8]

[1]University of Colorado, USA, [2]LOCEAN-IPSL, Sorbonne Universités (UPMC, Univ. Paris 06)-CNRS-IRD-MNHN, France, [3]NOAA/Pacific Marine Environmental Laboratory (PMEL), USA, [4]Indian Institute of Tropical Meteorology (IITM), India, [5]CSIRO Ocean and Atmosphere, Australia, [6]Texas A&M University, [7]NASA Jet Propulsion Laboratory (JPL), USA, [8]California Institute of Technology, USA

21.1 Background

Despite the huge societal demand for improved understanding of sea level change over the Indian Ocean, our knowledge of sea level variability and its major drivers, particularly at decadal and multi-decadal timescales, remains limited due to the lack of observational records. Sea level change refers to the anthropogenic change associated with greenhouse gas forcing. Tide gauges are invaluable for directly detecting multi-decadal and centennial trends and variability of relative sea level and have shown sea level to be rising at a rate of 1$\sim$2 mm yr-1 around the Indian coast on average, based on records of 40 yrs and longer (Unnikrishnan and Shankar, 2007). However, archaeological records at Saint Paul Island in the south Indian Ocean show no statistically significant trend for the 1874-2009 period (Testut et al., 2010) and a century-long tide gauge record at Mumbai documents significant inter-decadal sea level variability (Shankar and Shetye, 1999). Hence, it is difficult to disentangle regional patterns of sea level variability and change over the Indian Ocean. Sea level has risen at all tide gauge locations since the 1960s, except at the Zanzibar station, where sea level has fallen during recent decades (Figure 21.1, black lines). The record length at Zanzibar, however, is only 20 yrs (from 1985 to early 2000s) and that from the Seychelles is even shorter. The sparseness of tide gauge stations, together with their limited duration, hampers the characterisation of spatial patterns of multi-decadal sea level trend over the Indian Ocean. Indeed, there are only a dozen data points over the entire region with records of more than 50yrs and only two over 100yrs (Bradshaw et al., 2015).

To compensate for this limitation, ocean reanalysis products, reconstructed sea level data, and OGCM simulations have been used to estimate basin-wide patterns of SLC (Han et al., 2010). The results show that sea level fall at Zanzibar is associated with a large-scale reduction over the southwest tropical Indian Ocean (Figure 21.1; Han et al., 2010; Timmerman et al., 2010; Dunne et al., 2012). This distinct spatial pattern is forced by the changing surface winds associated with changing Indian Ocean Walker and Hadley circulations (Han et al., 2010). While the multi-decadal trend of surface winds appears largely associated with natural variability, AGCM and large-ensemble climate model experiments suggest that $\sim$20% of the Seychelles sea level reduction could be forced by Indian Ocean warming (Han et al., 2010; 2018) attributed to anthropogenic greenhouse gas forcing (Du and Xie, 2008; Dong et al., 2014). The regional patterns and magnitudes of sea level change at multi-decadal timescales, however, are strongly dependent on the datasets and models used (Nidheesh et al., 2013; Han et al., 2018), illustrating a critical need for sustained, basin-scale observations.

The advent of satellite altimetry has revolutionized our ability to detect basin-scale patterns of sea level variations since the early 1990s (Lee et al., 2017). Overlying the multi-decadal sea level trend is large-amplitude variability at intraseasonal-to-decadal timescales. On intrasea-

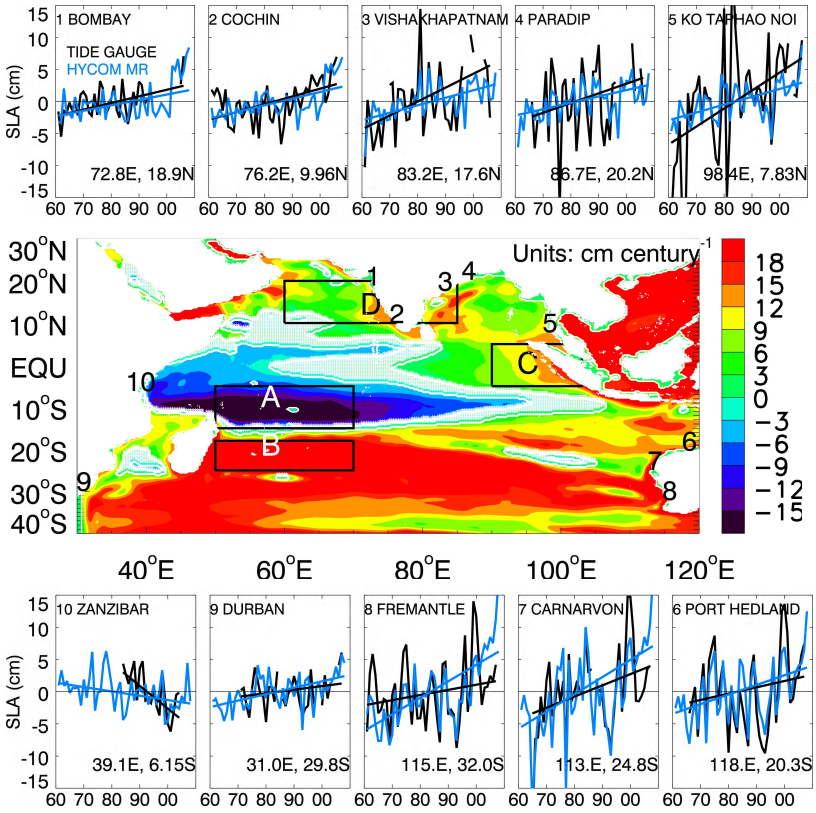

Figure 21.1 Tide gauge observed and OGCM simulated annual mean sea level anomalies (SLA) and their trends during 1961-2008. The 10 tide gauge stations with records longer than 30 years (20 years for Zanzibar) are shown. All trends exceed 95% significance except for stations 6 and 9. Middle color panel shows trend of HYCOM SLA for 1961-2008. Light blue/green regions are below and the rest above 95% significance. Figure from Han et al., (2010).

sonal timescales, strong sea level variability is associated with equatorial Kelvin and Rossby waves (e.g., Han et al., 2005; Fu et al., 2007; Iskandar and McPhaden, 2011; Nagura and McPhaden, 2012), which propagate into the Northern Indian Ocean coastal waveguide (Vialard et al., 2009b), and with basin-resonance at 90-day period (Han et al., 2005). Mesoscale eddies induced by oceanic internal variability can also have a significant contribution to sea level variability in some regions of the Indian Ocean (Li and Han, 2015) and they dominate the smaller-scale ($<6°$) sea level variance globally (Sérazin et al., 2015).

On seasonal and interannual timescales, variability is associated with the mean seasonal cycle and the Indian Ocean Dipole (Perigaud and Delecluse, 1992; Fu and Smith, 1996; Shankar et al., 2010; Nagura and McPhaden, 2010b; McPhaden and Nagura, 2014). Interannual signals associated with the IOD also propagate into the northern Indian Ocean via the coastal waveguide, which can affect surface anoxic events and thus marine ecosystems (Parvathi et al., 2017). On decadal timescales sea level differences between the east and west coasts of the tropical south Indian Ocean have been used to infer changes in the lower limb of the shallow overturning circulation and linkages to the Pacific shallow overturning circulation (Lee et al., 2004; Lee and McPhaden, 2008; Feng et al., 2010; Thompson et al., 2016; Srinivasu et al., 2017).

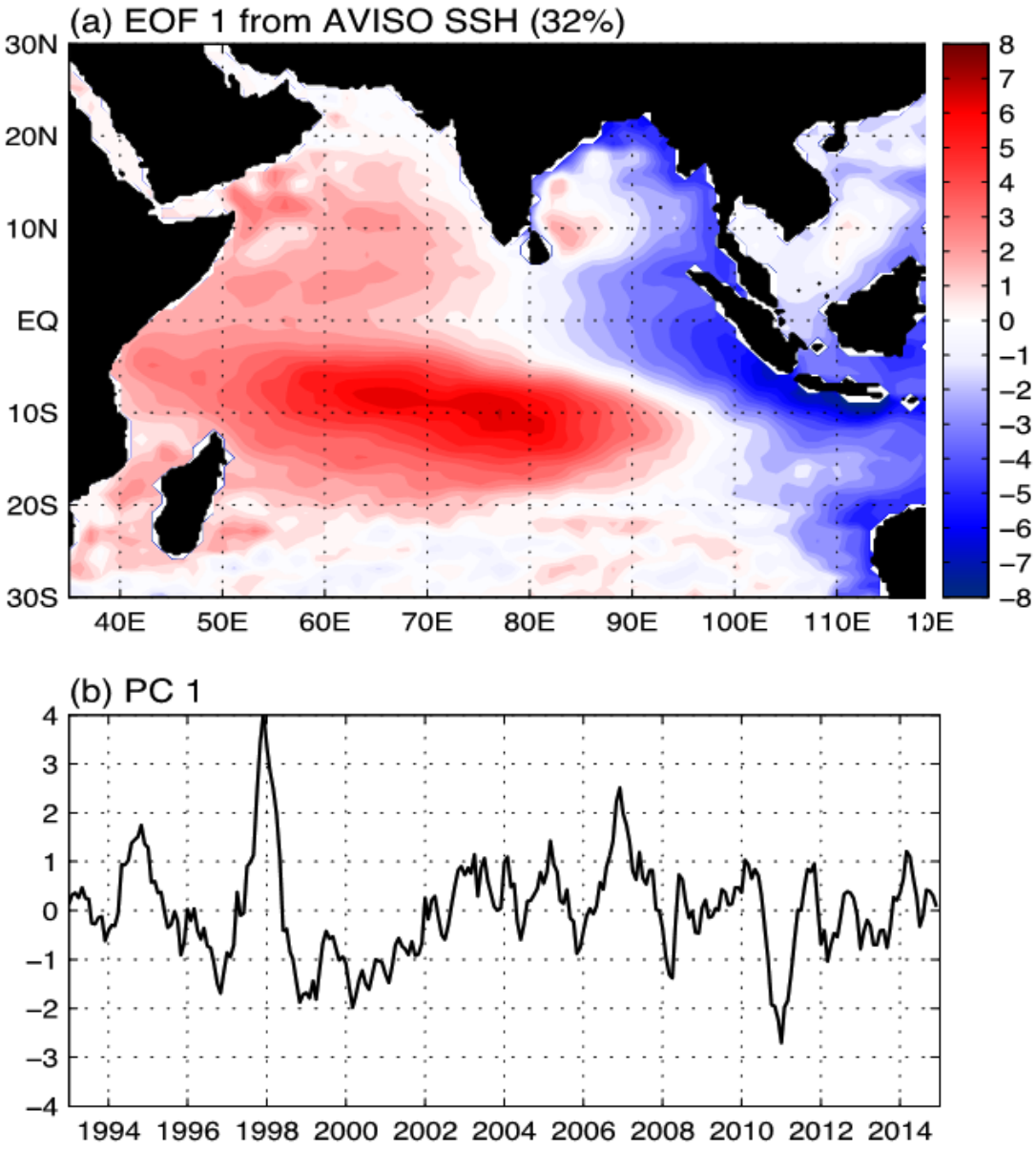

Figure 21.2 The leading EOF of SSH (a) and PC1 (b), based on AVISO monthly interannual anomalies from 1993-2014 with linear trend removed. This spatial pattern of SSH anomaly is associated with the IOD and ENSO; the 1994, 1997 and 2006 positive IOD events are evident from PC1, and the 1997 positive IOD co-occurred with El Niño.

Among the many factors that can cause sea level to change regionally (Church et al., 2013; Stammer et al., 2013; Kopp et al., 2015), surface wind patterns - with a large proportion being associated with natural modes such as the MJO, monsoon, ENSO and IOD - are shown to be a major factor (Li and Han, 2015; reviews by Stammer et al., 2013 and Han et al., 2017; Han et al., 2018). For instance, a distinct spatial pattern of sea level variability at interannual timescale is associated with the IOD and ENSO (Figure 21.2) and primarily driven by IOD- and ENSO-related surface winds (Rao et al., 2002; McPhaden and Nagura, 2014; Deepa et al., 2018; Zhang and Han, 2019). ENSO can affect Indian Ocean sea level through both an atmospheric bridge via surface winds, and an oceanic connection via the ITF. ENSO-associated winds can cause large sea level variability in the thermocline ridge region (Xie et al., 2002; Deepa et al.,

2018; Zhang and Han, 2019), while its effect via the ITF is primarily confined to the southeast Indian Ocean, particularly near the west coast of Australia (Trenary and Han, 2012; Feng et al., 2013). Similar conclusions hold for the effects of the Interdecadal Pacific Oscillation on decadal sea level variations in the Indian Ocean (e.g., Feng et al., 2004, 2010; Trenary and Han, 2013; Nidheesh et al., 2013; Li et al., 2017; Srinivasu et al., 2017; Han et al., 2018).

Recent studies suggest that the influence of the ITF on decadal sea level variability over the south Indian Ocean has increased since the early 1990s (Trenary and Han, 2013). Most of the "missing heat" of the global warming hiatus since $\sim$2002 has been transported from the Pacific into the Indian Ocean via a strengthening ITF (Lee et al., 2015; Nieves et al., 2015; Vialard, 2015), with a large proportion being concentrated in the southeast Indian Ocean (Li et al., 2017). Changes in rainfall over the Indonesian Seas have also been implicated in the strengthening of the Throughflow (Hu and Sprintall, 2017). Given that the tropical Indian Ocean has warmed far more rapidly than the global mean during 1950–2015 (Roxy et al., 2014; Cheng et al., 2017), the possible contributions of the "extra heat" and of other dominant contributors to the Indian Ocean heat budget, such as the Agulhas Current and subtropical gyre circulation, demand immediate attention in the context of decadal sea level variability.

On long time scales, while anthropogenic land ice melt increases global sea level by adding mass into the ocean, its freshwater buoyancy flux and gravitational effects induce regional patterns of SLC (Stammer and Hüttemann, 2008; Stammer et al., 2011; Slangen and Lenaerts, 2016; Mitrovica et al., 2001). Moreover, the long term Glacial Isostatic Adjustment (GIA; Peltier, 2004) since the Last Glacial Maximum also induces regional SLC. These gravitational and GIA effects are estimated to be of considerable magnitude in the Indian Ocean ($\sim$1 mm/yr; Slangen et al., 2012; 2014; Slangen and Lenaerts, 2016).

21.2 Sea level as a driver of the IndOOS

Sea level is an integral effect of surface and subsurface oceanic processes. In addition to surface winds, ocean heat content, or thermosteric sea level, is a primary contributor to regional sea level patterns, and salinity, or halosteric sea level, also has significant contributions in many regions (Shankar and Shetye, 1999; Fukumori and Wang, 2013; Nidheesh et al., 2013; Llovel and Lee, 2015). *In situ* temperature and salinity profiles over the upper 700 m of the ocean from XBT and, more recently, the Argo program, can explain a large portion of the observed sea level variability and change (Fukumori and Wang, 2013; Nidheesh et al., 2013; Srinivasu et al., 2017). But there remain significant differences from total sea level, as observed with satellite observations since the 1990s and reanalysis products since the 1950s (Han et al., 2018). Consequently, more continuous and deep ocean observations are needed to capture missing steric sea level variations and close the global sea level change budget.

Efforts have been made to generate reliable multidecadal records of sea level for climate studies using the existing patchy observations of sea level, temperature, winds, and air-sea fluxes. This has been done by quality control of existing historic datasets, by assimilating observations into numerical models to create reanalysis products, and by applying statistical techniques to extend basin- and global-scale datasets to earlier, data-sparse periods to create reconstructed products. There is a non-negligible spread among these products, especially before the satellite era, leading to significant uncertainties in multidecadal trends and decadal variations. There are also significant differences among reconstructed sea level datasets before the satellite era, regarding both global mean sea level change and regional multidecadal trends (Nidheesh et al., 2017). An increase in the number of tide gauge stations with colocated GNSS (Global Navigation Satellite System) stations to measure land movement associated with GIA and other

effects would help. Continuous effort is needed, not only to enhance and sustain high quality observations, but to further advance statistical techniques and improve data archaeology in order to improve the quality and increase the data records of multidecadal historical, reanalysis, and reconstructed datasets.

21.3 Essential Ocean Variables

Our knowledge of regional sea level variability and change at decadal and longer timescales remains rudimentary. Given the large uncertainty in reanalysis products and model simulations, long and continuous records of sea level from tide gauges and satellite altimetry are crucial. Multiple satellite merged records with a quarter degree resolution do exist since the early 1990s, but are still too short for understanding anthropogenic change. And consistent *in situ* measurements are essential for inter-calibrating successive satellite missions in order to yield these continuous merged records. The importance of wind-driven ocean circulation, as well as the dominance of thermosteric, and to a lesser extent halosteric drivers of sea level call for sustained observations of the following EOVs: Velocity, full-depth temperature and salinity, surface winds, and sea surface height.

21.4 Actionable recommendations

A. Maintain the existing network of tide gauge stations, including the recently added tide gauge in the Seychelles-Chagos thermocline ridge (Bradshaw et al., 2015). Enhance engagement and cooperation of coastal and island states in the Indian Ocean, with a focus on new tide gauges around the SCTR (Mauritius, French “Iles éparses”). Add GNSS stations co-located with tide gauges to measure land movement (Chapter 5).

B. Maintain the Argo network to obtain basin-wide estimation of thermosteric and halosteric sea level contributions.

C. Enhance deep ocean observations using deep ocean moorings and deep Argo to assess the effect of deep ocean variability on sea level change.

D. Maintain RAMA-2.0, particularly the meridional sections at 67°E and 80°E where sea level variability is large over the thermocline ridge (Figures 21.1 and 21.2), and the zonal sections at the equator, 2°N and 2°S that capture IOD signals, and all moorings in the eastern equatorial Indian Ocean for temperature and velocity measurements.

E. Maintain the IX01 XBT line to monitor the ITF.

F. Maintain the trans-Indian Ocean GO-SHIP line at $\sim$32°S, including crossings of the Leeuwin and Agulhas currents at the boundaries, for decadal basin-wide heat budget.

G. Maintain satellite altimetry missions, satellite missions measuring vector winds at the ocean surface, and Earth gravity satellite missions such as GRACE and GOCE (ESA’s Gravity field and steady-state Ocean Circulation Explorer) that capture changes of mass distribution in the ocean. Enhance resolution and coastal retrieval of sea surface height from satellite, such as the upcoming SWOT mission.

22. Decadal Variability and Predictability

Jérôme Vialard[1], Weiqing Han[2], Ming Feng[3], Tomoki Tozuka[4], Michael J. McPhaden[5], Mathew K. Roxy[6], Matthieu Lengaigne[1], and A.G. Nidheesh[6]

[1]LOCEAN-IPSL, Sorbonne Universités (UPMC, Univ. Paris 06)-CNRS-IRD-MNHN, France, [2]University of Colorado, USA, [3]CSIRO Oceans and Atmosphere, Australia, [4]University of Tokyo, Japan, [5]NOAA/Pacific Marine Environmental Laboratory (PMEL), USA, [6]Indian Institute of Tropical Meteorology (IITM), India

22.1 Indian Ocean contribution to climate predictability

Modes of decadal internal climate variability have been identified in the Pacific (Interdecadal Pacific Oscillation or IPO; Alexander et al., 2010; Liu et al., 2012) and Atlantic (Atlantic Multi-decadal Oscillation or AMO; Liu et al., 2012), but decadal variability in the Indian Ocean is a "grey area" (Han et al., 2014a) due to lack of data and dedicated studies. This is a problem for attributing climate change signals in the basin. For instance, is the rapid $\sim$1°C Indian Ocean surface warming between 1950 and 2015 (compared to the $\sim$0.6°C global average) due to a faster response to climate change in this basin or to natural decadal climate variability (Lau and Weng, 1999; Alory et al., 2007; Roxy et al., 2014)?

Indian Ocean decadal variability may have played an important role in the recent global surface warming "hiatus". A negative IPO phase during 2000-2010 has meant a colder Pacific Ocean that absorbed more heat than usual from the atmosphere. This vertical heat redistribution led to a slowdown of global surface warming (Kosaka and Xie, 2013). At the same time, fast surface warming in the Indian Ocean may have contributed to this negative IPO phase by enhancing the Walker circulation (Luo et al., 2012; Han et al., 2014b; Hamlington et al., 2014; Li et al., 2015; Dong and McPhaden, 2017), while a significant fraction of the Pacific heat uptake has been fluxed to the Indian Ocean via the Indonesian Throughflow (Lee et al., 2015; Nieves et al., 2015; Liu et al., 2016; Gastineau et al., 2018).

The Indian Ocean has contributed to more than 30% of the upper 700m global oceanic heat content increase during the last decade (Lee et al., 2015). Whether this extra heat in the Indian Ocean will re-surface or stay at depth during the coming decades could influence the evolution of global surface temperature (Vialard et al., 2015), making the Indian Ocean a potentially important region for decadal climate predictions. The Indian Ocean is also the region of highest skill for decadal surface temperature predictions due to relatively weak internal variability (Guemas et al., 2012), offering potential prospects for decadal regional climate projections.

There is a strong need to characterize natural decadal variability of the Indian Ocean in order to attribute regional climate change signals and to better predict global climate evolution over the coming decades.

22.2 Decadal variability and its predictability

The Pacific and Indian Oceans are closely connected through their common warm pool, which energizes the planetary-scale Walker circulation. This results in a close connection of the two basins at interannual timescales (Chapter 19). The eastward shift of the Walker circulation during El Niño events induces subsidence over the Indian Ocean, leading to a basin-scale surface warming through enhanced solar fluxes and local air-sea feedbacks (Klein et al., 1999; Xie et

al., 2009). El Niño events also tend to trigger positive Indian Ocean Dipole events (Chapter 19; Annamalai et al., 2003). A close connection between the two basins can also be expected at decadal timescales.

The leading mode of decadal Indian Ocean SST variability is a relatively homogenous basin-scale signal (Figure 22.1a), referred to as the decadal Indian Ocean Basin-mode (decadal IOB). The decadal IOB is in phase with the IPO (Tozuka et al., 2007, Han et al., 2014b, Dong et al., 2016) and "pacemaker" experiments with specified SST in the equatorial Pacific are able to reproduce its observed phase, demonstrating that decadal modulation of ENSO is its primary driver (Dong et al., 2016b). Century-long paleo-proxies from coral records also show decadal SST variability in phase with ENSO in the southwestern Indian Ocean (Cole et al., 2000; Cobb et al., 2001). However, Han et al., (2014b) find that phase-locking between the IOB and IPO has broken down since the 1980s, with a negative IPO phase coinciding with an anomalously warm Indian Ocean over 2000-2010. This may be a consequence of the faster surface warming trend of the Indian Ocean relative to the Pacific (Chapter 21, Chapter 23; Luo et al., 2012; Han et al., 2014b; Dong and McPhaden, 2017) and possibly of volcanic eruptions on decadal time-scales (W. Han, pers. Comm.). The resultant unusual SST pattern, cold Pacific and warm Indian Ocean, may have contributed to a strengthening of the Pacific easterlies (Dong and McPhaden, 2017), resulting in unprecedented sea-level rise in the western Pacific (Han et al., 2014b) and in heat transfer to the Indian Ocean via a strengthened ITF (Lee et al., 2015, Nieves et al., 2016).

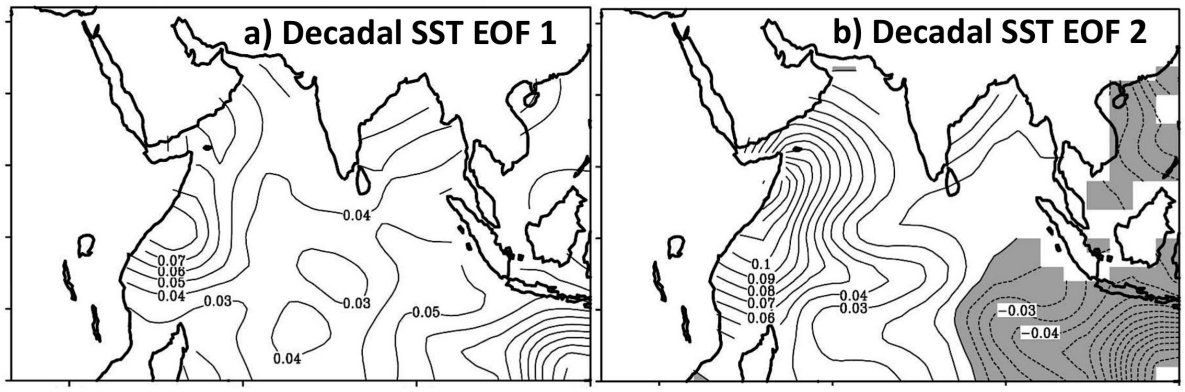

Figure 22.1 Spatial patterns of the (a) first (37% of total variance) and (b) second (14% of total variance) Empirical Orthogonal Function of decadal (9-35 years) observed SST (ERSST product). Adapted from Tozuka et al., (2007).

The second mode of decadal tropical Indian Ocean SST variability appears to be associated with an east-west SST dipole (Figure 22.1b) which has been interpreted as a decadal modulation of the IOD (Ashok et al., 2004, Tozuka et al., 2007). However, large gaps in the Indian Ocean SST dataset prior to the satellite era (Deser et al., 2010; Izumo et al., 2014) cause large uncertainties and discrepancies between observations and models. Similarly, there is a large spread in the decadal sea level variability reconstructed from observations over the Indian Ocean (Figure 22.2, Nidheesh et al., 2017; Chapter 21). While some products (Nidheesh et al., 2017) and the short altimetry record (Lee and McPhaden, 2008) suggest coherent variations with the IPO, others suggest that the IOD decadal modulation is relatively independent from the IPO (Ashok et al., 2004; Tozuka et al., 2007; Nidheesh et al., 2013). The large uncertainties in long records of observed SST (Izumo et al., 2014), sea level (Nidheesh et al., 2017), and wind (Nidheesh et al., 2013) in the Indian Ocean curtail our assessment of decadal IOD-IPO coupling and the role of the Walker Circulation.

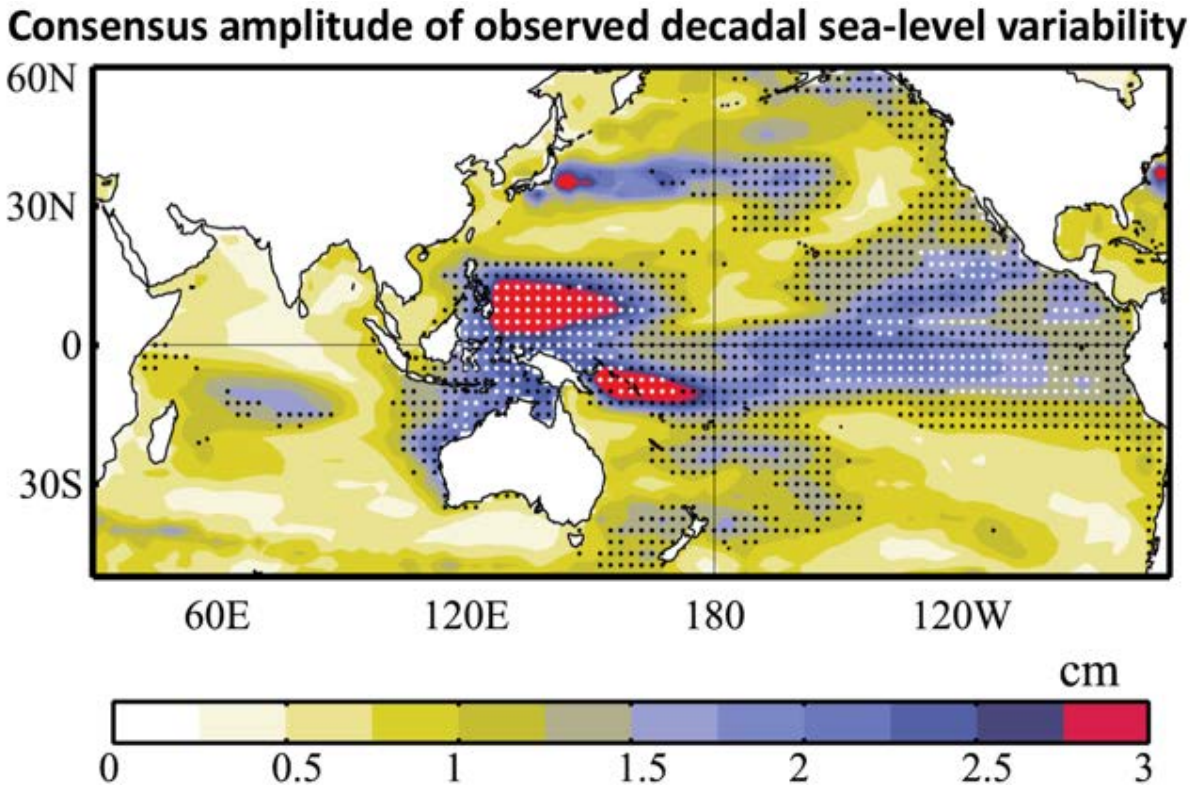

Figure 22.2 Standard deviation of the ensemble-mean decadal sea-level variability from ten gridded, observationally-derived sea-level products over the 1960-2010 period. Black (white) dots indicate regions where the inter-product spread is smaller (twice smaller) than the standard deviation of the ensemble-mean, i.e. where sea-level decadal variability is well constrained. Adapted from Nidheesh et al., (2017). Decadal sea-level variability is much more uncertain in the Indian Ocean than in the Pacific and there are two regions of strong variability near the west coast of Australia and in the Southern tropical Indian Ocean.

Modeling studies have identified significant decadal variations in sea-level (Nidheesh et al., 2018), mixed-layer depth, and SST variations (Yamagami and Tozuka, 2015) in the southern tropical Indian Ocean, to the east of Madagascar. These decadal fluctuations may be associated with variations in anticyclonic wind curl, as is the case at interannual timescale for the subtropical Dipole (Chapter 19). Again, large gaps in the observational record in this region (Deser et al., 2010) make it difficult to verify these model results.

In addition to the Walker Circulation atmospheric bridge, the Indian Ocean is connected to the Pacific via the Indonesian Throughflow. There is transport of mass, heat, and freshwater from the Pacific to the Indian Ocean via the Throughflow (Gordon et al., 2010) and these transports increase during La Niña events, with sea level rise along the west coast of Australia and Leeuwin Current strengthening as a result (Feng et al., 2003). The ITF also acts as a waveguide, with negative IPO phases inducing robust, positive, decadal sea level signals in the eastern equatorial Indian Ocean off the west coast of Australia, associated with regional warming (Figure 22.2; Nidheesh et al., 2017; Feng et al., 2004). The multidecadal negative IPO phase between the late 1990s and 2013 favored more frequent marine heatwaves off western Australia, called Ningaloo Niños (Chapter 12), with devastating consequences for ecosystems (Feng et al., 2013, Feng et al., 2015a). Modulation of eastern Indian Ocean heat content by the IPO via the Throughflow also appears to influence the IOD, with more frequent positive IODs during positive IPO phases (Ummenhofer et al., 2017), although those changes may have occurred via the atmospheric bridge. Finally, as noted earlier, a large fraction of the anomalous

heat uptake in the Pacific during the last decade of the negative IPO phase was transferred to the Indian Ocean via the Throughflow (e.g. Lee et al., 2015; Nieves et al., 2015).

Recent studies have suggested a regional decadal sea level rise in the northern Indian Ocean, partially attributed to decadal fluctuations in the cross equatorial overturning cell (Schott et al., 2002; Thompson et al., 2016), with a possible role of air-sea fluxes (Srinivasu et al., 2017). Dong and McPhaden, (2016a) argue that, despite this northern signal, heat content has increased more in the southern Indian Ocean over the last decade, with most of the heat input from the Throughflow remaining south of the equator, leading to a decadal interhemispheric SST gradient change with potential impacts on monsoon intensity. However, once again large uncertainties (Figure 22.2) prevent a thorough assessment of decadal mass and heat content variability in the northern Indian Ocean.

Studies of Indian Ocean decadal predictability are scant. Guemas et al., (2012) indicate that the signal associated with anthropogenic climate change stands out from the internal "noise" in the basin, elevating predictability at decadal timescales. Yet, prospects for decadal predictions of internal climate variability in the Indian Ocean are unclear. The decadal basin mode is largely forced by ENSO decadal variations (Dong et al., 2016b), which may themselves not be predictable (Wittenberg et al., 2014). And while the IOD may be more independent from ENSO at decadal time scales (Ashok et al., 2004; Tozuka et al., 2010; Nidheesh et al., 2018), there is no clear mechanism for an IOD decadal memory based on the oceanic state (Tozuka et al., 2010). Memory associated with the oceanic mixed layer depth (Yamagami and Tozuka, 2015) and planetary wave propagations (Nidheesh et al., 2018) may, on the other hand, imply predictability for the subtropical southern Indian Ocean.

22.3 Decadal variability as a driver of the IndOOS

A better description of Indian Ocean decadal climate variability is a must for detecting climate change signals in this under-sampled basin and for global decadal climate projections. The overall picture is incomplete and many unresolved questions remain. For instance, is the recent apparent decoupling between the IPO and decadal IOB a result of external forcing, whereby anthropogenic climate change and/or volcanic eruptions has led to rapid upper-ocean warming in the Indian Ocean? And did such forcing contribute to the unusually fast sea level rise in the western Pacific and resultant heat transfer to the Indian Ocean during 2000-2010? Is decadal IOD modulation coupled with the IPO through the Walker Circulation or through the Throughflow, or is it independent? Is the northern Indian Ocean are sea level and heat content decadally modulated through changes in shallow overturning strength? How does decadal interhemispheric SST gradient variability, associated with modulation of the ITF, impact the monsoons? Are there other modes of decadal climate variability intrinsic to the Indian Ocean? What combination of physical processes - air-sea heat exchange, changes in ocean circulation and upper ocean heat content, planetary waves - give rise to the observed decadal time scale variations?

To answer these questions sustained, basin-scale observations are needed at monthly time scale over several decades.

22.4 Essential Ocean Variables

Required essential ocean variables are: sea surface temperature, sea surface height, ocean surface wind stress, net surface heat flux and constituent turbulent and radiative components,

and upper-ocean temperature, salinity, and velocity, particularly within the Indonesian Throughflow and off the western coast of Australia, the eastern pole of the IOD, the Seychelles-Chagos thermocline ridge, and the northern tropical Indian Ocean where recent, unprecedented sea level rise has been observed. High resolution, sub-surface temperature, salinity, and velocity are also needed in key, narrow oceanic currents to constrain volume, heat, and freshwater budgets, including in the Agulhas and Leeuwin Currents and the Somali Current.

22.5 Actionable recommendations

A. Maintain the IX01 XBT line with at least fortnightly resolution to monitor geostrophic mass and heat transport of the ITF. Increase salinity measurements with enhancement of regional Argo floats or a pilot glider program along IX01.

B. Complete and maintain RAMA-2.0 in order to observe and diagnose surface and upper ocean variability in key regions, such as the equatorial band and SCTR, and for calibration of satellite SST and wind retrievals.

C. Maintain the IndOOS Argo network.

D. Maintain satellite observations and intercalibration-work that can provide basin-scale wind, sea level, and SST records that span several decades, including in rainy/cloudy regions.

E. Maintain the existing network of island and coastal tide gauge stations, and ensure open accessibility to these data. Upgrade stations in the western Arabian Sea and on the horn of Africa with GNSS stations to monitor vertical land movements.

F. Develop collaborations with the paleo-proxy community to provide long records of SST variability in the IOD eastern pole and of sea level variability near the west coast of Australia (Zinke et al., 2015), in the Chagos archipelago, and Mascarene Islands.

23. Heat Content and its Major Flux Components

Lisa Beal[1] and Elaine McDonagh[2,3]

[1]University of Miami, USA, [2]NORCE, Norwegian Research Centre, Bjerknes Centre for Climate Research, Bergen, Norway, [3]NOC, National Oceanography Centre, Southampton, UK

23.1 Current Understanding and Societal Impact

To date, the world's oceans have absorbed 93% of the global heat gain due to anthropogenic increases in greenhouse gases over the last 150 years (Cheng et al., 2017). The oceans are acting as a buffer to global warming. Although the Indian Ocean is the smallest of the world's oceans, it has accounted for more than one quarter of global ocean heat gain over the last twenty years (Lee et al., 2015; Cheng et al., 2017) and perhaps as much as 45% over the upper 700 m in the last ten years (Figure 23.1; Desbruyères et al., 2017).Since 1950 the Indian Ocean has warmed about 1°C at the surface, compared to a global average of 0.6°C. This rapid warming may be due to a faster response to climate change, or to natural decadal variability (Lau and Weng, 1999; Alory et al., 2007; Roxy et al., 2014). Oceanic heat content influences the climate of Indian Ocean rim countries through its feedback on winds, rainfall, storm intensity, and sea level rise (Han et al., 2014a; Chapter 21). And can influence fisheries and marine ecosystems due to associated changes in stratification, oxygen, and nutrient levels (Roxy et al., 2016). Warming trends in the equatorial Indian Ocean are predicted to drive decreases in rainfall over eastern Africa, resulting in larger undernourished populations (Funk et al., 2008). Sea level rise has accelerated along the coasts of India and Australia since the late 1990s and greater than global increases have been estimated along the coasts of Indonesia, Sumatra, Oman, and Madagascar (Han et al., 2010; Watson et al., 2011). Understanding more about Indian Ocean heat content change and predicting future changes will require sustained observations of its dominant flux components as part of IndOOS.

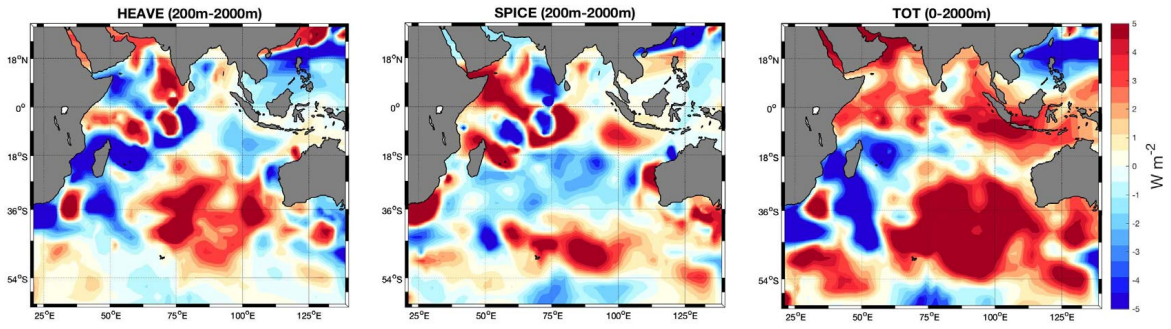

Figure 23.1 Trend in ocean heat content over the upper 2000 m since the late 1990's, based on blended Argo and repeat hydrography data. Heave represents the change in temperature at a fixed depth related to movement of isopycnals due to wind forcing or subduction of warmer/cooler waters. Spice represents density-compensated changes in temperature which have no dynamical signal. TOT is the total heat content trend. After Fig 7, Desbruyères et al., (2017).

In contrast to the Atlantic and Pacific Oceans, the Indian Ocean is insulated from surface heat loss at cold northern latitudes by the Asian continent and receives an influx of warm tropical waters via the Indonesian Throughflow. As a result, there is, on average, large heat gain within the basin, which is exported across its open southern boundary (Ganachaud and Wunsch, 2000;

Lumpkin and Speer, 2007; Hernández-Guerra and Talley, 2016) to balance heat loss in both the Atlantic and Southern Oceans (Talley, 2013).

The heat budget of the entire Indian Ocean, north of its open southern boundary around 35°S, is dominated by three oceanic flux components estimated to have similar magnitude (Figure 23.2): An inflow of fresh tropical waters via the Indonesian Throughflow (Sprintall et al., 2009; Zhang et al., 2018; Roberts et al., 2017), a vertical overturning circulation (0-2000 m) linking upwelling in the northern hemisphere and in the equatorial gyre with subduction and inflow of Southern Ocean waters at the southern reaches of the basin (Schott et al., 2004; Schott et al., 2009; Han et al., 2014), and a horizontal subtropical gyre circulation dominated by the warm and salty waters of the Agulhas Current at the western boundary (Bryden and Beal, 2001).

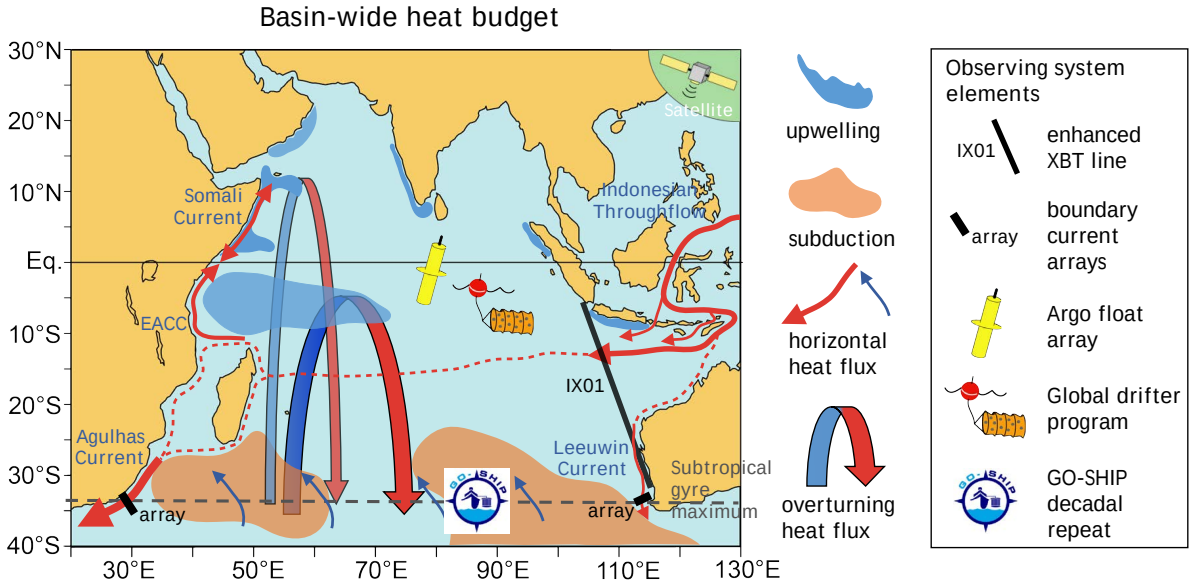

Figure 23.2 The dominant components of the Indian Ocean heat budget and required observing system elements. The components are: The Indonesian Throughflow, the cross-equatorial and subtropical overturning cells linking regions of upwelling with regions of subduction, and the horizontal subtropical gyre circulation linking equatorward flow across the interior with the poleward Agulhas Current at the western boundary.

Estimates of the steady Indian Ocean heat budget have varied widely, with basin-wide divergences between 0.1 and 1 PW and exports, based on mass-conserving global inversions, from 0.25 to 1.55 PW (e.g. McDonald et al., 1998; Ganachaud and Wunsch, 2000; Bryden and Beal, 2003; Lumpkin and Speer, 2007; Sultan et al., 2007; Hernández-Guerra and Talley, 2016). These estimates have been underpinned by three hydrographic occupations across the open southern boundary of the basin over the last 30 years (1987, 2002, and 2009) and are highly sensitive to the fluxes and temperatures of the ITF (Sprintall et al., 2009) and Agulhas Current (Bryden and Beal, 2001), although the exact dependencies are uncertain (McDonagh et al., 2008; Hernández-Guerra and Talley, 2016).

The Indonesian Throughflow (ITF) is thought to be shoaling and strengthening as a result of strengthening Pacific Trade winds and increasing rainfall over the Indonesian Seas (Wijffels et al., 2008; Feng et al., 2011; Sprintall and Révelard, 2014b; Hu & Sprintall, 2017) and has been put forward as the main proponent of rapid Indian Ocean heat gain (Lee et al., 2015; Zhang et al., 2018). However, patterns of heat content change across the Indian Ocean are complex (Figure 23.1), dependent also on changes in the other dominant flux components of the heat

budget, which in turn are linked to the dynamical and thermohaline response of the basin. For instance, in the tropics, warming at the surface and at depth is dissected by cooling of upper thermocline waters in between, thought to be driven by a local divergence of heat due to weakening of the cross-equatorial overturning cell (Trenory and Han, 2008; Han et al., 2015), while in the extra-tropics cooling has been related to shoaling of the thermocline transmitted from the Pacific and to changes in the ITF (Han et al., 2015). However, there is some evidence that a stronger ITF is consistent with reduced heat content of the Indian Ocean (Hernández-Guerra and Talley, 2016) and such uncertainties relate, in large part, to the enormous variability in depth and temperature transport of the incoming ITF on multiple timescales (Sprintall et al., 2009).

The largest warming trends are concentrated far from the ITF, throughout the southern Indian Ocean (Alory et al., 2007, Desbruyères et al., 2017) and in the Agulhas system (Wu et al., 2012), and have been related to a strengthening and poleward expansion of the subtropical gyre in response to strengthening Westerlies (Palmer et al., 2004; McDonagh et al., 2005), as well as to decadal changes in Indian Ocean thermocline and mode waters, which have reversed from freshening (Bindoff and McDougall, 2000) to becoming saltier (McDonagh et al., 2005). However, major uncertainties remain. Isopycnal surfaces in the southwestern Indian Ocean appear to have moved upward on average, causing a cooling trend that contrasts with warming at the surface and elsewhere in the basin (Figure 23.1, Desbruyères et al., 2017). And, paradoxically, while the ITF and gyre transports appear to be increasing, neither the Agulhas nor Leeuwin Currents have strengthened (Beal and Elipot, 2016; Zhang et al., 2018). Instead, a small increase in southward heat transport appears related to warming in these currents (Hernández-Guerra and Talley, 2016; Zhang et al., 2018). This paradox calls for a fit-for-purpose observing system that can, first and foremost, balance the mass budget of the basin.

Over the long-term the Agulhas is expected to strengthen and the Throughflow potentially to weaken with climate change (Yang et al., 2016; Feng et al., 2017), although for the latter wind and rainfall effects may be competing (Hu & Sprintall, 2017). In addition, long-term warming of the ocean is inevitable. Abyssal warming below 4000 m (Purkey and Johnson, 2010; Desbruyeres et al., 2017) and a possible reduction in Antarctic bottom water formation may have already contributed to a reduction in the deep Indian Ocean overturning cell (Katsumata et al., 2013; Hernández-Guerra and Talley, 2016). Although changes in the deep cell have little effect on the heat budget, abyssal warming makes an important contribution to thermosteric sea level rise.

In the past decade of the IndOOS most targeted assets have been concentrated within the equatorial region, yet subsurface temperature and salinity in the southern Indian Ocean are a good place to look for climate change signals (Banks and Wood, 2002), not least because natural variability is smaller than in the tropics. The greatest rates of heat content changes have been in the Southern Indian Ocean and Agulhas system (Cai et al., 2007; Wu et al., 2012; Alory et al., 2007; Yang et al., 2016). With Argo it is possible to map the distribution of heat content change across the basin (Desbruyeres et al., 2017), yet to understand this distribution and the time scale of storage — how long will the Indian Ocean continue to warm at a rapid pace? Where will the heat go next? — and to try to reconcile tropical drivers with those at higher latitudes, it is necessary to also monitor the major heat flux components in the subtropics. Here the horizontal gyre component, dominated by the Agulhas Current, and the upper-ocean overturning cell, which appears largely separated from the deep cell at about 2000 m depth, contribute almost equally to the heat budget (Sloyan and Rintoul, 2001; Bryden and Beal, 2001; Hernández-Guerra and Talley, 2016). Almost nothing is known about the seasonal-to-decadal variability of these components nor their response to changes in the Indonesian Throughflow, which is typically modelled as a barotropic export although its buoyancy flux must surely cause

baroclinic change within the basin. It is also possible that other components, such as the warm, southward Leeuwin Current, play important roles in the time-varying heat budget even though their mean contributions are small (Zhang et al., 2018).

23.2 Essential Ocean Variables

To gain a better understanding of how wind and thermohaline changes impact the basin-wide Indian Ocean heat budget and vice versa we need to measure variability and change in its major flux components. This requires the collection of temperature, salinity, velocity, and where possible oxygen data along the open southern boundary of the basin, latitudes $\sim$32°-34°S (Figure 23.2). 34°S is the latitude of climatological mean maximum wind curl. Daily observations of these EOVs at 10 km (inshore)—50 km (offshore) horizontal resolution, and 100 m (upper)—1000 m (bottom) vertical resolution are needed to capture the intense, narrow Agulhas Current and its heat flux at the western boundary, and similarly for the Leeuwin Current at the eastern boundary. Moorings in 2000 m (or more) of water as part of these arrays will double as end-point moorings to capture geostrophic, basin-wide, upper-ocean overturning, in a similar manner to the overturning array of the North Atlantic (Rayner et al., 2011). Across the interior, profiles (down to 2000 m) of EOVs T,S,O_2 at monthly resolution are needed to capture inflows of intermediate waters, changes in mode waters, and constrain gyre circulation. Decadal GO-SHIP sections (full-depth), which include the collection of silicates, CFCs and other properties, are required to provide important constraints on circulation and heat flux estimates (Robbins and Toole, 1997) as well as measures of abyssal warming. These *in situ* observations must be augmented by sustained, consistent satellite observations of sea level, sea surface temperature, and wind stress to obtain estimates of barotropic fluxes and meridional Ekman transport.

23.3 Actionable Recommendations

A. Re-establish and maintain an Agulhas System volume, heat, and freshwater array at the western boundary near 34°S, including an “end-point” mooring to measure interior geostrophic overturning down to $\sim$2000 m.

B. Enhance and maintain a Leeuwin Current array to measure volume, heat, and freshwater flux at the eastern boundary near 34°S, including an “end-point” mooring down to $\sim$2000 m.

C. Enhance XBT line IX01 with automated launchers and more regional Argo float deployments (for salinity) to monitor the geostrophic volume and heat fluxes of the Indonesian Throughflow.

D. Maintain the Argo program throughout the Indian Ocean to map interior heat content change.

E. Maintain satellite observations of SST, SSH, and surface winds.

F. Maintain decadal repeats of GO-SHIP line I5 at $\sim$32°S.

24. Carbon Cycle, Acidification, and Ecological Impacts

Raleigh Hood

University of Maryland Center for Environmental Science, USA

24.1 Current understanding and societal Impact

The oceanic uptake of atmospheric CO_2 is estimated to be 2.6 Gigatonnes (Gt) of carbon per year, which is nearly comparable to the uptake by land (LeQuere et al., 2015). As such, the oceanic sink plays an important role in the global carbon cycle acting to slow the increase of atmospheric CO_2 (Sabine et al., 2004; Takahashi et al., 2009) and therefore also global climate change. Thus, it is important to accurately quantify the oceanic sink and understand the factors that drive it's spatial and temporal variability in order to accurately project future atmospheric CO_2 levels and global climate change (Takahashi and Sutherland, 2013).

It has been estimated that the Indian Ocean as a whole accounts for $\sim$1/5 of the global oceanic uptake of atmospheric CO_2 (Takahashi et al., 2002). The Arabian Sea is a source of CO_2 to the atmosphere because of elevated pCO_2 within the upwelling systems of the southwest monsoon (Figure 24.1; Takahashi et al., 2009; 2014). Overall, the Indian Ocean north of 14°S loses CO_2 at a rate of 0.12 PgC/yr (Takahashi et al., 2002; 2009; 2014). Whether the Bay of Bengal is a CO_2 source or sink remains ill-defined due to sparse sampling in both space and time (Figure 24.1; Bates et al., 2006a). The southern Indian Ocean appears to be a strong net CO_2 sink, -0.44 PgC/yr in the band 14°S-50°S (Figure 24.1). The biological pump, representing the sum of all the biologically mediated processes that export carbon, and the solubility pump, representing the dissolution of CO_2 and its physical transport, are estimated to contribute equally to the CO_2 flux in the South Indian Ocean region (Valsala et al., 2012), but the factors that maintain this sink are unclear. Cold temperatures certainly increase CO_2 solubility in the austral winter, but there is also evidence that chemical and biological factors are important (Piketh et al., 2000; Wiggert et al., 2006).

A synthesis of the seasonal, annual, and interannual air-sea CO_2 fluxes based on both observations (Takahashi et al., 2009) and models (ocean, atmospheric inversions), shows that the sea-air CO_2 uptake derived from models (-0.37 PgC/yr) is not inconsistent with the estimates from observations (-0.24 PgC/yr), given the uncertainties (Sarma et al., 2013). However, models underestimate the flux in the northwestern region of the Indian Ocean and overestimate the flux in the Bay of Bengal. This suggests that the atmospheric inversions, which estimate the surface CO_2 fluxes that best fit the spatiotemporal patterns of measured atmospheric CO_2 given a defined, time-evolving atmospheric transport from numerical models (Sarma et al., 2013), are not well constrained. More observations of ocean carbon flux are needed to constrain these models. Compared to other oceans there have been few observations in the Indian Ocean (north of 20ºS) in recent years (Bakker et al., 2014, see also www.socat.info).

The uptake of anthropogenic CO_2 by the global ocean induces fundamental changes in seawater chemistry that could have dramatic impacts on upper ocean ecosystems. Estimates based on the Intergovernmental Panel on Climate Change (IPCC) business-as-usual emission scenarios suggest that atmospheric CO_2 levels could approach 800 ppm near the end of this century (Feely et al., 2009). The associated global trend of increasing oceanic CO_2 concentrations will lead to lower pH and acidification of the Indian Ocean over the coming decades, with potential negative impacts on coral reefs and other calcifying organisms (Doney et al., 2010). The average surface pH values for the northern (20°E-120°E, 0°-24.5°N) and southern

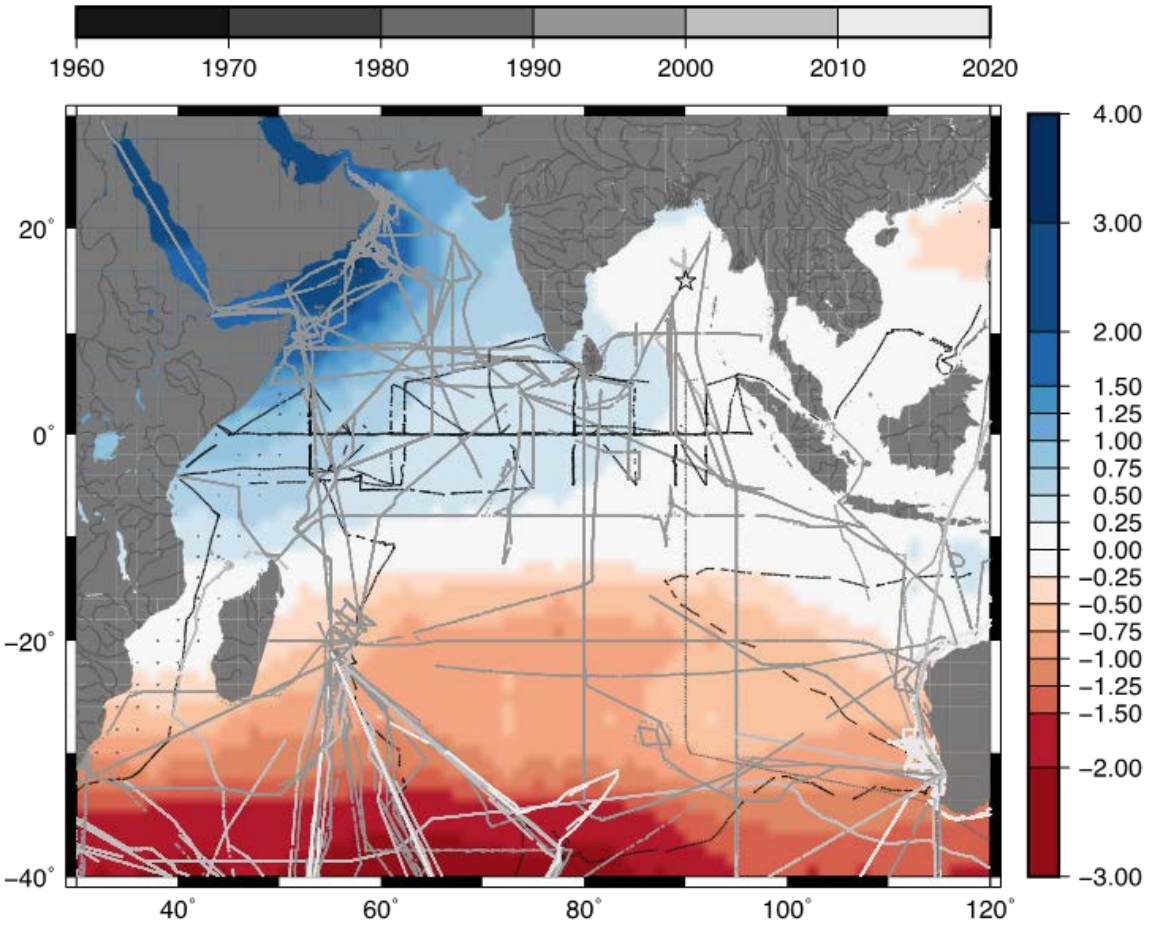

Figure 24.1 Annual CO_2 flux (mol C m^{-2} yr^{-1}) referenced to the year 2000 (Takahashi et al., 2009) over the Indian Ocean. Data points colored by year of collection (Takahashi & Sutherland, 2016) are overlaid as points. Major rivers are depicted over the continents.

(20°E-120°E, 0°-40°S) Indian Ocean in 1995 were 8.068 $\pm$ 0.03 and 8.092 $\pm$ 0.03, respectively (Feely et al., 2009), the lowest of the major ocean basins. The causes for basin differences are not understood (Takahashi et al., 2014). Very low surface pH ($<$ 7.9) in the Arabian Sea during summer results from upwelling of more acidic subsurface waters during the southwest monsoon (Takahashi et al., 2014). There are only a few studies on the temporal evolution of surface ocean acidification in the Indian Ocean because of the lack of time-series measurements. The results of a recently published study from the eastern Bay of Bengal indicate a decrease in pH of 0.2 in the period from 1994 to 2012 (Rashid et al., 2013), which is much faster than the global rate of 0.1 over the last 100 years (IPCC, 2007).

The large-scale coral bleaching events of 1998, 2005, and 2011 caused by marine heatwaves highlight the susceptibility of the Indian Ocean to warming (McClanahan et al., 2007; Moore et al., 2012; Chapter 12). Ocean acidification has the potential to exacerbate these negative impacts on coral reef areas. For example, the 1998 bleaching event affected higher trophic levels by altering the age distribution of commercially harvested fish (Graham et al., 2007). Coral reef ecosystems may be at greater risk than previously thought because of the combined effects of acidification, human development, and global warming (Hoegh-Guldberg et al., 2007). In addition, some commercially fished species, like shelled mollusks, are directly vulnerable to ocean

acidification (Hoegh-Guldberg et al., 2014). A study on modern planktonic foraminifera off Somalia suggests that human-induced ocean acidification reduced the rate at which foraminifera calcify, resulting in lighter shells (de Moel et al., 2009). The Southern Ocean sector of the Indian Ocean could experience major disruptions in upper levels of pelagic food webs due to the effects of acidification on calcifying pteropods, which are preyed on by many higher trophic level organisms (Bednarsek et al., 2012).

In addition to the direct impacts of acidification, increasing CO_2 in the upper ocean could lead to increased primary productivity for some species, like diazotrophs (Hutchins et al., 2007), altering rates of nitrogen fixation and therefore the biogeochemistry of particulate organic matter formation and remineralization. Decreasing pH also shifts the chemical equilibrium from ammonia (NH_3) to ammonium (NH_4^+), which may alter key biological processes such as microbial nitrification and nitrogen assimilation by phytoplankton (Gattuso and Hansson, 2011).

Understanding current carbon uptake by the Indian Ocean is critical for understanding how the global carbon cycle and climate are evolving under the impact of human activities. Understanding and predicting rates of carbon uptake and ocean acidification are also fundamental to understanding the biogeochemical and ecological future of the Indian Ocean.

24.2 The Carbon Cycle as a Driver of IndOOS

The carbon cycle research community has set a goal of being able to constrain regional fluxes to 0.2 Pg C year^{-1}, which translates into measuring the atmospheric fCO_2 (fugacity to CO_2 which is similar to partial pressure) to within 0.1 µatm and the seawater fCO_2 to within 2 μatm (Pierrot et al., 2009). These observations can be obtained from ships, moorings, gliders, wave gliders and Argo floats, with ships, gliders and wave gliders providing less frequent spatial transects, and moorings and Argo floats providing complimentary continuous measurements.

The GO-SHIP program (Chapter 7) is working to provide decadal resolution of the changes in inventories of heat, freshwater, carbon, oxygen, nutrients and transient tracers, covering the ocean basins from coast to coast and from top to bottom, with global measurements of the highest quality and accuracy to detect these changes. GO-SHIP has several lines in the Indian Ocean that are part of the global decadal survey (Figure 7.2). All of these lines include carbon system measurements. Some of these lines have national commitments for occupation over the next 5 to 10 years. These surveys will be crucial for filling in the current large spatial gaps in carbon system measurement in the Indian Ocean (Figure 24.1).

The development and deployment of Moored Autonomous pCO_2 ($MAPCO_2$) systems have dramatically improved our ability to characterize the temporal variability in the carbon system, sea–air gas exchange, and biogeochemical processes (Sutton et al., 2014). The $MAPCO_2$ system provides high-resolution data that can measure interannual, seasonal, and sub-seasonal dynamics and constrain the impact of short term biogeochemical variability on CO_2 flux. The deployment of a $MAPCO_2$ system at the Bay of Bengal Ocean Acidification mooring site, established at 15°N, 90°E in November 2013, is providing the first continuous surface water carbon system measurements along with physical measurements in the northern Indian Ocean (Figure 24.2; Hood et al., 2019). Deployments of $MAPCO_2$ systems on RAMA moorings could help to fill in the large temporal gaps between GO-SHIP carbon system measurements.

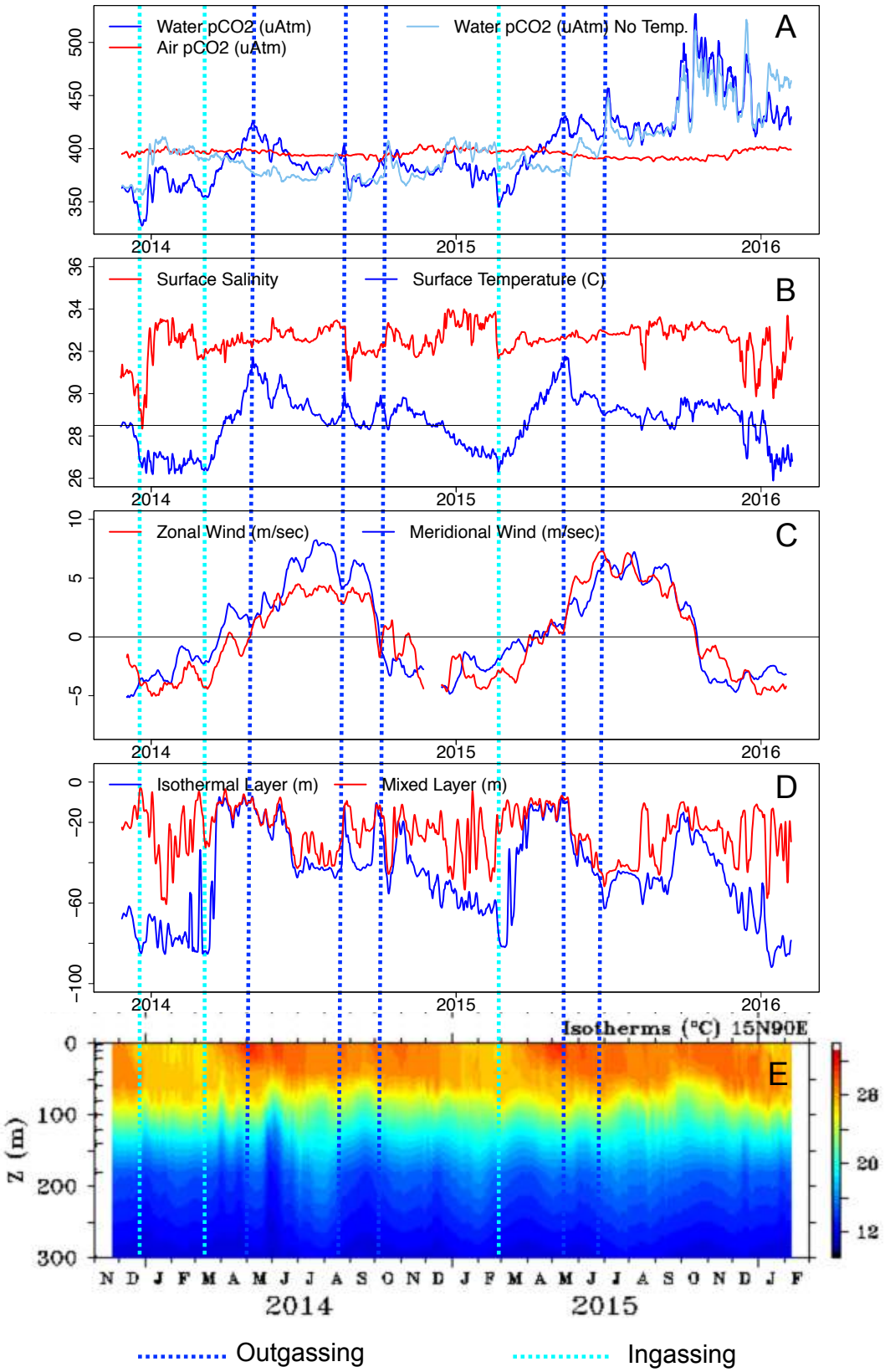

Figure 24.2 Time series plots from Bay of Bengal mooring. (A) pCO_2 in the water (dark blue), in the air (red) and with the temperature effect removed (light blue); (B) surface temperature (blue) and salinity (red); (C) zonal (red) and meridional (blue) wind speed; (D) isothermal layer (blue) and mixed layer (red) depth; and (E) water column temperature down to 300 meters depth.

In addition to GO-SHIP and the deployment of MAPCO$_2$ systems on RAMA moorings, carbon system measurements can be made underway from ships of opportunity and also from gliders, wave gliders, and Argo floats. The Ship of Opportunity CO_2 program (SOOP-CO_2) has outfitted numerous ships with automated instruments that take surface water pCO_2 measurements. These data, along with an improvement in the determination of gas transfer and in global wind products, have led to a 20% decrease in the uncertainty of global sea-air CO_2 flux estimates (https://www.aoml.noaa.gov/ocd/ocdweb/occ_soop.html). Several of the transects depicted in Figure 24.1 were collected as part of the SOOP-CO_2 program. Increasing the number of SOOP-CO_2 measurements in the Indian Ocean could help to fill in spatial gaps in carbon system measurements. Similarly, deployment of gliders and wave gliders equipped with automated instruments could help to fill in spatial gaps. However, the feasibility of motivating and maintaining routine deployments of these vehicles / sensors as part of IndOOS is unclear.

The SOCCOM (Southern Ocean Carbon and Climate Observations and Modeling) project (https://soccom.princeton.edu/content/overview) is deploying Argo floats in the Southern Ocean that are equipped with biogeochemical sensors that can be used to constrain the carbon system. The project will ultimately increase the number of carbon system measurements made monthly in the Southern Ocean by 10-30 times. These deployments include the Indian Ocean sector of the Southern Ocean. BGC-Argo floats have also been deployed in the northern and southeastern Indian Ocean (for example, https://research.csiro.au/iobioargo/), though whether or not these measurements can be used to determine carbon system parameters is uncertain. Increasing the number biogeochemical Argo float measurements in the Indian Ocean could help to fill in both temporal and spatial gaps in carbon system measurements.

24.3 Essential Ocean Variables

The observations required to constrain the carbon system at a point in space and time are any two of Dissolved Inorganic Carbon (DIC), Total Alkalinity (TA), partial pressure of carbon dioxide (pCO_2) and pH, plus temperature and salinity. The products that can be derived from these carbon system measurements include saturation state (aragonite, calcite), dissolved carbonate ion concentration, air-sea flux of CO_2, anthropogenic carbon, and the change in total carbon.

24.4 Actionable Recommendations

A. Deploy MAPCO$_2$ systems at RAMA Flux Reference Sites (Figure ES.1 and Table 24.1) that provide all the additional atmospheric and physical oceanographic measurements needed to calculate pH and air-sea flux of CO_2. The central Arabian Sea site should be a top priority because of large seasonal variability in air-sea CO_2 flux and acidic, low oxygen waters. Additional deployments should target regions with high temporal variability in CO_2 fluxes and / or rapidly increasing pH. Proposals should be motivated to obtain international funding for the purchase of additional systems. A first step would be to contact the carbon group at NOAA's Pacific Marine Environmental Laboratory (https://www.pmel.noaa.gov-/CO_2/).

B. Increase the number of SOOP-CO_2 measurements, particularly in the southern central Indian Ocean and also in the northern Arabian Sea and Bay of Bengal. (contact the Ocean Carbon Cycle group at NOAA's Atlantic Oceanographic and Meteorology Laboratory, which leads the SOOP-CO_2 consortium, https://www.aoml.noaa.gov/ocd/ocdweb/occ_soop.html).

C. Undertake analyses to determine whether BGC-Argo measurements can be used to determine carbon system parameters. Critical considerations are the specific biogeochemical measurements needed and whether alkalinity can be estimated accurately enough in the highly variable salinity regimes of the northern and equatorial Indian Ocean. If successful then additional BGC-Argo float deployments should be motivated, particularly in the Arabian Sea and the Bay of Bengal.

Table 24.1 Positions of the 7 RAMA Flux Reference Mooring sites

Mooring Location	Mooring Position
Western Equatorial Indian Ocean	Equator, 55°E
Southwestern Tropical Indian Ocean	16°S, 55°E
Central Arabian Sea	15°N, 65°E
Seychelles-Chagos Thermocline Ridge	8°S, 67°E
Central Equatorial Indian Ocean	Equator, 80°E
Central Bay of Bengal	15°N, 90°E
Southeastern Tropical Indian Ocean	5°S, 95°E

25. Anthropogenic Climate Change

Mathew K. Roxy[1], Lijing Cheng[2], Tianjun Zhou[2], Paul J. Durack[3], Weiqing Han[4] and Jérôme Vialard[5]

[1]Indian Institute of Tropical Meteorology (IITM), India, [2]Institute of Atmospheric Physics Chinese Academy of Sciences (IAP-CAS), China, [3]Lawrence Livermore National Laboratory (LLNL), USA, [4]University of Colorado, USA, [5]LOCEAN-IPSL, Sorbonne Universités (UPMC, Univ. Paris 06)-CNRS-IRD-MNHN, France

25.1 Background

The Indian Ocean is responding quickly to anthropogenic climate change, with increasing surface temperatures and heat content, rising sea level, and an intensified water cycle (IPCC, 2013). Changes in the Indian Ocean can affect the monsoon system, resulting in extreme droughts, rainfall, and flooding events (Roxy et al., 2015; Kay et al., 2015). Studies show that the warming trend of the Indian Ocean has far reaching impacts, modulating the Pacific climate (Luo et al., 2012, Han et al., 2014b, Hamlingon et al., 2014), affecting the North Atlantic Oscillation (Hoerling et al., 2004), enhancing the positive Southern Annular Mode (Loveday et al., 2015), and causing West Sahel and Mediterranean droughts (Giannini et al., 2003; Hoerling et al., 2012). Marine de-oxygenation and acidification may have already caused a dramatic shift in the ecosystem of the eastern Arabian Sea (chapters 16,20). These changes to the climate system are impacting food, water, and energy security of Indian Ocean rim countries. Oceanic measurements and information are needed to be able to predict, mitigate, and adapt to change.

25.2 Detection and attribution of long-term changes in the Indian Ocean

Warming in the Indian Ocean: Approximately 93% of the heat due to anthropogenic global warming has been absorbed by the oceans since the 1950s (Glecker et al., 2012; Pierce et al., 2012; IPCC, 2013; Gnanaseelan et al., 2017; Cheng et al., 2017). Indian Ocean SST exhibits a basin wide warming during this period (Figure 25.1a; Lau and Weng, 1999; Alory et al., 2007; Ihara et al., 2008; Du and Xie, 2008; Rao et al., 2012; Roxy et al., 2014, Dong et al., 2014a,b). Between 1950 and 2015 global mean SST warmed by 0.67°C and the tropical mean SST warmed by 0.83°C, while the tropical Indian Ocean has warmed the most, by 1.04°C (from ERSST v4 data).

The Indian Ocean basin-mean temperature, from the surface to 2000 m depth, has warmed consistently during 1960-2015, with an ocean heat content (OHC) increase north of 34°S of 0.41 x 10^{22} Joules per decade (Cheng et al., 2017), most of it occurring over the upper 300 m (Pierce et al., 2006; Cheng et al., 2015). OHC over the upper 700 m increased abruptly after 1998 (Figure 25.1b), to a rate of 1.60 x 10^{22} Joules per decade. This Indian Ocean warming has accounted for more than 28% of the global ocean heat gain over the past two decades, despite representing only 12% of the global ocean area. The greatest increase in OHC occurred in the southern Indian Ocean subtropical gyre (Levitus et al., 2012). These studies suggest that the Indian Ocean has been an important heat sink over the last two decades, offsetting accelerating anthropogenic global warming elsewhere. Yet substantial uncertainties remain in long-term changes in OHC due to insufficient data coverage (Wang et al., 2017). Some analyses indicate that global ocean warming is underestimated in some ocean datasets due to poor sampling of

the Southern Hemisphere (Gille, 2008, Durack et al., 2014b) and limitations of the objective analysis methods used to fill data gaps (Cheng et al., 2017, Wang et al., 2017). Data coverage is also sparse below 1500 m, with only 60% of Argo floats successfully reaching profiling depths of 2000 m in 2010, and lack of observations in the Indonesian Seas may cause bias in the global and regional scale OHC changes (Schuckmann and Le Traon, 2011).

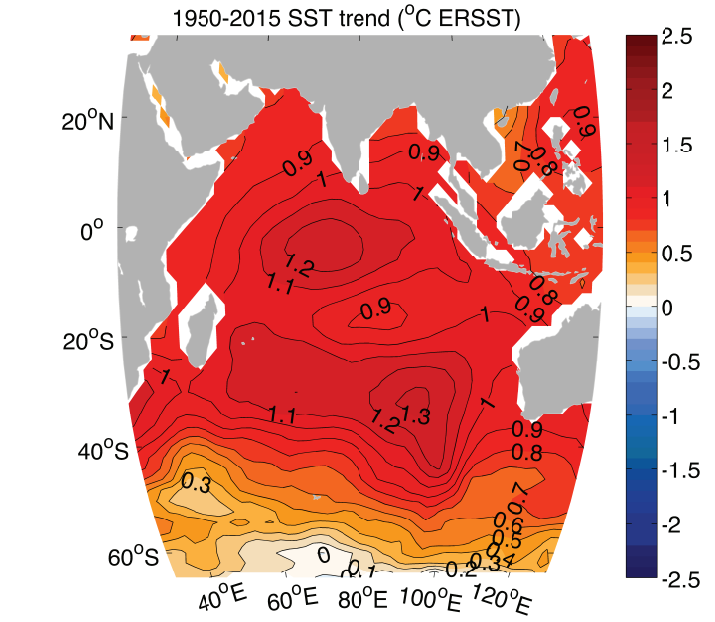

(a)

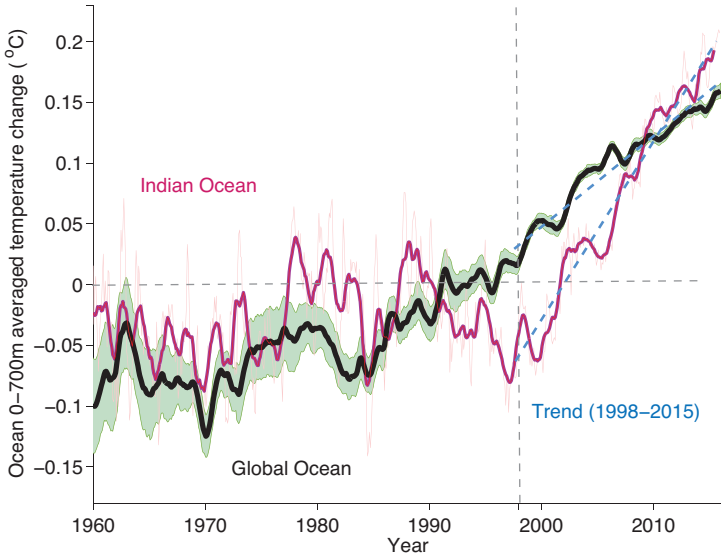

(b)

Figure 25.1 a) 1950-2015 SST trend (ERSST v4) represented by total change in 66 years, and b) 12-month running mean time series of the 0-700m averaged temperature for the Global Ocean (black, with green shading for 95% confidence interval) and Indian Ocean (purple, with thin line showing monthly time series). The 1998 to 2015 linear trends for both series are displayed as blue dashed lines. Data are from IAP-Gridded dataset (Cheng et al., 2017).

Climate model simulations indicate that anthropogenic forcing accounts for about 90% of the surface warming trend in the Indian Ocean (Dong et al., 2014a,b), which is primarily attributed to atmospheric forcing via radiative and turbulent fluxes associated with anthropogenic greenhouse gases (Barnett et al., 2005; Pierce et al., 2006; Knutson et al., 2006; Du and Xie, 2008). In contrast, observations (Yu et al., 2007, Rao et al., 2012, Ummenhofer et al., 2017) point to a negative surface heat flux trend over the Indian Ocean for the period 1984-2007 (Rao et al., 2012), which therefore cannot explain the observed surface warming. Considerable uncertainty exists about the sign of the net heat flux in some parts of the Indian Ocean (Yu et al., 2007) and surface fluxes over the global ocean continue to exhibit large biases (Chapter 10). Simulated regional patterns are due to anthropogenic aerosols, which have regional cooling effects (Figure 25.2), ocean dynamics (Dong et al., 2014b, Rahul and Gnanaseelan, 2016, Luo et al., 2016b), and local air-sea interaction (Liu et al., 2015, Rahul and Gnanaseelan, 2016, Yao et al., 2016).

Superimposed on the anthropogenic trend are considerable decadal variations in Indian Ocean SST (Chapter 22). Although external forcing accounts for most of the warming trend over the 1958–2005 period (Dong et al., 2014b), decadal variability induced by the Interdecadal Pacific Oscillation weakened the trend by about 50% during IPO's cold phase, and vice-versa during its warm phase, contributing about 10% to the global warming hiatus since 1999 (Dong et al., 2016b). The recent negative IPO phase also increased Indian Ocean heat content from 2003–2012, and is linked to an increase in heat transport from the Pacific via the ITF (Lee et al., 2015). Ummenhofer et al., (2017) suggest that this Pacific control of multidecadal Indian Ocean heat content via the ITF operates over the entire 1958–2007 period.

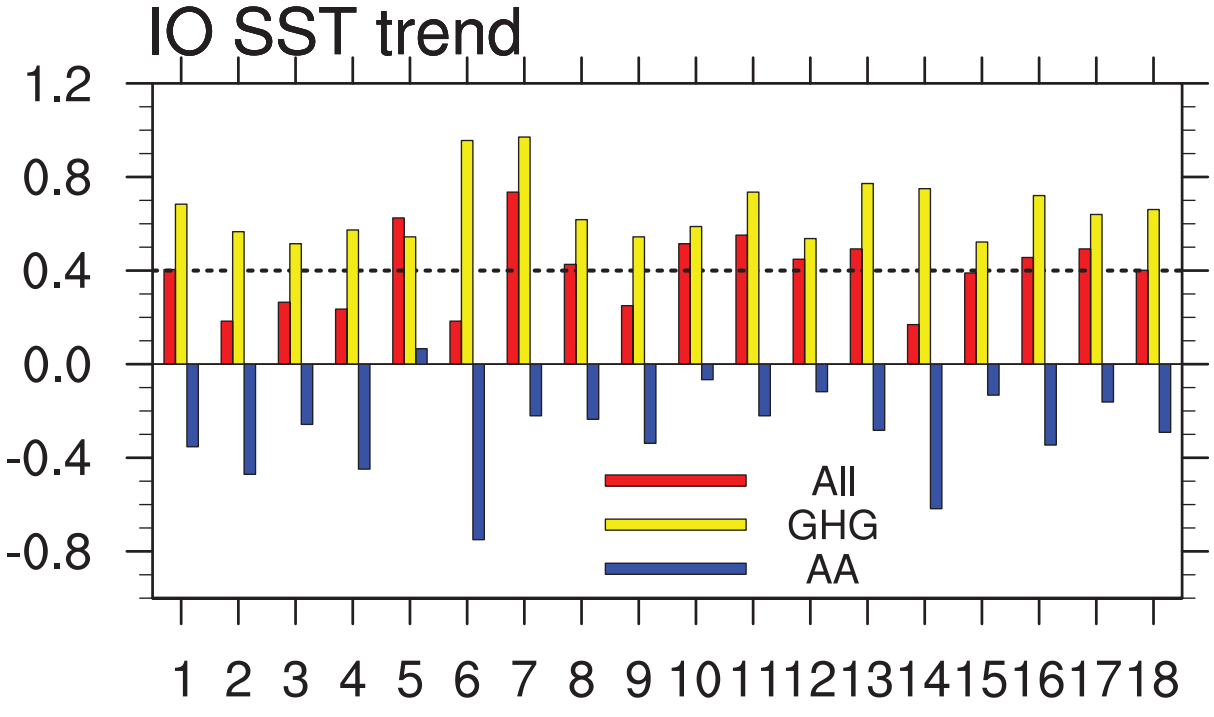

Figure 25.2 Indian Ocean (40°S-15°N, 40°E-100°E) SST trends (K per century) during 1870-2005 under all anthropogenic forcing (red), greenhouse gas only forcing (yellow), and aerosol only forcing (blue, All-GHG-None) from 17 CMIP5 models and their multi-model ensemble (number 18). The dashed line represents the trend from observations (Dong and Zhou, 2014a).

The frequency of extreme positive IOD events is projected to increase threefold by the end of the 21st century (Cai et al., 2014) and many future projections indicate an IOD-like pattern of

mean warming, although large biases remain in the mean state and in IOD variance of the simulations (Li et al., 2016). The historical climate model simulations under CMIP5 using observed greenhouse gas forcing do not reproduce the zonal SST gradient or the observed warming pattern over the Indian Ocean (Cai and Cowan, 2013; Roxy et al., 2015). Internal variability and ENSO forcing also play a major role in the IOD-like response (Yang et al., 2015; Hui and Zheng, 2018). More long-term observations and coordinated modeling studies are needed before we can reliably detect and attribute regional SST changes in the Indian Ocean.

Sea level change: Anthropogenic change in ocean temperature affects sea level change (SLC), with thermal expansion accounting for 35% of the global sea level rise during 1993–2010 (IPCC, 2013). SLC measured by satellite altimeter and averaged over the entire Indian Ocean (30°E–120°E, 30°S–30°N) is 5.6 mm/year during 2004-2013. Over the northern Indian Ocean (30°E–120°E, 5°S–30°N) it is 6.1 mm/year and dominated by thermosteric effects (Thompson et al., 2016; Srinivasu et al., 2017). It is unclear whether this fast SLC over the northern Indian Ocean is due to superimposition of natural decadal variability (Srinivasu et al., 2017) or a regional signature of global warming and more investigation is needed. The largest SLC has occurred along the northern and eastern coasts of the Bay of Bengal during 1993–2012 (Unnikrishnan et al., 2015).

Prior to the satellite era, distinct spatial patterns of SLC have been detected using tide gauge data and OGCM simulations, with rising sea level along most coasts of Indian Ocean rim countries (Mumbai, Kochi, Vishakhapatnam in India, Durban in South Africa, and Fremantle and Port Hedland in Australia) since the 1960s and falling sea level in the southwest tropical basin (Han et al., 2010). An enhancement of the Indian Ocean regional Walker and Hadley cells, along with changes in the Somali Current, are suggested to be the major causes for these basin-wide patterns, which are partially attributed to anthropogenic warming (Han et al., 2010).

Changes in salinity: The strong salinity contrast between the Arabian Sea, where evaporation dominates, and the Bay of Bengal, where precipitation and runoff dominate, has amplified since 1950. *In situ* measurements show an increase in salinity over the Arabian Sea and a freshening trend over the Bay of Bengal (Hosoda et al., 2009; Durack and Wijffels, 2010), while in the subtropical gyre there is a strong near-surface salinity trend which penetrates into the upper thermocline (Hosoda et al., 2009; Durack & Wijffels, 2010; Skliris et al., 2014) and a very large and consistent freshening below, associated with subduction of Subantarctic Mode Water south of Australia (Sallee et al., 2009). The latter feature is one of the largest freshening signals of the global ocean (Durack and Wijffels, 2010; Helm et al., 2010; Skliris et al., 2014). A freshening plume of low salinity ITF waters is also visible, extending from the east along 12°S into the central Indian Ocean. And increasingly saline Red Sea Waters lead to increased salinity down to 1000 m in the northern Indian Ocean, particularly in the Arabian Sea intermediate waters. These Indian Ocean salinity changes are consistent with those in the Pacific and Atlantic Oceans. Enhancement of both horizontal and vertical salinity gradients is the signature of an intensified hydrological cycle, whereby fresh regions are becoming fresher, and salty regions are becoming saltier (Figure 25.3).

Studies focused on the independent and combined changes in salinity and temperature in the Indian, Atlantic, and Pacific Oceans have been able to attribute observed changes to anthropogenic influence over the three ocean basins (Figure 25.3, Stott et al., 2008; Gleckler et al., 2012; Pierce et al., 2012; Terray et al., 2012; Durack et al., 2014a).

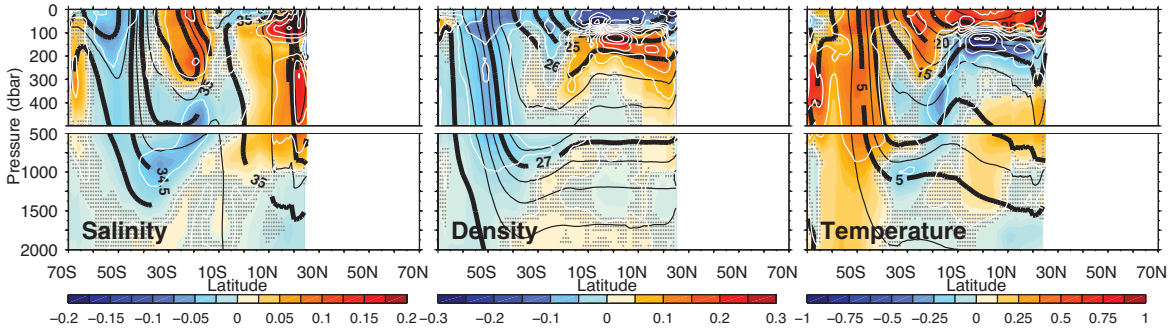

Figure 25.3 Zonally-averaged linear trend of salinity changes (left), neutral density changes (middle), and potential temperature changes (right), for the Indian Ocean during 1950 to 2000. Mean fields are shown as black lines. Regions where the linear trend is not significant at the 90% confidence level are stippled in grey (IPCC, 2013).

Biogeochemical change: Warming-induced increases in stratification in the Indian Ocean have led to a decrease in the transport of dissolved oxygen from surface to subsurface waters, leading to enlargement of oxygen minimum zones (Chapter 20, Stramma et al., 2010) and to a reduction in marine phytoplankton in the western Arabian Sea (Roxy et al., 2016). A 30% reduction in phytoplankton was found during 1998-2013 based on observations and 20% during 1950-2005 based on CMIP5 hindcast simulations. Variability and change in the marine carbon cycle, primary productivity, and ecosystems of the Indian Ocean remain poorly constrained due to few historic baseline data and even fewer measurements over the last decade (Chapters 16, 20, 24).

25.3 Essential Ocean Variables

Long term changes in Indian Ocean SST (Chapter 18), heat content (Chapter 23), salinity, and sea level (Chapter 21), among others, are ongoing. However, natural decadal climate variability can obscure the anthropogenic trends and sustained, long-term observations of key variables are needed to distinguish them and be able to skilfully predict future changes.

EOVs include: *In situ* temperature, salinity, oxygen, and core nutrients, plus velocity. Monitoring of key mass, heat, and salt transports entering the basin via the Indonesian Throughflow and exiting across 34°S, including the Leeuwin and Agulhas boundary currents, will better constrain basin-wide budgets. Sustained measurements of air-sea heat fluxes and constituent turbulent and radiative components are needed to address uncertainties and the inconsistency with SST trends. Basin scale measurements of SST, SSS, and subsurface temperature and salinity are needed to better constrain long-term heat and salt content trends. Basin-scale sea level measurements provide regional sea level signals and also indicate long term, large-scale wind changes alongside surface wind and wind stress measurements. Regions of particular importance include the equator and warm pool to monitor the Indian Ocean Walker circulation, the Somali Current that strongly influences the southwest monsoon, and the southwestern Indian Ocean where changes in wind stress curl may have induced a decrease in sea level.

25.4 Actionable recommendations

A. Maintain and complete the RAMA-2.0 array. Add MAPCO$_2$ systems at RAMA Flux Reference Sites for pH and air-sea flux of CO$_2$. Expand into the Arabian Sea at 10°N, 60°E, where air-sea flux uncertainties are large.

B. Maintain the Argo array and enhance coverage near the ITF to capture freshening signals. Develop a BGC-Argo program of 200 floats to measure oxygen and core nutrients and estimate productivity. Deploy deep Argo floats to constrain estimates of total heat content and sea level change.

C. Monitor boundary fluxes of volume, heat, and freshwater in Agulhas and Leeuwin Currents. Explore the feasibility of a long-distance glider line along 32°S.

D. Sustain the GO-SHIP repeat hydrographic sections in the Indian Ocean (Chapter 7) to quantify long-term change and provide calibrations for Argo. Add observations of phytoplankton community structure on GO-SHIP lines

E. Maintain the IX01 XBT line to monitor the geostrophic volume and heat transport of the ITF. Pilot a glider program along IX01 line for improved monitoring.

F. Maintain satellite observations of SST, SSS, sea level and winds which are inter-calibrated between missions for climate-quality data. Ongoing satellite missions and their measurements are a vital part of the IndOOS.

G. Model experiments that go hand-in-hand with observations to separate the role of climate change, internal variability, and ENSO forcing on regional SST.

H. Maintain and augment the tide-gauge network, in particular on the islands of the southwestern tropical Indian Ocean. Ensure open distribution and common processing of the data, and add colocated GNSS stations to measure land motion.

Synthesis

Lisa M. Beal, Mathew K. Roxy, and Jérôme Vialard

Out of this review process, including three international workshops and the above 25 chapters, have come 136 actionable recommendations aimed at consolidating, improving, and enhancing the IndOOS to better meet the scientific and societal demands for ocean and climate information and products throughout the next decade and beyond.

Here we synthesize the main findings and outcomes of the review into a roadmap for the future of the IndOOS. First, the overarching successes and limitations of the current IndOOS design are highlighted in terms of the important oceanic and climatic phenomena that need to be captured. Second, the many actionable recommendations for an evolution to IndOOS-2 are carefully prioritized, in terms of the observing system components, to present a clear path forward. Finally, we discuss some of the challenges inherent in implementing these recommendations, including the need for increased engagement and partnerships with and among Indian Ocean rim countries under the framework of the Global Ocean Observing System (GOOS, www.goosocean.org).

Evaluating the IndOOS in terms of the oceanic and climatic phenomena we need to observe and predict

The preceding chapters detail how the IndOOS and its components have revolutionized our scientific understanding of the Indian Ocean and its links to weather and climate and, at the same time, how there are significant limitations to our knowledge and predictive capabilities that can be overcome with future adjustments and enhancements to the IndOOS. Here we synthesize the findings of those chapters, highlighting the most significant successes and limitations of the IndOOS in the context of the important climatic phenomena of the Indian Ocean and their timescales.

Extreme events: The RAMA moorings have allowed case studies of the Indian Ocean's response to, and feedback on, tropical cyclogenesis, showing, for instance, that strong salinity stratification in the Bay of Bengal can cause rapid intensification of TCs, while weakened stratification in the thermocline ridge region related to El Niño events reduces TC activity there

(Chapter 12). These observations are particularly important since air-sea coupling and cooling under cyclones is not well observed from satellites due to intense rainfall. New satellite technologies are needed to observe SST in all weathers. Coastal tide gauges measure the storm surges associated with tropical cyclones, as well as the amplitude of tsunamis, but there are few in the tropical southwest Indian Ocean where cyclones make landfall (Chapters 5,12). An essential input for TC forecasts, and for weather forecasting more generally, is sea level pressure data and upper ocean (200 m) temperature and salinity and while RAMA sites provide some observations in cyclogenesis regions, improved vertical and spatial data coverage is needed (Chapters 4,9,12).

Marine heat waves can have devastating effects on marine life, including coral bleaching. Argo data have successfully characterized the persistence of these events below the surface mixed layer, where signals are invisible to satellites. Yet, marine heat waves along the west coast of Australia, related to Ningaloo Niño, are strongly associated with anomalies in the Leeuwin Current, where fluxes of temperature and salinity from the Indonesian Seas and along the West Australia shelf and slope are poorly captured (Chapters 12,19).

Subseasonal variability: Much has been learned about the MJO and MISO from the IndOOS, phenomena that are important to understand for their influence on monsoon rainfall and hydroclimate (Chapters 9,13,14,15). The Argo dataset has revealed the spatial scale of the oceanic coupling to these intraseasonal oscillations and high frequency RAMA data have captured the dynamical response within the equatorial waveguide, as well as the thermo-dynamical response in regions of strong coupling, such as the SCTR and Bay of Bengal. Subseasonal-to-seasonal prediction models rely on these datasets to initialize their forecasts. Basin-scale fluctuations in SST, SSH, surface wind, and convective perturbations associated with the MJO and MISO and their active and break phases have been characterized and analyzed using satellite data.

Despite these successes, recent field experiments and model simulations point to the need to measure the diurnal cycle of fine vertical structure temperature and salinity (order 1 m over the upper 10 m) of the surface ocean in the 10°N-10°S band and Bay of Bengal in order to better capture MJO and MISO initiation and propagation and improve forecasts (Chapters 9,13,14). Direct measurements of air-sea fluxes are also desirable in key regions of strong subseasonal air-sea coupling, such as in the SCTR, eastern equatorial Indian Ocean, and Bay of Bengal. More generally, air-sea flux products are subject to large errors at all timescales, and need to be better constrained for a wide range of scientific and operational purposes (Chapters 10,14,15). The largest SST signals associated with the MJO occur in the Timor Sea, between Australia and Indonesia, making this a prime site to establish new *in situ* measurements, with the potential to improve subseasonal-to-seasonal forecasting, including predictions of hydroclimate over Australia (Chapters 9,13,15). In summary, the current spatio-temporal coverage of upper ocean stratification (T, S) within the tropics does not capture diurnal signals thought to be important for subseasonal forecasting (Chapters 1,13,14).

The monsoons: Strong seasonal current variations in the Indian Ocean, in particular the Somali Current of the southwest monsoon and the inter-monsoon Wyrtki jets along the equator, dominate the redistribution of heat around the basin and across the equator. They are also linked to strong seasonal variations in upwelling and primary productivity (Chapters 16,18). However, these seasonal circulations are not faithfully represented by coupled models, giving rise to strong biases in the representation of the monsoons and monsoon rainfall (Annamalai et al., 2017). Velocity data at some RAMA sites have allowed major steps forward in describing and understanding the Wyrtki jets and a climatology of the surface seasonal circulation at the basin scale is relatively well captured by surface drifters and satellite data. The accumulation

of Argo data has led to progressive improvements in the mapping of the subsurface thermohaline climatology and geostrophic currents. Nevertheless, contemporary dynamical forecast systems have little skill beyond two months and could be improved by filling observational gaps to improve oceanic initial conditions (Chapter 9). Most important is to occupy the two empty RAMA sites in the western equatorial Indian Ocean and make more direct measurements of surface meteorological fluxes (Chapters 2,9,10). Also essential are observations in the Somali Current system and its associated upwelling cells and cross-equatorial fluxes, which are persistently undersampled by drifters and floats (Chapters 1 & 4), a problem for all boundary fluxes and upwelling systems of the Indian Ocean (Chapters 17,18). New technologies and integrated approaches are desirable to overcome the logistical constraints of sustained observing systems near boundaries and to include biogeochemical observations that can track ecosystem variability (Chapter 8).

Interannual variability: The Indian Ocean Dipole affects climate, rainfall, sea level, and ecosystems throughout the Indian Ocean region and is well described from the combination of RAMA, Argo, and satellite data, which capture the equatorial dynamics, subsurface signals and predictors, and basin-scale surface response (SST, SSH, wind, and SSS), respectively. These data also provide important sources of information for initializing coupled forecast models, by providing subsurface oceanic conditions in the equatorial region and constraining surface fluxes used to force the ocean models. Observations of ocean dynamics and sea level in the SCTR are particularly important for both the IOD and IOBM and a moored velocity time series and more sea level measurements from island tide gauges would capture regional signals better (Chapters 13,14,21). A lack of observations in the eastern pole of the IOD, which harbors smaller spatial scales and includes the upwelling systems of Java-Sumatra, limit our understanding of the dynamics there (Chapters 18,19). New technologies, such as gliders, may provide a feasible way to make sustained measurements closer to the coast in the future (Chapter 8). More observations of oxygen, nutrients, and bio-optics are needed to characterize the subsurface biogeochemical responses to the IOD (Chapter 20). The interannual variability of mass and heat fluxes into the Indian Ocean from the Pacific are relatively well constrained by the IX01 XBT line across the Indonesian Throughflow but more salinity measurements are needed to measure freshwater variability in the ITF, which can dominate over thermal changes (Chapters 3,17). Interannual variability of the subtropical gyre, home to the subtropical dipole and Ningaloo Niño modes, should be constrained with sustained observations of the Agulhas and Leeuwin Currents (Chapters 11,17). While the mean transport of the Agulhas is almost two orders of magnitude larger than the Leeuwin Current, both appear to be important components of interannual variability in the basin-wide heat budget (Chapter 23).

Decadal variability and change: The IndOOS was established little more than a decade ago and climate variability at long time scales across the Indian Ocean remains poorly understood. There are a handful of continuous multidecadal records, among them tide gauges in the north and east of the basin (Chapter 5) and the exceptional 35-yr IX01 XBT section across the ITF (Chapter 3). The combination of the Fremantle tide gauge and IX01 XBT line, for instance, have allowed estimates of decadal fluctuations in the exchanges of mass and heat between the Pacific and Indian Oceans. Evidence for multi-decadal trends in dissolved oxygen, carbon uptake, and ocean acidification come from repeat GO-SHIP hydrographic lines (Chapters 7,20,24), but almost nothing is known about the background variability of these parameters.

Since the mid 2000s there have been enough Argo data to track the large oceanic heat gain of the Indian Ocean over the last decade and the IX01 XBT data have shown that this heat gain is largely due to an intensification of the ITF. Satellite ocean color suggests a reduction of primary productivity related to this warming. Satellite altimetry data have revealed patterns of re-

gional sea level variability and change and Argo data can quantify much of the thermosteric and halosteric contributions to sea level change (Chapters 21, 25). However, the relative paucity and irregularity of past oceanic observations compared to the Pacific and Atlantic make it difficult to separate natural decadal climate variability from anthropogenic change in the Indian Ocean. For instance, fast sea level change in the northern Indian Ocean may be due to natural decadal variability, while observations and models disagree about the sign of the surface heat flux trend within the Indian Ocean since the 1980's (Chapter 25). These deficiencies point to the need for sustained observing with some strategic enhancements to the IndOOS.

Thermohaline changes deeper than 2000 m contribute significantly to decadal heat and sea level variability, but remain unobserved between GO-SHIP decadal surveys (Chapters 11,21,22). There are no sustained measurements of air-sea flux of CO_2 for the Indian Ocean, nor systematic observations of nutrients, bio-optics, and oxygen (Chapters 16,18,20,24). More measurements of vertical land motion need to be colocated with tide gauge records to provide absolute measures of sea level change (Chapters 5,21,22,25). Since decadal variations of heat storage seemed to play an important role in the recent hiatus of global surface warming, there is a strong need to improve our understanding of the dynamics of Indian Ocean heat storage via better measurements of the surface (air-sea fluxes), entrance (ITF), and exit (largely Agulhas and Leeuwin currents) fluxes. The sign of net surface heat flux trends in the Indian Ocean is uncertain in regions (Chapters 10,25), calling for more direct flux measurements, including in the subduction zone of the subtropical gyre. New automated surface platforms may provide the answer to accessing this remote region, where a RAMA site has proven unsustainable (Chapters 2,8,10). Sustained measurements of temperature, salinity, and velocity in the Agulhas Current, which acts as an integrator of variability across the entire subtropical gyre, are highly desirable (Chapters 17,21,22,23,25). These observations would improve ocean state estimates and reanalyses, products that are used to initialize ocean models and form the basis of global energy budget estimates (Chapter 11).

Biogeochemical cycles and change: Sustained observations of biogeochemical parameters in the Indian Ocean have not been a part of the IndOOS until now. The need to integrate these measurements is important enough to be emphasized independently of the physical drivers and time scales above. Uptake of anthropogenic CO_2 and ocean acidification, combined with growth of oxygen minimum zones in the Arabian Sea and Bay of Bengal, are inducing fundamental changes in ocean chemistry that may have already had dramatic impacts on upper ocean ecosystems (Chapters 16,20,24). Pilot programs for biogeochemical measurements have been conducted on some IndOOS platforms in the past, for example subsurface fluorescence measurements and air-sea CO_2 flux estimates at RAMA moorings and the Indian-Australian Bio-Argo program, and these must pave the way for a full integration of biogeochemical measurements over the next decade. Key regions that call for BGC measurements are the strongly productive Arabian Sea, including its upwelling and oxygen minimum zones, the oxygen minimum zone of the Bay of Bengal, the upwelling regions of the SCTR and Sumatra-Java coast, and the subtropical subduction zone of the South Indian Ocean.

Prioritization of Actionable Recommendations

There are many recommendations that have arisen from this review process - 136 in all - and hence it is important to carefully prioritize them in order to provide a clear and actionable roadmap for implementation. For example, of the many adjustments and enhancements to the IndOOS that have been recommended within the chapters herein, which will lead to the greatest improvements in scientific understanding, products, and forecasts? How can we best guide principal investigators, program managers, institute directors, and other decision makers

as to the most optimal use of resources?

We took a number of approaches to the refinement, consolidation, and prioritization of the recommendations during this three-year review process. First, all chapters and recommendations were reviewed by an independently appointed board of six international experts: Peter Dexter (IOC), Marjolaine Krug (OOPC), Richard Matear (IOGOOS), Jay McCreary (CLIVAR), Coleen Moloney (IMBeR), and Susan Wijffels (CLIVAR). These experts also attended the second IndOOS review workshop, where chapters and recommendations were presented by lead authors for further review and discussion.

Second, on the last day of the same workshop all recommendations were discussed in break-out groups of 5-7 scientists. Groups were asked to organize the recommendations into three tiers: high priority, desirable, and low priority, taking into consideration the following requirements, as suggested by the review board. Does the actionable recommendation:

a. Provide sustained observations to characterize and advance our understanding of key phenomena?

b. Provide data to evaluate, validate, and initialize climate predictions and forecasting?

c. Support integration of satellite and *in situ* observations including calibration and validation?

d. Provide observations to track the evolving state of the ocean?

Following the workshop, all written reviews, meeting notes, discussion points, and break-out group results pertaining to each chapter were collated by the Editors and sent to authors, who subsequently revised and refined their chapters and recommendations over the following six months.

With the final versions of chapters and recommendations in hand, all actionable recommendations were cross referenced in a spreadsheet by the Editors so that their impact could be assessed objectively as regards the number of scientific and societal drivers each address and their unique importance. In this way, priorities for the observing system were further refined. For instance, the Argo program is of highest priority, being cited in 13 of 17 chapters, while the establishment of SOOP-CO_2 measurements are also a high priority because there are currently no long-term measurements of surface carbon flux in the Indian Ocean.

Finally, a draft of the Executive Summary, including tiered lists of actionable recommendations, was sent out for final comments from the review board and from the CLIVAR and wider science communities and presented and discussed during the third and final IndOOS review workshop. At this stage a handful of remaining queries, errors, or omissions were followed up by the Editors with the relevant chapter authors and/or observing system component scientists, and adjustments made where necessary. For instance, discussions with SIBER and SCOR members about the lack of observations of ecosystem change in the Indian Ocean during the final workshop led to an additional recommendation to establish a Continuous Plankton Recorder survey.

This rigorous community-led review and discussion process has resulted in a list of prioritized actionable recommendations, laid out in the Executive Summary, that form a framework for implementing an IndOOS more capable of meeting societal demands for climate information and prediction in the future.

IndOOS-2: 2020-2030

In the Executive Summary actionable recommendations resulting from this review are first synthesized into four Core Findings and then grouped into Tiers, with further prioritization as numbered letters - A1, A2 etc. Tiers are defined as follows:

Tier I - High Priority: *Maintain and consolidate essential capacities, while better considering practicalities.*

Tier II - Desirable: *Extend IndOOS capacities to better address scientific and operational drivers.*

Tier III - Lower Priority: *Pilot projects to investigate efficacy, sustainability, and potential for integration into the IndOOS.*

Here, after a brief summary of the four Core Findings, we instead synthesize the actionable recommendations according to observing system component - e.g. the tide gauge network - noting their level of priority by tier. This organization is intended to provide another point of reference for program managers, institute leaders, and individual scientists, including members of IO-GOOS and the Indian Ocean Resources Forum, who are working towards implementation of IndOOS-2.

Core findings

1. We recommend that IndOOS coverage of the Arabian Sea and western equatorial Indian Ocean, including biogeochemical measurements, be rapidly intensified.

2. We recommend enhanced vertical and temporal resolution of upper-ocean measurements in regions of high variability of SST, air-sea fluxes of CO_2, and primary productivity - at the eastern equatorial boundary near Sumatra, in the southeastern Arabian Sea, in the Seychelles-Chagos Thermocline Ridge, and in the Bay of Bengal - and the addition of near-surface biogeochemical observations in these regions.

3. We recommend expansion of the IndOOS into key shelf/slope regions and into the deep ocean, with the establishment of boundary flux arrays in the Agulhas and Leeuwin Currents, an enhancement of Indonesian Throughflow monitoring, and an increase in observations of the deep ocean below 2000 m, initially targeted to the subtropics.

4. We recommend an increase in biogeochemical measurements throughout the basin, initially targeted to regions of high variability and change, such as the Arabian Sea, Bay of Bengal, and eastern equatorial Indian Ocean.

Actionable recommendations by observing system component

Argo: The current Indian Ocean Argo array consists of about 600 floats north of 40°S. Argo is an extraordinarily successful program, providing subsurface oceanic data (temperature, salinity, pressure) that can track variability and change across the basin at seasonal time scales and longer. These data are used to constrain ocean state and circulation estimates and to initialize weather, ocean, and climate models and forecasts (Chapters 1,12,14,15,18,19,21,22,23,25). **The Argo network should be maintained at highest priority (Tier I).**

Long-term observations of the ITF have been made at the 35-yr IX01 XBT line. More measurements of salinity are needed in the vicinity of the line to account for significant changes in the freshwater budget and improve transport estimates (Chapters 3,17,23,25). **The number of Argo profiles within the region of the IX01 XBT line should be enhanced (Tier I).**

The success of Argo makes it an ideal platform on which to integrate vital biogeochemical observations into the IndOOS over the coming decade. These observations are needed to track variability and change in oxygen minimum zones, marine productivity, ocean acidification, and potentially carbon uptake (Chapters 16,18,20,24). Nutrient, bio-optical, and oxygen sensors have matured and the BGC-Argo program is organized and ready to expand. **We recommend 200 BGC-Argo profilers (design density of the BGC-Argo program) throughout the Indian Ocean, initially targeted to key regions of strong variability and change, such as upwelling and oxygen minimum zones, and areas of strong air-sea fluxes of CO_2, including the Arabian Sea, Bay of Bengal, eastern equatorial Indian Ocean, and SCTR (Tier II).**

New Deep-Argo profilers are also poised to go operational. Observations of the deep ocean are needed to track natural and anthropogenic decadal to multi-decadal ocean heat and freshwater content, attribute causes of regional sea level rise, and constrain reanalyses and state estimates (Chapters 11,21,23,25). 250 Deep-Argo floats north of 40°S would provide optimal 5° x 5° resolution. **We recommend the establishment of a Deep-Argo program, with initial deployments in the subtropical southern Indian Ocean where decadal changes in deep ocean heat content are largest (Tier II).**

In the tropics, greater temporal and vertical resolutions of observations are needed to capture upper ocean variability important to MJO and MISO initiation and propagation and potentially improve forecasts of the monsoons (Chapters 1,9,13,14). This might be done through a **pilot project to double the frequency of Argo profiling within the tropical band, 10°N-10°S (Tier III).** Specialized Argo missions may also improve coverage in key regions such as the Somali Current system, where a **pilot project including shallow, fast profiling of BGC-Argo floats would help characterize the upwelling (Tier III).**

RAMA: The RAMA moorings relay 10-minute data of upper ocean and surface meteorological conditions in real-time via satellite, monitoring the fast ocean dynamics of the equatorial band and providing essential information for weather and climate analyses and forecasting (Chapters 9,10,12,13,14,15,19,21,22). EOVs measured by RAMA include ocean surface and subsurface temperature, salinity, and velocity, as well as variables needed to calculate wind stress and surface heat flux. Due to challenging logistics related to ship time and vandalism some RAMA sites have been unsustainable and others left unoccupied. **Highest priority is to consolidate RAMA to a new design, RAMA-2.0 (33 sites versus the original 46), and complete the array by occupying three remaining sites in the western equatorial Indian Ocean (Tier I).** A reduced array maintains key scientific capacity while providing more flexibility to add new sensors, upgrade technology, and add new sites (Chapter 2).

Key processes of the near-surface ocean need to be better measured to meet the need for improved sub-seasonal to seasonal forecasting and surface flux products (Chapters 9,10). These measurements will refine our understanding of the MJO and MISO and their influence on monsoon rainfall and hydro-climate (Chapters 13,14,15), while direct measures of surface fluxes are needed to validate bulk algorithmic estimates (Chapter 10, 14). **We recommend direct flux measurements and increased vertical resolution of temperature and salinity sensors be added at RAMA flux reference sites (Tier II).** The region of highest intra-seasonal variability of SST and rainfall is found to the northwest of Australia. **A new RAMA flux reference site between Australia and Indonesia in the outflow of the ITF (14°S, 115°E) has strong potential to improve hydroclimate predictions (Tier II).**

RAMA moorings can serve as platforms for a host of new sensors including measurements of marine biogeochemistry and ecosystem dynamics (Chapters 2,24). **We recommend adding $MAPCO_2$ systems and biogeochemical measurements at RAMA Flux Reference sites, targeting regions with high variability in CO_2 fluxes and/or rapidly increasing pH as priority (Tier II).**

There is a mooring network in the northern Indian Ocean - OMNI - led by India that also records high resolution ocean and near-surface meteorological data. The Ministry of Earth Sciences (MoES) of India announced in June 2018 that the data from OMNI outside the Indian EEZ would be made freely available at data standards similar to that of RAMA. **A coordinated moored network, combining RAMA and OMNI is a priority and will improve operational efficiency as well as data accessibility and standards (Tier I).**

Tide gauge network: Tide gauges measure sea level continuously at given coastal points, capturing tides, tsunamis, and storm surges as well as local sea level variability and change. When combined with measurements of vertical land motion, they can provide referenced data for calibration of satellite altimetry, estimates of anthropogenic sea level rise, and combined reconstructions of long-term regional sea level changes (Chapters 5,12,17,18,21,22,25). **The core tide gauge network should be sustained, with the addition of co-located vertical land motion measurements prioritized at stations where records are longest (Tier I).** Island stations are highly effective for calibrations and reconstructions and **more stations are needed on the islands of the southwest tropical Indian Ocean, as well as along the coasts of Thailand and Africa (Tier I).**

Satellite remote sensing: Satellites are a crucial component of the IndOOS, providing the only comprehensive, basin-wide view of the ocean. **The capacity to monitor key essential ocean variables, such as all-weather SST, SSH, surface wind and wind stress, Chl, SSS, deep-atmospheric convection, and precipitation must be maintained (Tier I)**. In particular, observing capacity for some important EOVs is currently not guaranteed by planned satellite missions. First, continuous coverage of surface winds requires three scatterometers in coordinated orbits, while currently two cover only 60% of the Indian Ocean at 6 hr interval (Chapters 6,12,21,22). Second, all-weather SST missions are vital to capture signals in regions of cloud and rainfall and SSS missions should be continued with improved accuracy and spatial resolution to better constrain mixed layer depth and barrier layer thickness in salinity-stratified regions such as the Bay of Bengal (Chapters 6,12,15,18,22). Finally, for observing energetic boundary current regions currently poorly sampled by IndOOS, **space-based capabilities for measuring meso- and sub-mesoscale fronts and eddies should be enhanced (Tier I)** (Chapters 6,12,17,21).

XBT network: The XBT network consists of transects made by voluntary observing ships that collect temperature observations over the upper 1 km of the ocean, sometimes complemented by other measurements. This network has allowed evaluation of multi-decadal changes in oceanic heat content, but is now largely superseded by Argo. However, XBT observations remain important in regions of high variability, intense narrow flows, and/or depths shallower than 2000 m, such as in the Indonesian Seas and Throughflow. **We recommend that IX01, across the ITF, is maintained at highest priority and equipped with automated XBT launchers to increase resolution and maximize data return (Tier I)** (Chapters 3,8,15,17,19,21,22,23,25).

The IX21 line is one of the few sustained measurements in the subtropical gyre, aside from Argo, and has potential for capturing long-term changes in the Agulhas system. **We recommend maintaining the IX21 line and adding measurements of pCO_2 (Tier I)** to provide the

only systematic carbon cycle measurements between decadal GO-SHIP lines (Chapters 3,24). IX14 across the Bay of Bengal has long been active, supported by Indian agencies, and **we recommend that IX14 data are shared with the international community and made easily accessible to become part of the IndOOS (Tier I).**

Surface drifters: Drifters measure near-surface currents and temperature at a design density of one drifter per 5° x 5°, with data retrievals every three hours via satellite, as part of the Global Drifter Program. A few drifters now also measure sea level pressure, important for initializing weather prediction models. **We recommend the drifter array be maintained at current design density and enhanced with more barometric pressure observations, with the optimal density of pressure observations to be evaluated at highest priority (Tier I)** (Chapters 4,12,15). More deployments are needed in severely under-sampled regions, such as the Somali Current system, the SCTR, and the ITF.

Boundary arrays and new technologies: Many recommendations from this review relate to an expansion of the IndOOS towards the coasts at key locations to better measure energetic boundary currents and upwelling systems and their related fluxes (Chapters 8,11,12,17,18,19, 20,21,23,25). Emerging technologies will provide new platforms and sensors that ease the logistics of this expansion. Boundary arrays should integrate a number of technologies to best cover the range of energetics and scales within the shelf-slope region, such as moored current meters and CTDs, CPIES (Current and Pressure recording Inverted Echo Sounder), gliders, autonomous underwater vehicles, and new Articulating or Lift-Assisted moored profilers. At highest priority **we recommend re-establishing an Agulhas Current volume, heat, and freshwater transport array (Tier II)** at the western boundary near 34°S, colocated with an altimeter ground track and including an “end-point” mooring to measure basin-wide geostrophic overturning down to 2000 m. **The Leeuwin Current array needs to be enhanced to measure full-depth volume, heat, and freshwater fluxes, including an end-point mooring (Tier II)**. We need to **monitor T/S fluxes, dissolved oxygen, and core nutrients within the Sumatra-Java upwelling region and South Java Current,** the eastern pole of the IOD, as well as **T/S fluxes, dissolved oxygen, and core nutrients along the west coast of India** where monsoon currents, upwelling, and the Arabian Sea oxygen minimum zone intersect and societal implications are greatest (**Tier II**).

There should be continued exploration of the Indian Ocean with new autonomous and expendable platforms and new sensor technologies (Tier III) that may revolutionize the IndOOS in the future, including directional wave spectra drifters (with SST and GPS sensors), χ-SOLO floats (turbulence), X-Spar floats, Saildrones, Wave Gliders, and Minimets.

GO-SHIP: GO-SHIP is an internationally-coordinated program of decadal, multi-disciplinary, trans-basin hydrographic surveys. A wide variety of measurements are made via GO-SHIP that are unobtainable through automated means, including physical, geochemical and trace properties of seawater to full ocean depth that are used to constrain ocean circulation and water mass changes over long time scales. Given the growing importance of decadal and multidecadal climate variability and change, GO-SHIP is an important part of the future of the IndOOS. **GO-SHIP occupations should continue at decadal interval and it is a priority to identify national or multi-national support for the occupation of I01E and I01W sections across the Bay of Bengal and Arabian Sea (Tier I)**.

Applications: In addition to actionable recommendations for each observing system component, a number of other priorities became clear during the process of this review. These recommendations involve data-mining, analyses, and collaborations towards the validation and

improvement of the products, models, and predictions that derive from the IndOOS.

We recommend **digitization of historic sea level data** from around the Indian Ocean. **To better target new biogeochemical observations, the locations of largest productivity variability need to be determined using satellite ocean color.** *In situ* chlorophyll and productivity observations need to be compared to satellite ocean color to **quantify the accuracy of satellite algorithms for primary productivity in the Indian Ocean** and develop regionally-tuned algorithms, if necessary. **Tropical convective parameterizations need to be improved** through more collaboration between oceanographers and the atmospheric reanalysis community. **Advancement of coupled ocean-atmosphere data assimilation techniques is of highest priority.** There is a need to **improve capabilities for reanalysis, prediction, and observing system evaluation** through stronger collaborations among data assimilators, modelers, and observationalists. **Collaborations with the paleo-proxy community can provide long records** of surface temperature variability in the IOD eastern pole and of sea level variability near the west coast of Australia, in the Chagos archipelago, and Mascarene Islands.

The way forward: Engagement, collaboration, and capacity building under the GOOS framework with support from the WCRP and IOC

Under the terms of reference for this decadal review we have scientifically evaluated the IndOOS and clearly articulated how the observing system should evolve to better meet societal demand for ocean and climate products and forecasts in the future. We hope we have provided a roadmap to address *the clear and urgent need for expansion of global ocean observing designed to meet the requirements of a broad suite of users*, as identified in the GOOS 2030 Strategy. Although falling outside the scope of this review, the necessity for implementation planning, resource building, and connection to end-users in the future success of IndOOS-2 are obvious and hence we briefly discuss here the challenges and how these efforts can be coordinated going forward.

Flat or declining financial support poses a serious threat to the IndOOS and to GOOS as a whole. Improvements and enhancements to the system will require increased investment from the nations currently involved, the engagement of new nations and institutions willing to provide resources, and a recommitment to the organization and governance of GOOS by the Intergovernmental Oceanographic Commission (IOC) of UNESCO, the World Meteorological Organisation (WMO), and the International Council for Science (ICSU) through their support of the World Climate Research Progam (WCRP).

There is a necessity for increased engagement of Indian Ocean rim countries for the future success of IndOOS. In particular, the expansion into coastal and upwelling regions will be reliant on increased involvement and cooperation of regional countries and agencies. These countries will need to invest in the long-term development of their ocean science human capacity so that skills can grow robustly and be passed on to the next generation of researchers and technicians, ensuring ownership and sustainability of regional observing system components. Equally essential is a commitment to the rigor of the scientific method, to observing best-practices, and to data sharing and dissemination. Distinguishing oceanic variability from change requires continuous or repeated observations that are carefully calibrated, inter-calibrated, and archived across decades of practice.

Political agreements for the opening of country's Exclusive Economic Zones to new platforms and technologies of the IndOOS are required, for example, to allow shallow-profiling Argo floats

and gliders to sample coastal upwelling zones.

Better connection to end-users will ensure that investments in the IndOOS are more fully realized. Many oceanographic datasets are still fragmented and heterogeneous, posing an impediment to decision-makers who need to analyse oceanographic data alongside economic and human-driven factors in support of economic or sustainable development decisions.

These implementation challenges are not new to ocean observing and can be addressed under the existing framework of the GOOS, of which IndOOS is a component. The recently published GOOS 2030 Strategy and upcoming Implementation Plan will provide further guidance. The core principles of GOOS are to: Implement through user-driven design; Maintain sustained observations; Ensure regular evaluation; Set global standards and best practices; Encourage open data sharing, and Develop capacity. Over the last three decades GOOS has successfully built a unified network around the independently funded observing system components of many different nations, acting on these core principles. To give an example of success for IndOOS, the RAMA partners have conducted 85 cruises on 21 different ships from 11 different nations, using 2053 days of ship time to deploy and recover 325 moorings in the 14 years since September 2004. This is an enormous success, not only for the IndOOS, but also in terms of international engagement, partnerships, and capacity building.

More will need to be done to connect Indian Ocean rim countries and institutions with the principles and tools of GOOS in the future. As the scientific advisory panel, regional implementation alliance, and resources forum for the IndOOS, respectively, the IORP, IO-GOOS and IndOOS Resource Forum (IRF) are essential in this. Multilateral partnerships for the IndOOS and its enhancement should be fostered through, and guided by, these bodies. They can help ensure that international resources are optimized, national cases for funding are strengthened, capacity building is conducted in priority areas, and data are shared. The IORP, IO-GOOS, and IRF need to be committed, proactive, well-coordinated, and more inclusive for a successful IndOOS-2. To achieve this they will need ongoing and improved financial and secretarial support from the WCRP and their sponsors, the IOC-UNESCO, WMO, and ICSU.

Acknowledgements

This review is dedicated to Gary Meyers (1941-2016), visionary and leader of Ocean Observing Systems. Gary was an eminent oceanographer who received many awards, including the 2006 Australian Meteorological and Oceanographic Society Medal for Leadership in Meteorology and Oceanography. He was the founding chair of the CLIVAR/IOC-GOOS Indian Ocean Panel, leading the initial design and development of a sustainable observing system for the Indian Ocean and effectuating the birth of IndOOS. The Indian Ocean scientific community will miss his warm personality, deep scientific knowledge, and inspiring leadership.

Dr Gary Meyers, CSIRO Hobart. Photo by Bruce Miller. Copyright CSIRO Australia

This review would not have been possible without the support of various sponsors and individuals. We thank the members of the review board for fruitful discussions and thoughtful feedback, both written and in person, on all the chapters and actionable recommendations of the review: Susan Wijffels and Jay McCreary (both nominated by CLIVAR), Coleen Moloney (IMBeR), Marjolaine Krug (OOPC), Richard Matear (IO-GOOS), and Peter Dexter (IOC). We acknowledge strong contributions from past and present members of the CLIVAR/IOC-GOOS IORP and IMBeR-IOGOOS SIBER panel, many of whom authored chapters and participated in workshops.

We especially thank Jing Li of the International CLIVAR Project Office who efficiently managed the logistics leading up to and during the review workshops, kept us (almost) on schedule by reminding us of commitments and deadlines during the review process, and oversaw the collation, type-setting, and proof-reading of the entire document. We also appreciate the excellent layout conducted by Mr Sandeep Sukhdeve from the International CLIVAR Monsoon Project Office (ICMPO) at Indian Institute of Tropical Meteorology (IITM), Pune, India.

WCRP, US-CLIVAR, IMBeR, IOGOOS, the UNESCO-IOC Perth Programme Office, the US NOAA, and the IUGG-IAPSO all provided financial support for the three workshops during which this review was undertaken. We thank the Indian Ocean Marine Research Centre (IOMRC), the Indonesian Institute of Sciences (LIPI) and the Indonesian Agency for Meteorology, Climatology and Geophysics (BMKG), and the Nelson Mandela University in South Africa for hosting the three IndOOS Review workshops.

References

Abhilash S, A.K. Sahai, S. Pattanaik, B.N. Goswami, and A. Kumar, 2014: Extended range prediction of active-break spells of Indian summer monsoon rainfall using an ensemble prediction system in NCEP climate forecast system. *International Journal of Climatology* , **34**, 98-113.

Abram, N. J., M. K. Gagan, M. T. McCulloch, J. Chappell, and W. S. Hantoro, 2003: Coral reef death during the 1997 Indian Ocean Dipole linked to Indonesian wildfires. *Science*, **301**, 952-955.

Achuthavarier, D., and V. Krishnamurthy, 2011: Role of Indian and Pacific SST in Indian summer monsoon intraseasonal variability. *J. Climate*, **24(12)**, 2915-2930.

Agarwal, N., R. Sharma, S. Basu, and V. K. Agarwal, 2008: Assimilation of sub-surface temperature profiles from Argo floats in the Indian Ocean in an Ocean General Circulation Model. *Current Science*, **95**, 495-501.

Ajayamohan, R.S., S. A. Rao, and T. Yamagata, 2008: Influence of Indian Ocean Dipole on poleward propagation of boreal summer intraseasonal oscillations. *J. Climate*, **21**, 5437-5454.

Aldrian, E., 2008: Dominant factors of Jakarta's three largest floods. *Jurnal Hidrosfir Indones*, **3**, 105-112.

Alexander, M., 2010: Extratropical Air-Sea Interaction, Sea Surface Temperature Variability, and the Pacific Decadal Oscillation. *Climate Dyn.: Why Does Climate Vary?*, 123-148.

Alford, M. H., M. C. Gregg, and M. Ilyas, 1999: Diapycnal mixing in the Banda Sea: Results of the first microstructure measurements in the Indonesian Throughflow. *Geophys. Res. Lett.*, **26**, 2741-2744.

Allison, E.H. et al., 2009: Vulnerability of national economies to the impacts of climate change on fisheries. *Fish and Fisheries*, **10**, 173-196: 10.1111/j.1467-2979.2008.00310. x.

Alory, G., S. Wijffels, and G.Meyers, 2007: Observed temperature trends in the Indian Ocean over 1960-1999 and associated mechanisms. *Geophys. Res. Lett.*, **34(2)**.

Anderson, J.E., and S. C. Riser, 2014: Near-surface variability of temperature and salinity in the near-tropical ocean: Observations from profiling floats. *J. Geophys. Res. Oceans*, **119**, 7433-7448, doi: 10.1002/2014JC010112.

Andres, M., S. Jan, T.B. Sanford, V. Mensah, **L. Centurioni**, and J.W. Book, 2015: Mean structure and variability of the Kuroshio from northeastern Taiwan to southwestern Japan. *Oceanography*, **28(4)**, 84-95, http://dx.doi.org/10.og.2015.84.g.2015.84.

Andres, M., V. Mensah, S. Jan, M.-H. Chang, …, S.B. Sanford, 2017: Downstream evolution of the Kuroshio's time-varying transport and velocity structure. *J. Geophys. Res. Oceans*, **122**, doi:10.1002/2016JC012519.

Annamalai, H., and M. J. Slingo, 2001: Active/break cycles: diagnosis of the intraseasonal

variability of the Asian Summer Monsoon. *Climate Dyn.*, **18(1)**, 85-102.

Annamalai, H., R. Murtugudde, J. Potemra, S. P. Xie, …B. Wang, 2003: Coupled dynamics over the Indian Ocean: Spring initiation of the zonal mode. *Deep-Sea Res. Part II: Topical Studies in Oceanography*, **50**, 2305-2330.

Annamalai, H., and K.R. Sperber, 2005: Regional heat sources and the active and break phases of boreal summer intraseasonal (30-50 day) variability. *J. Atmos. Sci.* , **62**, 2726-2748.

Annamalai, H., P. Liu, and S-P. Xie, 2005a: Southwest Indian Ocean SST variability: Its local effect and remote influence on Asian monsoons. *J. Climate*, **18**, 4150-4167.

Annamalai, H., J. Potemra, R. Murtugudde, and J.P. McCreary, 2005b: Effect of preconditioning on the extreme climate events in the tropical Indian Ocean. *J. Climate*, **18**, 3450-3469.

Annamalai, H., B. Taguchi, K.R. Sperber, J.P. McCreary, …, A. Moise., 2015: Persistence of systematic errors in the Asian-Australian monsoon precipitation in climate models: a way forward. *CLIVAR Exchanges, Special Issue on Monsoons: Advancing understanding of monsoon variability and improving prediction*, **66**, 19-23.

Annamalai, H., B. Taguchi, J. P McCreary, M. Nagura, and T. Miyama, 2017: Systematic errors in south Asian monsoon simulation: Importance of Equatorial Indian Ocean processes. *J. Climate*, **30 (19)**, 8159-8178, doi:10.1175/JCLI-D-16-0573.1.

Anutaliya, A., U. Send, J.L. McClean, J. Sprintall, …, E.J. Metzger, 2017: An undercurrent off the east coast of Sri Lanka. *Ocean Sci.*, **13**, 1035-1044, https://doi.org/10.5194/os-13-1035-2017.

Ashok, K., Z. Guan, and T. Yamagata, 2001: Impact of the Indian Ocean dipole on the relationship between the Indian monsoon rainfall and ENSO. *Geophys. Res. Lett.*, **28**, 4499-4502.

Ashok, K., Z. Guan, and T. Yamagata, 2003: Influence of the Indian Ocean Dipole on the Australian winter rainfall. *Geophys. Res. Lett.*, **30**, doi:10.1029/2003GL017926.

Ashok, K., Z. Guan, N.H. Saji, and T. Yamagata, 2004: Individual and combined influences of the ENSO and Indian Ocean Dipole on the Indian summer monsoon. *J. Climate*, **17**, 3141-3155.

Astier, N., M. Plu, and C. Claud, 2015: Associations between tropical cyclone activity in the Southwest Indian Ocean and El Niño Southern Oscillation. *Atmos. Sci. Lett.*, **16**, 506-511, doi:10.1002/asl.589.

Bakker, D. C. E., and et al., 2014: An update to the Surface Ocean CO_2 Atlas (SOCAT version 2). *Earth Systems Science Data*, **6**, 69-90.

Bakun, A., 1990: Global climate change and intensification of coastal ocean upwelling. *Science*, **247(4939)**, 198-201.

Balaguru, K., P. Chang, R. Saravanan, L. R. Leung,J.-S. Hsieh, 2012: Ocean barrier layers' effect on tropical cyclone intensification. *PNAS*, **109**, 14343-14347, doi:10.1073/pnas.1201364109

Balaguru, K., S. Taraphdar, L. R. Leung, and G. R. Foltz, 2014: Increase in the intensity of post-monsoon Bay of Bengal tropical cyclones. *Geophys. Res. Lett.*, **41**, 3594-3601, doi:10.1002/2014GL060197.1

Balmaseda, M.A., F. Hernandez, and A. Storto, et al., 2015: The ocean reanalysis Intercomparison project (ORA-IP). *J. Oper. Oceanogr.*, **8**, 80-97, doi:10.1080/1755876X.2015.1022329.

Bange, H.W. et al., 2001: Nitrous oxide emissions from the Arabian Sea: A synthesis. *Atmos. Chem. Phys.*, **1**, 61-71.

Bange, H.W., S. Wajih, A. Naqvi, and L.A. Codispoti, 2005: The nitrogen cycle in the Arabian Sea. *Prog. Ocean.*, **65**, 145-158.

Bange, H.W., 2009: Nitrous oxide in the Indian Ocean. In: J. D. Wiggert, R.R. Hood, S.W.A. Naqvi, K.H. Brink and S.L. Smith (Editors), Indian Ocean Biogeochemical Processes and Ecological Variability. *Geophysical Monograph. American Geophysical Union, Washington, D. C.*, 205-216.

Barange, M. et al., 2014: Impacts of climate change on marine ecosystem production in societies dependent on fisheries. *Nature Climate Change*, **4**: 211-216, 10.1038/nclimate2119.

Barber, R.T., J. Marra, R.R. Bidigare, L.A. Codispoti, …, S.L. Smith, 2001: Primary productivity and its regulation in the Arabian Sea during 1995. *Deep-Sea Res. Part II*, **48**, 1127-1172, doi: 1110.1016/S0967-0645(1100)00134-X.

Barnett T.P., D.W. Pierce, K.M. Achuta Rao, P.J. Gleckler, …, W.M. Washington, 2005: Penetration of human-induced warming into the world's oceans. *Science*, **309 (5732)**, 284-287

Bates, N. R., A. C. Pequignet, and C. L. Sabine, 2006: Ocean carbon cycling in the Indian Ocean: I. Spatio-temporal variability of inorganic carbon and air-sea CO_2 gas exchange. *Global Biogeochemical Cycles*, **20**, GB3020.

Beal, L. M., and T. K. Chereskin, 2003: The volume transport of the Somali Current during the 1995 southwest monsoon. Deep-Sea Res. Part II: Topical Studies in Oceanography 50.12 (2003), 2077-2089.

Beal, L.M., V. Hormann, R. Lumpkin, and G.R. Foltz, 2013: The Response of the Surface Circulation of the Arabian Sea to Monsoonal Forcing. *J. Phys. Oceanogr.*, **43**, 2008-2022, doi:https://doi.org/10.1175/JPO-D-13-033.1

Beal, L. M., et al., 2015: Capturing the transport variability of a western boundary jet: Results from the Agulhas Current Time-Series Experiment (ACT). *J. Phys. Oceanogr.* **45.5 (2015)**, 1302-1324.

Beal, L.M., and S. Elipot, 2016: Broadening not strengthening of the Agulhas Current since the early 1990s. *Nature*, **540**, 570-573, doi:10.1038/nature19853.

Bednarsek, N., G. A. Tarling, D. C. E. Bakker, S. Fielding, …, E. J. Murphy, 2012: Extensive dissolution of live pteropods in the Southern Ocean. *Nature Geoscience*, **5**, 881-85.

Behera, S. K., R. Krishnan, and T. Yamagata, 1999: Unusual ocean-atmosphere conditions in the tropical Indian Ocean during 1994. *Geophys. Res. Lett.*, **26**, 3001-3004.

Behera, S. K., and T. Yamagata, 2001: Subtropical SST dipole events in the southern Indian Ocean. *Geophys. Res. Lett.*, **28**, 327-330.

Behrenfeld, M.J., and P.G. Falkowski, 1997: Photosynthetic rates derived from satellite-based chlorophyll concentration. *Limnology and Oceanography*, **42(1)**, 1-20.

Bellon, G., A.H. Sobel and J. Vialard, 2008: Ocean-atmosphere coupling in the monsoon intraseasonal oscillation: a simple model study. *J. Climate*, **21**, 5254-5270.

Bellon, G., and A. Sobel, 2008a: Poleward-propagating intraseasonal mon- soon disturbances in an intermediate-complexity axisymmetric model. *J Atmos Sci.*, **65**, 470-489.

Bellon, G., and A. Sobel, 2008b: Instability of the axisymmetric monsoon ow and intraseasonal oscillation. *J Geophys Res.*, **113**, **D07109**, doi:10.1029/2007-JD008968

Benthuysen, J.A., E.C. J. Oliver, M. Feng, and A.G. Marshall, 2018: Extreme Marine Warming Across Tropical Australia During Austral Summer 2015-2016. *J. Geophys. Res.*, **123**, 1301-1326, doi:10.1002/2017JC013326.9.

Benthuysen, J., R. Furue, J. McCreary, N. Bindoff, and H. Phillips, 2014: Dynamics of the Leeuwin Current: Part 2. Impacts of mixing, friction, and advection on a buoyancy-driven eastern boundary current over a shelf. *Dyn. Atmos. Oceans*, **65**, 39-63.

Bessafi M., and M.C. Wheeler, 2006: Modulation of south Indian ocean tropical cyclones by the Madden-Julian oscillation and convectively coupled equatorial waves. *Mon. Wea. Rev.* **134**, 638-656.

Biastoch, A., C.W. Boening, F.U. Schwarzkopf, and J.R.E. Lutjeharms, 2009: Increase in Agulhas leakage due to poleward shift of Southern Hemisphere westerlies. *Nature*, **462**, 495-498.

Bindoff, N. L., and T. J. McDougall, 2000: Decadal changes along an Indian Ocean section at 32 S and their interpretation. *J. Phys. Oceanogr.*, **30(6)**, 1207-1222.

Biogeochemical-Argo Planning Group, 2016: The scientific rationale, design and Implementation Plan for a Biogeochemical-Argo float array. Edited by Ken Johnson and Hervé Claustre. doi:10.13155/46601.

Birkett, C., R. Murtugudde, and R. Allan, 1999: Indian Ocean climate event brings floods to East Africa's lakes and the Sudd Marsh. *Geophys. Res. Lett.*, **26 (8)**, 1031-1034.

Black, E., J. Slingo, and K.R. Sperber, 2003: An observational study of the relationship between excessively strong short rains in coastal East Africa and Indian Ocean SST. *Mon. Wea. Rev.*, **131**, 74-94.

Boos, W.R., and Z. Kuang, 2010: Mechanisms of poleward propagating, intraseasonal convective anomalies in cloud system-resolving models. *J Atmos Sci.* **67**, 3673-3691

Bopp, L., L. Resplandy, A. Untersee, P.L. Mezo, and M. Kageyama, 2017: Ocean (de)oxy-

genation from the Last Glacial Maximum to the twenty-first century: insights from Earth System models. *Phil. Trans. R. Soc.*, **A 375**, doi:10.1098/rsta.2016.0323.

Bopp, L., L. Resplandy, J.C. Orr, S.C. Doney , …, M. Vichi, 2013: Multiple stressors of ocean ecosystems in the 21st century: projections with CMIP5 models. *Biogeosciences*, **10**, 6225-6245, doi:10.5194/bg-10-6225-2013.

Bourlès, B., R. Lumpkin, M.J. McPhaden, F. Hernandez, …, J. Trotte, 2008: The PIRATA Program: History, Accomplishments, and Future Directions. *Bull. Amer. Meteor. Soc.*, **89**, 1111-1125.

Bourlès, B., M. Araujo, M.J. McPhaden, P. Brandt, …, R. Perez, 2019: PIRATA: A sustained observing system for tropical Atlantic Climate research and forecasting. *Earth Space Science*, **6**, 577-616, doi:https://doi.org/10.1029/2018EA000428.

Bradshaw E., L. Rickards, and T. Aarup, 2015: Sea level data archaeology and the Global Sea Level Observing System (GLOSS). *Geophysical Research Journal* , **6**, 9-16.

Brandt, P., M. Dengler, and A. Rubino, et al., 2003: Intraseasonal variability in the southwestern Arabian Sea and its relation to the seasonal circulation. *Deep-Sea Res. Part II*, **50**, 2129-2141.

Brunke, M. A., X. Zeng, and S. Anderson, 2002: Uncertainties in sea surface turbulent flux algorithms and data sets. *J. Geophys. Res.*, **102**, doi: 10.1029/2001JC000992.

Bryden, H. L., and L.M. Beal, 2001: Role of the Agulhas Current in Indian Ocean circulation and associated heat and freshwater fluxes. *Deep-Sea Res. Part I*, **48(8)**, 1821-1845.

Burns, J. M., B. Subrahmanyam, E.S. Nyadjro, and V. S. N. Murty, 2016: Tropical cyclone activity over the Southwest tropical Indian Ocean. *J. Geophys. Res.*, **121**, 6389-6402, doi:10.1002 2016JC011992.2

Bushinsky, S.M., S.R. Emerson, S.C. Riser, and D.D. Swift, 2016: Accurate oxygen measurements on modified Argo floats using *in situ* air calibrations. *Limnology and Oceanography-Methods*, **14(8)**, doi:10.1002/lom3.10107, 491-505.

Cai, W., T. Cowan, M. Dix, L. Rotstayn, …, S. Wijffels, 2007: Anthropogenic aerosol forcing and the structure of temperature trends in the southern Indian Ocean. *Geophys. Res. Lett.*, **34(14)**.

Cai, W., T. Cowan, and M. Raupach, 2009a: Positive Indian Ocean Dipole events precondition southeast Australia bushfires. *Geophys. Res. Lett.*, **36 (L19710)**, doi:10.1029/2009GL 039902.

Cai, W., T. Cowan, and A. Sullivan, 2009b: Recent unprecedented skewness towards positive Indian Ocean Dipole occurrences and their impact on Australian rainfall. *Geophys. Res. Lett.*, doi:10.1029/2009GL037604.

Cai, W., A. Pan, D. Roemmich, T. Cowan, and X. Guo, 2009c: Argo profiles a rare occurrence of three consecutive positive Indian Ocean Dipole events, 2006-2008. *Geophys. Res. Lett.*, **36 (L08701)**, doi:10.1029/2008GL037038.

Cai, W., and T. Cowan, 2013: Why is the amplitude of the Indian Ocean Dipole overly large in CMIP3 and CMIP5 climate models? *Geophys. Res. Lett.* **40**, 1200-1205.

Cai, W., S. Borlace, M. Lengaigne, P. Van Rensch, …, L. Wu, 2014a: Increasing frequency of extreme El Nino events due to greenhouse warming. *Nature Climate change*, **4(2)**, 111-116.

Cai, W., A. Santoso, G. Wang, E. Weller, …, T. Yamagata, 2014b: Increased frequency of the Indian Ocean Dipole events due to greenhouse warming. *Nature*, **510**, 254-258.

Cai, W., G. Wang, A. Santoso, M.J. McPhaden, …, M. Lengaigne, 2015: Increased frequency of extreme La Nina events under greenhouse warming. *Nature Climate Change*, **5(2)**, 132-137.

Camargo, S.J., M.C. Wheeler, and A.H. Sobel, 2009: Diagnosis of the MJO modulation of tropical cyclogenesis using an empirical index, *J. Atmos. Sci.*, doi:10.1175/2009JAS3101.1.

Centurioni, L., L. Braasch, E. Di Lauro, P. Contestabile, …, D. Vicinanza, 2017: A new strategic wave measurement station off Naples port main breakwater. *Coastal Engineering Proceedings*, **1(35)**, 36.

Centurioni, L.R., 2018: Drifter Technology and Impacts for Sea Surface Temperature, Sea-Level Pressure, and Ocean Circulation Studies, in Observing the Oceans in Real Time, edited by R. Venkatesan, A. Tandon, E. D'Asaro and M.A. Atmanand. *Springer International Publishing, Cham*, 37-57, doi:10.1007/978-3-319-66493-4_3.

Chen, G., W. Han, Y. Li and D. Wang, 2016: Interannual Variability of Equatorial Eastern Indian Ocean Upwelling: Local versus Remote Forcing. *J. Geophys. Res.*, doi: 10.1175/JPO-D-15-0117.1.

Cheng, L., F. Zheng, and J. Zhu, 2015: Distinctive ocean interior changes during the recent warming slowdown. *Scientific Reports*, **5**, 14346; doi: 10.1038/srep14346.

Cheng, L., J. Abraham, G. Goni, T. Boyer, …, J. Zhu, 2016: XBT Science: Assessment of Instrumental Biases and Errors. *Bull. Amer. Meteor. Soc.*, **97**, 924-933, https://doi.org/10.1175/BAMS-D-15-00031.1 1

Cheng L., K. Trenberth, J. Fasullo, T. Boyer, …, J. Zhu, 2017: Improved estimates of ocean heat content from 1960 to 2015, *Science Advances*, **3**, doi:e1601545.

Church J.A., N.J.White, and J.R. Hunter, 2006: Sea-level rise at tropical Pacific and Indian Ocean islands. *Global and Planetary Change*, **53**, 155-168.

Cione, J.J., and E. W. Uhlhorn, 2003: Sea surface temperature variability in hurricanes: Implications with respect to intensity change. *Mon. Wea. Rev*, doi:10.1029/2004GL021980.

Clarke, A.J., and X. Liu, 1994: Interannual sea level in the northern and eastern Indian Ocean. *J. Phys. Oceanogr.*, **24**, 1224-1235.

Cobb, K.M., C.D. Charles, and D.E. Hunter, 2001: A central tropical Pacific coral demonstrates Pacific, Indian, and Atlantic decadal climate connections. *Geophys. Res. Lett.*, **28**, 2209-2212, doi:10.1029/2001GL012919.

Codispoti, L.A. et al., 2001: The oceanic fixed nitrogen and nitrous oxide budgets: Moving targets as we enter the anthropocene? *Sci. Mar.*, **65**, 85-105.

Cole, J. E., R. B. Dunbar, T. R. McClanahan, and N. A. Muthiga, 2000: Tropical Pacific forcing of decadal SST variability in the western Indian Ocean over the past two centuries. *Science*, **287**, 617-619, doi:10.1126/science.287.5453.617.

Currie, J.C., M. Lengaigne, J. Vialard, D.M. Kaplan, …, O. Maury, 2013: Indian Ocean Dipole and El Nin?o/Southern Oscillation impacts on regional chlorophyll anomalies in the Indian Ocean. *Biogeosciences*, **10**, 6677-6698, doi:10.5194/bg-10-6677-2013.

D'Arrigo, R., and R. Wilson, 2008: El Nino and Indian Ocean influences on Indonesian drought: implications for forecasting rainfall and crop productivity. *International Journal of Climatology*, **28**, 611-616.

D'Arrigo, R., N. Abram, C. Ummenhofer, J. Palmer, and M. Mudelsee, 2011: Reconstructed streamflow for Citarum River, Java, Indonesia: linkages to tropical climate dynamics. *Climate Dyn.*, **36**, 451-462.

Dai A. et al., 2009: Changes in Continental Freshwater Discharge from 1948 to 2004. J. *Climate*, **22**, 2773-2792.

de Boisséson, E., Balmaseda, M.A., Vitart, F., and K.Mogensen, 2012: Impact of the sea surface temperature forcing on hindcasts of Madden-Julian Oscillation events using the ECMWF model, *Ocean Sci.*, **8**, 1071-1084, https://doi.org/10.5194/os-8-1071-2012.

de Moel, H., G.M. Ganssen, F.J.C. Peeters, S.J.A. Jung, …, R.E. Zeebe, 2009: Planktonic foraminiferal shell thinniing in the Arabian Sea due to anthropogenic ocean acidification?. *Biogeosciences*, **6**, 1917-25.

deCastro, M., M.C. Sousa, F. Santos, J.M. Dias, and M. Gómez-Gesteira, 2016: How will Somali coastal upwelling evolve under future warming scenarios? *Sci. Rep.*, **6**, 30137, doi:10.1038 srep30137.

Deckker, P., 2016: The Indo-Pacific warm pool: critical to world oceanography and world climate. *Geoscience Letters*, **3:20**, doi: 10.1186/s40562-016-0054-3.

Dee, D.P., and Co-authors, 2011: The ERA-Interim reanalysis: Configuration and performance of the data assimilation system. *Quart. J. Roy. Meteor. Soc.*, **137**, 553-597, doi:10.1002/qj.828.

Deepa, J. S.; C. Gnanaseelan; R. Kakatkar; A. Parekh; J. S. Chowdary, 2018: The interannual sea level variability in the Indian Ocean as simulated by an Ocean General Circulation Model. *International Journal of Climatology*, **38 (3)**, 1132-1144.

Del Sole, T., and J. Shukla., 2002: Linear prediction of Indian monsoon rainfall. *J. Climate*, **15**, 3645-3658.

DeMaria, M., M. Mainelli, and L.K. Shay, 2005: Further improvements to the Statistical Hurricane Intensity Prediction Scheme (SHIPS). *Wea. Forecasting*, **20**, 531-543.

DeMaria, M., C.R. Sampson, J.A. Knaff, and K.D. Musgrave, 2013: Is Tropical Cyclone Intensity

Guidance Improving? *Bull. Amer. Meteor. Soc.*, 130725143726000, doi:10.1175/BAMS-D-12-00240.1.

DeMott, C.A., N.P. Klingaman, and S.J. Woolnough 2015: Atmosphere-ocean coupled processes in the Madden-Julian oscillation, *Rev. Geophys.*, **53**, 1099-1154, doi:10.1002/2014RG000478.

Depczynski, M. et al., 2013: Bleaching, coral mortality and subsequent survivorship on a West Australian fringing reef. *Coral Reefs*, **32**, 233-238.

Desbruyères, D., E.L. McDonagh, B.A. King, and V. Thierry, 2017: Global and full-depth ocean temperature trends during the early 21st century from Argo and repeat hydrography. *J. Climate*, **30(6)**, 1985-1997, 10.1175/JCLI-D-16-0396.1

Deser, C., M.A. Alexander, S.P. Xie, and A.S. Phillips, 2010: Sea surface temperature variability: Patterns and mechanisms. *Annual review of marine Science*, **2**, 115-143.

Doi, T., S.K. Behera, and T. Yamagata, 2013: Predictability of Ningaloo Nino/Nina. *Sci. Rep.*, **3**, 2892, doi:10.1038/srep02892.

Doi, T., S.K. Behera, and T. Yamagata, 2016: Improved seasonal prediction using the SINTEX-F2 coupled model. *J. Adv. Modeling Earth Sys.*, **8**, 1847-1867.

Doi, T., A. Storto, S.K. Behera, A. Navarra, and T. Yamagata, 2017: Improved prediction of the Indian Ocean Dipole Mode by use of subsurface ocean observations. *J. Climate*, **30**, 7953-7970.

Dombrowsky, E., L. Bertino, and G.B. Brassington, et al., 2009: GODAE systems in operation. *Oceanography*, **22(3)**, 80-95, doi:http://dx.doi.org/10.5670/oceanog.2009.68.

Domingues, C., M. Maltrud, S. Wijffels, J. Church, and M. Tomczak, 2007: Simulated Lagrangian pathways between the Leeuwin Current System and the upper-ocean circulation of the southeast Indian Ocean. *Deep-Sea Res. Part II*, **54**, 797-817, doi:10.1016/j.dsr2.2006.10.003.

Domingues, C. M., J.A. Church, N.J. White, P.J. Gleckler, …, J.R. Dunn, 2008: Improved estimates of upper-ocean warming and multi-decadal sea-level rise. *Nature*, **453**, 1090-1095.

Doney, S.C., 2010: The growing human footprint on coastal and open-ocean biogeochemistry. *Science*, **328**, 1512-16.

Doney, S.C. et al., 2012: Climate change impacts on marine ecosystems. *Ann. Rev. Mar. Sci.*, **4**, doi:10.1146/annurev-marine-041911-111611.

Dong, L., T. Zhou, and X. Chen, 2014: Changes of Pacific decadal variability in the twentieth century driven by internal variability, greenhouse gases, and aerosols. *Geophys. Res. Lett.*, **41**, 8570-8577.

Dong, L., and T. Zhou, 2014a: The Indian Ocean Sea Surface Temperature Warming Simulated by CMIP5 Models during the 20th Century: Competing Forcing Roles of GHGs and Anthropogenic Aerosols. *J. Climate*, **27**, 3348-3362.

Dong L., T. Zhou, B. Wu, 2014b: Indian Ocean warming during 1958-2004 simulated by a climate system model and its mechanism. *Climate Dyn.*, **42 (1-2)**, 203-217.

Dong, L., and M.J. McPhaden, 2016a: Interhemispheric SST gradient trends in the Indian Ocean prior to and during the recent global warming hiatus. *J. Climate*, doi: http://dx.doi.org/10.1175/JCLI-D-16-0130.1

Dong L., T. Zhou, A. Dai, F. Song, …, X. Chen, 2016b: The Footprint of the Inter-decadal Pacific Oscillation in Indian Ocean Sea Surface Temperatures. *Scientific Reports*,**6**:21251, doi:10.1038/srep21251.

Dong, L., and M.J. McPhaden, 2017: Why Has the Relationship between Indian and Pacific Ocean Decadal Variability Changed in Recent Decades? *J. Climate 30*, 1971-1983.

Donguy, J-R., and G. Meyers, 1995: Observations of Geostrophic transport in the tropical Indian Ocean. *Deep-Sea Res. Part I Oceanographic Research Papers*, **42(6)**, 1007-1028, doi: 10.1016/0967-0637(95)00047-A.

Donohue, K.A., D.R. Watts, K.L. Tracey, A.D. Greene and M. Kennelly, 2010: Mapping circulation in the Kuroshio Extension with an array of Current and Pressure recording Inverted Echo Sounders. *J. Atmos. Oceanic Technol.*, **27**, 507-527, doi:10.1175/2009JTECHO686.1.

Donohue, K.A., K.L. Tracey, D.R. Watts, M.P. Chidichimo, and T.K. Chereskin, 2016: Mean Antarctic Circumpolar Current transport measured in Drake Passage. *Geophys. Res. Lett.*, **43(22)**, 11,760-11,767, doi: 10.1002/2016GL070319. l.

Downes, S. M., N. L. Bindoff, and S. R. Rintoul, 2009: Impacts of Climate Change on the Subduction of Mode and Intermediate Water Masses in the Southern Ocean. *J. Climate*, **22**, 3289-3302.

Drushka, K., J. Sprintall, and S. T. Gille, 2012: *In situ* observations of Madden-Julian oscillation mixed layer dynamics in the Indian and western Pacific Oceans. *J. Climate*, **25**, 2306-2328?2.

Du Y., and S.P. Xie, 2008: Role of atmospheric adjustments in the tropical Indian Ocean warming during the 20th century in climate models. *Geophys. Res. Lett.*, **35 (8)**.

Du, Y., S.-P. Xie, G. Huang, and K. Hu, 2009: Role of Air-Sea Interaction in the Long Persistence of El Nino-Induced North Indian Ocean Warming*. *J. Climate*, **22**, 2023-2038, doi:10.1175/2008JCLI2590.1.

Du, Y., S.-P. Xie, Y.-L. Yang, X.-T. Zheng, …, G. Huang, 2013: Indian Ocean variability in the CMIP5 multimodel ensemble: The basin mode. *J. Climate*, **26**, 7240-7266.

Du, Y., Y. Zhang, M. Feng, T. Wang, …, S. Wijffels, 2015: Decadal trends of the upper ocean salinity in the tropical Indo-Pacific since mid-1990s. *Scientific Reports*, **5**, doi:10.1038/srep16050.

Dufois, F., N.J. Hardman-Mountford, M. Fernandes, B. Wojtasiewicz, …, R. Toresen, 2017: Observational insights into chlorophyll distributions of subtropical South Indian Ocean eddies, *Geophys. Res. Lett.*, **44(7)**, 3255-3264, doi:10.1002/2016gl072371.

Dunne, R.P., S.M. Barbosa, P.L. Woodworth, 2012: Contemporary sea level in the Chagos Archipelago, central Indian Ocean. *Global and Planetary Change*, 82-83, 25-37.

Durack, P.J., and S.E. Wijffels, 2010: Fifty-year trends in global ocean salinities and their relationship to broad-scale warming. *J. Climate*, **23 (16)**, 4342-4362.

Durack, P. J., S. E. Wijffels, and R. J. Matear, 2012: Ocean Salinities Reveal Strong Global Water Cycle Intensification During 1950 to 2000. *Science*, **336**, 455-458.

Durack, P. J., S. E. Wijffels, and P. J. Gleckler, 2014a: Long-term sea-level change revisited: the role of salinity. *Environ. Res. Lett.*, **9(11)**, 114017.

Durack, P.J., P.J. Gleckler, F.W. Landerer, and K.E. Taylor, 2014b: Quantifying underestimates of long-term upper-ocean warming. *Nature Climate Change*, **4(11)**, 999-1005.

Durack, P. J., T. Lee, N. T. Vinogradova, and D. Stammer, 2016: Keeping the lights on for global ocean salinity observation. *Nature Climate Change*, **6(3)**, 228-231.

Durand, F. et al., 2004: Impact of temperature inversions on SST evolution in the South-Eastern Arabian Sea during the pre-summer monsoon season. *Geophys. Res. Lett.*, **31**, L01305, doi:10.1029/2003GL018906

Duvel, J. P., R. Roca, and J. Vialard, 2004: Ocean mixed layer temperature variations induced by intraseasonal convective perturbations over the Indian Ocean. *J. Atmos. Sci.*, **61**, 1004-1022.

Duvel J.P., and J. Vialard, 2007: Indo-Pacific sea surface temperature perturbations associated with intraseasonal oscillations of tropical convection. *J. Climate* **20**, 3056-3082.

Ebuchi, N., H.C. Graber, and M.J. Caruso, 2012: Evaluation of Wind Vectors Observed by QuikSCAT/SeaWinds Using Ocean Buoy Data. *J. Atmos. Oceanic Tech.*, doi:https://doi.org/10.1175/1520-0426(2002)019<2049:EOWVOB>2.0.CO;2.

Edward, J. K., and Co-authors, 2018: Coral mortality in the Gulf of Mannar, southeastern India, due to bleaching caused by elevated sea temperature in 2016. *Current Science*.

Eigenheer, A., and D. Quadfasel, 2000: Seasonal variability of the Bay of Bengal circulation inferred from TOPEX/POSEIDON altimetry. *J. Geophys. Res.*, **105**, 3243-3252.

Ekau, W., H. Auel, H.O. Portner, and D. Gilbert, 2010: Impacts of hypoxia on the structure and processes in pelagic communities (zooplankton, macro-invertebrates and fish). *Biogeosciences*, **7**, 1669-1699: 10.5194/bg-7-1669-2010.

Elipot, Shane, and Lisa M. Beal, 2015: Characteristics, energetics, and origins of Agulhas Current meanders and their limited influence on ring shedding. *J. Phys. Oceanogr.*, **45.9**, 2294-2314.

Elsner, J.B., J.P. Kossin, and T.H. Jagger, 2008: The increasing intensity of the strongest tropical cyclones. *Nature*, **455**, 92-95, doi:10.1038/nature07234.

Eppley, R.W., 1972: Temperature and phytoplankton growth in the sea. *Fish. Bull.*, **70**, 1063-

1085.

Eriksen C.C., T.J. Osse, R.D. Light, T. Wen, T.W. Lehman, et al., 2001: Seaglider: a long-range autonomous underwater vehicle for oceanographic research. *IEEE J. Ocean. Eng.*, **26**, 424-36.

Evan, A.T., and S.J. Camargo, 2011: A Climatology of Arabian Sea Cyclonic Storms. *J. Climate*, **24**, 140-158, doi:10.1175/2010JCLI3611.1.

FAO, 2004: The State of the World Fisheries and Aquaculture. In Food and Agriculture Organization of the United Nations. Rome, Italy.

Feely, R.A., C.L. Sabine, J.M. Hernandez-Ayon, D. Ianson, and B. Hales, 2008: Evidence for upwelling of corrosive ”acidified” water onto the continental shelf. *Science*, **320**, 1490-92.

Feely, R.A., S.C. Doney, and S.R. Cooley, 2009: Ocean acidification: Present conditions and future changes in a high-CO_2 world, *Oceanography*, **22**, 36-47.

Felton, C.S., B. Subrahmanyam, and V.S.N. Murty, 2013: ENSO-Modulated Cyclogenesis over the Bay of Bengal*. *J. Climate*, **26**, 9806-9818, doi:10.1175/JCLI-D-13-00134.1.

Feng, M., G. Meyers, A. Pearce, and S. Wijffels, 2003: Annual and Interannual Variations of the Leeuwin Current at 32°S. *J. Geophys. Res.*, **108(11)**, 33-55.

Feng, M., Y. Li, and G. Meyers, 2004: Multidecadal variations of Fremantle sea level: Footprint of climate variability in the tropical Pacific, *Geophys. Res. Lett.*, **31**, L16302, doi:10.1029/2004 GL019947.

Feng, M., M.J. McPhaden, and T. Lee, 2010: Decadal variability of the Pacific subtropical cells and their influence on the southeast Indian Ocean. *Geophys. Res. Lett.*, **37**, L09606, doi:10.1029/2010GL042796.

Feng, M., C. Boning, A. Biastoch, E. Behrens, …, Y. Masumoto, 2011: The reversal of the multi-decadal trends of the equatorial Pacific easterly winds, and the Indonesian Throughflow and Leeuwin Current transports. *Geophys. Res. Lett.*, **38**, L11604, doi:10.1029/2011GL047291.

Feng M., M.J. McPhaden, S. Xie, and J. Hafner, 2013: La Nina forces unprecedented Leeuwin Current warming in 2011. *Sci Rep*, **3**, doi:10.1038/srep01277.

Feng, M., H.H. Hendon, S.-P. Xie, A.G. Marshall, …, A. Pearce, 2015a: Decadal increase in Ningaloo Nino since the late 1990s, *Geophys. Res. Lett.*, **42**, doi:10.1002/2014GL062509.

Feng, M., A. Marshall, and H.H. Hendon, 2015b: A review of progress in understanding the Ningaloo Niño. *CLIVAR Exchanges*, **68**, 4-6.

Feng, M., J. Benthuysen, N. Zhang, and D. Slawinski, 2015c: Freshening anomalies in the Indonesian Throughflow and impacts on the Leeuwin Current during 2010-2011. *Geophys. Res. Lett.*, **42**, 8555-8562.

Feng, M., X. Zhang, B. Sloyan, and M. Chamberlain, 2017: Contribution of the deep ocean to the centennial changes of the Indonesian Throughflow, *Geophys. Res. Lett.*, **44(6)**,2859-

2867. doi:10.1002/2017GL072577.

Feng, M., N. Zhang, Q. Liu, and S. Wijffels, 2018: The Indonesian Throughflow, its variability and centennial change. *Geoscience Letters*, **5:3**, doi:https://doi.org/10.1186/s40562-018-0102-2.

Ffield, A., and A.L. Gordon,1996: Tidal mixing signatures in the Indonesian seas, *J. Phys. Oceanogr.*, **26**, 1924-1937.

Ffield, A. and R. Robertson, 2008: Temperature finestructure in the Indonesian Seas. *J. Geophys. Res.*, **113**, C09009, doi:10.1029/2006JC003864.

Foltz, G.R., J. Vialard, P. Kumar, and M.J. McPhaden, 2010: Seasonal mixed layer heat balance of the southwestern tropical Indian Ocean. *J. Climate*, **23**, 947-965. https://doi.org/10.1175/2009JCLI3268.1.

Fonteneau, A., V. Lucas, E. Tewkai, A. Delgado, and H. Demarcq, 2008: Mesoscale exploitation of a major tuna concentration in the Indian Ocean. *Aquatic Living Resources*, **21**, 109-21.

Fore, A.G., S.H. Yueh, and W. Tang, et al., 2016: Combined Active/Passive Retrievals of Ocean Vector Wind and Sea Surface Salinity with SMAP. *IEEE Transactions on Geoscience and Remote Sensing*, **54**,12, doi:10.1109/TGRS.2016.2601486.

Forget, G., J.-M. Campin, P. Heimbach, C. Hill, …, C. Wunsch, 2015: ECCO version 4: an integrated framework for non-linear inverse modeling and global ocean state estimation. *Geosci. Model Dev.*, **8**, 3071-3104.

Fratantoni, D.M., J.K. O'Brien, C. Flagg, and T. Rossby, 2017: AXIS—An Autonomous Expendable Instrument System. *J. Atmos. Oceanic Technol.*, **34**, 2673-2682, https://doi.org/10.1175/JTECH-D-17-0054.1.100

Freitag, H. P., C. Ning, P. Berk, D. Dougherty, …, D. Zimmerman, 2016: Atlas, T-Flex, Bailong Meteorological Sensor Comparison Test Report. *NOAA Tech. Memo. OAR PMEL-148, NOAA/Pacific Marine Environmental Laboratory, Seattle, WA*, **31**, doi:10.7289/V57942PP.

Fréon, P., J. C. Coetzee, C.D. Van der Lingen, A.D. Connell, …, L. Hutchings, 2010: A review and tests of hypotheses about causes of the KwaZulu-Natal sardine run. *African Journal of Marine Science*, **32(2)**, 449-479.

Fu X., B. Wang, T. Li, and J.P. McCreary, 2003: Coupling between north- ward-propagating, intraseasonal oscillations and sea surface tem- perature in the Indian Ocean. *J Atmos Sci* **60**, 1733-1753.

Fu, L., and R. Smith, 1996: Global ocean circulation from satellite altimetry and high-resolution computer simulation. *Bull. Amer. Meteor. Soc.*, **77**, 2625-2636.

Fu, L, 2007: Intraseasonal Variability of the Equatorial Indian Ocean Observed from Sea Surface Height, Wind, and Temperature Data. *J. Phys. Oceanogr.*, **37**, 188-202. doi: 10.1175/JPO3006.1.

Fu, X., W. Wang, J.-Y. Lee, B. Wang, …, S. Weaver, 2015: Distinctive Roles of Air-Sea Cou-

pling on Different MJO Events: A New Perspective Revealed from the DYNAMO/CINDY Field Campaign. *Mon. Wea. Rev.*, **143 (3)**, 794-812.

Fujii, Y., et al., 2015: Evaluation of the tropical Pacific observing system from the ocean data assimilation perspective. *Quart. J. Roy. Meteor. Soc.*, doi: 10.1002/qj.2579. **Oct. 2015.**

Fukumori, I., and O. Wang, 2013: Origins of heat and freshwater anomalies underlying regional decadal sea level trends, *Geophys. Res. Lett.*, **40**, 563-567, doi:10.1002/grl.50164

Funk, C., M. D. Dettinger, J. C. Michaelsen, J. P. Verdin, …, A. Hoell, 2008: Warming of the Indian Ocean threatens eastern and southern African food security but could be mitigated by agricultural development. *Proceedings of the National Academy of Sciences*, **105(32)**, 11081-11086.

Furue, R., J.P. McCreary, J. Benthuysen, H. Phillips, and N. Bindoff, 2013: Dynamics of the Leeuwin Current: Part 1. Coastal flows in an inviscid, variable-density, layer model. *Dyn. Atmos. Oceans*, **63**, 24-59.

Furue, R., K. Guerreiro, H.E. Phillips, J. P. McCreary and N. Bindoff, 2017: On the Leeuwin Current System and its linkage to zonal flows in the South Indian Ocean as inferred from a gridded hydrography. *J. Phys. Oceanogr.* **47**, 583-602. doi: 10.1175/JPO-D-16-0170.1

Gadgil, S., P.N. Vinayachandran, P.A. Francis, S. Gadgil, 2004: Extremes of the Indian summer monsoon rainfall, ENSO and equatorial Indian Ocean oscillation. *Geophys. Res. Lett.*, **31**, L12213.

Ganachaud, A., and C. Wunsch, 2000: Improved estimates of global ocean circulation, heat transport and mixing from hydrographic data. *Nature*, **408 (6811)**, 453-457.

Gasparin F., D. Roemmich, J. Gilson, B. Cornuelle, 2015: Assessment of the upper-ocean observing system in the equatorial Pacific: The role of Argo in resolving intraseasonal to interannual variability. *J. Atmos. Oceanic Technol.*, **32 (9)**, 1668-1688.

Gastineau, G., A.R. Friedman, M. Khodri, et al., 2018: Global ocean heat content redistribution during the 1998-2012 Interdecadal Pacific Oscillation negative phase. *Climate Dyn..*, doi:https://doi.org/10.1007/s00382-018-4387-9.

Gattuso, J.-P., and L. Hansson, 2011: Ocean Acidification. *Oxford University Press: Oxford, UK.*

Gaube, P., D.B. Chelton, P.G. Strutton, and M.J. Behrenfeld, 2013: Satellite observations of chlorophyll, phytoplankton biomass, and Ekman pumping in nonlinear mesoscale eddies. *J. Geophys. Res.: Oceans*, **118(12)**, 6349-6370. doi:10.1002/2013JC009027.

Ge, X., W. Wang, A. Kumar and Y. Zhang, 2017: Importance of the vertical resolution in simulating SST diurnal and intraseasonal variability in an ocean general circulation model. *J. Climate*, **30**, 3963-3978.

Ghofar, A., 2005: Marine fisheries management plan in Indonesia a case study of the Bali Strait fishery. *Indonesian Journal of Marine Sciences*, **10**, 177-84.

Giannini A., R. Saravanan, and P. Chang, 2003: Oceanic forcing of Sahel rainfall on interannual to interdecadal time scales. *Science*, **302**, 1027-1030.

Gille, S.T., S.G.L. Smith, and M. Lee, 2003: Measuring the sea breeze from QuikSCAT scatterometry. *Geophys. Res. Lett.*, *30*, doi:10.1029/2002gl016230.

Gille, S.T., 2008: Decadal-scale temperature trends in the Southern Hemisphere ocean. *J. Climate*, **21(18)**, 4749-4765.

Girish kumar, M.S., M. Ravichandran, and W. Han, 2013: Observed intraseasonal thermocline variability in the Bay of Bengal. *JGR-Oceans*, **118**, 3336-3349, doi:10.1002/jgrc.20245.

Gleckler, P.J., B.D. Santer, C.M. Domingues, D.W. Pierce, …, P.M. Caldwell, 2012: Human-induced global ocean warming on multidecadal timescales. *Nature Climate Change*, **2(7)**, 524-529.

Gnanaseelan C., M.K. Roxy, and A. Deshpande, 2017: Variability and Trends of Sea Surface Temperature and Circulation in the Indian Ocean. In: Rajeevan MN, Nayak S (eds) Observed Climate Variability and Change over the Indian Region. *Springer Singapore, Singapore*, 165-179. doi:10.1007/978-981-10-2531-0_10.

Gomes, H.R., J.I. Goes, S.G.P. Matondkar, E.J. Buskey, …, P. Thoppil, 2014: Massive outbreaks of Noctiluca scintillans blooms in the Arabian Sea due to spread of hypoxia. Nature Communications 5m 4862.

Good, S. A., M. J. Martin and N. A. Rayner, 2013: EN4: quality controlled ocean temperature and salinity profiles and monthly objective analyses with uncertainty estimates. *J. Geophys. Res.: Oceans*, **118**, 6704-6716, doi:10.1002/2013JC009067

Gopalakrishna, V. V., R. R. Rao, K. Nisha, M. S. Girishkumar, …, S. Rajesh, 2008: Observed anomalous upwelling in the Lakshadweep Sea during the summer monsoon season of 2005. *J. Geophys. Res.*, doi:10.1029/2007JC004240.

Gordon, A. L., J. Sprintall, H. M. Van Aken, D. Susanto, …, S. Wirasantosa, 2010: The Indonesian throughflow during 2004-2006 as observed by the INSTANT program. *Dyn. Atmos. Oceans*, **50**, 115-128.

Goswami, B.N., 2011: South Asian Summer Monsoon. In: Lau WKM, Waliser DE (eds) Intraseasonal variability of the atmosphere- ocean climate system, *2nd edn. Springer, Heidelberg*.

Goswami, B.N., and R.S. Ajaya Mohan, 2001: Intraseasonal oscillations and interannual variability of the Indian summer monsoon. *J. Climate*, **14(6)**, 1180-1198.

Goswami B.N., R.S. Ajaya Mohan, P.K. Xavier, and D. Sengupta, 2003: Clus- tering of synoptic activity by Indian summer monsoon intrasea- sonal oscillations. *Geophys Res Lett*, **30(8)**, 1431

Goswami, B.N., 2005: South Asian monsoon. In Intraseasonal variability in the atmosphere-ocean climate system. *Springer Berlin Heidelberg*, 19-61.

Graham, N.A.J., S.K. Wilson, S. Jennings, N.V.C. Polunin, …, T.M. Daw, 2007: Lag effects

in the impacts of mass coral bleaching on coral reef fish, fisheries, and ecosystems. *Conservation Biology*, **21**, 1291-300.

Grodsky, S.A., J.A. Carton, and R. Murtugudde, 2001: Anomalous surface currents in the tropical Indian Ocean. *Geophys. Res. Lett.*, **28 (22)**, 4207-4210, doi:10.1029/2001GL013592.

Gruber, N., 2011: Warming up, turning sour, losing breath: ocean biogeochemistry under global change. *Philosophical Transactions of the Royal Society a-Mathematical Physical and Engineering Sciences*, **369**, 1980-1996, doi: 10.1098/rsta.2011.0003.

Grunseich, G., B. Subrahmanyam, and B. Wang, 2013: The Madden-Julian oscillation detected in Aquarius salinity observations. *Geophys. Res. Lett.*, **40**, 5461-5466, doi:10.1002/2013GL 058173.

Guan, B, T. Lee, and D. Waliser, et al., 2014: Aquarius Surface Salinity and the Madden-Julian Oscillation: the Role of Salinity in Surface Layer Density and Potential Energy. *Geophys. Res. Lett.*, **41**, doi:10.1002/2014GL059704.

Gudka, M., D. Obura, J. Mwaura, S. Porter, and S. Yahya, 2018: Impact of the 3rd global coral bleaching event on the Western Indian Ocean in 2016. 1 .

Guemas, V., S. Corti, J. Garcia-Serrano, F.J. Doblas-Reyes, …, L. Magnusson, 2013: The Indian Ocean: The region of highest skill worldwide in decadal climate prediction. *J. Climate*, **26**, 726-739.

Halkides, D.J., and T. Lee, 2009: Mechanisms controlling seasonal-to-interannual mixed layer temperature variability in the southeastern tropical Indian Ocean. *J. Geophys. Res.*, **114**, C02012, doi:10.1029/2008JC004949.

Halkides, D.J., D.E. Waliser, T. Lee, D. Menemenlis, and B. Guan, 2015: Quantifying the processing controlling intraseasonal mixed-layer temperature variability in the tropical Indian Ocean. *J. Geophys. Res. Oceans*, **120**, 692-715, doi:10.1002/2014JC010139.

Hamlington, B.D., M.W. Strassburg, R.R. Leben, W. Han, …, K.Y. Kim, 2014: Uncovering an anthropogenic sea-level rise signal in the Pacific Ocean. *Nature Climate Change*, **4(9)**, 782-785.

Han, W., J.P. McCreary, D.L.T. Anderson, and A.J. Mariano., 1999: Dynamics of the eastern surface jets in the equatorial Indian Ocean. *J. Phys. Oceanogr.*, **29**, 2191-2209.

Han, W., D.M. Lawrence, and P.J. Webster, 2001: Dynamical response of equatorial Indian Ocean to intraseasonal winds: zonal flow. *Geophys. Res. Lett.*, **28**, 4215-4218. doi: 10.1029 /2001GL013701.

Han, W., and P.J. Webster, 2002: Forcing Mechanisms of Sea-Level Interannual Variability in the Bay of Bengal, *J. Phys. Oceanogr.*, **32**, 216-239.

Han, W., 2005: Origins and dynamics of the 90-day and 30-60-day variations in the equatorial Indian Ocean. *J. Phys. Oceanogr.*, **35**, 708-728. https://doi.org/10.1175/JPO2725.1.10

Han, W., T. Shinoda, L-L. Fu, and J. McCreary, 2006: Impact of atmospheric intraseasonal

oscillations on the Indian Ocean dipole. *J. Phys. Oceanogr.*, **36**, 670-690.

Han, W., D. Yuan, W. T. Liu and D. J. Halkides, 2007: Intraseasonal variability of the Indian Ocean sea surface temperature during boreal winter: Madden - Julian Oscillation verus submonthly forcing and processes. *J. Geophys. Res.*, **112**, C04001, doi:10.1029/2006JC003791.2

Han, W., G.A. Meehl, B. Rajagopalan, J. Fasullo, A. Hu, …, S. Yeager, 2010: Patterns of Indian Ocean Sea Level Change in a Warming Climate. *Nature Geoscience*, **3**, 546-550.

Han, W., J. Vialard, M.J. McPhaden, T. Lee, …, W.P. De Ruijter, 2014a: Indian Ocean decadal variability: A review. *Bull. Amer. Meteor. Soc.*, **95**, 1679-1703.

Han, W., G.A. Meehl, A. Hu, M.A. Alexander, …, X.W. Quan, 2014b: Intensification of decadal and multi-decadal sea level variability in the western tropical Pacific during recent decades. *Climate Dyn.*, **43**, 1357-1379.

Han, W., G. Meehl, D. Stammer, A. Hu, …, P. Thompson, 2017: Spatial Patterns of Sea Level Variability Associated with Natural Internal Climate Modes. *Surveys in Geophysics*, **38**, 217-250.

Han W., D. Stammer, G.A. Meehl, A. Hu, …, L. Zhang, 2018: Multi-Decadal Trend and Decadal Variability of the Regional Sea Level over the Indian Ocean since the 1960s: Roles of Climate Modes and External Forcing, *Climate*, **6(2)**, 51, doi: https://doi.org/10.3390/cli6020051

Hatayama, T., 2004: Transformation of the Indonesian Throughflow water by vertical mixing and its relation to tidally generated internal waves. *J. Oceanography*, **60 (3)**, 569-585.

Helm, K.P., N. L. Bindoff, and J.A. Church, 2010: Changes in the global hydrological-cycle inferred from ocean salinity. *Geophys. Res. Lett.*, **37**, L18701.

Hendon H.H., and B. Liebmann, 1990: The intraseasonal (30-50 day) oscillation of the Australian summer monsoon. *J Atmos Sci*, **47**, 2909-2924.

Hendon, H.H., and B. Liebmann, 1990: A composite study of onset of the Australian monsoon. *J. Atmos. Sci.*, **47**, 2227-2240.

Hendon, H.H., 2003: Indonesian rainfall variability: Impacts of ENSO and local air-sea interaction. *J. Climate*, **16**, 1775-1790.

Hermes, J. and C.J.C. Reason, 2008: Annual cycle of the South Indian Ocean (Seychelles-Chagos) thermocline ridge in a regional ocean model. *J. Geophys. Res.*, **113**, C04035. doi:10.1029/2007JC004363.

Hermes, J.C. and C.J.C. Reason, 2009: The sensitivity of the Seychelles-Chagos thermocline ridge to large-scale wind anomalies. *ICES Journal of Marine Science* , **66(7)**, 1455-1466.

Hernández-Guerra, A., and L.D. Talley, 2016: Meridional overturning transports at 30 S in the Indian and Pacific Oceans in 2002-2003 and 2009. *Progress in Oceanography*, **146**, 89-120.

Heron, S.F., J.A. Maynard, R. van Hooidonk, and C.M. Eakin, 2016: Warming Trends and Bleaching Stress of the World's Coral Reefs 1985-2012. *Sci Rep*, **6**, 38402, doi:10.1038/srep

38402.2,

Hobday, A.J., and Co-authors, 2016: A hierarchical approach to defining marine heatwaves. Progress in Oceanography, 141, 227-238, doi:10.1016/j.pocean.2015.12.014.

Hoegh-Guldberg, O., P.J. Mumby, A.J. Hooten, R.S. Steneck, …, M.E. Hatziolos, 2007: Coral reefs under rapid climate change and oceand acidification. *Science*, **318**, 1737-42.

Hoerling, M., J.W. Hurrell, T. Xu, G. Bates, and A. Phillips, 2004: Twentieth century north Atlantic climate change. Part II: understanding the effect of Indian Ocean warming. *Climate Dyn.*, **23**, 391-405.

Hoerling, M., J. Eischeid, J. Perlwitz, X. Quan, …, P. Pegion, 2012: On the Increased Frequency of Mediterranean Drought. *J. Climate*, **25**, 2146-2161.

Holgate, S.J., A. Matthews, P.L. Woodworth, L.J. Rickards, …, J. Pugh, 2013: New data systems and products at the Permanent Service for Mean Sea Level. *Journal of Coastal Research*, **29**, 493-504, doi:10.2112/JCOASTRES-D-12-00175.1.

Hood, R., W. Yu, Y. Masumoto, J. Wiggert, …, L.E. Beckley, 2012: SIBER and IOP: Joint activities and science results. *CLIVAR Exchanges*, **17 (1)**, 17-20, National Oceanography Centre, Southampton, UK.

Hood, R.R., H.W. Bange, L. Beal, L.E. Beckley, …, W. Yu. 2015: Science Plan of the Second International Indian Ocean Expedition (IIOE-2): A Basin-Wide Research Program. *Scientific Committee on Oceanic Research, Newark, Delaware, USA*.

Hood, R.R., L.E. Beckley, and J.D. Wiggert, 2017: Biogeochemical and ecological impacts of boundary currents in the Indian Ocean. *Prog. Ocean.*, **156**, 290-325: http://dx.doi.org/10.1016/j.pocean.2017.04.011.

Hood, R. R., V. J. Coles, A. J. Sutton, and M. J. McPhaden, 2019: Physical forcing of air-sea carbon flux in the Bay of Bengal. *Geophys. Res. Lett.*

Horányi, A., C. Cardinali, and L. Centurioni, 2017: The global numerical weather prediction impact of mean-sea-level pressure observations from drifting buoys. *Quart. J. Roy. Meteor. Soc.*, **143(703)**, 974-985, doi:10.1002/qj.2981

Horii, T., H. Hase, I. Ueki, and Y. Masumoto, 2008: Oceanic precondition and evolution of the 2006 Indian Ocean Dipole. *Geophys. Res. Lett.*, **35**, L03607, doi:10.1029/2007GL032464.

Horii, T., I. Ueki, and K. Ando, 2018: Coastal upwelling events along the southern coast of Java during the 2008 positive Indian Ocean Dipole. *J. Oceanography*, **74**, 499-508, doi:10.1007/s10872-018-0475-z.

Hormann, V., L.R. Centurioni, A. Mahadevan, S. Essink, …, B. P. Kumar, 2016: Variability of near-surface circulation and sea surface salinity observed from Lagrangian drifters in the northern Bay of Bengal during the waning 2015 southwest monsoon. *Oceanography*, **29 (2)**,124-133, http://dx.doi.org/10.5670/oceanog.2016.45. 1

Hosoda, S., T. Suga, N. Shikama, and K. Mizuno, 2009: Global surface layer salinity change

detected by Argo and its implication for hydrological cycle intensification. *Journal of Oceanography*, **65(4)**, 579-586.

Howden, S.D., and R. Murtugudde, 2001: Effects of river inputs into the Bay of Bengal. *J. Geophys. Res.*, **106(C9)**, 19825-19843. doi:10.1029/2000JC000656

Hoyos, C.D., and P.J. Webster, 2007: The role of intraseasonal variability in the nature of Asian monsoon precipitation. *J. Climate*, **20**, 4402-4424, https://doi.org/10.1175/JCLI4252.1. 1

Hu, S., and J. Sprintall, 2016: Interannual variability in the Indonesian Throughflow: the salinity effect. *J. Geophys. Res.*, **21**, 2596-2615.

Hu, S., and J. Sprintall, 2017: Observed strengthening of interbasin exchange via the Indonesian seas due to rainfall intensification, *Geophys. Res. Lett.*, **44(3)**, 1448-1456.

Huang, B., Y. Xue, and D. W. Behringer, 2008: Impacts of Argo salinity in NCEP Global Ocean Data Assimilation System: The tropical Indian Ocean. *J. Geophys. Res.*, **113**, C08002, doi:10.1029/2007JC004388.

Hui, C., and X. T. Zheng, 2018: Uncertainty in Indian Ocean Dipole response to global warming: the role of internal variability. *Climate Dyn.*, 1-15.

Hutchins, D. A., F.-X. Fu, Y. Zhang, M. E. Warner, …, M. R. Mulholland, 2007: CO_2 control of Trichodesmium N2 fixation, photosynthesis, growth rates, and elemental ratios: Implications for past, present, and future ocean biogeography. *Limnology and Oceanography*, **52**, 1293-304.

Ihara C., Y. Kushnir, and M.A. Cane, 2008: Warming trend of the Indian Ocean SST and Indian Ocean dipole from 1880 to 2004. *J. Climate*, **21 (10)**, 2035-2046, doi:Doi 10.1175/2007jcli1945.1

Inness, P.M., and J.M. Slingo, 2006: The interaction of the Madden-Julian Oscillation with the Maritime Continent in a GCM, *Quart. J. Roy. Meteor. Soc.*, **132 (618)**, 1645-1667.

International CLIVAR Project Office, 2006: Understanding the Role of the Indian Ocean in the Climate System - Implementation Plan for Sustained Observations. *January. International CLIVAR Project Office, CLIVAR Publication Series No.100*.

IOC, 2012: The Global Sea Level Observing System (GLOSS) Implementation Plan - 2012.*UNESCO/Intergovernmental Oceanographic Commission*, 37pp. (IOC Technical Series No. 100). doi:http://unesdoc.unesco.org/images/0021/002178/217832e.pdf.

IOC, 2015: Tsunami warning and mitigation systems to protect coastal communities. *Indian Ocean Tsunami Warning and Mitigation System 2005-2015*. doi:http://unesdoc .unesco.org/images/0023/002336/233627e.pdf.

IPCC, 2013: IPCC WGI Fifth Assessment Report, Chapter 13 Sea Level Change.

IPCC, 2013: IPCC WGI Fifth Assessment Report, Chapter 3 - Observations: Ocean.

IPCC, 2007: The Physical Science Basis. Contribution of Working Group I to the Fourth Assessment Report of the Intergovernmental Panel on Climate Change, S. Solomon et al., Eds.

(Cambridge Univ. Press, Cambridge, UK, and New York, 2007).

Iskandar, I., W. Mardiansyah, Y. Masumoto, and T. Yamagata, 2005: Intraseasonal Kelvin Waves along the Southern Coast of Sumatra and Java. *J. Geophys. Res.*, **110**, C04013, doi:10.1029/2004JC002508.

Iskandar, I., and M.J. McPhaden, 2011: Dynamics of wind-forced intraseasonal zonal current variations in the equatorial Indian Ocean. *J. Geophys. Res.*, **116**, C06019.

Izumo, T., C. de Boyer Montégut, J.J. Luo, S.K. Behera, …, T. Yamagata, 2008: The role of the western Arabian Sea upwelling in Indian monsoon rainfall variability. *J. Climate*, **21**, 5603-5623.

Izumo, T., M. Lengaigne, J. Vialard, J-J. Luo, …, G. Madec, 2014: Influence of Indian Ocean Dipole and Pacific recharge on following year's El Nino: interdecadal robustness. *Climate Dyn.*, **42**, 291-310.

Jayakumar A., J. Vialard, M. Lengaigne, C. Gnanaseelan, …, B.P. Kumar, 2011: Processes controlling the surface temperature signature of the Madden-Julian Oscillation in the thermocline ridge of the Indian Ocean. *Climate Dyn.* **37**, 2217-2234.

Johns, W.E., M.O. Baringer, L.M. Beal, S.A. Cunningham, T. Kanzow, ..., R. Curry, 2011: Continuous, array-based estimates of Atlantic Ocean heat transport at 26.5°N. *J. Climate*, **24(10)**, 2429-2449.

Jongaramrungruang S., H. Seo, and C.C. Ummenhofer, 2017: Intraseasonal rainfall variability in the Indian Ocean during the summer monsoon: coupling with the ocean and modulation by the Indian Ocean Dipole. *Atmos. Sci. Lett.*, **18**, 88-95.

Kanzow, T., S.A. Cunningham, W.E. Johns, J.J. Hirschi, …, J. Collins, 2010: Seasonal variability of the Atlantic meridional overturning circulation at 26.5 N. *J. Climate*, **23(21)**, 5678-5698.

Kaplan, D.M., E. Chassot, J.M. Amande, S. Dueri, …, A. Fonteneau, 2014: Spatial management of Indian Ocean tropical tuna fisheries: potential and perspectives. ICES *J. Mar. Sci.*, **71(7)**, 1728-1749, doi:10.1093/icesjms/fst233.

Karmakar, N., A. Chakraborty, and R.S. Nanjundiah, 2015: Decreasing intensity of monsoon low-frequency intraseasonal variability over India. *Environ. Res. Lett.*, **10**, 054018

Kataoka, T., T. Tozuka, and T. Yamagata, 2012: The Indian Ocean subtropical dipole mode simulated in the CMIP3 models. *Climate Dyn.*, **39**, 1385-1399.

Kataoka, T., T. Tozuka, S.K. Behera, and T. Yamagata, 2014: On the Ningaloo Nino/Nina. *Climate Dyn.*, **43**, 1463-1482.

Kataoka, T., T. Tozuka, and T. Yamagata, 2017: Generation and decay mechanisms of Ningaloo Nino/Nina. *J. Geophys. Res. Oceans*, doi:10.1002/2017JC012966.

Kataoka, T., S. Masson, T. Izumo, T. Tozuka, and T. Yamagata, 2018: Can Ningaloo Nino/Nina Develop Without El Nino-Southern Oscillation? *Geophys. Res. Lett.*, **45**, 7040-7048, doi:10.1029/2018GL078188.o

Kato, S., N.G. Loeb, F.G. Rose, D.R. Doelling, …, R.A. Weller, 2013: Surface irradiances consistent with CERES-derived top-of-atmosphere shortwave and longwave irradiances. *J. Climate*, **26**, 2719-2740, doi: http://dx.doi.org/10.1175/JCLI-D-12-00436.1.

Katsumata, K., and S. Masuda, 2013: Variability in Southern Hemisphere Ocean Circulation from the 1980s to the 2000s. *J. Phys. Oceanogr.*, **43(9)**, 1981-2007.

Katsumata, M., P.E. Ciesielski, and R.H. Johnson, 2011. Evaluation of budget analyses during MISMO. *Journal of Applied Meteorology and Climatology*, **50**, 241-254.

Kay S., and co-authors, 2015: Modeling the increased frequency of extreme sea levels in the Ganges-Brahmaputra-Meghna delta due to sea level rise and other effects of climate change. *Environmental Science Process Impacts*, **17**, 1311-22.

Keerthi, M.G., M. Lengaigne, M. Levy, J. Vialard, …, P.M. Muraleedharan, 2017: Physical control of interannual variations of the winter chlorophyll bloom in the northern Arabian Sea. *Biogeosciences*, **14(15)**, 3615-3632.

Kemball-Cook S., and B. Wang, 2001: Equatorial waves and air-sea inter- action in the boreal summer intraseasonal oscillation. *J. Climate*, **14**, 2923-2942.

Kemball-Cook, S., B. Wang, and X. Fu, 2002: Simulation of the ISO in the ECHAM4 model: The impact of coupling with an ocean model, *J. Atmos. Sci.*, **59**, 1433-1453.

Kessler, W.S., M.J. McPhaden, and K.M. Weickmann, 1995: Forcing of intraseasonal Kelvin waves in the equatorial Pacific Ocean. *J. Phys. Oceanogr.*, **23**, 608-625.

Kessler, W.S., and R. Kleeman, 2000: Rectification of the Madden-Julian oscillation into the ENSO cycle. *J. Climate*, **13**, 3560-3475.

Kido, S., T. Kataoka, and T. Tozuka, 2016: Ningaloo Nino simulated in the CMIP5 models. *Climate Dyn.*, **47**, 1469-1484.

Kido, S., and T. Tozuka, 2017: Salinity variability associated with the positive Indian Ocean Dipole and its impact on the upper ocean temperature. *J. Climate*, **30**, 7885-7907.

Kim, D., K. Sperber, W. Stern, D. Waliser, …, M.I. Lee, 2009: Application of MJO simulation diagnostics to climate models. *J. Climate*, **22(23)**, 6413-6436.

Kim, D.M., M.I. Lee, H.M. Kim, S.D. Shubert and J. Yoo, 2014: The Modulation of Tropical Storm Activity in the Western North Pacific by the MJO in GEOS-5 AGCM Experiments, *Atmos. Sci. Lett*, **15 (4)**, 335-341

Kim, H.-M., C.D. Hoyos, P.J. Webster, and I.-S. Kang, 2008: Sensitivity of MJO simulation and predictability to sea surface temperature variability. *J. Climate*, **21**, 5304-5317.

King, M., 2014: Priorities for installation of continuous Global Navigation Satellite System (GNSS) near to tide gauges. *Technical Report. University of Tasmania. October 2014*, doi: 10.13140/RG.2.1.1781.7049.

Klein, S.A., B.J. Soden, and N.C. Lau, 1999: Remote sea surface temperature variations dur-

ing ENSO: evidence for a tropical atmospheric bridge. *J. Climate*, **12**, 917-932.

Klingaman, N.P., X. Jiang, P.K. Xavier, J. Petch, …, S.J. Woolnough, 2015: Vertical structure and physical processes of the Madden-Julian oscillation: Synthesis and summary. *J. Geophys. Res.: Atmospheres*, **120(10)**, 4671-4689.

Knutson T.R., T.L. Delworth, K.W. Dixon, I.M. Held, …, R.J. Stouffer, 2006: Assessment of twentieth-century regional surface temperature trends using the GFDL CM2 coupled models. *J. Climate*, **19 (9)**,1624-1651

Knutson, T.R., J.J. Sirutis, M. Zhao, R.E. Tuleya, …, D. Chavas, 2015: Global Projections of Intense Tropical Cyclone Activity for the Late Twenty-First Century from Dynamical Downscaling of CMIP5/RCP4.5 Scenarios. *J. Climate*, **28**, 7203-7224, doi:10.1175/JCLI-D-15-0129.1.1

Kobayashi, S., and co-authors, 2015: The JRA-55 Reanalysis: General specifications and basic characteristics. *J. Meteor. Soc. Japan*, **93**, 5-48, doi:10.2151/jmsj.2015-001.

Koch-Larrouy, A., G. Madec, P. Bouruet-Aubertot, T. Gerkema, …, R. Molcard, 2007: On the transformation of PacificWater into Indonesian Throughflow Water by internal tidal mixing. *Geophys. Res. Lett.*, **34**, L04,604, doi:10.1029/2006GL028405.

Koch-Larrouy, A., M. Lengaigne, P. Terray, G. Madec, and S. Masson, 2010: Tidal mixing in the Indonesian Seas and its effect on the tropical climate system, *Climate Dyn.*, **34**, 891-904, doi:10.1007/s00382-009-0642-4

Koch-Larrouy, A., A. Atmadipoera, P. van Beek, G. Madec, …, M. Souhaut, 2015: Estimates of tidal mixing in the Indonesian archipelago from multidisciplinary INDOMIX *in situ* data, *Deep-Sea Res.*, **106**, 136-153.2

Kopp, R.E., C.C. Hay, C.M. Little, and J.X. Mitrovica, 2015: Geographic Variability of Sea-Level Change, *Curr. Clim. Change. Rep.*, **1**, 192-204.

Kosaka, Y., and S.-P. Xie, 2013: Recent global-warming hiatus tied to equatorial Pacific surface cooling. *Nature*, **501**, 403-407, doi:10.1038/nature12534.

Kossin, J.P., T.L. Olander, and K.R. Knapp, 2013: Trend Analysis with a New Global Record of Tropical Cyclone Intensity. *J. Climate*, **26**, 9960-9976, doi:10.1175/JCLI-D-13-00262.1.

Krishnamurthy, L., and V. Krishnamurthy, 2016: Decadal and interannual variability of the Indian Ocean SST. *Climate Dyn.*, **46**, 57-70.

Krishnamurti, T.N., and D. Subrahmanyam, 1982: The 30-50 day mode at 850 mb during MONEX. *J. Atmos. Sci.*, **39(9)**, 2088-2095.

Krishnamurti, T.N., D.K. Oosterhof, and A. V. Metha, 1988: Air-sea interaction on the timescale of 30-50 days. *J. Atmos. Sci.*, **45**, 1304-1322.

Krishnamurti, T.N., A. Chakraborty, R. Krishnamurti, W.K. Dewar, and C.A. Clayson, 2007: Passage of intraseasonal waves in the subsurface oceans. *Geophys. Res. Lett.*, **34**, L14712.

Krug, M., S. Swart, and J. Gula, 2017: Submesoscale cyclones in the Agulhas current. *Geo-*

phys. Res. Lett., **44(1)**, 346-354.

Kuleshov, Y., L. Qi, R. Fawcett, and D. Jones, 2008: On tropical cyclone activity in the Southern Hemisphere: Trends and the ENSO connection. *Geophys. Res. Lett.*, **35**, L14S08, doi:10.1029/2007GL032983.

Lachkar, Z., S. Smith, M. Levy, and O. Pauluis, 2016: Eddies reduce denitrification and compress habitats in the Arabian Sea. *Geophys. Res. Lett.*, **43**, 9148-9156, doi:10.1002/2016gl069876.

Lau, K.M., and S. Yang, 1996: Seasonal variation, abrupt transition, and intraseasonal variability associated with the Asian summer monsoon in the GLA GCM, *J. Climate*, **9(5)**, 965-985.

Lau K.M., and P.H. Chan, 1988: Intraseasonal and interannual variations of tropical convection: a possible link between the 40-50 day oscillation and ENSO? *J Atmos Sci*, **45**, 506-521.

Lau K.M., and H.Y. Weng, 1999: Interannual, decadal-interdecadal, and global warming signals in sea surface temperature during 1955-97. *J. Climate*, **12 (5)**, 1257-1267

Lau K.M., and D.E. Waliser, 2011: Intraseasonal variability of the atmosphere ocean climate system, 2nd edn. *Springer, Heidelberg*, 613.

Leber, G.M., L.M. Beal,.and S Elipot, 2017: Wind and current forcing combine to drive strong upwelling in the Agulhas Current. *J. Phys. Oceanogr.*, **47(1)**, 123-134.

Lee, P.-F., I.-C. Chen, and W.-N. Tzeng, 2005: Spatial and temporal distibution patterns of Bigeye Tuna (Thunnus obesus) in the Indian Ocean. *Zoological Studies*, **44(2)**, 260-270.

Lee, S.S., B. Wang, D.E. Waliser, J.M. Neena, and J.Y. Lee, 2015: Predictability and prediction skill of the boreal summer intraseasonal oscillation in the Intraseasonal Variability Hindcast Experiment. *Climate Dyn.*, **45(7-8)**, 2123-2135.

Lee, S-K., W. Park, M.O. Baringer, A.L. Gordon, …, Y. Liu, 2015: Pacific origin of the abrupt increase in Indian Ocean heat content during the warming hiatus, *Nature Geoscience*, doi:10.1038 /ngeo2438.

Lee, T., 2004: Decadal weakening of the shallow overturning circulation in the South Indian Ocean. *Geophys. Res. Lett.*, **31**, L18305, doi:10.1029/2004GL020884.

Lee, T., and M.J. McPhaden, 2008: Decadal phase change in large-scale sea level and winds in the Indo-Pacific region at the end of the 20th century, *Geophys. Res. Lett.*, **35**, doi:10.1029/2007 GL032419.

Lee, T., T. Awaji, M.A. Balmaseda, E. Greiner, and D. Stammer, 2009: Ocean state estimation for climate research. *Oceanography*, **22(3)**, 160-167, doi:http://dx.doi.org/10.5670/oceanog. 2009.74.0

Lee, T., T. Awaji, M. Balmaseda, et al., 2010: Consistency and fidelity of Indonesian-throughflow total volume transport estimated by 14 ocean data assimilation products. *Dyn. Atmos. Oceans.* doi:10.1016/j.dynatmoce.2009.12.004.

Lee, T., 2016: Consistency of Aquarius sea surface salinity with Argo products on various spa-

tial and temporal scales. *Geophys. Res. Lett.*, **43**, doi:10.1002/2016GL068822.

Lee, T., J.T. Farrar, S. Arnault, B. Meyssignac, W. Han, T. Durland, 2017: Monitoring and interpreting the tropical oceans by satellite altimetry. Chapter 7 in satellite altimetry textbook "Satellite Altimetry Over Ocean and Land Surfaces", Editors D. Stammer and A. Cazenave, *CRC Press, Taylor and Francis Group*. 644, doi:https://doi.org/10.1201/ 9781315151779.

Lengaigne, M., and Co-authors, 2018: Influence of air-sea coupling on Indian Ocean tropical cyclones. *Climate Dyn.*, **88**, 93-22, doi:10.1007/s00382-018-4152-0.

Levine, R.C., A.G. Turner, D. Marathayil, and G.M. Martin, 2013: The role of northern Arabian Sea surface temperature biases in CMIP5 model simulations and future projections of Indian summer monsoon rainfall. *Climate Dyn.*, **41**, 155-172.

Levitus S., J.I. Antonov, T.P. Boyer, O.K. Baranova, …, E.S. Yarosh., 2012: World ocean heat content and thermosteric sea level change (0-2000 m), 1955-2010. *Geophys. Res. Lett.*, **39**, (10).

L'Heureux, M. L., S. Lee, and B. Lyon, 2013: Recent multidecadal strengthening of the Walker circulation across the tropical Pacific. *Nature Climate Change*, **3**, 571-576.

Li, G., S.P. Xie, and Y. Du, 2016: A robust but spurious pattern of climate change in model projections over the tropical Indian Ocean. *J. Climate*, **29(15)**, 5589-5608.

Li, Q., D.M. Farmer, T.F. Duda, and S. Ramp, 2009: Acoustical measurement of nonlinear internal waves using the inverted echo sounder. *J. Atmos. Oceanic Technol.*, **26(10)**, 2228-2242, doi:10.1175/2009JTECHO652.1.

Li, Y., W. Han, T. Shinoda, C. Wang, …, J.-W. Wang, 2013: Effects of the diurnal cycle in solar radiation on the tropical Indian Ocean mixed layer variability during wintertime Madden-Julian oscillation. *J. Geophys. Res. Oceans*, **118**, 4945-4964, doi:10.1002/jgrc.20395.

Li, Y., W. Han, T. Shinoda, C. Wang, …, J.-W. Wang, 2014: Revisiting the Wintertime Intraseasonal SST Variability in the Tropical South Indian Ocean: Impact of the Ocean Interannual Variation. *J. Phys. Oceanogr.*, **44(7)**, 1886-1907.

Li, Y., and W. Han, 2015: Decadal Sea level Variatoins in the Indian Ocean Investigated with HYCOM: Roles of Climate Modes, Ocean Internal Variability and Stochastic Wind Forcing. *J. Climate*, **28**, 9143-9165.

Li, Y., W. Han, W. Wang, M. Ravichandran, …, T. Lee, 2017a: Bay of Bengal Salinity Stratification and Indian Summer Monsoon Intraseasonal Oscillation: 1. Intraseasonal variability and causes. *J. Geophys. Res. Oceans*, doi: 10.1002/2017JC012692

Li, Y., W. Han, W. Wang, M. Ravichandran, …, T. Shinoda, 2017b: Bay of Bengal Salinity Stratification and Indian Summer Monsoon Intraseasonal Oscillation: 2. Impact on SST and convection. *J. Geophys. Res. Oceans*, doi: 10.1002/2017JC012692.

Liang, X., and L. Yu, 2016: Variations of the global net air-sea heat flux during the "hiatus" period (2001-2010). *J. Climate*, **29**, 3647-3660, doi: 10.1175/JCLI-D-15-0626.1.

Liang, X., M. Spall, and C. Wunsch, 2017: Global ocean vertical velocity from a dynamically consistent ocean state estimate. *J. Geophys. Res.: Oceans*, **122**, doi:10.1002 /2017JC012985.

Liebmann, B., H. H. Hendon, and J. D. Glick, 1994: The relationship between tropical cyclones of the eastern Pacific and Indian Oceans and the Madden-Julian oscillation. *J. Meteor. Soc. Japan*, **72**, 401-411.

Liebmann, B., M. P. Hoerling, C. Funk, I. Bladé, …, J. K. Eischeid, 2014: Understanding recent eastern Horn of Africa rainfall variability and change. *J. Climate*, **27**, 8630-8645.

Lien, R.-C., B. Ma, Y.-H. Cheng, C.R. Ho, …, M.-H. Chang, 2014: Modulation of Kuroshio Transport by Mesoscale Eddies at the Luzon Strait Entrance. *J. Geophys. Res. Oceans*, **119**, doi:10.1002/2013JC009548.

Lin, I. I., C.-H. Chen, I.-F. Pun, W. T. Liu, and C.-C. Wu, 2009: Warm ocean anomaly, air sea fluxes, and the rapid intensification of tropical cyclone Nargis (2008). *Geophys. Res. Lett.*, **36**, L03817, doi:10.1029/2008GL035815.

Liu, H., Y. Tang, D. Chen, and T. Lian, 2017: Predictability of the Indian Ocean Dipole in the coupled models. *Climate Dyn.*, **48**, 2005-2024.

Liu, L., S.-P. Xie, X.-T. Zheng, T. Li, …, W. Yu, 2014: Indian Ocean variability in the CMIP5 multi-model ensemble: the zonal dipole mode. *Climate Dyn.*, **43**, 1715-1730.

Liu, Q., M. Feng, D. Wang, and S. Wijffels, 2015: Interannual variability of the Indonesian Throughflow transport: a revisit based on 30-year expendable bathythermograph data. *J. Geophys. Res.*, **120**, 8270-8282, doi:10.1002/2015JC011351.

Liu, W., J. Lu, and S.P. Xie, 2015: Understanding the Indian Ocean response to double CO_2. *Ocean Dynamics*, **65(7)**, 1037-1046.

Liu, W., S.P. Xie, and J. Lu, 2016: Tracking ocean heat uptake during the surface warming hiatus. *Nature Communications*, **7**.

Liu, Z., 2012: Dynamics of interdecadal climate variability: a historical perspective. *J. Climate*, **25**, 1963-1995.

Lix, J.K., and Co-authors, 2016: Differential bleaching of corals based on El Niño type and intensity in the Andaman Sea, southeast Bay of Bengal. *Environ Monit Assess*, **188**, 175, doi:10.1007/s10661-016-5176-8.

Llewellyn, L.E., S. English, and S. Barnwell, 2016: A roadmap to a sustainable Indian Ocean blue economy. *Journal of the Indian Ocean Region*, **12(1)**, 52-66.

Llovel, W., and T. Lee, 2015: Importance and origin of halosteric contribution to sea level change in the southeast Indian Ocean during 2005-2013. 42, 1148-1157. *Geophys. Res. Lett.*, doi: 10.1002/2014GL062611.

Lough, J.M., K.D. Anderson, and T.P. Hughes, 2018: Increasing thermal stress for tropical coral reefs, 1871-2017. *Sci Rep*, **8**, 6079, doi:10.1038/s41598-018-24530-9.

Lucas, A.J., J.D. Nash, R. Pinkel, J.A. MacKinnon, …, A. Le Boyer, 2016: Adrift upon a salinity-stratified sea: A view of upper-ocean processes in the Bay of Bengal during the southwest monsoon. *Oceanography*, **29(2)**, 134-145, https://doi.org/10.5670/oceanog.2016.46.7

Lukas R., and E.J. Lindstorm, 1991: The mixed layer of the western equatorial Pacific Ocean. *J. Geophys. Res.*, **96**, 3343-3357, doi:10.1029/90JC01951

Lumpkin, R., and K. Speer, 2007: Global ocean meridional overturning. *J. Phys. Oceanogr.*, **37 (10)**, 2550-2562.

Luo, J.-J., S. Masson, S. Behera, and T. Yamagata, 2007: Experimental forecasts of the Indian Ocean Dipole using a coupled OAGCM. *J. Climate*, **20**, 2178-2190.

Luo, J.-J., S. Behera, Y. Masumoto, H. Sakuma, and T. Yamagata, 2008: Successful prediction of the consecutive IOD in 2006 and 2007. *Geophys. Res. Lett.*, **35**, L14S02, doi:10.1029/2007GL032793.

Luo, J.-J., W. Sasaki, and Y. Masumoto, 2012: Indian Ocean warming modulates Pacific climate change. *Proceedings of the National Academy of Sciences*, **109(46)**, 18701-18706.

Luo, J.-J., et al., 2016a: Current status of intraseasonal-seasonal-to-interannual prediction of the Indo-Pacific climate, in Indo-Pacific Climate Variability and Predictability. *World Sci. Publ. Co, chap. 3*, 63-107.

Luo, Y., J. Lu, F. Liu, and X. Wan, 2016b: The positive Indian Ocean Dipole-like response in the tropical Indian Ocean to global warming. *Advances in Atmospheric Sciences*, **33(4)**, 476-488.

Macdonald, A.M., 1998: The global ocean circulation: a hydrographic estimate and regional analysis. *Progress in Oceanography*, **41(3)**, 281-382.

Madden R.A., and P.R. Julian., 1994: Observations of the 40-50-day tropical oscillation: a review. *Mon. Wea. Rev.*, **122**, 814-837.

Madden, R.A., and P. R. Julian, 1972: Description of global-scale circulation cells in the tropics with a 40-50 day period. *J. Atmos. Sci.*, **29**, 1109-1123.

Mahadevan, A., T. Paluszkiewicz, M. Ravichandran, D. Sengupta, and A. Tandon, 2016a: Introduction to the special issue on the Bay of Bengal: From monsoons to mixing. *Oceanography*, **29**, 14-17.

Mahadevan, A., G. Spiro Jaeger, M. Freilich, M. Omand, …, D. Sengupta, 2016b: Freshwater in the Bay of Bengal: Its fate and role in air-sea heat exchange. *Oceanography*, **29(2)**, 72-81, doi:http://dx.doi.org/10.5670/oceanog. 2016.40.5

Mahowald, N.M. et al., 2006: Change in atmospheric mineral aerosols in response to climate: Last glacial period, pre-industrial, modern and doubled-carbon dioxide climates. *J. Geophys. Res.*, **111**, doi:10.1029/2005JD006653.

Malan, N., C.J.C. Reason, and B.R. Loveday, 2013: Variability in tropical cyclone heat potential

over the Southwest Indian Ocean. *J. Geophys. Res*, **118**, 6734-6746, doi:10.1002/2013JC008958.

Maloney, E.D., and D. L. Hartmann, 2000a: Modulation of eastern North Pacific hurricanes by the Madden-Julian oscillation. *J. Climate*, **13**, 1451-1460.

Maloney, E.D., and D.L. Hartmann, 2000b: Modulation of hurricane activity in the Gulf of Mexico by the Madden-Julian Oscillation. *Science*, **287**, 2002-2004, doi:10.1126/science.287.5460.2002.

Manatsa, D., B. Chipindu, and S. K. Behera, 2012: Shifts in IOD and their impacts on association with East African rainfall. *Theor. Appl. Climatol.*, **110**, 115-128.

Manatsa, D., and S.K. Behera, 2013: On the epochal strengthening in the relationship between rainfall of East Africa and IOD. *J. Climate*, **26**, 5655-5673.

Marshall, A.G., and H.H. Hendon, 2014: Impacts of the MJO in the Indian Ocean and on the Western Australian coast. *Climate Dyn.* **42**, 579-595. doi:10.1007/s00382-012-1643-2.

Marshall, A.G., H.H. Hendon, M. Feng, and A. Schiller, 2015: Initiation and amplification of the Ningaloo Nino. *Climate Dyn.*, **45**, 2367-2385, doi:10.1007/s00382-015-2477-5.

Masson, S., C. Menkes, P. Delecluse, and J.-P. Boulanger, 2003: Impacts of salinity on the eastern Indian Ocean during the termination of the fall Wyrtki Jet. *J. Geophys. Res.*, **108**, 3067 (doi:10.1029/2001JC000833)

Masson, S., et al., 2005: Impact of barrier layer on winter-spring variability of the southeastern Arabian Sea. *Geophys. Res. Lett.*, **32**, L07703, doi:10.1029/2004GL021980.

Masumoto, Y., W. Yu, G. Meyers, N. D'Adamo, …, L. Yu, 2010: Observing systems in the Indian Ocean. In Proceedings of the "OceanObs'09: Sustained Ocean Observations and Information for Society" Conference (Vol. 2), Venice, Italy, 21-25 September 2009, Hall, J., D.E. Harrison, and D. Stammer, Eds., ESA Publication WPP-306.

McClanahan, T.R., M. Ateweberhan, N.A.J. Graham, S.K. Wilson, …, J.H. Bruggemann. 2007: Western Indian Ocean coral communities: bleaching responses and susceptibility to extinction. *Marine Ecology Progress Series*, **337**, 1-13.

McClean, J.L., D.P. Ivanova, and J. Sprintall, 2005: Remote origins of interannual variability in the Indonesian Throughflow region from data and a global Parallel Ocean Program simulation. *J. Geophys. Res.*, **110**, C10013, doi: 10.1029/2004JC002477.

McCreary, J.P., S.R. Shetye, and P.K. Kundu, 1986: Thermohaline forcing of eastern boundary currents: With application to the circulation off the west coast of Australia. *J. Mar. Res.*, **44**, 71-92, doi:10.1357/002224086788460184.

McCreary J.P. Jr, P.K. Kundu, and R.L. Molinari, 1993: A numerical investigation of dynamics, thermodynamics and mixed-layer processes in the Indian Ocean. *Prog Oceanogr*, **31**, 181-2440

McCreary, J.P., R. Murtugudde, J. Vialard, P.N. Vinayachandran, …, S. Shetye, 2009: Biophysical Processes in the Indian Ocean, in Indian Ocean Biogeochemical Processes and Ecological Variability. *American Geophysical Union*, 9-32, doi:10.1029/2008GM000768.

McCreary, J.P. et al., 2013: Dynamics of the Indian-Ocean oxygen minimum zones. *Prog. Ocean.*, **112**, 15-37, doi:10.1016/j.pocean.2013.03.002.

McDonagh, E.L., H.L. Bryden, B.A. King, R.J. Sanders, …, R. Marsh, 2005: Decadal changes in the south Indian Ocean thermocline. *J. Climate*, **18**, 1575-1590, doi:https://doi.org/10.1175/JCLI3350.1.

McDonagh, E.L., H.L. Bryden, B.A. King, and R.J. Sanders, 2008: The circulation of the Indian Ocean at 32 S. *Progress in Oceanography*, **79 (1)**, 20-36.

McPhaden, M.J., 1999: Genesis and evolution of the 1997-98 El Niño. *Science*, **283**, 950-954.

McPhaden, M.J., 2002: Mixed layer temperature balance on intraseasonal timescales in the equatorial Pacific Ocean, *J. Climate*, **15**, 2632 - 2647.

McPhaden, M.J., G. Meyers, K. Ando, Y. Masumoto, …, W. Yu, 2009: RAMA: The research moored array for African-Asian-Australian monsoon analysis and prediction. *Bull. Amer. Meteor. Soc.*, **90**, 459-480, doi:10.1175/2008BAMS2608.1.

McPhaden, M.J., K. Ando, B. Bourlès, H.P. Freitag, …, W. Yu, 2010: The global tropical moored buoy array. In Proceedings of the"OceanObs'09: Sustained Ocean Observations and Information for Society" Conference (Vol. 2), Venice, Italy, 21-25 September 2009, Hall, J., D.E. Harrison, and D. Stammer, Eds., ESA Publication WPP-306.

McPhaden, M.J., and M. Nagura, 2014: Indian Ocean Dipole interpreted in terms of Recharge Oscillator theory. *Climate Dyn.*, **42**, 1569-1586. doi 10.1007/s00382-013-1765-1.

McPhaden, M.J., Y. Wang, and M. Ravichandran, 2015: Volume transports of the Wyrtki Jets and their Relationship to the Indian Ocean Dipole. *J. Geophys. Res.*, **120**, 5302-5317, doi:10.1002/2015JC010901.

McPhaden, M.J., M. Ravichandran, K. Ando, V.S.N. Murty, and W. Yu, 2016: Unpublished manuscript available from NOAA/PMEL. *RAMA-2.0.*, **11**

Menard, F., F. Marsac, E. Bellier, and B. Cazelles, 2007: Climatic oscillations and tuna catch rates in the Indian Ocean: a wavelet approach to time series analysis. *Fish. Oceanogr.*, **16**, 95-104.

Menezes, V.V., H.E. Phillips, A. Schiller, C. Domingues, and N.L. Bindoff, 2013: Salinity dominance on the Indian Ocean Eastern Gyral Current. *Geophys. Res. Lett.* **40**, 1-6, doi:10.1002/2013GL057887.

Menezes, V.V., M.L. Vianna, and H.E. Phillips, 2014a: Aquarius sea surface salinity in the South Indian Ocean: Revealing annual-period planetary waves, *J. Geophys. Res. Oceans*, **119**, 3883-3908, doi:10.1002/2014JC009935.5

Menezes, V.V., H.E. Phillips, A. Schiller, N.L. Bindoff, …, M.L. Vianna, 2014b: South Indian Countercurrent and associated fronts. *J. Geophys. Res. Oceans*, **119**, 6763-6791.

Meyers, G., 1996: Variation of Indonesian Throughflow and the El Nino- Southern Oscillation, *J. Geophys. Res.*, 101(C5), **12**, 255-12, 263.

Meyers, G., R.J. Bailey, and A.P. Worby, 1995: Geostrophic transport of Indonesian Throughflow, *Deep-Sea Res. Part I*, **42(7)**, 1163-1174.

Michida, Y., and H. Yoritaka, 1996: Surface currents in the area of the Indo-Pacific throughflow and in the tropical Indian Ocean observed with surface drifters. *J. Geophys. Res.*, **101 (C5)**, 12475-12482, doi: 10.1029/96JC00035.97

Molinari, R.L., D. Olson, and G. Reverdin, 1990: Surface current distributions in the tropical Indian Ocean derived from compilations of surface buoy trajectories. *J. Geophys. Res.*, **95 (C5)**, 7217-7238, doi: 10.1029/JC095iC05p07217.5

Moore, J.A.Y., L.M. Bellchambers, M.R. Depczynski, R.D. Evans, …, S.K. Wilson, 2012: Unprecedented mass bleaching and loss of coral across 12 of latitude in Western Australia in 2010-11. *PLoS ONE*, **7(12)**: e51087, doi:10.1317/journal.pone.0051807.

Morioka, Y., T. Tozuka, and T. Yamagata, 2010: Climate variability in the southern Indian Ocean as revealed by self-organizing maps. *Climate Dyn.*, **35**, 1075-1088.

Morris, T., J. Hermes, and L. Beal et al., 2017: The importance of monitoring the Greater Agulhas Current and its inter-ocean exchanges using large mooring arrays. *South African Journal of Science*, **113**, 708, 10.17159/sajs.2017/20160330.

Morrison, J.M. et al., 1999. The oxygen minimum zone in the Arabian Sea during 1995. *Deep-Sea Res. Part II*, **46**, 1903-1931.

Moum, J.N., and J.D. Nash, 2009: Mixing measurements on an equatorial ocean mooring. *J. Atmos. Oceanic Technol.*, **26(2)**, 317-336, doi:http://dx.doi.org/10.1175 /2008JTECHO617.1.

Moum, J.N., A. Perlin, J.D. Nash, and M.J. McPhaden, 2013a: Seasonal sea surface cooling in the equatorial Pacific cold tongue controlled by ocean mixing. *Nature*, **500 (7460)**, 64-67.

Moum, J.N., and Co-authors, 2013b: Air-sea interactions from westerly wind bursts during the November 2011 MJO in the Indian Ocean. *Bull. Amer. Meteor. Soc.*, **95**, 1185-1199.

Murakami, H., M. Sugi, and A. Kitoh, 2012: Future changes in tropical cyclone activity in the North Indian Ocean projected by high-resolution MRI-AGCMs. *Climate Dyn.*, **40**, 1949-1968, doi:10.1007/s00382-012-1407-z.

Nagai, T., and T. Hibiya, 2015: Internal tides and associated vertical mixing in the Indonesian Archipelago. *J. Geophys. Res.*, **120**, 3373-3390, doi:10.1002/2014JC010592.

Nagura M., et al., 2013: Longitudinal biases in the Seychelles Dome simulated by 35 ocean-atmosphere coupled general circulation models. *J. Geophys. Res. Oceans*, **118**, doi:10.1029 /2012JC008352.

Nagura, M., and M.J. McPhaden, 2010a: Dynamics of zonal current variations associated with the Indian Ocean Dipole. *J. Geophys. Res.*, **115**, C11026, doi:10.1029/2010JC006423.

Nagura, M., and M.J. McPhaden, 2010b: Wyrtki Jet dynamics: Seasonal variability. *J. Geophys. Res.*, **115**, C07009, doi:10.1029/2009JC005922.

Nagura, M., and M.J. McPhaden, 2012: The dynamics of wind-driven intraseasonal variability in the equatorial Indian Ocean, *J. Geophys. Res.*, **117**, C02001, doi:10.1029/2011JC007405.

Nagura, M., T. Terao and M. Hashizume, 2015: The role of temperature inversions in the generation of seasonal and interannual SST Variability in the far northern Bay of Bengal. *J. Climate*, **28**, 3671-3693.

Nagura, M., J.P. McCreary and H. Annamalai, 2018: Origins of coupled-model biases in the Arabian-Sea climatological state. *J. Climate*, **31 (5)**, 2005-2029, doi:10,1175/JCLI-D-17-0417.1

Napitu, A.M., A.L. Gordon, and K. Pujiana, 2015: Intraseasonal Sea Surface Temperature Variability across the Indonesian Seas. *J. Climate*, **28**, 8710-8727.

Naqvi, S.W.A. et al., 1998: Severe fish mortality associated with ”red tide” observed in the sea of Cochin. *Current Science* , **75**, 543-544.

Naqvi, S.W.A. et al., 2010: Marine hypoxia/anoxia as a source of CH_4 and N_2O. *Biogeosciences*, **7**, 2159-2190, doi:10.5194/bg-7-2159-2010.

Nauw, J.J. et al., 2008: Observations of the southern East Madagascar Current and undercurrent and countercurrent system.” *J. Geophys. Res.: Oceans*, **113**.C8.

Neale, R., and J. Slingo, 2003: The Maritime Continent and its role in the global climate: A GCM Study. *J. Climate*, **16**, 834-848.

Neena, J.M., and B.N. Goswami, 2010: Extension of potential predictability of Indian summer monsoon dry and wet spells in recent decades. *Quart. J. Roy. Meteor. Soc.* **136**, 583-592.

Neena, J.M., D. Waliser, and X. Jiang, 2016: Model performance metrics and process diagnostics for boreal summer intraseasonal variability. *Climate Dyn.*, 1-23.

Neetu, S., M. Lengaigne, E.M. Vincent, J. Vialard, …, F. Durand, 2012: Influence of upper-ocean stratification on tropical cyclone-induced surface cooling in the Bay of Bengal. *J. Geophys. Res*, **117**, C12020, doi:10.1029/2012JC008433.03.

Neetu, S., M. Lengaigne, J. Vialard, G. Samson, …, I. Suresh, 2019: Premonsoon/Postmonsoon Bay of Bengal Tropical Cyclones Intensity: Role of Air-Sea Coupling and Large-Scale Background State. *Geophys. Res. Lett.*, **46(4)**, 2149-2157, doi:10.1029/2018GL0 81132.-1.

Neumann B., A.T. Vafeidis, J. Zimmermann, and R.J. Nicholls, 2015: Future Coastal Population Growth and Exposure to Sea-Level Rise and Coastal Flooding - A Global Assessment. *PLoS ONE*, **10(3)**, e0118571. doi:10.1371/journal.pone.0118571

Nicholson, S.E., 2015: Long-term variability of the East African “short rains” and its links to large-scale factors. *International Journal of Climatology*, doi:10.1002/joc.4259.

Nidheesh, A.G., M. Lengaigne, J. Vialard, A.S. Unnikrishnan and H. Dayan, 2013: Decadal and long-term sea level variability in the tropical Indo-Pacific Ocean. *Climate Dyn.*, **41**, 381-402.

Nidheesh, A.G., M. Lengaigne, J. Vialard, T. Izumo, …, C. de Boyer Montégut, 2017: Robustness of observationally-derived decadal sea-level variability in the Indo-Pacific region, *Geophys. Res. Lett.*, **44**, 7391-7400, doi:10.1002/2017GL073955.

Nidheesh, A.G., M. Lengaigne, J. Vialard, T. Izumo, …, R. Krishnan, 2019: Natural decadal sea-level variability in the Indian Ocean: Lessons from CMIP models. *Climate Dyn.*, doi:https://-doi.org/10.1007/s00382-019-04885-z

Nieves, V., J. K. Willis, and W. C. Patzert, 2015: Recent hiatus caused by decadal shift in Indo-Pacific heating. *Science*, **349**, 532-535, doi:10.1126/science.aaa4521.

Nyadjro, E. S., B. Subrahmanyam, V. S. N Murty, and J. F. Shriver, 2012: The role of salinity on the dynamics of the Arabian Sea mini warm pool. *J. Geophys. Res.Oceans*, **117(C9)**.

Oh J.H., K.Y. Kim, and G.H. Lim, 2012: Impact of MJO on the diurnal cycle of rainfall over the western Maritime Continent in the austral summer. *Climate Dyn.*, **38**, 1167-1180.

Oke, P. R., and A. Schiller, 2007: Impact of Argo, SST, and altimeter data on an eddy-resolving ocean reanalysis. *Geophys. Res. Lett.*, **34**, L19601.

Oliver, E.C.J., S.E. Perkins-Kirkpatrick, N.J. Holbrook, and N.L. Bindoff, 2018: Anthropogenic and Natural Influences on Record 2016 Marine Heat waves. *Bull. Amer. Meteor. Soc.*, **99**, S44-S48, doi:10.1175/
BAMS-D-17-0093.1.

Palastanga, V., P.J. van Leeuwen, M.W. Schouten, and W.P.M. de Ruijter, 2007: Flow structure and variability in the subtropical Indian Ocean: Instability of the South Indian Ocean Countercurrent, *J. Geophys. Res.*, **112**, C01001, doi:10.1029/2005JC003395.

Palmer, M.D., C.D. Roberts, and M. Balmaseda, et al., 2017: Ocean heat content variability and change in an ensemble of ocean reanalyses. *Climate Dyn.*, doi:10.1007/s00382-015-2801-0.

Parvathi, V., I. Suresh, M. Lengaigne, C. Ethé, …, S.W.A. Naqvi, 2017: Positive Indian Ocean Dipole events prevent anoxia along the west coast of India, *Biogeosciences*, **14**, 1541-1559.

Patanjali Kumar Ch., B. Ajay Kumar, E. Uma Devi, R. S. Mahendra, M.V. Sunanda, M. Pradeep Kumar, J. Padmanabham, S. Dipankar and T. Srinivasa Kumar, 2015: The admissible tsunamigenic source region of 24 September 2013 land-based earthquake - application of backward ray tracing technique, *Current Science*, **108(9)**, 1712-1716.

Penny, S.G., and T.M. Hamill, 2017: Coupled data assimilation for integrated earth system analysis and prediction. *Bull. Amer. Meteor. Soc.*, **98**, ES169-ES172, doi:https://doi.org/10.1175
/BAMS-D-17-0036.1.

Perigaud, C., and P. Delecluse, 1992: Annual sea level variations in the southern tropical Indian Ocean from Geosat and shallowwater simulations. *J. Geophys. Res.*, **97**, 20,169-20,178.

Perry, C.T., and K.M. Morgan, 2017: Bleaching drives collapse in reef carbonate budgets and reef growth potential on southern Maldives reefs. *Sci Rep*, **7**, 40581, doi:10.1038/srep40581.

Phillips, H.E., S.E. Wijffels, and M. Feng, 2005: Interannual variability in the freshwater content of the Indonesian-Australian Basin, *Geophys. Res. Lett.*, **32**, L03603

Pierce, D.W., T.P. Barnett, K.M. AchutaRao, P.J. Gleckler, …, W.M. Washington, 2006: Anthropogenic warming of the oceans: observations and model results. *J. Climate* , **19 (10)**, 1873-1900.

Pierrot, D., C. Neill, K. Sullivan, R. Castle, …, C.E. Cosca, 2009: Recommendations for autonomous underway pCO_2 measuring systems and data-reduction routines. *Deep-Sea Res. Part II: Topical Studies in Oceanography*, **56**, 512-22.

Piketh, S.J., P.D. Tyson, and W. Steffen, 2000: Aeolian transport from southern Africa and iron fertilization of marine biota in the South Indian Ocean. *South African Journal of Science*, **96**, 244-46.

Potemra, J.T., 2005: Indonesian Throughflow transport variability estimated from satellite altimetry. *Oceanography*, **18**, 94-103.

Pradeep K., J. Padmanabham, S. Dipankar and T. Srinivasa Kumar, 2015: The admissible tsunamigenic source region of 24 September 2013 land-based earthquake - application of backward ray tracing technique. *Current Science*, **108(9)**, 2015, 1712-1716.

Prakash, P., S. Prakash, H. Rahaman, M. Ravichandran, and S. Nayak, 2012: Is the trend in chlorophyll-a in the Arabian Sea decreasing? *Geophys. Res. Lett.*, **39**, L23605.

Praveen, V., R.S. Ajayamohan, V. Valsala, and S. Sandeep, 2016: Intensification of upwelling along Oman coast in a warming scenario. *Geophys. Res. Lett.*, **43(14)**, 7581-7589.

Price, J.F., 1981: Upper Ocean Response to a Hurricane. *J. Phys. Oceanogr*, **11**, 153-175.

Probyn, T.A., B.A. Mitchellinnes, P.C. Brown, L. Hutchings, and R.A. Carter, 1994: *Review of primary production and related processes on the Agulhas-Bank*.

Pujiana, K. and M.J. McPhaden, 2018: Ocean's response to the convectively coupled Kelvin waves in the eastern equatorial Indian Ocean. *J. Geophys. Res.*, doi:https://doi.org/10.1029/2018 JC013858.

Pujiana, K., J.N. Moum, and W.D. Smyth, 2018: The role of turbulence in redistributing upper-ocean heat, freshwater, and momentum in response to the MJO in the equatorial Indian Ocean. *J. Phys. Oceanogr.*, **48**, 197-220.

Purkey, S.G., and G.C. Johnson, 2010: Warming of global abyssal and deep Southern Ocean waters between the 1990s and 2000s: Contributions to global heat and sea level rise budgets. *J. Climate*, **23(23)**, 6336-6351.

Qiu, Y., W. Cai, L. Li, and X. Guo, 2012: Argo profiles variability of barrier layer in the tropical Indian Ocean and its relationship with the Indian Ocean Dipole. *Geophys. Res. Lett.*, **39**, L08605, doi:10.1029/2012GL051441.

Rabalais, N.N. et al., 2010: Dynamics and distribution of natural and human-caused hypoxia. *Biogeosciences*, **7**, 585-619.

Rahaman, H., D.W. Behringer, S.G. Penny, and M. Ravichandran, 2016: Impact of an upgraded model in the NCEP Global Ocean Data Assimilation System: The Tropical Indian Ocean, *J. Geophys. Res. Oceans*, **121**, 8039-8062, doi:10.1002/2016JC012056.

Rahul, S., and C. Gnanaseelan, 2016: Can large scale surface circulation changes modulate the sea surface warming pattern in the tropical Indian Ocean? *Climate Dyn.*, **46(11-12)**, 3617-3632.

Rajeevan, M., J. Srinivasan, K.N. Kumar, C. Gnanaseelan, and M.M. Ali, 2013: On the epochal variation of intensity of tropical cyclones in the Arabian Sea. *Atmos. Sci. Lett.*, **14**, 249-255, doi:10.1002/asl2.447.

Rajendran, K., and A. Kitoh, 2006: Modulation of tropical intraseasonal oscillations by ocean atmosphere coupling. *J. Climate*, **19(3)**, 366-391.

Ram, A. et al., 2014: Nutrients, hypoxia and Mass Fishkill events in Tapi Estuary, India. *Estuar. Coast. Shelf Sci.*, **148**, 48-58, doi:10.1016/j.ecss.2014.06.013.

Ramachandran, S., A. Tandon, and J. MacKinnon, et al., 2017: Submesoscale processes at shallow salinity fronts: Observations from the Bay of Bengal during the winter Monsoon, Submitted to *J. Phys. Oceanogr.*

Ramanantsoa, J.D., P. Penven, M. Krug, J. Gula and M. Rouault, 2018: Uncovering a New Current: The Southwest MAdagascar Coastal Current. *Geophys. Res. Lett.*, **45(4)**, 1930-1938.

Ramsay, H.A., S.J. Camargo, and D. Kim, 2011: Cluster analysis of tropical cyclone tracks in the Southern Hemisphere. *Climate Dyn.*, **39**, 897-917, doi:10.1007/s00382-011-1225-8.

Ramsay, H.A., M.B. Richman, L.M. Leslie, H.A. Ramsay, and M.B. Richman, 2017: The Modulating Influence of Indian Ocean Sea Surface Temperatures on Australian Region Seasonal Tropical Cyclone Counts. *J. Climate*, **30**, 4843-4856, doi:10.1175/JCLI-D-16-0631.1.6

Rao, S.A., S.K. Behera, Y. Masumoto, and T. Yamagata, 2002: Interannual variability in the subsurface tropical Indian Ocean. *Deep-Sea Res. Part II*, **49**, 1549-1572.

Rao, S.A., and T. Yamagata, 2004: Abrupt termination of Indian Ocean dipole events in response to intraseasonal disturbances. *Geophys. Res. Lett.*, **31**, L19306, doi:10.1029 /2004GL020842.

Rao, S.A., and S.K. Behera, 2005: Subsurface influence on SST in the tropical Indian Ocean: Structure and interannual variability. *Dyn. Atmos. Oceans*, **39**, 103-139.

Rao S.A., A.R. Dhakate, S.K. Saha, S. Mahapatra, …, S.K. Sahu., 2012: Why is Indian Ocean warming consistently? *Climatic change*, **110 (3-4)**, 709-719.

Rao, R.R., and R. Sivakumar, 2003: Seasonal variability of sea surface salinity and salt budget

of the mixed layer of the north Indian Ocean. *J. Geophys. Res.*, **108(C1)**, 3009, doi:10.1029/2001JC000907.

Rashid, T., S. Hoque, and F. Akter, 2013: Ocean acidification in the Bay of Bengal. *Scientific Reports*, **2**, 699.

Ratheesh, S., R. Sharma, S. Basu, 2014: An EnOI assimilation of satellite data in an Indian Ocean circulation model. *IEEE Transactions on Geoscience Remote Sensing*, **52**, 4106-4111.

Ravichandran, M., M.S. Girishkumar, and S. Riser, 2012: Observed variability of chlorophyll-a using Argo profiling floats in the southeastern Arabian Sea. *Deep-Sea Res. Part I: Oceanographic Research Papers*, **65**, 15-25.

Ray, R., and R.D. Susanto, 2016: Tidal mixing signatures in the Indonesian seas from high-resolution sea-surface temperature. *Geophys. Res. Lett.*, **43**, doi:10.1002/2016GL069485

Rayner, D., J.J.M. Hirschi, T. Kanzow, W.E. Johns, …, L.M. Beal, 2011: Monitoring the Atlantic meridional overturning circulation. *Deep-Sea Res. Part II: Topical Studies in Oceanography*, **58(17-18)**, 1744-1753.

Rayner, N.A., D.E. Parker, E. B. Horton, C.K. Folland, …, A. Kaplan, 2003: Global analyses of sea surface temperature, sea ice, and night marine air temperature since the late nineteenth century. *J. Geophys. Res.*, **108**, 4407, 10.1029/2002JD002670.

Reason, C.J.C., 2001: Subtropical Indian Ocean SST dipole events and southern African rainfall. *Geophys. Res. Lett.*, **28**, 2225-2227.

Reason, C.J.C., 2002: Sensitivity of the southern African circulation to dipole sea-surface temperature patterns in the south Indian Ocean. *International Journal of Climatology*, **22**, 377-393.

Resplandy, L., M. Levy, G. Madec, S. Pous, …, D. Kumar, 2011: Contribution of mesoscale processes to nutrient budgets in the Arabian Sea. *J. Geophys. Res.*, **116**, doi:10.1029/2011jc007006.

Resplandy, L. et al., 2012: Controlling factors of the oxygen balance in the Arabian Sea's OMZ. *Biogeosciences*, **9**, 5095-5109, doi:10.5194/bg-9-5095-2012.

Reul, N., S. Fournier, and J. Boutin, et al., 2013: Sea surface salinity observations from space with the SMOS satellite: A new means to monitor the marine branch of the water cycle. *Surv. Geophys.*, 681-722.

Reverdin, G., D.L. Cadet, and D. Gutzler, 1986: Interannual displacements of convection and surface circulation over the equatorial Indian Ocean. *Quart. J. Roy. Meteorol. Soc.*, **112**, 43-67.

Ridderinkhof, H., et al., 2010: Seasonal and interannual variability in the Mozambique Channel from moored current observations. *J. Geophys. Res.: Oceans*, **115**.C6.

Ridderinkhof, W., et al., 2013: Dipoles of the South East Madagascar Current. *Geophys. Res. Lett.*, **40.3 (2013)**, 558-562.

Rienecker M.M., and co-authors, 2011: MERRA—NASA's Modern-Era Retrospective Analy-

sis for Research and Applications. *J. Climate*, doi:10.1175/JCLI-D-11-00015.1.

Riser, S.C., J. Nystuen, and A. Rogers, 2008: Monsoon effects in the Bay of Bengal inferred from profiling float-based measurements of wind speed and rainfall. *Limnology and Oceanography*, **53**, 2080-2093.

Riser, S.C., H.J. Freeland, D. Roemmich, S. Wijffels, …, S.R. Jayne, 2016: Fifteen years of ocean observations with the global Argo array. Nature Clim. Change, 6, 145-153.

Rixen, T., A. Baum, B. Gaye, B. Nagel, 2014: Seasonal and interannual variations in the nitrogen cycle in the Arabian Sea. *Biogeosciences*, **11**, 5733-5747: doi:10.5194/bg-11-5733-2014.

Robbins, P.E., J.M. Toole, 1997: The dissolved silica budget as a constraint on the meridional overturning circulation of the Indian ocean. *Deep-Sea Res. Part I*, **44 (5)**, 879-906.

Roberts, C.D., M.D. Palmer, R.P. Allan, D.G. Desbruyeres, …, D. Smith, 2017: Surface flux and ocean heat transport convergence contributions to seasonal and interannual variations of ocean heat content. *J. Geophys. Res. Oceans*, **122(1)**, 726-744.

Robertson, A.W., A. Kumar, M. Peña, and F. Vitart, 2015: Improving and promoting subseasonal to seasonal prediction. *Bull. Amer. Meteor. Soc.*, **96**, ES49-ES53. doi: http://dx.doi.org/10.1175/BAMS-D-14-00139.1Clim

Rossby, T., R. Curry, and J. Palter, 2017: Packing science into a shipping vessel. *Eos, Trans. Amer. Geophys. Union* , doi:https://doi.org/10.1029/2017EO071319. Published on 28 April 2017.

Rossi V., M. Feng, C. Pattiaratchi, M. Roughan and A.M. Waite, 2013: On the factors influencing the development of the sporadic upwelling in the Leeuwin Current system. *J. Geophys. Res.*, doi:10.1002/jgrc.20242.

Roundy, P.E., 2008: Analysis of convectively coupled Kelvin waves in the Indian Ocean MJO. *J. Atmos. Sci.* , **65(4)**, 1342-1359.

Roxy M.K., and Y. Tanimoto, 2007: Role of SST over the Indian Ocean in Influencing the Intraseasonal Variability of the Indian Summer Monsoon. *J Meteorol Soc Jpn*, **85(3)**, 349-358.

Roxy M.K., K. Ritika, P. Terray, and S. Masson, 2014: The curious case of Indian Ocean warming. *J. Climate* **27 (22)**, 8501-8509. doi:10.1175/JCLI-D-14-00471.1

Roxy M.K., K. Ritika, P. Terray, R. Murtugudde, …, B.N.Goswami, 2015: Drying of Indian subcontinent by rapid Indian Ocean warming and a weakening land-sea thermal gradient. *Nature Communications*, **6**, 7423. doi:10.1038/ncomms8423.

Roxy M.K., A. Modi, R. Murtugudde, V. Valsala, …, M. Lévy, 2016: A reduction in marine primary productivity driven by rapid warming over the tropical Indian Ocean. *Geophys. Res. Lett.*, **43**, 826-833, doi:810.1002/2015GL066979.

Rudnick D.L., and S.T. Cole, 2011: On sampling the ocean using underwater gliders. *J. Geophys. Res.*, **116**, C08010, doi:10.1029/2010JC006849.

Rudnick, D.L., 2016: Ocean Research Enabled by Underwater Gliders. *Annual Review of Marine Science*, **8**, 9.1-9.23, doi:10.1146/annurev-marine-122414-033913.

Sabeerali, C., 2014: Modulation of monsoon intraseasonal oscillations in the recent warming period. *JGR-Atmospheres*, **119 (9)**, 5185-5203.

Saha A., S. Ghosh, A. Sahana, and E. Rao, 2014: Failure of CMIP5 climate models in simulating post-1950 decreasing trend of Indian monsoon. *Geophys. Res. Lett.*, **41 (20)**, 7323-7330.

Saha, S., S. Moorthi, and H.-L. Pan et al., 2010: The NCEP Climate Forecast System Reanalysis. *Bull. Amer. Meteor. Soc.*,doi: https://doi.org/10.1175/2010BAMS3001.1.

Saji, N.H., B.N.Goswami, P.N. Vinayachandran, and T. Yamagata, 1999: A dipole mode in the tropical Indian Ocean. *Nature*, **401**, 360-363.

Saji, N. H., and T. Yamagata, 2003: Possible impacts of Indian Ocean Dipole mode events on global climate. *Climate Research*, **25**, 151-169.

Saji, N. H., S.-P. Xie, and T. Yamagata, 2006: Tropical Indian Ocean variability in the IPCC twentieth-century climate simulations. *J. Climate*, **19**, 4397-4417.

Sallée, J.B., K. Speer, S. Rintoul, and S. Wijffels, 2010: Southern Ocean thermocline ventilation. *J. Phys. Oceanogr.*, **40(3)**, 509-529.

Sarma, V.V.S.S., A. Lenton, R.M. Law, N. Metzl, …, V. Valsala. 2013: Sea-air CO_2 fluxes in the Indian Ocean between 1990 and 2009. *Biogeosciences*, **10**, 7035-52.

Sartimbul, A., H. Nakata, E. Rohadi, B. Yusuf, and H. P. Kadarisman, 2010: Variations in chlorophyll-a concentration and the impact on Sardinella lemuru catches in Bali Strait. Indonesia, *Progress in Oceanography*, **87**, 168-74.

Schott, A.F., and J. P. McCreary Jr., 2001: The monsoon circulation of the Indian Ocean. *Progress in Oceanography*, **51**, 1-123.

Schott, A.F., M. Dengler, and R. Schoenefeldt, 2002: The shallow overturning circulation of the Indian Ocean. *Progress in Oceanography*, **53**, 57-103.

Schott, F.A., S.-P. Xie, and J. P. McCreary Jr., 2009: Indian Ocean circulation and climate variability. *Rev. Geophys.*, **47**, RG1002, doi:10.1029/2007RG000245.

Schuckmann K.V.„ and P-YL.Traon, 2011: How well can we derive Global Ocean Indicators from Argo data? Ocean Science 7 (6), 783-791. Seitzinger, S.P. et al., 2010: Global river nutrient export: A scenario analysis of past and future trends. *Global Biogeochemical Cycles*, **24**, doi: 10.1029/2009gb003587.

Sen Gupta, A., S. McGregor, E. van Sebille, A. Ganachaud, …, A. Santoso, 2016: Future changes to the Indonesian Throughflow and Pacific circulation: The differing role of wind and deep circulation changes, *Geophys. Res. Lett.*, **43**, 1669-1678.

Send U., R.A. Weller, D. Wallace, F. Chavez, …, R. Feely, 2010: OceanSITES. In: Hall J, Harrison DE, Stammer D, editors. Proceedings of OceanObs'09: Sustained ocean observa-

tions and information for society (Vol. 2). Venice, Italy: ESA Publication WPP-306, 21-25. doi:10.5270/OceanObs09.cwp.79.

Sengupta, D., B.N. Goswami, and R. Senan, 2001a: Coherent intraseasonal oscillations of ocean and atmosphere during the Asian summer monsoon, *Geophys. Res. Lett.*, **28(21)**, 4127-4130.

Sengupta D, and M. Ravichandran, 2001b: Oscillations of Bay of Bengal sea surface temperature during the 1998 summer monsoon. *Geo. phys. Res. Lett.*, **28**, 2033-2036.

Sengupta, D., G.N. Bharath Raj, M. Ravichandran, J. Sree Lekha, and F. Papa, 2016: Near-surface salinity and stratification in the north Bay of Bengal from moored observations, *Geophys. Res. Lett.*, **43**, 4448-4456, doi:10.1002/2016GL068339.

Seo, K.-H., J.-K. E. Schemm, W. Wang, and A. Kumar, 2007: The boreal summer intraseasonal oscillation simulated in the NCEP climate forecast system: The effect of sea surface temperature, Mon. *Weather Rev.*, **135(5)**, 1807-1827.

Seo, H., S.P. Xie, R. Murtugudde, M. Jochum and A.J. Miller, 2009: Seasonal effects of Indian Ocean freshwater forcing in a regional coupled model. *J. Climate*, **22**, 6577-6596.

Seo, H., A.C. Subramanian, A.J. Miller, and N.R. Cavanaugh, 2014: Coupled impacts of the diurnal cycle of sea surface temperature on the Madden-Julian Oscillation. *J. Climate*, **27**, 8422-8443.

Sérazin, G., T. Penduff, S. Grégorio, B. Barnier, …, L. Terray, 2015: Intrinsic variability of sea level from Global Ocean simulations: Spatiotemporal scales. *J. Climate*, **28**, 4279-4292.

Shankar, D., and S.R. Shetye, 1999: Are interdecadal sea level changes along the Indian coast influenced by variability of monsoon rainfall? *J. Geophys. Res.*, **104**, 26031-26042.

Shankar, D., P.N. Vinayachandran, and A.S. Unnikrishnan, 2002: The monsoon currents in the north Indian Ocean. *Progress in oceanography*, **52(1)**, 63-120.

Shankar, D., S.G. Aparna, J.P. McCreary, I. Suresh, …, M.A. Al Saafani, 2010: Minima of interannual sea-level variability in the Indian Ocean. Prog. *In Oceanogr.*, **84**, 225-241.

Sharma, R., N. Agarwal, A. Chakraborty, S. Mallick, …, A. Tandon, 2016: Large-scale air-sea coupling processes in the Bay of Bengal using space-borne observations. *Oceanography*, **29**, 192-201.

Shenoi, S.S.C., P.K. Saji, and A.M. Almeida, 1999: Near- surface circulation and kinetic energy in the tropical Indian Ocean derived from Lagrangian drifters. *J. Mar. Res.*, **57 (6)**, 885-907.

Shenoi, S.S.C., D. Shankar and S.R. Shetye., 2002: Differences in heat budgets of the near surface Arabian Sea and Bay of Bengal: Implications for the summer monsoon. *J. Geophys. Res* , **107**, NO. C6, 3052, 10.1029/2000JC000679.

Sherin, V.R., F. Durand, V.V. Gopalkrishna, S. Anuvinda, …, F. Papa, 2018: Signature of Indian Ocean Dipole on the western boundary current of the Bay of Bengal. *Deep-Sea Res. Part I: Oceanographic Research Papers*, **136**, 91-106.

Shinoda, T., and H. H. Hendon, 1998: Mixed layer modeling of intraseasonal variability in the tropical western Pacific and Indian Oceans. *J. Climate*, **11**, 2668-2685.

Shinoda, T., H. H. Hendon, and J. Glick, 1998: Intraseasonal variability of surface fluxes and sea surface temperature in the tropical western Pacific and Indian Oceans. *J. Climate*, **11**, 1685-1702.

Shinoda, T., 2005: Impact of diurnal cycle of solar radiation on intraseasonal SST variability in the western equatorial Pacific. *J. Climate*, **18**, 2628-2636.

Shinoda, T., and W. Han, 2005: Influence of Indian Ocean dipole on atmospheric subseasonal variability. *J. Climate*, **18**, 3891-3909.

Shroyer, E., D.L. Rudnick, J.T. Farrar, B. Lim, S.K. Venayagamoorthy, …, J. N. Moum, 2016: Modification of upper-ocean temperature structure by subsurface mixing in the presence of strong salinity stratification. *Oceanography*, **29 (2)**, 62-71.

Shukla, J., and M. Fennessy, 1994: Simulations and predictability of monsoons, in Proceedings of the International Conference on Monsoon variability and predictability, Tech. *Rep. WCRP*, 567-575, World Climate Research Programme, Geneva, Switzerland.

Siedler, G., M. Rouault, and J. Lutjeharms, 2006: Structure and origin of the subtropical South Indian Ocean Countercurrent, *Geophys. Res. Lett.*, **33**, L24609, doi:10.1029/2006GL027399.

Sikka D.R., and S. Gadgil, 1980: On the maximum cloud zone and the ITCZ over Indian longitudes during the southwest monsoon. *Mon. Wea. Rev.*, **108**, 1840-1853.

Sivareddy, S., A. Paul, T. Sluka, M. Ravichandran, and E. Kalnay, 2017: The pre-Argo ocean reanalyses may be seriously affected by the spatial coverage of moored buoys, *Scientific Reports*, **7**: 46685.

Skliris, N., R. Marsh, S.A. Josey, S.A. Good, …, R.P. Allan, 2014: Salinity changes in the World Ocean since 1950 in relation to changing surface freshwater fluxes. *Climate Dyn.*, **43(3-4)**, 709-736.

Sloyan, B.M., and S.R. Rintoul, 2001: The Southern Ocean limb of the global deep overturning circulation. *J. Phys. Oceanogr.*, **31(1)**, 143-173.

Smith, N.R., and C.J. Koblinsky, 2001: Global Ocean Data Assimilation Experiment (2001) Observing the Oceans in the 21st Century: a Strategy for Global Ocean Observations? ISBN 10: 0642706182, ISBN 13: 9780642706188.

Smith, R. L., A. Huyer, J. S. Godfrey, and J. A. Church, 1991: The Leeuwin Current off Western Australia, 1986-1987. *J. Phys. Oceanogr.*, **21**, 323-345, doi:10.1175/1520-0485(1991)021,0323: TLCOWA.2.0.CO;2.

Sobel, A.H., E.D. Maloney, G. Bellon, and D.M. Frierson, 2008: The role of surface heat fluxes in tropical intraseasonal oscillations. *Nature Geoscience*, **1(10)**, 653-657.

Sperber K.R., et al., 2000: Predictability and the relationship between subseasonal and in-

terannual variability during the Asian summer monsoon. *Quart. J. Roy. Meteor. Soc.*, **126**, 2545-2574.

Sperber K.R., et al., 2001: Dynamical seasonal predictability of the Asian summer monsoon. *Mon. Wea. Rev.*, **129**, 2226-2248 Sperber KR, Annamali H, Kang I-S, Kitoh A, Moise A, Turner A.

Sperber, K.R., 2004: Madden-Julian variability in NCAR CAM2.0 and CCSM2.0. *Climate Dyn.*, **23**, 259-278.

Sperber K.R., and H. Annamalai, 2008: Coupled model simulations of boreal summer intraseasonal (30-50 day) variability, Part I: systematic errors and caution on use of metrics. *Climate Dyn.*, **31**, 345-372.

Sperber, K.R. et al., 2013: The Asian monsoon: an intercomparison of CMIP3vs CMIP5 simulations of the late 20th century. *Clim. Dyn*. **41**, (9-10), 2711-2744, doi:10.1007/s00382-012-1607-6.

Sprintall, J., S. Wijffels, T. Chereskin and N. Bray, 2002: The JADE and WOCE I10/IR6 Throughflow Sections in the Southeast Indian Ocean. Part 2: Velocity and transports. *Deep-Sea Res. Part II*, **49**, 1363-1389.

Sprintall, J., S.E. Wijffels, R. Molcard, and I. Jaya, 2009: Direct estimates of the Indonesian throughflow entering the Indian Ocean: 2004-2006. *J. Geophys. Res.*, **114**, C07001, doi:10.1029/2008JC005257.

Sprintall, J., A.L. Gordon, A. Koch-Larrouy, T. Lee, …, S.E. Wijffels, 2014a: The Indonesian seas and their role in the coupled ocean-climate system. *Nature Geoscience*, **7(7)**, 487-492.

Sprintall, J., and A. Révelard, 2014b: The Indonesian Throughflow response to Indo-Pacific climate variability. *J. Geophys. Res.*, **119**, 1161-1175, doi:10.1002/2013JC009533.

Srinivas Kumar T., Shailesh Nayak K., Ch. Patanjali Kumar, R.B.S. Yadav, …, S.S.C. Shenoi, 2012: Successful monitoring of April 11, 2012 off coast of Sumatra tsunami by Indian Tsunami Early Warning Center (ITEWC). *Current Science*, **102 (11)**, 1519-1526.

Srinivasu U., M. Ravichandran, W. Han, S. Sivareddy, …, S.Nayak, 2017: Causes for the reversal of North Indian Ocean decadal sea level trend in recent two decades. *Climate Dyn.*, 1-18. doi:10.1007/s00382-017-3551-y.

Srokosz, M.A., J. Robinson, H. McGrain, E.E. Popova, and A. Yool, 2015: Could the Madagascar bloom be fertilized by Madagascan iron?, *J. Geophys. Res.: Oceans*, **120(8)**, 5790-5803, doi:10.1002/2015JC011075.

Stammer, D., A. Cazenave, R. M. Ponte, and M. E. Tamisiea, 2013: Causes for contemporary regional sea level changes. *Annual Review of Marine Science*, **5**, 21-46.

Stockdale T.N., M.A. Balmaseda, and A. Vidard, 2006: Tropical Atlantic SST prediction with coupled ocean-atmosphere GCMS. *J. Climate 19*, 6047 - 6061.

Storto, A., S. Masina, and M. Balmaseda, et al., 2017: Steric sea level variability (1993-2010) in

an ensemble of ocean reanalyses and objective analyses. *Climate Dyn.*, doi:10.1007/s00382-015-2554-9.

Stott, P.A., R.T. Sutton, and D.M. Smith, 2008: Detection and attribution of Atlantic salinity changes. *Geophys. Res. Lett.*, **35(21)**.

Stramma, L., S. Schmidtko, L.A. Levin, and G.C. Johnson, 2010: Ocean oxygen minima expansions and their biological impacts. *Deep-Sea Res. Part I: Oceanographic Research Papers*, **57(4)**, 587-595. 10.1016/j.dsr.2010.01.005.

Strutton, P.G., V.J. Coles, R.R. Hood, R.J. Matear, …, H.E. Phillips, 2015: Biogeochemical variability in the central equatorial Indian Ocean during the monsoon transition. *Biogeosciences*, **12(8)**, 2367-2382, doi:10.5194/bg-12-2367-2015.

Suhas, E., J.M. Neena, and B.N. Goswami, 2013: An Indian monsoon intraseasonal oscillations (MISO) index for real time monitoring and forecast verification. *Climate Dyn.*, **40(11-12)**, 2605-2616.

Suresh I., J. Vialard, and M. Lengaigne, et al., 2013: Origins of wind-driven intraseasonal sea level variations in the North Indian Ocean coastal waveguide. *Geophys. Res. Lett.*, **40**, 5740-5744, doi:10.1002/2013GL058312.

Susanto, R.D., G. Fang, I. Soesilo, Q. Zheng, …, B. Sulistyo, 2010: New Surveys of a Branch of the Indonesian Throughflow, EOS Trans. *AGU*, **91 (30)**, doi:10.1029/2010EO300002

Susanto, R.D., A. L. Gordon, and Q. Zheng, 2001: Upwelling along the coasts of Java and Sumatra and its relation to ENSO, *Geophys. Res. Lett.*, **28**, 8, 1599-1602, doi:10.1029/2000GL011844.

Susanto, R.D., and J. Marra, 2005: The effect on 1997/98 El Nino on chlorophyll-a concentration along the southern coasts of Java and Sumatra, *Oceanography*, **18**, 4, 124-127, doi:10.5670/oceanog.2005.13

Susanto, R.D., A.L. Gordon and J. Sprintall, 2007: Observations and Proxies of the Surface Layer Throughflow in Lombok Strait, *J. Geophys. Res. Oceans*, **112**, No. C3, C03S92, 10.1029/2006JC003790.

Susanto, R.D., Z. Wei, T.R. Adi, B. Fan, …, G. Fang, 2013: Karimata throughflow from December 2007 to November 2008, *Acta Oceanol. Sin.*, **32**,5, 1-6, doi: 10.1007/s13131-013-0307-3.

Susanto, R.D., and Y.T. Song, 2015: Indonesian Throughflow proxy from satellite altimeters and gravimeters, *J. Geophys. Res. Oceans*, **120**, doi:10.1002/2014JC010382.

Susanto, R.D., Z. Wei, T. R. Adi, Q. Zheng, …, A. Setiawan, 2016: Oceanography Surrounding Krakatau Volcano in the Sunda Strait, Indonesia, *Oceanography*, **29**, 2, 228-237, doi:http://dx.doi.org/10.5670/ oceanog.2016.31.

Sutton, A.J., C.L. Sabine, S. Maenner-Jones, N. Lawrence-Slavas, …, A. Kozyr. 2014: A high-frequency atmospheric and seawater pCO_2 data set from 14 open-ocean sites using a moored autonomous system. *Earth System Science Data*, **6**, 353-66.

Sutton, A.J., C.L. Sabine, R.A. Feely, W.-J. Cai, …, D.C. Vandemark, 2016: Using present-day observations to detect when anthropogenic change forces surface ocean carbonate chemistry outside pre-industrial bounds. *Biogeosciences*, **13**, 5065-5083, doi:10.5194/bg-13-5065-2016.

Takahashi, T., S.C. Sutherland, C. Sweeney, A. Poisson, …, Y. Nojiri. 2002: Global sea-air CO_2 flux based on climatological surface ocean pCO_2, and seasonal biological and temperature effects. *Deep-Sea Res. Part II*, **49**, 1601-23.

Takahashi, T., S.C. Sutherland, R. Wanninkhof, C. Sweeney, …, H.J.W. deBaar, 2009: Climatological mean and decadal change in surface ocean pCO_2, and net sea-air CO_2 flux over the global oceans. *Deep-Sea Res. Part II: Topical Studies in Oceanography*, **56(8-10)**, 554-577.

Takahashi, T., S.C. Sutherland, D. Chipman, J.G. Goddard, …, D.R. Munro, 2014: Climatological distributions of pH, pCO_2, total CO_2, alkalinity, and $CaCO_3$ saturation in the global surface ocean, and temporal changes at selected locations. *Marine Chemistry*, **164**, 95-125.

Takayabu Y.N., T. Iguchi, M. Kachi, A. Shibata, and H. Kanzawa, 1999: Abrupt termination of the 1997-1998 El Nino in response to a Madden-Julian oscillation. *Nature*, **402**, 279-282.

Talley, L.D., 2008: Freshwater transport estimates and the global overturning circulation: Shallow, deep and throughflow components. *Progress in Oceanography*, **78(4)**, 257-303.

Talley, L.D., G.L. Pickard, W.J. Emery, and J.H. Swift, 2011: Descriptive Physical Oceanography: an introduction. *Academic Press*, **Sixth edition**.

Talley, L.D., 2013: Closure of the global overturning circulation through the Indian, Pacific and Southern Oceans: Schematics and transports. *Oceanography*, **26 (1)**, 80-97.

Tangang, F.T., L. Juneng, E. Salimun, P.N. Vinayachandran, …, T. Yasunari, 2008: On the roles of the northeast cold surge, the Borneo vortex, the Madden- Julian oscillation, and the Indian Ocean dipole during the extreme 2006/2007 flood in southern peninsular Malaysia. *Geophys. Res. Lett.*, **35**, L14S07, doi:10.1029/2008GL033429.

Tanizaki, C., T. Tozuka, T. Doi, and T. Yamagata, 2017: Relative importance of the processes contributing to the development of SST anomalies in the eastern pole of the Indian Ocean Dipole and its implication for predictability. *Climate Dyn.*, doi:10.1007/s00382-016-3382-2.

Terray, L., L. Corre, S. Cravatte, T. Delcroix, …, A. Ribes, 2012: Near-surface salinity as nature's rain gauge to detect human influence on the tropical water cycle. *J. Climate*, **25(3)**, 958-977.

Testut L., B.M. Miguez, G. W¨oppelmann, P. Tiphaneau, …, M. Karpytchev, 2010: Sea level at Saint Paul Island, southern Indian Ocean, from 1874 to the present. *J. Geophys. Res.*, **115**, C12028.

Thadathil, P., et al., 2007: Observed seasonal variability of barrier layer in the Bay of Bengal, *J. Geophys. Res* , **112**, C02009, doi:10.1029/2006JC003651

Thadathil, P., I. Suresh, S. Gautham, S. Prasanna Kumar, …, A. Hegde, 2016: Surface layer temperature inversion in the Bay of Bengal: Main characteristics and related mechanisms. *J. Geophys. Res*, **121**, 5682-5696, doi:10.1002/2016JC011674.5

Thompson, P.R., C.G. Piecuch, M.A. Merrifield, J.P. McCreary, and E. Firing, 2016: Forcing of recent decadal variability in the Equatorial and North Indian Ocean. *J. Geophys. Res. Oceans*, **121**, 6762-6778, doi:10.1002/2016JC012132.

Thompson, R.O.R.Y., 1984: Observations of the Leeuwin Current off Western Australia. *J. Phys. Oceanogr.*, **14**, 623-628, doi:10.1175/1520-0485

Tian B., D.E. Waliser, E.J. Fetzer, 2006: Modulation of the diurnal cycle of tropical deep convective clouds by the MJO. *Geophys. Res. Lett.* **33**, L20704.

Timmermann, A., S. McGregor, and F.F. Jin, 2010: Wind effects on past and future regional sea level trends in the southern Indo-Pacific. *J. Climate*, **23**, 4429-4437.

Todd R.E., D.T. Rudnick, R.E. Davis, and M.D. Ohman, 2011: Underwater gliders reveal rapid arrival of El Niño effects off California's coast. *Geophys. Res. Lett.*, **38**, L03609

Todd, R.E., W.B. Owens, and D.L. Rudnick, 2016: Potential vorticity structure in the North Atlantic western boundary current from underwater glider observations. *J. Phys. Oceanogr.*, **46(1)**, 327-348, doi:10.1175/JPO-D-15-0112.1.

Todd, R.E., D.L. Rudnick, J.T. Sherman, W.B. Owens, and L. George, 2017: Absolute velocity estimates from autonomous underwater gliders equipped with Doppler current profilers. *J. Atmos. Oceanic Technol.*, **34(2)**, 309-333, doi:10.1175/JTECH-D-16-0156.1.

Toole, J.M., M. Andres, I.A. Le Bras, T.M. Joyce, and M.S. McCartney, 2017: Moored observations of the Deep Western Boundary Current in the NW Atlantic: 2004-2014, *J. Geophys. Res.: Oceans*, **122**, doi:10.1002/2017JC012984.

Tozuka, T., J.J. Luo, S. Masson, and T.Yamagata, 2007: Decadal modulations of the Indian Ocean dipole in the SINTEX-F1 coupled GCM. J. Climate, 20, 2881-2894.

Tozuka, T., T. Kataoka, and T. Yamagata, 2014: Locally and remotely forced atmospheric circulation anomalies of Ningaloo Nino/Nina. *Climate Dyn.*, **43**, 2197-2205.

Trenary L., and W. Han, 2012: Intraseasonal-to-interannual variability of South Indian Ocean sea level and thermocline: Remote versus local forcing. *J. Phys. Oceanogr.*, **42**, 602-627.

Trenary L., and W. Han, 2013: Local and remote forcing of decadal sea level and thermocline depth variability in the south Indian Ocean. *JGR-Oceans*, **118**, 381-398.

Trenberth K, K.J. Fasullo, K.V. Schuckmann, and L. Cheng, 2016: Insights into Earth's energy imbalance from multiple sources. *J. Climate*, **29**, 7495-7505.

Turner, A.G., and H. Annamalai., 2012: Climate change and the South Asian summer monsoon. *Nature Climate Change*, **2**, 587-595, doi:10.1038/nclimate1495.

Unnikrishnan, A.S., and D. Shankar, 2007: Are sea-level-rise trends along the coasts of the north Indian Ocean consistent with global estimates? Global and Planet. *Change*, **57**, 301-307.

Ummenhofer, C.C., A. Sen Gupta, M.J. Pook, and M.H. England, 2008: Anomalous rainfall

over southwest Western Australia forced by Indian Ocean sea surface temperatures. *J. Climate*, 21, 5113-5134.

Ummenhofer, C.C., M.H. England, G.A. Meyers, P.C. McIntosh, …, A.S. Taschetto, 2009a: What causes Southeast Australia's worst droughts? *Geophys. Res. Lett.*, **36** (L04706), doi:10.1029/2008GL036801.

Ummenhofer, C.C., A. Sen Gupta, M.H. England, and C.J.C. Reason, 2009b: Contributions of Indian Ocean sea surface temperatures to enhanced East African rainfall. *J. Climate*, **22**, 993-1013.

Ummenhofer, C.C., A. Sen Gupta, A.S. Taschetto, and M.H. England, 2009c: Modulation of Australian precipitation by meridional gradients in east Indian Ocean sea surface temperature. *J. Climate*, **22**, 5597-5610.

Ummenhofer, C.C., A. Sen Gupta, and M.H. England, 2009d: Effect of tropical and subtropical Indian Ocean dipoles in driving precipitation around Indian Ocean rim countries. *9th International Conference for Southern Hemisphere Meteorology and Oceanography*, **Feb. 9-13, 2009**, Melbourne, Australia.

Ummenhofer, C.C., A. Sen Gupta, Y. Li, A.S. Taschetto, and M.H. England, 2011a: Multi-decadal modulation of the El Niño-Indian monsoon relationship by Indian Ocean variability. *Environ. Res. Lett.*, **6**, (034006), doi:10.1088/1748-9326/6/3/034006.

Ummenhofer, C.C., A. Sen Gupta, P.R. Briggs, M.H. England, …, J.S. Risbey, 2011b: Indian and Pacific Ocean influences on Southeast Australian drought and soil moisture. *J. Climate*, **24**, 1313-1336.

Ummenhofer, C.C., A. Biastoch, and C.W.W. Böning, 2017: Multi-decadal Indian Ocean variability linked to the Pacific and implications for preconditioning Indian Ocean Dipole events. *J. Climate*, **30**, 1739-1751.

Ummenhofer, C.C., M. Kulüke, and J.E. Tierney, 2018: Extremes in East African hydroclimate and links to Indo-Pacific variability on interannual to decadal timescales. *Climate Dyn.*, **50**, 2971-2991.

Unnikrishnan, A.S., A.G. Nidheesh, and M. Lengaigne, 2015: Sea-level-rise trends off the Indian coasts during the last two decades. *Current Science*, **108(5)**, 966-970.

Vallivattathillam P., S. Iyyappan, M. Lengaigne, C. Ethe, …, and W. Naqvi, 2017: Positive Indian Ocean Dipole events prevent anoxia off the west coast of India. *Biogeosciences* , **14**, 1541-1559.

Valsala, V., S. Maksyutov, and R. Murtugudde, 2012: A window for carbon uptake in the southern subtropical Indian Ocean. *Geophys. Res. Lett.*, **39**, L17605. doi:10.1029/2012GL052857

Vaquer-Sunyer, R., and C.M. Duarte, 2008: Thresholds of hypoxia for marine biodiversity. *Proc. Natl. Acad. of Sci.*, **105**, 15452-15457: doi:10.1073/pnas.0803833105.

Vargas-Hernandez, J.M., S. Wijffels, G. Meyers, and N.J. Holbrook, 2014: Evaluating SODA for IndoPacific Ocean decadal climate variability studies. *J. Geophys. Res.: Oceans*, **119**,

7854-7868.

Vecchi, G.A., and D.E. Harrison, 2002: Monsoon breaks and subseasonal sea surface temperature variability in the Bay of Bengal. *J. Climate*, **15(12)**, 1485-1493.

Vecchi, G.A., and D.E. Harrison, 2004: Interannual Indian rainfall variability and Indian Ocean sea surface temperature anomalies. In Earth Climate: The Ocean-Atmosphere Interaction, C. Wang, S.-P. Xie, and J.A. Carton (eds.), American Geophysical Union, Geophysical Monograph 147, Washington D.C., 247-260.

Vecchi, G.A., B.J. Soden, 2007: Global warming and the weakening of the tropical circulation. *J. Climate*, **20**, 4316-4340.

Vialard, J., G.R. Foltz, M.J. McPhaden, J.P. Duvel, and C. de Boyer Montégut, 2008: Strong Indian Ocean sea surface temperature signals associated with the Madden-Julian Oscillation in late 2007 and early 2008. *Geophys. Res. Lett.*, **35**, L19608, doi:10.1029/2008GL035
238.

Vialard, J., J.P. Duvel, M.J. McPhaden, P. Bouruet-Aubertot, …, S. Kennan, 2009a: Cirene: Air Sea Interactions in the Seychelles-Chagos thermocline ridge region, *Bull. Amer. Meteor. Soc.*, **90**, 45-61.

Vialard, J., S.S.C. Shenoi, J.P. McCreary, D. Shankar, …, S.R. Shetye, 2009b: Intraseasonal response of the northern Indian Ocean coastal waveguide to the Madden-Julian oscillation, *Geophys. Res. Lett.*, **36**, L14606, doi:10.1029/2009GL038450.

Vialard, J., A. Jayakumar, C. Gnanaseelan, M. Lengaigne, …, B.N. Goswami, 2012: Processes of 30-90 day sea surface temperature variability in the Northern Indian Ocean during boreal summer. *Climate Dyn.*, **38**, 1901-1916.

Vialard, J., K. Drushka, H. Bellenger, M. Lengaigne, …, J.P. Duvel, 2013: Understanding Madden-Julian-Induced sea surface temperature variations in the North Western Australian Basin. *Climate Dyn.*, **41**, 3203-3218, doi:10.1007/s00382-012-1541-7.

Vialard, J., 2015: Hiatus heat in the Indian Ocean. Nature Geoscience, doi:10.1038/ngeo2442.

Vic C., X. Capet, G. Roullet, and X. Carton, 2017: Western boundary upwelling dynamics off Oman. *Ocean Dynamics*, doi:10.1007/s10236-017-1044-5.

Vinayachandran, P.N., V.S. N. Murty, and V. Ramesh Babu, 2002a: Observations of barrier layer formation in the Bay of Bengal during summer monsoon. *J. Geophys. Res.*, 107(C12), 8018, doi:10.1029/2001JC000831.

Vinayachandran, P.V., D. Shankar, J. Kurian, F. Durand, and S.S.C. Shenoi, 2002b: Arabian Sea mini warm pool and monsoon onset vortex. *Current Science*, **93**, 203-214.

Vinayachandran, P.N., and T. Yamagata, 1998: Monsoon response of the sea around Sri Lanka: Ge neration of thermal domes and anticyclonic vortices. *J. Phys. Oceanogr.*, **28**, 1946 - 1960.

Vinayachandran, P.N., and N.H. Saji, 2008: Mechanisms of South Indian Ocean intraseasonal cooling, *Geophys. Res. Lett.*, **35**, L23607, doi:10.1029/2008GL035733.

Vinayachandran, P.N., 2009: Impact of Physical Processes on Chlorophyll Distribution in the Bay of Bengal, in Indian Ocean Biogeochemical Processes and Ecological Variability, edited, pp. 71-86. *American Geophysical Union*, doi:10.1029/2008GM000705.

Vincent, E.M., M. Lengaigne, G. Madec, J. Vialard, …, S. Jullien, 2012a: Processes setting the characteristics of sea surface cooling induced by tropical cyclones. *J. Geophys. Res.*, **117**, C02020, doi:10.1029/2011JC007396.

Vincent, E.M., M. Lengaigne, J. Vialard, G. Madec, …, S. Masson, 2012b: Assessing the oceanic control on the amplitude of sea surface cooling induced by tropical cyclones. *J. Geophys. Res.*, 117, C05023, doi:10.1029/2011JC007705.

Vincent, E.M., K.A. Emanuel, M. Lengaigne, J. Vialard, and G. Madec, 2014: Influence of upper ocean stratification interannual variability on tropical cyclones. *JAMES*, **6**, 680-699, doi:10.1002/2014MS000327.

Vitart, F., 2009: Impact of the Madden Julian Oscillation on tropical storms and risk of landfall in the ECMWF forecast system. *Geophys. Res. Lett.*, **36**, L15802, doi:10.1029/2009GL039089

Vitart, F., 2014: Evolution of ECMWF sub-seasonal forecast skill scores. *Quart. J. Roy. Meteor. Soc*, **140**, 1889-1899.

Vitart, F., C. Ardilouze, A. Bonet, A. Brookshaw, …, H. Hendon, 2016: The sub-seasonal to seasonal prediction (S2S) project database. *Bull. Amer. Meteor. Soc.*, Early online release, doi: http://dx.doi.org/10.1175/BAMS-D-16-0017.1.

Wainwright, L., G. Meyers, S. Wijffels, and L. Pigot, 2008: Change in the Indonesian Throughflow with the climatic shift of 1976/77. *Geophys. Res. Lett.*, **35**, L03604, doi:10.1029/2007GL03 1911.

Wajsowicz R.C., 2007: Seasonal-to-interannual forecasting of tropical Indian Ocean sea surface temperature anomalies: Potential predictability and barriers. *J. Climate 20*, 3320-3343.

Wajsowicz, R.C., 2005: Potential predictability of tropical Indian Ocean SST anomalies. *Geophys. Res. Lett.*, **32**, L24702, doi: 10.1029/2005GL024169.

Waliser, D.E., R. Murtugudde, and L. E. Lucas, 2003: Indo-Pacific Ocean response to atmospheric intraseasonal variability: 1. Austral summer and the Madden-Julian Oscillation. *J. Geophys. Res.*, **108(C5)**, 3160, doi:10.1029/2002JC001620.

Waliser, D.E., R. Murtugudde, and L. E. Lucas, 2004: Indo-Pacific Ocean response to atmospheric intraseasonal variability: 2. Boreal summer and the intraseasonal oscillation. *J. Geophys. Res*, **109**, C03030, doi:10.1029/2003JC002002.

Waliser D.E., 2006: Intraseasonal variations. In: Wang B (ed) The Asian monsoon. *Springer, Heidelberg*, 787.

Wang G., L. Cheng, J. Abraham, and C. Li, 2017: Consensuses and discrepancies of basin-scale ocean heat content changes in different ocean analyses. *Climate Dyn.*, doi: 10.1007/s00382-017-3751-5. Wang T.Y., Y. Dy, W. Zhuang, and J.B. Wang, 2015: Connection of sea level vari-

ability between the tropical western Pacific and the southern Indian Ocean during recent two decades. *Science China-Earth Sci.*, **58**, 8,1387-1396. doi: 10.1007/s11430-014-5048-4.

Wang, L.-P., C.J. Koblinksky, and S. Howden, 2001: Annual Rossby waves in the Southern Indian Ocean: why does it appear to break down in the middle ocean? *J. Phys. Oceanogr.*, **31**, 54-74.

Wang, W., M. Chen, and A. Kumar, 2009: Impacts of ocean surface on the northward propagation of the boreal summer intraseasonal oscillation in the NCEP climate forecast system. *J. Climate*, **22(24)**, 6561-6576.

Wang, W., A. Kumar, J.X. Fu, and M. Hung, 2015: What is the Role of the Sea Surface Temperature Uncertainty in the Prediction of Tropical Convection Associated with the MJO?. *Mon. Wea. Rev.*, **143**, 3156-3175, doi:https://doi.org/10.1175/MWR-D-14-00385.1

Warner, S.J., J. Becherer, K. Pujiana, E.L. Shroyer, …, J.N. Moum, 2016: Monsoon mixing cycles in the Bay of Bengal: A year-long subsurface mixing record. *Oceanography*, **29(2)**,158-169, http://dx.doi.org/10.5670/oceanog.2016.48.

Watson, P.J., 2011: Is there evidence yet of acceleration in mean sea level rise around mainland Australia?. *Journal of Coastal Research*, **27(2)**, 368-377.

Webster P.J., V.O. Magana, T.N. Palmer, J. Shukla, …, T. Yasunari, 1998: Monsoons: processes, predictability, and the prospects for prediction. *J Geophys Res.* **103**, 14451-14510.

Webster, P.J., and R. Lukas, 1992: TOGA COARE: Coupled Ocean Atmosphere Response Experiment. *Bull. Amer. Meteor. Soc.*,**73**, 1377-1416.

Webster, P.J., A. M. Moore, and J. P. Loschnigg, et al., 1999: Coupled oceanic-atmospheric dynamics in the Indian Ocean during 1997-98. *Nature*, **401**, 356-360.

Webster, P.J., et al., 2002: The JASMINE pilot study, *Bull. Amer. Meteor. Soc.*, **83**, 1603-1630.

Wei, Z. X., G. H. Fang, R. D. Susanto, T. R. Adi, …, X. M. Gao, 2016: Tidal elevation, current and energy flux in the area between the South China Sea and Java Sea. *Ocean Sci.*, **12**, 2831-2861, doi:10.5194/osd-12-2831-2015.

Weickmann, K.M., G.R. Lussky, and J.E. Kutzbach, 1985: Intraseasonal (30-60 day) fluctuations of outgoing longwave radiation and 250mb streamfunction during northern winter. *Mon. Wea. Rev.*, **113**, 941-961.

Weller, R.A., and S.P. Anderson, 1996: Surface meteorology and air-sea fluxes in the western equatorial Pacific warm pool during the TOGA Coupled Ocean Atmosphere Response Experiment. *J. Climate*, **9**, 1959-1990.

Weller, R.A., M.F. Baumgartner, S.A. Josey, A.S. Fischer, and J. Kindle, 1998: Atmospheric forcing in the Arabian Sea during 1994- 1995: Observations and comparisons with climatology and models. *Deep-Sea Res.*, **45**, 1961-1999.

Weller, R.A., and Co-authors, 2016: Air-sea interaction in the Bay of Bengal. *Oceanography*,

29(2), 28-37.

Wentz, F.J., L. Ricciardulli, and E. Rodriquez, 2017: Evaluating and Extending the Ocean Wind Climate Data Record. *IEEE J*. Selected Topics in Applied Earth Observations and Remote Sensing, 10, 5, 2165-2185. doi: 10.1109/JSTARS.2016.2643641.

Wernberg, T., D.A. Smale, F. Tuya, M.S. Thomsen, …, C.S. Rousseaux, 2013: An extreme climatic event alters marine ecosystem structure in a global biodiversity hotspot. Nature Climate change, 3, 78-82, doi:10.1038/nclimate1627.

Wernberg, T., and Co-authors, 2016: Climate-driven regime shift of a temperate marine ecosystem. *Science*, **353**, 169-172, doi:10.1126/science.aad8745.

Wheeler, M., and G.N. Kiladis, 1999: Convectively coupled equatorial waves: Analysis of clouds and temperature in the wavenumber-frequency domain. *Journal of the Atmospheric Sciences*, **56(3)**, 374-399.

Wheeler, M.C., and H.H. Hendon, 2004: An all-season real-time multivariate MJO index: Development and index for monitoring and prediction. *Mon. Wea. Rev.*, **132**, 1917-1932.

Wiggert, J.D., R.G. Murtugudde, and J.R. Christian, 2006: Annual ecosystem variability in the tropical Indian Ocean: results of a coupled bio-physical ocean general circulation model. *Deep-Sea Res. Part II*, **53**, 644-676.

Wiggert, J.D., J. Vialard, and M.J. Behrenfeld, 2009a: Basin-wide modification of dynamical and biogeochemical processes by the Indian Ocean Dipole. In: Indian Ocean Biogeochemical Processes and Ecological Variability, J.D. Wiggert, R.R. Hood, S.W.A. Naqvi, S.L. Smith, and K.H. Brink (ed.), *American Geophysical Union*, Washington, D. C, 385-408.

Wijesekera H.W., E. Shroyer, A. Tandon, M. Ravichandran, …, M. Baumgartner, 2016: ASIRI: An ocean-atmosphere initiative for Bay of Bengal. *Bull. Amer. Meteor. Soc..* **97(10)**,1859-84.

Wijffels, S., and G. Meyers, 2004: An intersection of oceanic waveguides: Variability in the Indonesian Throughflow region. *J. Phys. Oceanogr.*, **34**, 1232-1253.

Wijffels, S.E., G. Meyers, and J.S. Godfrey, 2008: A 20-yr average of the Indonesian Throughflow: Regional currents and the interbasin exchange. *J. Phys. Oceanogr.*, **38**, 1965-1978, doi:10.1175/2008JPO3987.1.

Williams, A.P. and C. Funk, 2011: A westward extension of the warm pool leads to a westward extension of the Walker circulation, drying eastern Africa. **Climate Dyn.**, **37**, 2417-2435.

Wishner, K.F. et al., 2008: Vertical zonation and distributions of calanoid copepods through the lower oxycline of the Arabian Sea oxygen minimum zone. *Prog. Ocean.*, **78**, 163-191, doi:10.1016/j.pocean.2008.03.001.

Woo, L.M., and C.B. Pattiaratchi, 2008: Hydrography and water masses off the western Australian coast. *Deep-Sea Res. Part I*, **55**, 1090-1104, doi:10.1016/j.dsr.2008.05.005.3

Woodruff, Scott D., S.J. Worley, S.J. Lubker, Z. Ji, …, C. Wilkinson. 2011: ICOADS Release 2.5: extensions and enhancements to the surface marine meteorological archive. *International*

Journal of Climatology, **31(7)**, 951-967, doi:10.1002/joc.2103.

Woodworth, P.L., G. W¨oppelmann, M. Marcos, M. Gravelle, and R.M. Bingley, 2017: Why we must tie satellite positioning to tide gauge data. *Eos, Trans. Amer. Geophys. Union* , **98**, doi:10.1029/2017EO064037. Published on 03 January 2017. doi:https://eos.org/opinions/why-we-must-tie-satellite-positioning-to-tide-gauge-data.

Woolnough, S.J., F. Vitart, and M.A. Balmaseda, 2007: The role of the ocean in the Madden-Julian Oscillation: Implications for MJO prediction. *Quart. J. Roy. Meteor. Soc.*, **133**, 117-128. doi:10.1002/qj.49.

Wu, L., W. Cai, L. Zhang, H. Nakamura, ..., P Chang, 2012: Enhanced warming over the global subtropical western boundary currents. *Nature Climate Change*, **2(3)**, 161.

Wyrtki, K., 1973: An equatorial jet in the Indian Ocean. *Science*, **181**, 262-264.

Xie, S.P., H. Annamalai, F. A. Schott, and J. P. McCreary Jr., 2002: Structure and mechanisms of South Indian Ocean climate variability. *J. Climate*, **15**, 864-878, doi:10.1175/1520-0442(2002)015<0864:SAMOSI>2.0.CO;

Xie, S.P., K. Hu, J. Hafner, H.Tokinaga, …, T. Sampe, 2009: Indian Ocean capacitor effect on Indo-western Pacific climate during the summer following El Niño. *J. Climate*, **22**, 730-747.

Xu, F., and A. Ignatov, 2010: Evaluation of *in situ* sea surface temperatures for use in the calibration and validation of satellite retrievals, **115(C9)**, doi:10.1029/2010JC006129.

Yamagata, T., S.K. Behera, J.-J. Luo, S. Masson, …, S.A. Rao, 2004: Coupled ocean-atmosphere variability in the tropical Indian Ocean. In Earth's climate: The ocean-atmosphere interaction. *Geophys. Monogr. Ser.*, **147**, 189-211.

Yang, H., G. Lohmann, W. Wei, M. Dima, …, J. Liu, 2016: Intensification and poleward shift of subtropical western boundary currents in a warming climate. *J. Geophys. Res.: Oceans*, **121(7)**, 4928-4945.

Yang, J., L. Yu, and C. Koblinksky et al., 2001: Dynamics of the seasonalvariations in the Indian Ocean from TOPEX/POSEIDON sea surface height and an ocean model. *Geophys. Res. Lett.*, **25**, 11, 1915-1918. doi: 10.1029/98GL01401.

Yang, J., Q. Liu, S.-P. Xie, Z. Liu, and L. Wu, 2007: Impact of the Indian Ocean SST basin mode on the Asian summer monsoon. *Geophys. Res. Lett.*, **34**, L02708, doi:10.1029/2006GL028571.

Yang, Y., S. P. Xie, L. Wu, Y. Kosaka, …, G.A. Vecchi, 2015: Seasonality and predictability of the Indian Ocean dipole mode: ENSO forcing and internal variability. *J. Climate*, **28(20)**, 8021-8036.

Yao, S.L., G. Huang, R.G. Wu, X. Qu, and D. Chen, 2016: Inhomogeneous warming of the tropical Indian Ocean in the CMIP5 model simulations during 1900-2005 and associated mechanisms. *Climate Dyn.*, **46(1-2)**, 619-636.

Yaremchuk, M., Z. Yu, and J. McCreary, 2005: River discharge into the Bay of Bengal in an inverse ocean model. *Geophys. Res. Lett.*, **32(16)**, doi:10.1029/2005GL023750.

Yasunari, T., 1979: Cloudiness fluctuations associated with the Northern Hemisphere summer monsoon. *J. Meteor. Soc. Japan*, **57**, 227-242.

Yasunari, T., 1980: A quasi-stationary appearance of 30 to 40 day period in the cloudiness fluctuations during the summer monsoon over India. *J. Meteor. Soc. Japan.*, **58**, 225-2297

Yokoi, T., T. Tozuka, and T. Yamagata, 2008: Seasonal Variation of the Seychelles Dome. *J. Climate*, **21**, 3740-3754, doi: 10.1175/2008JCLI1957.1

Yoneyama, K., C. Zhang, and C.N. Long, 2013: Tracking pulses of the Madden-Julian Oscillation. *Bull. Amer. Meteor. Soc.*, **94**, 1871-1891.

Yu, L., and M.M. Rienecker, 1999: Mechanisms for the Indian Ocean warming during the 1997-98 El Niño. *Geophys. Res. Lett.*, **26**, 735-738, 10.1029/1999GL900072.

Yu, L., X. Jin, and R.A. Weller, 2007: Annual, seasonal, and interannual variability of air-sea heat fluxes in the Indian Ocean. *J. Climate*, **20(13)**, 3190-3209.

Yu, L., and M.J. McPhaden, 2011: Ocean Preconditioning of Cyclone Nargis in the Bay of Bengal: Interaction between Rossby Waves, *Surface Fresh Waters, and Sea Surface Temperatures**. **41**, 1741-1755, doi:10.1175/2011JPO4437.1.

Yu, L., X. Jin, S.A. Josey, T. Lee, …, Y. Xue, 2017: The Global Ocean Water Cycle in Atmospheric Reanalysis, Satellite, and Ocean Salinity. *J. Climate*, **30**, 3829-3852, doi:https://doi.org/10.1175/JCLI-D-16-0479.1.

Yu L., and X. Jin, 2018: A regime-dependent algorithm for retrieving near-surface air temperature and specific humidity from multi-microwave sensors. *Remote Sens. Environ.*, **215**, 199-216. https://doi.org/10.1016/j.rse.2018.06.001.

Yu W., R. Hood, N. D'Adamo, M. McPhaden, …, Y. Masumoto, 2016: The EIOURI Science Plan, available at http://www.iioe-2.incois.gov.in/IIOE-2/pdfviewer.jsp?docname=EIOURI_Science
_Plan.pdf

Yuan, C., T. Tozuka, J.-J. Luo, and T. Yamagata, 2014: Predictability of the subtropical dipole modes in a coupled ocean-atmosphere model. *Climate Dyn.*, **42**, 1291-1308.

Yuan, J., and J. Cao, 2012: North Indian Ocean tropical cyclone activities influenced by the Indian Ocean Dipole mode. Sci. *China Earth Sci*, **56**, 855-865, doi:10.1007/s11430-012-4559-0.

Zaba K.D., D.L. Rudnick, 2016: The 2014-2015 warming anomaly in the Southern California Current System observed by underwater gliders. *Geophys. Res. Lett.*, **43**, 1241-8.

Zeitzschel, B., 1973: The biology of the Indian Ocean. Springer-Verlag, Berlin.

Zhang, C., 2005: Madden-Julian Oscillation. *Rev. Geophys.*, **43**, RG2003, doi:10.1029/2004RG000158.

Zhang, C., M. Dong, S. Gualdi, H.H. Hendon, …, and W. Wang, 2006: Simulations of the Madden-Julian oscillation in four pairs of coupled and uncoupled global models. *Climate Dyn.*, **27**, 573-592.

Zhang, C., 2013: Madden-Julian Oscillation: Bridging weather and climate. *Bull. Amer. Meteor. Soc.*, doi:10.1175/BAMS-D-12-00026.1.

Zhang, C., and J. Ling, 2017: Barrier Effect of the Indo-Pacific Maritime Continent on the MJO: Perspectives from Tracking MJO Precipitation. *J. Climate*, **30(9)**, 3439-3459.

Zhang, N., M. Feng, H.H. Hendon, A.J. Hobday, and J. Zinke, 2017: Opposite polarities of ENSO drive distinct patterns of coral bleaching potentials in the southeast Indian Ocean. *Sci Rep*, **7**, 2443, doi:10.1038/s41598-017-02688-y.

Zhang, X and W. Han, 2019: Effects of climate modes on interannual variability of upwelling in the tropical Indian Ocean, *J. Climate*, in revision.

Zhang, Y.-C., W.B. Rossow, A.A. Lacis, V. Oinas, and M.I. Mishchenko, 2004: Calculation of radiative fluxes from the surface to top of atmosphere based on ISCCP and other global data sets: Refinements of the radiative transfer model and the input data. *J. Geophys. Res.*, **109**, D19105, doi:10.1029/2003JD004457.

Zhang, Y., Y. Du, S. Zheng, Y. Yang, and X. Cheng, 2013: Impact of Indian Ocean dipole on the salinity budget in the equatorial Indian Ocean. *J. Geophys. Res. Oceans*, **118**, 4911-4923.

Zhang, Y., M. Feng, Y. Du, H. E. Phillips, …, and M. J. McPhaden, 2018: Strengthened Indonesian Throughflow drives decadal warming in the Southern Indian Ocean, *Geophys. Res. Lett.*, **45**, 6167-6175.

Zhao et al., 2018: The GFDL Global Atmosphere and Land ModelAM4.0/LM4.0: Documentation and Simulations with Prescribed SSTs - Part I: Simulation Characteristics, JAMES.

Zheng, X.T., S.-P. Xie, G.A. Vecchi, Q. Liu, and J. Hafner, 2010: Indian Ocean Dipole response to global warming: Analysis of ocean-atmospheric feedbacks in a coupled model. *J. Climate*, **23**, 1240-1253.

Zheng, Z.-W., C.R. Ho, and N.J. Kuo, 2008: Importance of pre-existing oceanic conditions to upper ocean response induced by Super Typhoon Hai-Tang. *Geophys. Res. Lett.*, **35**, L20603.

Zhou, L., and R. Murtugudde, 2010: Influences of Madden-Julian oscillations on the eastern Indian Ocean and the maritime continent. *Dyn. Atmos. Oceans*, **50**, 257-274.

Zhou, L., R. Murtugudde, D. Chen, and Y. Tang, 2017: A central Indian Ocean mode and heavy precipitation during the Indian summer monsoon. *J. Climate*, **30**, 2055-2067.

Zhuang, W., M. Feng, Y. Du, A. Schiller, and D. Wang, 2013: Low-frequency sea level variability in the southern Indian Ocean and its impacts on the oceanic meridional transports. *J. Geophys. Res. Oceans*, **118**, 1302-1315, doi:10.1002/jgrc.20129.

Zilberman, N.V., D.H. Roemmich, S.T. Gille, and J. Gilson, 2018: Estimating the velocity and transport of Western Boundary Current systems: a case study of the East Australian Current

near Briabane. *J. Atmos. Oceanic. Tech.*, **35**, 1313-1329, doi:https://doi.org/10.1175/JTECH-D-17_0153.1

Zinke, J., A. Rountrey, M. Feng, S.P. Xie, and D. Dissard, 2014: Corals record long-term Leeuwin current variability including Ningaloo Nino/Nina since 1795. *Nature*.

Zinke, J., A. Hoell, J.M. Lough, M. Feng, …, M.T. McCulloch, 2015: Coral record of south-east Indian Ocean marine heatwaves with intensified Western Pacific temperature gradient. *Nature communications*, **6**.

Appendix A: List of Acronyms

ACT	Agulhas Current Time-Series experiment
ADCP	Acoustic Doppler Current Profiler
AMO	Atlantic Multi-decadal Oscillation
AMOC	Atlantic Meridional Overturning Circulation
AOML	Atlantic Oceanographic and Meteorological Laboratory, NOAA
ARGO	Global Array of temperature/salinity profiling floats
ASCA	Agulhas System Climate Array
ASCLME	Agulhas and Somali Current Large Marine Ecosystem
ASIRI	Air-Sea Interactions Regional Initiative
ASUKA	Affiliated Surveys of the Kuroshio off Cape Ashizuri
ATLAS	Autonomous Temperature Line Acquisition System
AUV	Autonomous Underwater Vehicle
AVHRR	Advanced Very High Resolution Radiometer
AVISO	Archiving, Validation and Interpretation of Satellite Oceanographic data
AXIS	Automated eXpendable Instrument System
BGC	Biogeochemical
BMKG	Indonesian Agency for Meteorology, Climatology and Geophysics
BoB	Bay of Bengal
BOBLME	Bay of Bengal Large Marine Ecosystem
CARICOOS	Caribbean Coastal Ocean Observing System
CDOM	Colored Dissolved Organic Matter
cDRAKE	Dynamics and transport of the Antarctic Circumpolar Current in Drake Passage
CERES	Clouds and the Earth's Radiant Energy System
CFC	Chlorofluorocarbon
CFSR	Climate Forecast System Reanalysis, NOAA
Chl	Chlorophyll
CLIVAR	Climate and Ocean: Variability, Predictability and Change
CLS	Collecte Localisation Satellites
COADS	Comprehensive Ocean-Atmosphere Data Set
CPIES	Current and Pressure-sensor-equipped Inverted Echo Sounder

CPUE	Catch Per Unit Effort
CREATE	Collaborative REAnalysis Technical Environment
CSIRO	Commonwealth Scientific and Industrial Research Organisation
CTD	Conductivity-Temperature-Depth
DBCP	Data Buoy Cooperation Panel, JCOMM
DCPS-PIES	Doppler Current Profiler Sensor and Pressure sensor equipped Inverted Echo Sounder
DIC	Dissolved Inorganic Carbon
DO	Dissolved Oxygen
DWS	Directional Wave Spectra
DYNAMO	Dynamics of the MJO field campaign
EBAF	Energy Balanced And Filled
ECCO	Estimating the Circulation and Climate of the Ocean group
ECMWF	European Centre for Medium-Range Weather Forecasts
ECVs	Essential Climate Variables
EEZ	Exclusive Economic Zone
ENSO	El Niño-Southern Oscillation
EOF	Empirical Orthogonal Function
EOVs	Essential Ocean Variables
ERA	ECMWF Reanalysis
ERS	Earth Remote Sensing
ERSST	Extended Reconstructed Sea Surface Temperature
ESA	European Space Agency
ESSO	Earth System Science Organisation
EUMETSAT	European Organisation for the Exploitation of Meteorological Satellites
FAO	Food and Agriculture Organization of the United Nations
FIO	First Institute of Oceanography, Ministry of Natural Resources of China
FLEAT	Flow Encountering Abrupt Topography
FR	Frequently Repeated
GCM	Global climate models
GCOS	Global Climate Observing System
GDP	Global Drifter Program
GEOSECS	Geochemical Ocean Sections Study

GEOTRACES	An International Study of Marine Biogeochemical Cycles of Trace Elements and their Isotopes
GEWEX	Global Energy and Water cycle Experiment
GHG	Greenhouse Gas
GIA	Glacial Isostatic Adjustment
GLOSS	Global Sea Level Observing System
GNSS	Global Navigation Satellite System
GO-SHIP	Global Ocean Ship-Based Hydrographic Investigations Program
GOCE	Gravity field and steady-state Ocean Circulation Explorer, ESA
GODAS	Global Ocean Data Assimilation System
GOOS	Global Ocean Observing System
GPM	Global Precipitation Measurement
GPS	Global Positionning System
GRACE	Gravity Recovery and Climate Experiment
Gt	Gigatonnes
GTS	Global Telecommunication System
HPLC	High Performance Liquid Chromatography
HR	High Resolution
HYCOM	Hybrid Coordinate Ocean Model
IBTrACS	International Best Track Archive for Climate Stewardship
ICOADS	International Comprehensive Ocean-Atmosphere Data Set
IGY	International Geophysical Year
IIOE-2	Second International Indian Ocean Expedition
IITM	Indian Institute of Tropical Meteorology
IMBeR	Integrated Marine Biosphere and Research
INCOIS	Indian National Centre for Ocean Information Services
IndOOS	Indian Ocean Observing System
IOBM	Indian Ocean Basin Mode
IOC	The Intergovernmental Oceanographic Commission of UNESCO
IOD	Indian Ocean Dipole
IO-GOOS	Indian Ocean component of the Global Ocean Observing System
IORP	Indian Ocean Region Panel
IOSD	Indian Ocean Subtropical Dipole
IPCC	Intergovernmental Panel on Climate Change

IPO	Inter-decadal Pacific Oscillation
IR	infrared
IRD	Institut de Recherche pour le Développement
IRF	IndOOS Resource Forum
ISCCP	International Satellite Cloud Climatology Project
ISO	Intra-Seasonal Oscillation
ISRO	Indian Space Research Organization
ISV	Intraseasonal to Seasonal Variability
ITCZ	Intertropical Convergence Zone
ITEWC	Indian Tsunami Early Warning Centre
ITF	Indonesian Throughflow
IUGG	International Union of Geodesy and Geophysics
JAMSTEC	Japan Agency for Marine-Earth Science and Technology
JCOMM	Joint WMO-IOC Technical Commission for Oceanography and Marine Meteorology
JGOFS	Joint Global Ocean Flux Study
JRA55	Japanese 55-year Reanalysis
KESS	The Kuroshio Extension System Study
LAMP	Lift-Assisted Moored Profiler
LD	Low Density
LDCs	least developed countries
LDL	Lagrangian Drifter Laboratory, SIO
LH	Latent Heat
LOCEAN	Laboratoire d'Océanographie et du Climat: Expérimentations et Approches Numériques
$MAPCO_2$	Moored Autonomous pCO_2
MC	Maritime Continent
MERRA	The Modern-Era Retrospective analysis for Research and Applications
MHW	Marine Heat Wave
MISO	Monsoon Intra-Seasonal Oscillation
MoES	Ministry of Earth Sciences, India
MJO	Madden-Julian Oscillation
NASA	The National Aeronautics and Space Administration
NCAOR	National centre for Antarctic and Ocean Research, India

NCEI	National Center for Environmental Information, NOAA
NCEP	National Center for Environmental Prediction, NOAA
NMEFC	National Marine Environmental Forecasting Center, State Oceanic Administration, China
NOAA	National Oceanic and Atmospheric Administration
NOCS	National Oceanography Centre Southampton
NWP	numerical weather prediction
OAFlux-HR	Objectively Analyzed Air-Sea Fluxes at High Resolution
ODA	Ocean data assimilation
OGCM	Ocean General Circulation Model
OHC	Ocean Heat Content
OKTV	Observations of Kuroshio Transport Variability
OMNI	Ocean Moored
OMZ	Oxygen Minimum Zones
ONR	Office of Naval Research
OOPC	Ocean Observations Panel for Climate
ORA-IP	Ocean ReAnalysis Intercomparison Project
OSE	Observing System Experiments
OSSE	Observing System Simulation Experiments
PAR	Photosynthetically Active Radiation
pCO_2	pressure of carbon dioxide
PIES	Pressure sensor-equipped Inverted Echo Sounders
PIRATA	Pilot Research Moored Array in the Atlantic
PMEL	Pacific Marine Environmental Laboratory, NOAA
PMW	Passive Microwave
PN	Line Pollution Nagasaki Line (Kuroshio)
PSMSL	Permanent Service for Mean Sea Level
QSCAT	QuikSCAT or Quick Scatterometer by NASA
RAMA	Research Moored Array for African-Asian-Australian Monsoon& Analysis and Prediction
REMUS	Remote Environmental Monitoring UnitS
RLR	Revised Local Reference
RMM	Rainfall Measuring Mission
S2S	Subseasonal-to-seasonal
SARAL	Satellite with ARgos and ALtika

SeaWiFS	Sea-Viewing Wide Field-of-View Sensor
SCTR	Seychelles-Chagos Thermocline Ridge
SH	Sensible Heat
SIBER	Sustained Indian Ocean Biogeochemistry and Ecosystem Research
SIDS	Small Island Developing States
SIO	Scripps Institution of Oceanography, USA
SK-II	Study of the Kuroshio-II
SKIM	Sea Surface Kinematics Multiscale of ESA
SLA	Sea Level Anomalies
SLC	Sea Level Change
SLP	Sea-level atmospheric pressure
SMAP	Soil Moisture Active Passive
SMOS	Soil Moisture and Ocean Salinity
SONEL	Service d'Observation du Niveau des Eaux Littorales
SOOP	Ship Of Opportunity Program
SOOP-CO_2	Ship of Opportunity CO_2 program
SOT	Ship Observation Team
SRB	Surface Radiation Budget
SSH	Sea Surface Height
SSS	Sea Surface Salinity
SST	Sea Surface Temperature
STD	Standard Deviation
STS	Sea Surface Temperature and Salinity
SVP	Surface Velocity Program
SWH	Significant Wave Height
SWOT	Surface Water Ocean Topography
SYNOP	Surface Synoptic Observations
T-Flex	Tropical Flex - new mooring design for greater number and types of instrumentation, using more off-the-shelf components
T/C	Temperature and Conductivity
T/S	Temperature and Salinity
TAlk	(TA) Total Alkalinity
TAO	Tropical Atmosphere Ocean
TC	Tropical Cyclone

TIO	Tropical Indian Ocean
TIP	Tropical Moored Buoy Implementation Panel
TOGA-COARE	Tropical Ocean Global Atmosphere Coupled Ocean Atmosphere Response Experiment
TPOS	Tropical Pacific Observing System
TRITON	Triangle Trans-Ocean Buoy Network
TRMM	Tropical Rainfall Measuring Mission
UNESCO	United Nations Educational, Scientific and Cultural Organization
VGPM	Vertically Generalized Productivity Model
VOS	Voluntary Observing Ship
WaCM	Wind and Current Mission of NASA
WCRP	World Climate Research Programme
WHOI	Woods Hole Oceanographic Institution
WMO	World Meteorological Organization
WOCE	World Ocean Circulation Experiment
XBT	eXpendable Bathy Thermograph
XCTD	Expendable Conductivity, Temperature and Depth

Appendix B: List of Contributors

Name	Organization	Country	Chapters
Thorkild Aarup	GLOSS/IOC	France	05
Kentaro Ando	JAMSTEC	Japan	02
Magdalena A. Andres*	Woods Hole Oceanographic Institution (WHOI)	USA	08*
Hariharasubramanian Annamalai*	University of Hawaii	USA	14*
Magdalena A. Balmaseda	European Centre for Medium-Range Weather Forecasts (ECMWF)	UK	09
David Barbary	Equipe cyclone, Laboratoire de l'Atmosphère et des Cyclones (UMR 8105, Meteo-France, CNRS, Reunion University), Saint-Denis de La Réunion, France		12
Lisa M. Beal* (Ed)	University of Miami	USA	17, 23*, Ex*, In, Sy*
Luca Centurioni	Scripps Institution of Oceanography	USA	04, 08
Lijing Cheng	Institute of Atmospheric Physics, Chinese Academy of Sciences	China	25
Rebecca Cowley	Commonwealth Scientific and Industrial Research Organisation (CSIRO)	Australia	03
Peter E. Dexter		Australia	Review Board
Takeshi Doi	Application Laboratory, JAMSTEC	Japan	19
Paul J. Durack	Lawrence Livermore National Laboratory	USA	25
Ming Feng*	CSIRO Oceans and Atmosphere, Perth, Western Australia, Australia	Australia	03*, 12, 17*, 21, 22

Médéric Gravelle	LIENS	France	05
Weiqing Han*	University of Colorado	USA	21*, 22, 25
Nicholas J. Hardman-Mountford	Oceans and Natural Resources Directorate, Commonwealth Secretariat	UK	01
Raleigh Hood*	University of Maryland, Cambridge	USA	18, 24*
Marjolaine Krug	Council for Scientific and Industrial Research	South Africa	Review Board
B. Ajay Kumar	ESSO-INCOIS	India	05
Arun Kumar	NOAA	USA	09
Craig Lee*	University of Washington	USA	08*
Tong Lee*	1. NASA Jet Propulsion Laboratory (JPL), USA; 2. California Institute of Technology, USA	USA	06*, 11*, 21
Matthieu Lengaigne*	LOCEAN-IPSL, Sorbonne Universités (UPMC, Univ. Paris 06)-CNRS-IRD-MNHN, Paris, France	France	12*, 22
Rick Lumpkin*	NOAA/Atlantic Oceanographic and Meteorological Laboratory	USA	04*
Jay McCreary	University of Hawaii	USA	Review Board
Yukio Masumoto*	University of Tokyo	Japan	18*
Richard Matear	Commonwealth Scientific and Industrial Research Organisation (CSIRO)	Australia	Review Board
Andrew Matthews	National Oceanography Centre	UK	05
Elaine McDonagh	1. NORCE, Norwegian Research Centre, Bjerknes Centre for Climate Research, Bergen, Norway; 2. NOC, National Oceanography Centre, Southampton, UK	Norway /UK	23
Michael J. McPhaden*	NOAA, PMEL/Tropical Moored Buoy Implementation Panel	USA	02*, 10, 18, 19, 21, 22,

Coleen Moloney	University of Cape Town	South Africa	Review Board
Motoki Nagura	JAMSTEC	Japan	14
Satheesh Neetu	CSIR-National Institute of Oceanography (NIO), Goa, India	India	12
A.G. Nidheesh	Indian Institute of Tropical Meteorology (IITM)	India	22
Helen Phillips	University of Tasmania	Australia	17
Hamish A.Ramsay	CSIRO, Oceans and Atmosphere, Aspendale, Victoria, Australia	Australia	12
Muthalagu Ravichandran*	1. National Centre for Polar and Ocean Research (NCPOR), India; 2. Indian National Centre for Ocean Information Services (INCOIS), India	India	01*, 02
Laure Resplandy	Princeton Environmental Institute		20
Kelvin Richards	University of Hawaii	USA	14
Mathew K. Roxy* (Ed)	Indian Institute of Tropical Meteorology (IITM)	India	21, 22, 25*, Ex, In, Sy
Toshiaki Shinoda*	Texas A&M University-Corpus Christi (TAMU)	USA	13*, 21
Emily L. Shroyer	Oregon State University	USA	08
Bernadette Sloyan*	1. CSIRO, Oceans and Atmosphere, Hobart Australia; 2. Centre for Southern Hemisphere Oceans Research, Hobart, Tasmania, Australia; 3. Co-Chair GO-SHIP	Australia	07*
Janet Sprintall	Scripps Institution of Oceanography	USA	03
Peter Strutton*	University of Tasmania	Australia	16*
Aneesh C. Subramanian*	University of Colorado	India /USA	09*
Raden D. Susanto	University of Maryland	Australia	17

Laurent Testut	LEGOS	France	05
Tomoki Tozuka*	University of Tokyo	Japan	19*, 22
T V Sudaya Bhaskar	Indian National Centre for Ocean Information Services (INCOIS)	India	01
Caroline C. Ummenhofer*	Woods Hole Oceanographic Institution (WHOI)	USA	15*
Alakkat S. Unnikrishnan*	CSIR-National Institute of Oceanography	India	05*
Jérôme Vialard* (Ed)	LOCEAN-IPSL, Sorbonne Universités (UPMC, Univ. Paris 06)-CNRS-IRD-MNHN, Paris, France	France	12, 21, 22*, 25, Ex, In*, Sy
Frederic Vitart	European Centre for Medium-Range Weather Forecasts (ECMWF), UK	UK	09
Kevin Walsh	School of Earth Sciences, University of Melbourne, Parkville, Victoria, Australia	Australia	12
Rik Wanninkhof	NOAA Atlantic Oceanographic and Meteorological Laboratory	NOAA	07
Susan Wijffels	Woods Hole Oceanographic Institution (WHOI)	USA	Review Board
Jerry Wiggert*	University of Southern Mississippi	USA	20*
Philip L. Woodworth	National Oceanography Centre	UK	05
Weidong Yu*	School of Atmospheric Sciences, Sun Yat-Sen University, Zhuhai, China	China	02, 18*
Lisan Yu*	Woods Hole Oceanographic Institution (WHOI)	USA	10*
Chidong Zhang	PMEL/NOAA	USA	09
Tianjun Zhou	Institute of Atmospheric Physics, Chinese Academy of Sciences	China	25

*= Lead authors, Ed = Editor, Ex = Executive Summary, In = Introduction, Sy = Synthesis